University of Sheffield

Department of Civil and Structural Engineering

Behaviour of Two Layer Railway Track Ballast Under Cyclic and Monotonic Loading

by
Andrew J. Key

A thesis submitted to the University of Sheffield
in partial fulfilment for the degree of
Doctor of Philosophy

Supervisor: Professor W. F. Anderson

September 1998

Summary

New railway track is laid to a specified level and alignment. However, with time and trafficking movements occur in the ballast bed and the underlying subgrade, and frequent maintenance is necessary to re-establish the correct geometry. This is currently done by the process of tamping, where extra material is vibrated under the sleeper to raise its level. Unfortunately this is not permanent, and the sleeper eventually reverts to its pre-maintenance state. Prior to mechanised tamping, track was relevelled by hand shovel packing in which the sleepers were raised and fine aggregate shovelled into the space under the sleeper, giving a permanent lift. A prototype of a mechanised version of this process, called the Stoneblower, has been developed and is currently undergoing field trials. It lifts the sleeper and blows single size stone smaller than the ballast into the void space, creating a two layer granular foundation for each sleeper.

In order to get a better understanding of the behaviour of a two layer granular foundation when subjected to repeated loading a laboratory study involving large scale cyclic triaxial testing of single size and two layer ballast has been carried out. This has been complemented by a large scale model study using a 'half sleeper rig' in which ballast beds similar to those produced by stoneblowing have been subjected to repeated loading simulating long term railway trafficking. These tests have been used to carry out a parametric study into stone angularity, stone size and layer geometry to assess their influence on the layered system, with the results being assessed primarily in terms of the resilient modulus and plastic deformation undergone by the material.

In the triaxial tests it was found that the layer of smaller material was the major controlling factor for the deformation. However, the layer of larger material tended to act as a restraint, effectively reducing the H/D ratio of the specimen. In the model testing, it was found that the smaller material dictated how the load was transmitted to the ballast bed, and this was then responsible for the majority of the settlement.

Acknowledgements

Many people have contributed to the work described here, and the author would like to take the opportunity to thank them.

The research was sponsored by the E.P.S.R.C. and help was provided both financially and practically by the Advanced Railway Research Centre at the University of Sheffield. Dr. Felix Schmid played a large part in this. Thanks must also go to Scientifics of Derby for allowing the author to use their equipment, and particularly Dr. Phil Sharpe for much practical advice and encouragement. In addition, the author is grateful to ARC Central and ECC Aggregates for supplying the testing material free of charge.

My supervisor, Prof. Bill Anderson must be thanked for asking me to do the research in the first place, and despite the pressures on his time for the constant supply of good ideas and guidance.

On the technical side, large amounts of effort have been expended by the technical staff at Sheffield to help set up the equipment and keep it running, particularly Tim Robinson, Paul Osborne and Mark Foster. Their efforts are much appreciated.

Finally I have to thank my parents and friends for their support, particularly Tracey for knowing how difficult a PhD is, and Rob, Kathryn and Rowan, without whom this thesis would still be a collection of computer files.

Andy Key, September 29th 1998

"If we knew what we were doing it wouldn't be called research, would it?"

- Albert Einstein

Contents

Chapter 4 - Transducer Calibration And Data Corrections

Chapter 5 - Materials And Triaxial Test Procedures

List of Tables

Chapter 4

Chapter 5

Chapter 6

Chapter 7

List of Figures

Chapter 2

Chapter 3

Chapter 4

Chapter 6

Chapter 7

Chapter 8

List of Plates

Chapter 3

Chapter 4

Chapter 5

Chapter 6

Chapter 7

List of Symbols

Chapter 2 - Literature Review

a_c	=	Corrected area of specimen
b	=	Constant
c_1	=	Constant
c_2	=	Constant
c_3	=	Constant
c_4	=	Constant
c_5	=	Constant
D	=	Specimen diameter
D_w	=	Diameter of vehicle wheels
D_0	=	Original diameter of membrane
d_{ekv}	=	Average grain size
d_0	=	Initial specimen diameter
d_{10}	=	Grading passed by 10% by mass of material
d_{50}	=	Grading passed by 50% by mass of material
d_{90}	=	Grading passed by 90% by mass of material
d_{max}	=	Maximum particle size
E	=	Young's modulus
E_m	=	Young's modulus of rubber membrane
E_r	=	Resilient modulus
F	=	Normal force at particle contact
G	=	Shear modulus
g	=	Acceleration due to the force of gravity
H	=	Height of specimen
H_s	=	Horizontal force required to initiate lateral displacement
K	=	Bulk Modulus
K_0	=	Coefficient of lateral earth pressure
K_1	=	Constant

K_2	=	Constant
K_3	=	Material constant
K_4	=	Constant
K_5	=	Constant
K_a	=	Constant
K_b	=	Constant
k_1	=	Material constant
k_2	=	Material constant
k_4	=	Constant
M	=	Membrane elastic modulus at 10% extension
N	=	Number of load cycles
n	=	Initial porosity of sample
P	=	Axle load
P_{di}	=	Static equivalent of dynamic wheel load
P_{st}	=	Static wheel load of vehicle
p'	=	Effective stress
p_m	=	Effective mean normal stress
p_r	=	Effective resilient normal stress
p_1	=	Effective minimum cyclic normal stress
p_2	=	Effective maximum cyclic normal stress
Q	=	Vertical load at wheel/rail contact point
q	=	Shear stress in compression
q_c	=	Cyclic deviator stress
q_m	=	Mean stress
q_r	=	Resilient stress
q_1	=	Effective minimum cyclic deviator stress
q_2	=	Effective maximum cyclic deviator stress
T_m	=	Mean stress
T_r	=	Resilient stress
t_0	=	Initial thickness of membrane
V	=	Velocity of vehicle
v	=	Poisson's ratio
W_r	=	Resilient strain
Y	=	Lateral force at wheel/rail contact point

α	=	Vertical acceleration required to initiate slip
ε	=	Axial strain
ε_{Ma}	=	Axial strain in specimen
ε_N	=	Permanent strain after N load cycles
ε_r	=	Recoverable strain on unloading section of cycle
ε_{sr}	=	Resilient shear strain
ε_v	=	Volumetric strain in specimen
ε_{vr}	=	Resilient volumetric strain
ε_1	=	Axial Strain
ε_3	=	Radial Strain
ε_{1LC}	=	Permanent strain after first load cycle
ϕ'	=	Angle of friction
γ	=	Constant
μ	=	Coefficient of friction
θ'	=	Bulk effective stress in loaded state
σ_a	=	Axial stress
σ_{am}	=	Corrected axial stress
σ_{rm}	=	Radial stress
σ'_{rm}	=	Corrected radial stress
σ_1	=	Axial stress on triaxial sample
σ_1'	=	Effective axial stress
σ_{0m}	=	Initial confining stress
σ_{1m}	=	Correction to measured compressive stress
σ_{3m}	=	Correction to minor principal stress
σ_3	=	Radial stress on triaxial sample
σ_3'	=	Effective radial stress

Chapter 6 - Results and Discussion

a	=	Magnitude of principal stress ratio at σ_3 = 1kPa
b	=	Empirical index related to degree of particle degradation
N	=	Number of load cycles
p'_c	=	Critical average stress for starting void ratio of material

p'_p	=	Average stress at peak deviator stress
q'_p	=	Peak deviator stress
R_p	=	Maximum principal stress ratio
α	=	Soil constant
β	=	Soil constant
ε_N	=	Permanent strain after N load cycles
γ	=	Constant
κ	=	Constant
λ	=	Constant
σ_3	=	Radial stress on triaxial sample

Chapter 1 - Introduction

1.1 Background

With the government shift towards public transport in the mid-nineties, the railway system in the UK is coming under increased pressure. It is continually required to carry more passengers at higher speed with increased reliability, and to do so at minimal cost. These pressures and constraints filter through to every sector of the railway infrastructure, and create new demands on the equipment and structures that were previously required to work to lower standards.

One such sector of the system is the railway track itself. In order to increase passenger revenue, journey times between major cities are being cut. This requires higher standards of planning, so that time built into the journey to account for delays from infrastructure work can be minimised. It also demands an increase in train speeds to cut the physical journey time. These factors put higher demands on the track, particularly in terms of maintenance. The increase in train speed requires the track to be lined and levelled to a higher standard, to avoid vibration and acceleration that would disturb passengers and increase wear on the rail vehicles. In addition, it requires maintenance to be carried out more quickly and less often in order to keep disruption to the timetable to a minimum.

To address these problems, there is major ongoing replacement of worn and maintenance intensive track infrastructure, and major investment in new maintenance equipment. This equipment includes the Pneumatic Ballast Injector, or 'Stoneblower'. This machine has been jointly developed by Pandrol - Jackson of America and British Rail / Railtrack in the UK over the past eighteen years. It is designed to line and level the track in a way that will maintain a higher standard of geometry than the maintenance machinery in current use, and at least double the current period between maintenance occasions.

Discussions with individuals connected with the Stoneblower project revealed that they had been concentrating on the mechanical engineering aspect of the machinery, and knew less

about the geotechnical aspects of the operation. For this reason, it was decided to carry out research into the fundamental behaviour of the type of angular materials used in railway track, particularly in the form of layered systems, which result from this form of maintenance.

The research fell into two distinct parts, element testing and model testing. The element testing was carried out in the form of cyclic load triaxial tests, conducted at the University of Sheffield Department of Civil and Structural Engineering, to investigate the behaviour of the individual materials used and the interaction between them when placed in layers. The model testing was carried out at Scientifics Ltd. of Derby, previously part of British Rail Research, on their Half Sleeper Rig. This piece of equipment was designed to model an individual sleeper within the track, and has been used previously by British Rail Research for much of their research into the fundamental behaviour of track materials. Here, it is used to assess how the materials will behave as a system, rather than just as materials as in the triaxial cell.

The research carried out is described in this thesis, along with the conclusions and recommendations for further work.

1.2 Thesis Structure

A review of the literature is presented in Chapter 2. This initially covers the background to railway track and the reasons for maintenance, along with the current methods to give more context to the work carried out. The loads encountered in typical track and the behaviour of the track materials under those loads are also reviewed. This section also reviews work on the behaviour of cohesionless materials under cyclic loading from pavement engineering, as much of this, whilst being specific to the well graded materials used in roads, is relevant to this application. Finally the methods of testing the materials are discussed.

Chapter 3 describes the development of the testing apparatus at Sheffield University. The calibrations and corrections applied to this testing are summarised in Chapter 4.

Chapter 5 provides details of the materials used in the testing programme, the testing procedure for the work carried out at the University of Sheffield, and the testing programme itself.

The results of the work carried out at the University of Sheffield, and the initial discussion of these results are presented in Chapter 6. Basic trends and anomalies are highlighted in terms of the different types of testing carried out, and the different test series presented in Chapter 5.

The model testing carried out is discussed in Chapter 7. The equipment used, procedures followed, and results obtained from this work are all presented here. This chapter also discusses the results obtained from the model testing, and some of the implications for use in full-scale track.

Finally, the results from both model testing and element testing are brought together and covered in more detail in Chapter 8. Further practical implications of the work are highlighted here, along with the conclusions and suggestions for beneficial and informative research in the future.

Chapter 2 - Literature Review

2.1 Introduction

Within the sphere of geotechnical materials, railway ballast is a fairly unique material. The combination of uniform grading and large particle size with an absence of fine material lead it to have somewhat different properties to other soils - in some cases, the small number of particles involved result in it behaving more as a discrete particle structure than a continuum. However, significant amounts of research have been carried out into the behaviour of this material, and these are presented in this chapter. Firstly though, background information on the nature of railway track and the loading placed upon it is described to give some context to the work on the ballast material.

2.2 Railway Track Components

The track can be split into four main components, the rail, the sleeper, the ballast bed / sub-ballast and the subgrade. Fig. 2.1 shows a typical cross section of track structure.

2.2.1 The Rail

The rails are steel members running longitudinally along the length of the track. Their job is to support the wheels of the train and to transfer the load to the sleepers spaced along their length with minimal distortion. The rails also control the direction of the vehicle, with the combination of the rail and wheel profiles enabling vehicles with solid axles to be guided around curves. The other job of the rails is to serve as a conductor for the signalling system, the vehicle completing the circuit between the rails to indicate its position.

The rail is built up from sections which were traditionally bolted together with drilled plates known as 'fishplates'. However, the discontinuity resulting from this caused vibration and extra dynamic loads at the joint, lowering passenger comfort and causing accelerated failure of the track around the joint. Hence nowadays, most of the important passenger and heavily used freight lines have been converted to continuously welded rail (CWR), where the sections are laid and then joined with molten metal.

2.2.2 The Sleeper

It is the job of the sleeper to receive the concentrated load from the rails and distribute it over the ballast at an acceptable bearing pressure. The sleeper is also the basis of the rail fastening system, holding the rails in the correct longitudinal position and at the correct distance apart (the gauge). Ballast is placed under and around the sleeper to help it resist the lateral and longitudinal forces exerted by the rail, hence anchoring it in position.

Sleepers can either be made of wood, or in recent times, of prestressed concrete. Concrete sleepers are potentially more durable than wood, stronger, heavier and more rigid, producing an overall stiffer track, which also has fuel consumption benefits. However, one school of thought says that wooden sleepers are more resilient and tend not to be abraded by the ballast in the way that concrete sleepers are.

2.2.3 The Ballast

This can be further divided into the main ballast, which is beneath the sleepers, the crib ballast which is between the sleepers, and the shoulder ballast, which is at either end of the sleepers.

The major job of the ballast is to distribute the relatively high bearing pressures under the sleeper over a wide area, until they are of an acceptable level for the material underneath (the subgrade). However, the ballast also has several other functions in the track; most importantly the interlocking ballast particles are able to resist the lateral and longitudinal forces on the sleepers to keep them in position. Also the ballast provides some of the resiliency and energy absorption of the track, facilitates the adjustment of line and level via the ability to rearrange the particles e.g. during tamping, permits adequate drainage of the track, protects the subgrade against frost and prevents growth of vegetation on the track (Bryer, 1989).

In the UK ballast consists of crushed rock, as the interlocking effect of the angular particles offers the highest degree of stability under the loads from passing vehicles. It is normally some form of igneous rock, as this is the only rock to offer sufficient strength and resistance to attrition to make a suitable ballast. The size chosen is generally the result of some form of compromise. A uniform grading is chosen as this offers the best drainage characteristics despite the fact that a well graded ballast would offer better strength - deformation

characteristics (Bryer, 1989). Nominal 35mm (50-28mm) particle size is chosen, as it is felt that this strikes the best balance in terms of strength and grading. If the particle size is too big, large forces ensue at contact points resulting in attrition and penetration of the ballast into the subgrade. If the particle size is too small, the loss of inertia reduces the resistance to movement and increases attrition, and the loss of voids can result in premature fouling.

In other countries, notably the USA, an ideal ballast is not always found locally and hence whatever materials are available in the vicinity are used, for example gravel, ash or limestone. Whilst this will lower the performance of the track, the economics of hauling high quality ballast to remote areas make it worthwhile.

2.2.4 The Sub-Ballast

This layer between the ballast and subgrade normally consists of some form of granular material of a broad grading, either crushed rock or sand/gravel mixtures. The sub-ballast has a number of functions. Firstly, it helps to further reduce the stress level on the subgrade. Secondly, it should be designed to help the drainage, both shedding water from the ballast above and draining any water that may be present at the top of the subgrade to avoid subgrade softening under load. Thirdly, it performs a separation function, preventing the ballast particles from penetrating into the subgrade (and possibly generating slurry in the process) and also stopping upward migration of the subgrade particles into the ballast. In order to fulfill this last function, the grading of the subgrade should be chosen to fit filtration rules, such as those given by Cedergren (1989).

Occasionally it may be found that track has no sub-ballast, or that it is comprised of fouled and unremoved ballast. Additionally, one or all of the above functions may be carried out by substituting the sub-ballast with a geotextile or a combination of geotextile and granular material.

2.2.5 The Subgrade

This is effectively the ground on which the track is placed, and may be naturally occurring soil or specially placed fill, e.g. on embankments. It is the main supporting medium for the track and provides the bulk of the resiliency.

In the majority of cases, the subgrade has been trafficked for many years, and so has reached a point of stable behaviour. Unless it has been weakened by poor drainage, it normally has a very low maintenance requirement.

2.3 The Maintenance Cycle

From the time it is first laid to the time it is replaced, the track goes through what is known as the Maintenance Cycle. When first laid, the track is perfectly straight and level apart from the gradual changes built in to follow the topography of the landscape. With the passage of railway traffic, however, geometrical imperfections start to appear both in longitudinal and lateral alignment due to differential settlements in the ballast layer. These gradually increase with further traffic, causing greater dynamic loads on the system and worsened ride quality for vehicles up to the point where the track has to be realigned. The magnitude of the imperfections is quantified as the Track Quality Index by measuring the standard deviation of the top of the rail profile relative to a smoothed track profile, obtained by filtering out all the short wavelengths (below about 20 m). When the standard deviation reaches a certain figure, the precise value of which depends on the nature of the traffic on the line (Waters, 1989), the track requires maintenance.

The generally accepted hypothesis, assuming there are no external influences such as subgrade failure, is that there is a rapid initial deterioration in geometry due to compaction and settlement of the newly laid ballast bed, and then track geometry deteriorates more slowly (Waters, 1989). This is shown in Fig.2.2. In this slower period, the ballast particles are moving slightly and degrading due to abrasion as the particles move relative to each other when loaded (Hay, 1981). Also, being angular material, the contact points tend to be very sharp and can break under the high contact forces, enlarging the contact area until equilibrium is reached. This all results in uneven volumetric change, and hence differential settlement.

Maintenance consists of resetting the line and level of the track. This is traditionally done using a Tamping Machine. Fig. 2.3 shows a schematic diagram of the tamping operation. The self propelled computer controlled vehicle lifts each sleeper in turn, moving it to the correct line and level, and then inserts metal spikes into the ballast bed either side of the sleeper. The spikes are vibrated and forced together, moving ballast from either side of the sleeper into the area beneath it and raising the ballast to the correct level. The machine then

moves on to the next sleeper. Extra stone is placed onto the cribs to replace that moved underneath the sleeper during tamping.

After the track maintenance has been carried out, the track does not then remain at its correct geometry but continues to deteriorate, again rapidly at first and then more slowly later. Not only this, but if the geometry is measured again it can be seen that the track tends to revert to the same shape it had before the maintenance was carried out. This is called the inherent track shape. This phenomenon is generally attributed to the fact that over short lengths the rail is very stiff, and so tends to force its shape onto the ballast bed (Waters, 1989). Over long distances, the ballast bed is much stiffer than the rail so tends to imprint its shape on the rail. The only way to stop this is to straighten the rail and flatten the ballast bed. In theory, tamping should flatten the ballast bed, but in reality all it does is dilate the ballast below the sleeper giving an apparent increase in volume (Selig and Waters 1994). As soon as rail traffic starts to run over the section again, this ballast becomes compacted and settles back to its original position. It is possible to get some permanent improvement in the ballast bed by tamping, but this involves high lifts. In this case, the ballast level is raised so much that extra ballast is actually pushed under the sleeper during the tamping process to achieve permanent lift. However, this method is unacceptable for routine maintenance because the lift required for this to work (>25mm - Waters, 1989) would result in increased levels over a period in time.

This continuous process of geometry loss followed by maintenance does not go on ad-infinitum. After each cycle, the decay in geometry occurs slightly faster than in the cycle before. Fig. 2.4 shows this phenomenon.

This behaviour is due to the progressive degradation of the ballast. Each tamping operation re-arranges the ballast particles in the bed, exposing new contact points to be broken and abraded with the net result that the previously angular particles eventually become more smooth and rounded. Interlocking stability will therefore be reduced. This problem is exacerbated by the loss of compaction and associated horizontal confining forces during the maintenance process, resulting in greater interparticle movement and abrasion (Selig and Waters, 1994). To compound the problem, the high forces involved in the tamping process itself can cause the ballast particles to break. In British Rail tests, between 2 and 4 kg of material less that 14mm in size were generated per tamp (maintenance operation on one

sleeper) (Wright, 1983). The fine material generated by ballast breakdown combines with material blown onto the track by wind, and material spilt from vehicles, to block the void spaces in the ballast. As the ballast becomes progressively more fouled it starts to lose its free drainage properties, and more water is retained. The water combines with the fine particles present to form a highly lubricating slurry causing further settlement (Selig and Waters, 1994). If the correct specification sub-ballast layers are not present the water may even cause failure of the subgrade at the ballast / subgrade interface, resulting in the generation of further slurry. Passing vehicles will then cause high pore pressures in the saturated area of the ballast and the slurry will be forced up into the track.

Eventually the level of maintenance required to maintain the track geometry increases to the point at which it ceases to be economically viable and the ballast must either be cleaned, where the fouling material is predominantly greater than silt sized, or replaced where the fouling material is smaller than silt size and can not be removed by cleaning.

2.4 Addressing the Problems of the Maintenance Cycle

The response of railway engineers to the problems of track maintenance has been to develop a new generation of techniques to reduce the frequency and level of work required to maintain the ballast bed. Some of these are listed below.

2.4.1 Railway Geotextiles

Geotextiles have been introduced to the railway environment increasingly in recent years. They have been put to two main uses:

1. Geotextiles have been used in an attempt to replace some or all of the functions of the sub-ballast including drainage, ballast/subgrade separation, prevention of slurry generation and prevention of slurry migration. This has been done with limited success as no geotextile has yet been produced with the required combination of properties to fulfil all these roles. The most successful use of geotextile as a subgrade replacement has been where the subgrade requirement is difficult or expensive to fulfil with the available materials and geotextiles have been used in combination with a granular material (Evans, 1993).
2. Geotextiles (usually geogrids) have been used as reinforcement within the trackbed. Research (Bathurst and Raymond, 1987, Raymond, 1992) has shown that geogrids can act as reinforcement when placed within a layer of granular material. In the railway

environment, this usually has to be placed at the base of the ballast bed to avoid being disturbed, e.g. by tamping, during the maintenance cycle. This method of reinforcement is believed to work by resisting tensile deformations in the granular material leading to increased stiffness of the granular layer and hence lower deformation. This results in the greatest improvements being shown with granular layers over particularly soft subgrades.

Other methods of strengthening granular materials with geotextiles do exist. One of these is strengthening with small pieces of polymeric mesh (mesh elements) randomly mixed with the material. (Mercer et al., 1984, Andrawes et al., 1986) The mesh elements interlock with the material at two levels. Firstly, the ribs of the individual mesh elements interlock with groups of particles to form aggregations which have tensile resistance. On a second level, these aggregations are locked together by adjacent mesh elements to form a coherent matrix (See Fig. 2.5) This gives an apparent cohesion to the material, which as Klugar (1975) showed for the case of ballast would give the track bed increased capacity or a reduction in the maintenance requirement. Mesh elements have been successfully used with sand sized particles and it is thought that it may be possible to reproduce this effect with larger grained materials such as ballast. As this strengthening system does not rely on surface friction it should be more suitable for railway ballast, with its low number of high stress contact points, than other systems such as fibre reinforcement, yet it should still allow adjustment and re-arrangement of the material to facilitate maintenance unlike the other main cohesion development system, Hot Mix Asphalt, which binds the ballast particles together permanently using a form of bitumen.

2.4.2 The Dynamic Track Stabiliser

This machine was developed to apply vertical load and horizontal vibration to the newly maintained track. This results in accelerated compaction of newly laid / maintained track, i.e. acceleration through the first section of the maintenance cycle, to show up any major geometric faults and help restore the lateral stability of the track. Disturbing the ballast bed reduces its ability to resist lateral forces on the sleeper and this could result in the track buckling due to longitudinal stresses in the continuously welded rail, particularly in hot weather as the rail tries to expand. The traditional way to overcome this was to restrict the speed of traffic over the track to avoid any undue lateral forces which could cause buckling, until the passing traffic had consolidated the ballast sufficiently to restore the lateral

stability. The Dynamic Track Stabiliser overcomes the need for this, with the consequent reduction in disruption to the timetable.

2.4.3 The Stoneblower

The other major innovation has been the Stoneblower. This machine uses the principle of 'measured shovel packing' to correct the track geometry. Before the introduction of mechanised maintenance, a team of labourers would lift the track and add a carefully controlled quantity of small stones under the sleeper to raise its level. Raising the sleeper by this method avoids damaging the ballast and disturbing the ballast bed, and thus theoretically the geometry of the track should only decay slowly after maintenance and it should require attention less frequently. This manual process was too time and labour intensive for use on an everyday basis, but the Stoneblower has automated it to the point where it only requires a similar number of man hours to maintenance by mechanical tamping. Fig. 2.6 shows a schematic diagram of the stoneblowing operation. The machine lifts each sleeper in turn and inserts a tube beside it. Compressed air then blows the correct quantity of stone under the sleeper, which is then lowered back into position. The machine then moves on to the next sleeper.

Early reports of the machine's performance suggest that it is able to clear up wet spots, and gives an improvement in time between maintenance periods of 500% on average (McMichael, 1997). However, the graph of improvement over tamping indicates a large degree of scatter, which cannot yet be explained. The behaviour of the treated track, with the layer of small stone overlying the original ballast, is also unknown. Its suitability for use in maintenance has been questioned by some engineers because it adds small stone to the trackbed, and this has conventionally been regarded as a bad practice as it could contribute to the fouling of the ballast.

2.4.3(a) Two Layer Systems

As can be seen from the above section, use of the Stoneblower to maintain track results in a two layer system, a layer of small stone overlying the main ballast bed. A certain amount of work has been done on two layer systems, mainly in respect of pavement engineering. This generally covers the interaction between a granular layer and either a bound layer (pavement surfacing) or subgrade material (fine grained, cohesive soil). Very little work, however, appears to have been done on the interaction of two cohesionless media. An exception to

this is a paper by Drnovsek (1970) considering an analytical method for determination of the direction and stress in a rupture line on one side of the contact between two different non-cohesive media. It is not, however, expected that ballast will fail in this manner as it is operating at well below its bearing capacity in the railway environment, and failure in the railway context is merely a question of servicability rather than any form of ultimate limit state.

The one other speciality to consider systems such as this is coastal engineering, in terms of coastal defences formed from large layers of rock particles, with smaller particles underneath forming a filter layer to prevent erosion of the subsoil. Examination of literature on this subject showed that the only failure mechanism considered for the system was the loss of particles in a normal direction to the layer, due to wave uplift and excessive pore pressure. However, the literature did briefly mention the stability of a sloping system under gravity, saying it should be considered as a Coulomb style wedge, with the two layers sliding over each other. In this case, the angle of shearing resistance, presumably of the top layer material but this is not specified, should be reduced by 30% to allow for the interaction of the layers (CIRIA, 1991).

2.5 Track Forces

To undertake any experimental work on railway ballast, it is necessary to have some idea of the forces which will be encountered in the field. These forces can be highly variable - dependant on the type of vehicle, its loading, its speed, the geometry in the track and any track or vehicle defects. For this reason, any analysis of forces can be at best general.
Esvled (1989) divided the track forces into the following broad categories:

- Quasi Static Loads

  Due to the weight of the vehicle and reaction forces from cornering.

- Dynamic loads

  Resulting from track irregularities due to differential settlements in the ballast bed, discontinuities and welds or joints, and corrugations, plus vehicles defects such as wheel flats and hunting phenomenon

In addition, the effects of temperature on CWR can result in considerable compressive forces leading to instability of the track and buckling.

2.5.1 Vertical Forces

The maximum permitted axle load on lines in the UK is currently 25 tonnes (250kN). The way this is transmitted to the ballast depends on the spacing of the sleepers and the stiffness of the rail. The greater the stiffness of the rail, the more it spreads the load between the sleepers in the locality of the axle. Increasing the spacing of the sleepers (analogous to supports for a beam) effectively reduces the stiffness of the rail. As a rule of thumb, the load is distributed approximately in the ratio of 50% to the sleeper directly below the axle and 25% each to the sleepers on either side (Hunt, 1996). The beam action of the rail also causes an uplift force on the sleepers either side of the loaded sleepers (see Fig. 2.7) which is resisted by the weight of the track and frictional forces between the sleeper and crib ballast. In poorer quality track where there is insufficient resistance this can result in a gap forming between the sleeper and ballast. As the sleeper becomes loaded it will fall back onto the ballast imparting an impact force and thus resulting in further damage to the ballast (Chiang, 1989)

Experiments carried out by Shenton (1974) using pressure cells mounted on the base of the sleeper and buried in the ballast have shown that for a 100kN loading on a sleeper, the maximum pressure on the ballast below is somewhere between 200 and 300 kPa, the exact value depending on the state and arrangement of the ballast below the sleeper. This is confirmed by figures quoted by Esveld (1989) and Raymond and Bathurst (1994). Due to the inherent flexibility of the sleeper most of the load is carried by the ballast under the area of the rail seat, hence this is where the maximum ballast pressures are to be found, with the ends and middle of the sleeper carrying much less of the load.

These triaxial compression conditions under the sleeper will be complemented by triaxial extension conditions on certain sections of the unloaded crib ballast on either side of the sleeper as shown in Fig. 2.8 (Tarumi, 1994).

In addition to these quasi static loads there is a possible dynamic increment of load due to the velocity of the load application. Measurements carried out by Frederick and Round (1985) and Harrison et al. (1986) have shown that the dynamic forces can increase the wheel load by 100% or more. Li and Selig (1998) report the following equation for calculation of equivalent wheel loads:

$$P_{di} = \left(1 + \frac{0.0052V}{D_W}\right) P_{si} \qquad 2.5.1$$

Where P_{di} is the static equivalent of the dynamic wheel load

P_{si} is the static wheel load of the vehicle

D_W is the diameter of the wheels of the vehicle (m)

V is the velocity of the vehicle (km/h)

It is not stated, but the dimensional inconsistency of this equation would suggest it to be empirically derived.

Most of the higher loads were observed to have come from passenger vehicles even though their static wheel load was relatively low. The high dynamic loadings were a result of high speeds and defects in the vehicles such as wheel flats or in the track, such as dipped welds. In the UK steps are being taken to identify and correct such faults. These dynamic faults will give rise to more rapid degradation of the ballast below the track, resulting in deterioration in the track geometry and hence further degradation. The high level of maintenance required to correct this will also degrade the ballast, therefore it is better to lay inherently good track and correct faults as soon as they appear.

2.5.2 Lateral Forces

Lateral loading is far more complex than vertical loading and less well understood (Hunt, 1996).

In the unloaded state, there can be lateral forces due to thermal stresses in continuously welded rail. As the rail heats up beyond the temperature at which it was laid, longitudinal compressive forces build up due to thermal expansion. This can lead to buckling of the track if there is insufficient lateral resistance. Most of the lateral resistance in this case comes from the passive resistance of the ballast shoulders, with frictional components from the base and sides of the sleeper being relatively minor.

In the loaded state, lateral forces come from a number of sources (Hunt, 1996). On straight track there are lateral components from the centering force on the conical wheelsets and associated hunting forces from instability of the bogie units. Lateral forces are usually

expressed in terms of Y/Q (see Fig. 2.9). Straight track typically gives maximum individual Y/Q forces of 0.4. These lateral forces tend to cancel each other out and total forces on the track are not high (see Fig. 2.10)

On curved track in addition to the forces mentioned above, there are components due to the reaction force of the vehicles cornering and possible wheel flange contact against the rail (Hunt, 1996). These have a magnitude in the region of Y/Q = 0.6 and act against the outer rail. In extreme cases of very tight curves or vehicles with wheel/suspension defects Y/Q > 0.6. Y/Q > 1 often leads to derailment. In these cases, one rail now has a greater lateral force component that the other, so there is a resultant force acting on the track. The exact force, however, depends on the geometry of the track and the speed. A high speed track having a high cant to minimise lateral forces can give large forces on the low rail if traversed by a low speed freight train (see Fig. 2.11).

A empirical value for the required lateral resistance of a loaded track in order to ensure stability was determined in the 1950's by the SNCF (the French national railway company) and is known as the Prud'homme formula.

$$H_s > 10 + \frac{P}{3} \qquad 2.5.2$$

where:

H_s = Horizontal Force (kN) required to initiate lateral displacement

P = Axle Load (kN)

DiPilato et al. (1983) derived that in the loaded state, the majority of the lateral resistance in the loaded state comes from the frictional resistance between the ballast bed and the bottom of the sleeper, although the crib and shoulder do make contributions.

2.6 Material Behaviour

In order to understand the behaviour of railway track, a knowledge of the behaviour of the ballast material supporting it is required. This section covers the published work on the behaviour of railway ballast, although it is known that other work has been carried out by companies such as British Rail and has never been published, and brings in relevant

information on large granular materials from other disciplines such as road pavement engineering.

2.6.1 Behaviour Under Monotonic Loading

Firstly, the behaviour of the ballast in common soil mechanics tests must be established to enable a comparison with other geotechnical materials.

Given the granular nature of the ballast, it would be expected to obey the rules of Critical State Soil Mechanics (CSSM) as proposed by Schofield and Wroth (1968). The premiss of this model is that when material is sheared under a given confining stress, the shear strength will eventually tend to a certain value. As the shear strength approaches this value, the packing of the particles in the material will also change so that the void ratio of the material always approaches a certain value, i.e. the material will either dilate or contract until it reaches the correct void ratio. Fig. 2.12 illustrates this behaviour. When the shear stress and void ratio of the material have reached these steady state values, the material is said to be at a Critical State. At this point, shearing is taking place at a constant volume and constant shear stress.

The void ratio and shear strength that the material reaches when at a critical state is determined by the characteristics of the particles within the material, and the confining stress to which the material is exposed. As the confining stress increases, the particles of the soil tend to be forced together, so the void ratio at the critical state decreases as confining stress increases. Conveniently, if this relationship is plotted on a graph of void ratio vs the logarithm of the confining stress it forms a straight line parallel and to the left of the normal consolidation line. The critical shear strength increases linearly with bulk effective stress, due to the fact that the ability to resist shear comes mainly from the friction between the particles, and that friction is determined by a linear equation of the form;

$$\tau = \mu F \qquad 2.6.1$$

Where F is the normal force at the interparticle contact, determined by the bulk effective stress to which the material is exposed.

μ is the coefficient of friction, determined by the particle surface characteristics

These relationships are illustrated in Fig. 2.13

It can be seen therefore, that if a soil is loosely packed (normally consolidated), and so lies between the normal consolidation and critical state lines on the plot of void ratio against confining stress, as the material is sheared it will contract until it lies on the critical state line, provided it is a drained test, thus expelling pore fluid. For this reason, these soils are known as being on the wet side of critical state.

If a soil is densely packed (heavily overconsolidated), and so lies to the left of the critical state line on the plot of void ratio against confining stress, the material will dilate as it is sheared until it reaches the critical state line, again providing the test is drained. Thus pore fluid will be taken in as the material is sheared, and so these materials are known as being on the dry side of critical state. However, the fact that the materials are dilating means that work is being done against the confining stresses on the material. In order to do this work in addition to overcoming the frictional element, additional shearing force is required. The magnitude of this additional shear force is determined by the rate of dilation of the material (Rowe, 1962, Schofield and Wroth, 1968, Atkinson and Bransby, 1978) and hence there will be a maximum value of shear resistance exhibited by the material at the point where the rate of dilation is the greatest (see Fig. 2.12 (b) and (c)). As the rate of dilation reduces, when the material nears its critical state, the shear resistance exhibited by the material will reduce to its critical state value.

As would be expected, the test generally used to characterise the stress-strain behaviour of a material such as this is the triaxial test. Such tests have been carried out by various authors, including Raymond and Davies (1978), Alva-Hurtado and Selig (1981) and Indraratna et al. (1998), and these tests have all been carried out in a saturated state, no doubt to ease measurement of volumetric strain during drained tests. No information has been found on how this will affect the results compared to testing the specimens in a dry state but the principle of effective stress would suggest that there should be no difference if no excess pore water pressure is set up.

The results of these tests show that railway ballast exhibits behaviour typical of a granular material. Fig. 2.14 shows a typical set of results from Alva-Hurtado and Selig (1981). As can be seen, an increase in the cell pressure results in an increase in maxiumum shear

resistance, as would be expected, and causes a greater tendency towards volumetric contraction. This is because the specimens are prepared with a constant void ratio, and at low cell pressures this makes them heavily overconsolidated with the result that they dilate strongly and exhibit a peak strength. As the cell pressure is increased, this initial void ratio approaches that of a normally consolidated specimen at that cell pressure (see Fig. 2.13 (b)) with a resulting decrease in the dilatant tendency, and eventually specimen contraction as the void ratio passes that of the critical state line.

Indraratna et al. (1998) encountered similar behaviour, although they explained the different aspects of the ballast behaviour in a rather odd and non unified way. Analysis of the basic data showed it fitted the critical state pattern well, with a decrease in confining pressure resulting in an increase in maximum principal stress ratio (σ_1'/σ_3'), with very low confining stresses giving values as high as 120. This is due to specimens with a fixed initial void ratio being increasingly overconsolidated as lower cell pressures are used. This will result in increased dilation at lower cell pressures, and a higher principal stress ratio. Hence this gives an increase in the 'angle of shearing resistance' as confining pressure drops and produces a markedly curved Mohr-Coulomb failure envelope, which would lead the observer to believe that an apparent cohesion was being observed if only the failure points at higher values of confining stress were plotted. This 'cohesion' effect is one of the main arguments for using angular materials with highly dilatant tendencies, such as railway ballast, as it will give lateral support to the track even with very little confinement (for example, at the shoulder). One point to note with the results of Indraratna et al. is that their specimens were contained by a rubber membrane 4mm thick, yet they claim that even at very low confinement pressures, the membrane correction was minimal.

Indraratna et al. (1998) also showed that a grading with a larger percentage of smaller material resulted in a greater tendency towards dilation, believed to be due to the denser packing from the smaller particles.

2.6.2 Behaviour Under Cyclic Loading

To accurately assess the behaviour of the materials in track, it is necessary to simulate the loading they would experience, i.e. many load applications from passing vehicles. This is technically known as repeated loading, as opposed to the usual monotonic loading, and is

characterised by reversals in the direction of stress increase. However, it is commonly known as cyclic loading, and will be referred to as such.

The idealised behaviour of granular materials under cyclic loading is shown in Fig. 2.15. It consists of both recoverable (elastic) and permanent (plastic) strains. Initially the plastic strains form the majority of the specimen deformation, but their magnitude decreases with increasing number of cycles until they are of much smaller magnitude than the elastic strains, and the behaviour of the material is essentially elastic. It should be noted, however, that plastic straining is still occurring in each cycle, and in systems such as railways subjected to very large numbers of load cycles further significant plastic strains can accumulate over time.

If this observed soil behaviour is considered in terms of conceptual models, it should in theory follow the same rationale as it does during monotonic loading. The soil does not know at any time whether it is undergoing monotonic or cyclic loading and so the same laws should apply regardless. On this basis, the material under cyclic loading should follow the rules of CSSM, as outlined in the previous section. If the commonly used theory for soil deformation under critical state behaviour, the Cam Clay model (Schofield and Wroth, 1968), is used to describe the observed behaviour, however, certain shortcomings are visible. The theory states that the soil undergoes elastic deformation until the stresses reach a certain point, after which the soil deforms plastically. The line describing the stresses at which this occurs on a plot of q/p space is known as a yield surface. After the soil has deformed plastically, the yield surface expands to the maximum stress previously encountered, i.e. the soil work hardens, until further loads are encountered. If this is applied to cyclic loading, however, it would mean that the soil would deform plastically on the first cycle, and then elastically from then on, which is not the case. Not only this, but it does not predict the hysteresis observed in the loading and unloading cycle. To overcome this, several models have been proposed (Brown and O'Reilly, 1991) with either yield surfaces that translate rather than expand, expand and contract with stress history, or have multiple nested yield surfaces representing a model of the block and spring variety illustrated in Fig. 2.21. These all model to some extent the features of cyclic loading described above, but require significant computing power to use, as every cycle in the load sequence must be evaluated. In addition, there is as yet little consensus on the quantatative expression of the observed behaviour of the materials under cyclic loading, especially concerning plastic

deformation, and so the models will be by that nature limited. For this reason, the theoretical soil mechanics approach to this project will only be concerned with the broad critical state framework underpinning the expected soil behaviour rather than particular theories. Therefore, only the observed behaviour of materials under cyclic loading will be covered in this section.

2.6.2(a) Plastic Deformations

So far, a consensus on the occurrence of plastic strain has yet to emerge, although there have been several equations proposed to describe the plastic behaviour of railway ballast under cyclic loading. All these equations must encompass the fact that the majority of the deformation occurs within the first few loading cycles as the particles within the material re-orient themselves into a system able to resist loadings to which they have not previously been exposed. Within the first few thousand load cycles, the material appears to stabilise, and from then on plastic deformation occurs at a very low level. If cumulative deformation is plotted against the number of load cycles the specimen has been exposed to, on a linear axis at whatever scale, this appears to show the majority of the deformation occurring at the start of the test and then a horizontal line thereafter. For this reason, most of the work is compared using the number of load cycles plotted on a logarithmic scale as this effectively compresses both the early and later deformations onto one plot.

The simplest formula for plastic deformation, which is commonly found in the literature (e.g. Shenton (1975), Alva-Hurtado and Selig (1981) and Ford (1995)) states that the permanent strain, ε_N, after N load cycles is given by:

$$\varepsilon_N = \varepsilon_{1LC}\left(1 + C^* \log(N)\right) \qquad 2.6.1$$

where:

$\varepsilon_{1\,LC}$ = permanent strain after the first load cycle

C = dimensionless constant controlling the rate of growth of deformation

If this equation is used, the plot of total settlement vs the logarithm of the number of load cycles should yield a straight line.

There have been several modifications proposed to this basic formula. Early testing work by the Office for Research and Experiments for the European Union of Railways (ORE, 1970) on laboratory and field studies suggested that;

$$\varepsilon_N = 0.082(100n - 38.2)(\sigma_1 - \sigma_3)^2(1 + 0.2\log N) \qquad 2.6.1(b)$$

Where:

n = initial porosity of the sample.

σ_1 = axial stress on the traixial specimen (in kPa)

σ_3 = radial stress on the triaxial specimen (in kPa)

The porosity of the sample and the loads placed upon it were found to be the key factors.

Alva-Hurtado (1980), on the other hand, proposed a slightly different modification to the basic equation based on cyclic load triaxial tests of 30mm granite ballast;

$$\varepsilon_N = (0.85 + 0.38\log N)\varepsilon_{1LC} + (0.05 - 0.09\log N)\varepsilon_{1LC}^2 \qquad 2.6.1(c)$$

Alva-Hurtado also tried to predict cyclic settlement from monotonic triaxial compression test results. However, this is not a particularly suprising relationship as a monotonic triaxial test is effectively the first cycle of a cyclic load test without any of the following cycles, and thus this approach could be used with a number of the predictive formulae. He did, however, conclude from these experiments that the settlement is highly dependent upon the ratio of applied deviator stress to maximum deviator stress at failure for the same cell pressure, i.e. how far up the stress-strain curve the cyclic load extends. Stewart (1986) extended this idea by normalising the behaviour of a 40mm granite ballast. By normalising applied deviator stress to deviator stress at failure for a given cell pressure, and normalising strain with an estimated strain at failure at the given cell pressure, a single hyperbolic curve was obtained and used to predict settlements under various loadings. However, the procedure required refinement, in some cases being remarkably accurate whilst in other cases being highly inaccurate.

A similar conclusion was reached by Lentz and Baladi (1980) who carried out cyclic and monotonic loading tests on specimens of highway subgrade sand. They found that the cyclic performance could be predicted by normalising with respect to parameters from a monotonic test on an identical specimen. Normalising the strain at 10,000 cycles with respect to 95% of the peak static strength strain combined with normalising the cyclic principal stress difference (σ_1-σ_3) with respect to the peak static strength produced a single hyperbolic curve, thus facilitating a simple characterisation of the material.

Shenton (1985), after examining and averaging field data from many different sources, proposed that a better approximation of plastic settlement is obtained by considering settlement to be proportional to the fifth root of the number of load cycles. However, this tended to underestimate the settlement beyond 10^6 cycles so another factor needed to be applied, giving:

$$\varepsilon_N = k_1 N^{0.2} + k_2 N \qquad 2.6.2$$

where k_1 and k_2 are material constants.
In this case the first term predominates up to 10^6 cycles and the latter term predominates thereafter. Given the lack of consistency of the acquired data, and the large degree of scatter, this could at best be described as an approximation to the behaviour in any particular case.

Sato (1995) reports that studies by the Japanese railway companies have concluded that track settlement can be represented by an equation of the type:

$$\varepsilon_N = \gamma\left(1 - e^{-\alpha N}\right) + \beta N \qquad 2.6.3$$

Where: N = number of cycles or cumulative load tonnage carried by track

α = vertical acceleration required to initiate slip, and can be measured for spring loaded plates of the ballast material on a vibrating table (see Fig. 2.16)

$\beta \propto$ sleeper pressure × peak acceleration experienced by the ballast particles, and is affected by the type and condition of the ballast material, and the presence of water.

γ = constant dependant on the initial packing of the ballast material

No information was given on the values of the constants used in this equation, the units of the variables or the derivation of the formula, although it is thought to have been based on experimental work.

The first term in this equation expresses the initial rapid settlement of the track involving ballast compaction, and the second term expresses the lateral movement of the ballast under the sleepers. As can be seen, both Sato and Shenton presume the settlement to be essentially linear after an initial compaction period, due to lateral movement of the ballast, whereas the other equations predict a logarithmic settlement pattern.

None of these formulae, apart from the ORE proposal, completely predict what the settlement of the track will be, they merely describe the observed settlements. The fifth root equation (equation 2.6.2), for example, has two coefficients to take account of all the factors affecting the settlement (degree of compaction and stress level being the most important, e.g. Knutson and Thompson, 1978) and these must be established for each case. Even the ORE formula is compromised by the lack of knowledge regarding actual forces on the ballast, particularly lateral forces. Sato's formula (equation 2.6.3) comes the closest of the others to being able to predict settlements that will occur as they have deduced many of the factors that influence the coefficients in the equation, but even in this case the track environment is too complex to model precisely. Equation 2.6.1 uses the first loading cycle to assess how all these factors affect the deformation, and bases further settlement predictions on this. It ties in well with results from several authors suggesting that settlement is governed by the magnitude of elastic strain. For example, Tam (1986) conducting experiments on dry sand, has shown that plastic volumetric strain increases in proportion to the elastic cyclic strain. Others, such as Raymond (1992), Raymond and Bathurst (1994) and Sharpe (1996) have reported that in ballast box tests, the use of a stiffer subgrade to reduce the elastic cyclic strain results in lower levels of settlement. Thus equation 2.6.1 observes how all the external factors affect the strains in the material, which will govern further settlement.

Analysis of data shows that the occurrence of plastic deformation with increasing principal stress under cyclic loading is highly non-linear, as it is under monotonic loading. Bathurst and Raymond (1994) indicated that plastic deformation after a given cumulative load (rather than number of cycles) was proportional to the peak cyclic load up to a certain breakpoint,

after which the deformation increased greatly. For this reason, it is the largest load encountered which will control the settlements in the ballast e.g. in the railway environment occasional large dynamic loads caused by wheelflats. Shenton (1975), Klugar (1975), Stewart (1986) and Diyaljee (1987) have all shown this experimentally with multi-stage cyclic loading experiments. In these, the cyclic loading was divided into several blocks, each block having a different load level. It was found that the smaller loads caused virtually no further settlement compared with the larger ones. If desired, it is possible to equate the amount of settlement produced by one load to an equivalent number of cycles produced by another load in a procedure described by Stewart (1986) and Ford (1995) similar to Miner's rule for cumulative stress damage used in other disciplines.

A point to note is that this means that variable N in equation 2.6.3 cannot represent the cumulative tonnage of load carried by the track as was stated by Sato (1995), because the settlement will depend on how the load is applied i.e. either a few cycles of high load, or many cycles of low load.

Tam (1986) discovered during cyclic load tests on dry sand that plastic volumetric strain with varying loads behaved in a similar non linear fashion to settlement. As the ratio of average deviator stress to confining stress increased, the plastic strain increased rapidly and the magnitude of the plastic volumetric strain (contraction) decreased rapidly. As failure was approached, there was a certain threshold point beyond which the magnitude of the volumetric strain increased again, but in dilation. The threshold point for dilation under cyclic loading may be found as in the illustration Fig. 2.17. If this is plotted on a diagram of Mohr's circles, stress paths with an average below this line will cause contraction, and ones with an average above the line will cause dilation. As ballast is always operating well below its failure stress in the railway environment, it will always undergo volumetric contraction.

2.6.2(b) Elastic Deformation

As stated in section 2.6 the rate of increase of plastic strain in granular materials decreases with increasing numbers of load cycles, until the behaviour of the material becomes essentially elastic. This elastic behaviour under cycling is understood to a much greater degree than the plastic behaviour.

The most important elastic characteristic is the resilient modulus, E_r, which is defined as:

$$E_r = \frac{q_c}{\varepsilon_r} \qquad 2.6.4$$

Where:

q_c = cyclic deviator stress

ε_r = recoverable strain on the unloading section of the cycle

This is shown graphically in Fig. 2.18.

Experiments by Hicks and Monismith (1971) and Kalcheff and Hicks (1973) on a well-graded crushed limestone of 40mm maximum size have shown that there is some scatter in the value of resilient modulus at the start of a test, but after approximately 100 cycles the value drops slightly and then stabilises. Brown (1974) found similar behaviour using a well-graded crushed granite of 5mm maximum size, but the value did not stabilise until approximately ten thousand cycles into the test, although this was conducted on partially saturated material with indeterminate pore pressures and so cannot be strictly compared with work on dry material. However, these tests were on well-graded materials. Work on railway ballast by Shenton (1975) and Alva-Hurtado (1980) suggested that resilient modulus gradually increases with cycling. Brown and O'Reilly (1991) also state that density has little affect on the value of resilient modulus, whereas Selig and Waters (1994) report work that shows compacted specimens of railway ballast have a significantly higher resilient modulus than uncompacted ones. This would suggest that the single sized nature of railway ballast leads it to have different behaviour to well-graded granular materials.

It is commonly acknowledged that resilient modulus is highly dependant on the stress state of the specimen, particularly confining stress, and this has led to the following commonly used relationship, e.g. Hicks and Monismith (1971), Kalcheff and Hicks (1973), Brown (1974):

$$E_r = K_a(\theta')^{K_b} \qquad 2.6.5$$

Where:

θ' = bulk effective stress in the loaded state

K_a, K_b = soil constants determined from laboratory tests

However, this does not take account of the fact that the value of the resilient modulus also depends on the degree of unloading, as shown in Fig 2.19. The phenomenon is caused by an apparent change of stiffness on reversal of stress increase (see Fig. 2.20). Brown and O'Reilly (1991) discuss this subject on a particulate scale and liken it to a model consisting of a series of blocks linked by springs (see Fig. 2.21). The greater the movement in a direction, the more particle slippage occurs, and so there is an exponential increase in straining as the force on the specimen decreases or increases. The net result is that the more the specimen is unloaded, and this pattern continues into sample extension, the lower the apparent stiffness (E_r). Another consequence of this is that for a given specimen strain, the stress on the specimen will be higher during the loading phase of the cycle than the unloading phase, i.e. the sample is exhibiting hysteresis, with the excess energy being dissipated in the form of interparticle friction. This ability to damp vibration is a very useful property in the railway environment.

Selig and Waters (1994) offer an alternative experimentally derived equation for the calculation of resilient modulus, especially tailored for granite ballast:

$$\varepsilon_r = \left[0.00116q(\sigma_3')^{-1.15}\right]^{\lambda} \qquad 2.6.6$$

where:

ε_r = resilient compressive strain

q = shear stress in compression (psi)

σ_3' = constant confining pressure (psi)

$\lambda = 0.78(\sigma_3')^{0.088}$

Whilst perhaps offering more accurate stress dependent values of resilient modulus, however, this formula still does not address the fundamental problem of effects due to degree of unloading.

One model of elastic behaviour that may be more appropriate is that proposed by Boyce et al. (1976). This model will not only take into account minimum load, but any stress path that can be applied to the material in the triaxial cell.

The Boyce model defines the stress path applied to the sample in p/q space in terms of the mean stress applied (p_m and q_m) and the resilient stress applied (p_r and q_r). See Fig. 2.22 for definitions of these terms. All stresses used are in kPa. These stresses are then resolved into two other directions, a and b, to give the stress path in 'a/b space', where the mean (T_m) and resilient (T_r) values are given by;

$$T_m(a) = \left(p_m + 4/3q_m\right)/p_m \qquad 2.6.7\ (a)$$

$$T_r(a) = \left(p_r + 4/3q_r\right)/p_m \qquad 2.6.7\ (b)$$

and

$$T_m(b) = \left(p_m - 2/3q_m\right)/p_m \qquad 2.6.8\ (a)$$

$$T_r(b) = \left(p_r - 2/3q_r\right)/p_m \qquad 2.6.8\ (b)$$

The resilient strain (W_r) in each direction, a and b, is then calculated using the T_m and T_r values in each direction and the following equation;

$$W_r = \left(\frac{p_m}{K_1}\right)^{K_2} \sinh\left[\frac{2T_r}{(T_m + 1)}\right] \qquad 2.6.9$$

Where K_1 and K_2 are material constants, and p_m is the average normal stress from Fig. 2.22.

The strains in a/b space can then be coverted into physical strains that can be used for the calculation of the resilient modulus, using the following equations;

$$W_r(a) = 7/3\varepsilon_1 + 2/3\varepsilon_3 \qquad 2.6.10\ (a)$$

$$W_r(b) = 1/3\varepsilon_1 + 3/8\varepsilon_3 \qquad 2.6.10\ (b)$$

It can be shown that when q_m, q_r and p_r are small compared with p_m, then the function W_r approximates to an equation of the form :

$$W_r \approx \left(\frac{1}{K_3} p_m\right)^{K_4} T_r \qquad 2.6.11$$

i.e. an expression similar to equation 2.4.6.

This equation also confirmed the work by Brown and Hyde (1975) showing that the response of the material will differ depending on whether the confining stress is cycled with the deviator stress, or kept constant. Hence values of Poisson's ratio obtained from cyclic load tests must be treated with care.

Caveats to the use of this model are that whilst values of K_1 and K_2 have been calculated for the material tested by Boyce, they will undoubtedly be different for other materials and the equations may need modifications to suit. Also, these results were obtained by averaging the values from several samples, with Boyce reporting that values varied from this by up to ±50% in different samples. Another point to note is that to keep the number of specimens required to a minimum, plastic deformation was minimised by only subjecting the sample to four load cycles at each effective stress tested. Given that resilient modulus has been shown to change as the test proceeds, e.g. Brown (1974), this could be a limiting factor in the validity of this model. However, the model may still be useful for extrapolating test data already accumulated to other loading stress paths.

Given the difficulty of using the above model for numerical analyses, Pappin and Brown (1980) re-analysed that and other data to propose a model based on volumetric strain and shear strain. They proposed that;

$$\varepsilon_{vr} = \delta\left[\left(\frac{p}{K_5}\right)^{0.33}\left(1-0.08(q/p)^2\right)\right] \qquad 2.6.12$$

Where;

K_5 = constant of value $1.9*10^{11}$ kPa

ε_{vr} = resilient volumetric strain

All stresses are again in kPa.

On the basis that volumetric strain is stress path independent, to calculate resilient volumetric strain, the values for each end of the stress path are calculated and the difference is the resilient value. The resilient shear strain, however, was not found to be stress path independent. To find the resilient shear stress value, the shear strains had to be normalised and then re-expanded to calculate the result. Hence the resilient shear strain (ε_{sr}) produced by a stress path from (p_1,q_1) to (p_2,q_2) is given by;

$$\varepsilon_{sr} = 0.00024\left\{\frac{q_2}{p_2+b} - \frac{q_1}{p_1+b}\right\}\left\{\frac{\left(p_r^2+q_r^2\right)^{0.5}}{p_m}\right\}^{0.4} \qquad 2.6.13$$

However, this must have had certain shortcomings, as it has been superseded in Brown and O'Reilly (1991) by another method based on volumetric and shear strain where;
Resilient Volumetric Strain:

$$\varepsilon_{vr} = \delta\left[\left(\frac{p'}{c_1}\right)^{c_2}\left(1-c_3\eta^2\right)\right] \qquad 2.6.14$$

Resilient Shear Strain:

$$\varepsilon_{sr} = \delta\left[\left(\frac{p'}{c_4}\right)^{c_5}\eta\right] \qquad 2.6.15$$

where:

$\eta = q_d/p$

c_1, c_2, c_3, c_4, c_5 = constants determined from experiments. For Granite, these are;

$c_1 = 7.37 * 10^{-5}$ kPa

$c_2 = 0.49$

$c_3 = 0.091$

$c_4 = 9.88 * 10^{-6}$ kPa

$c_5 = 0.36$

This also allows calculation of stress dependent values of bulk and shear modulus (K and G respectively).

$$K = \frac{p'}{\varepsilon_{vr}} \qquad 2.6.16$$

$$G = \frac{q}{3\varepsilon_{sr}} \qquad 2.6.17$$

and from this Young's modulus (E) and Poisson's ratio (ν):

$$E = \frac{9GK}{3K+G} \qquad 2.6.18$$

$$\nu = \frac{3K-2G}{2(3K+G)} \qquad 2.6.19$$

This gives stress dependent values for Young's modulus and Poisson's ratio which can be plotted in the form of a contour map on p/q axes.

Boyce (1980) also presented another model for non linear elastic behaviour based on bulk modulus and shear modulus. He proposed that the elastic behaviour was purely derived from particle deformation at points of contact, hence should follow the rules of interaction of spherical particles interacting proposed by Timoshenko and Goodier (1970). This results in the following relationships;

$$K = K_1 p^{(1-K_2)} / \left(1 - \beta q^2 / p^2\right) \qquad 2.6.20$$

$$G = K_3 p^{(1-K_2)} \qquad 2.6.21$$

Where $\beta = \left(1-K_2\right)K_1/6K_3$

K_1, K_2 and K_3 are material constants.

Unlike the previous two models, this is a theoretical rather than empirical model based around the premise that the resilient behaviour is dictated purely by deformation at particle

contacts, and is perhaps therefore less appropriate for large resilient strains where particle slip may occur.

All of the above equations have 'constants' to take account of various material parameters, and which need to be adjusted as the conditions vary. Tests (e.g. Alva-Hurtado and Selig, 1981) had suggested that the degree of specimen compaction was one of these. Cyclic loading on many specimens by Kolisoja (1997) showed that for a given material and set of test conditions, the resilient modulus increased linearly with the percentage of solid material in the specimen (=1-porosity). If the link between resilient deformation and plastic deformation is correct (Raymond, 1992, Raymond and Bathurst, 1994, Sharpe, 1996) then this would confirm the findings of the ORE (equation 2.6.1(b)) who included porosity as a factor controlling deformation. This is because an increase in density would lead to an increase in resilient modulus, and thus the reduced resilient deformation would lead to reduced plastic deformation.

2.6.2(c) Effect of Particle Size During Cyclic Load Tests

Janardhanam and Desai (1983) attempted to test railway ballast in a true triaxial device, as opposed to a conventional triaxial cell which is only axisymmetrical, to gain a better idea of the ballast properties. However, the device was only able to take cubical samples of 100mm size, and so would have given very unrepresentative results with material of 30mm average particle size. For this reason, materials with smaller particle size and grading curves parallel to the original ballast were tested. These materials had average particle sizes of 16mm and 7mm.

Having undertaken cyclic 'conventional' triaxial tests in this apparatus, the results showed that at low confining pressures, the resilient modulus increases linearly with particle size. Increasing confining pressures resulted in the rate of increase of resilient modulus reducing with increase in particle size. These trends are shown in Fig. 2.23. The actual modulus values quoted should be treated with caution, as the tests only consisted of four load cycles with increasing values of deviator stress, thus the material would not have had a chance to stabilise. Also, the tests were compared with results by another author using material of a larger grain size. However, it could be assumed that the general trends shown would be valid.

It is also worth noting that the material with a smaller grain size gave consistently higher levels of axial strain for any given combination of confining pressure and deviator stress.

The general trends shown were confirmed in work by Kolisoja (1997). In a series of large scale triaxial tests (specimens of 300 mm diameter) Kolisoja found that the constant K_1 in equation 2.4.5 formed a linear relationship with a parameter d_{ekv} (in mm), this being representative of the average grain size where;

$$d_{ekv} = \left(d_{10} + d_{50} + d_{90}\right) / 3 \qquad 2.6.22$$

i.e. resilient modulus increasing linearly as the grain size increases. The absolute value of K_1 was found to vary with the type of material tested but the principle of the relationship was found to be the same.

2.7 Methods of Conducting Cyclic Load Tests

There are several experimental methods of determining the cyclic load response of granular materials, with varying degrees of sophistication. Among the more popular are the simple shear apparatus, the consolidometer, the triaxial test, the hollow cylinder apparatus and the resonant column apparatus. Brown and O'Reilley (1991) review all of these in more detail. Of the listed experimental methods, the triaxial test is the most commonly used for cyclic load testing, and a considerable body of work has been accumulated on its use. The cyclic load triaxial test is carried out in a similar manner to the conventional triaxial test, except that the axial (deviator) load, and occasionally the cell pressure, are cycled between pre-determined levels.

2.7.1 Stress Levels

The axial loads for the test are quite simple to determine, being deduced from the peak vertical and dead loads imposed on a typical ballast bed. The cell pressure is more difficult to determine, as much less is known about the lateral loads present in a ballast bed. In addition, it should be noted that the triaxial test is axisymmetrical, and so cannot truly represent the state of a ballast bed which will have differing principal stresses laterally and longitudinally.

Little is known about the lateral loads present in track beds for several reasons. Firstly it is presumed that it will be highly dependent on the physical state of the bed and its stress history. Secondly, it is difficult to investigate the in-situ state of granular materials without causing disturbance to them, and hence potentially changing the results. Thirdly, an accurate model of the ballast bed has so far proved elusive, meaning predictive values are unreliable. Previously, most of the computer models generated have been based on elastic layer theories, and thus in the case of a subgrade soil overlain by a relatively stiff ballast layer, have predicted tensile stresses at the base of the ballast bed. This is obviously inaccurate, and shows that the ballast models used are grossly oversimplified.

In an attempt to investigate the lateral loads in a ballast bed, Stewart et al. (1984) carried out box tests in which the sides of the box of 600mm by 300mm by 480mm deep were instrumented to measure lateral stresses. On the side panels, they found that the ballast just below the sleeper level experienced a lateral stress of just above 56kPa on initial loading of 270 kPa. When the load was removed, a residual horizontal stress of 17.5kPa remained. With further cycling, the horizontal stress when loaded gradually reduced, and the residual stress left when the load was removed increased, until the two converged around the 28kPa level at about 1000 cycles. Midway down the bed, the pattern was repeated with the loaded and unloaded stresses converging around the 28kPa mark, but starting off closer together. At the base of the bed, the stresses remained fairly constant at around 14kPa. On the end panels (i.e. between sleepers) similar behaviour occurred but with lower magnitudes of stress, as would be expected. From these results it was postulated that the residual stresses, combined with the high coefficient of lateral earth pressure (K_0) values found from the tests could account for why the expected tensile stresses at the base of the ballast bed would not cause failure. The superposition of the tensile stresses at the base of the bed over the residual horizontal stresses would still result in a net compressive stress, avoiding the failure condition. On removal of loading (and the tensile stresses), the high K_0 value would allow the residual stress to remain despite the fact that they are much higher than the vertical stress i.e. the vertical (initially major principal stress) has now become the minor principal stress. This process is described in more detail by Selig (1987).

It must be noted that this rotation of principal stress is likely to affect settlement in the base of the ballast bed as the change in principal stress direction can cause increased rates of compressive volumetric strains (Brown and O'Reilley, 1991) This will result in higher

plastic strains than would otherwise be expected, or predicted from any of the models mentioned above, which are all plane strain based, and hence greater permanent deformation. Little research has been done into the impact this is likely to have on the track bed environment. McDonald and Raymond (1984) have conducted repeated cyclic (compression - extension) triaxial tests and simple shear tests on dense dry sand and found that compression - extension tests, giving the rotation of principal stress as described in the previous paragraph, actually result in less permanent deformation than conventional repeated compression tests. However, limitations of the equipment and perhaps a lack of knowledge of the true conditions within the ballast bed, meant that the results were inconclusive with respect to the design of railway pavements.

If an attempt is being made to accurately replicate the stress regime in a road pavement or track bed the cell pressure should be cycled along with the axial load in the triaxial test, but as can be seen from the work by Stewart et al. (1984) the horizontal forces tend to a residual value, so it could be argued that it is not necessary to cycle cell pressure. Work by Brown and Hyde (1975) concludes that it is not necessary to cycle cell pressure if the constant value is equal to the mean cyclic pressure that would otherwise be applied. However, this is not valid for the determination of Poisson's ratio, so the results are better interpreted in terms of volumetric and shear strain.

2.7.2 Loading Pattern

Many researchers have carried out investigations into the effect of loading frequency and waveform on the cyclic load response of granular materials, some of which are listed by Lee and Vernese (1978). Lee and Vernese observed that in most cases, frequency and loading waveform had no effect on the results. This conflicts with reports by Gaskin et al. (1978) and Sato (1995) which suggest that the settlement of ballast is affected by the peak acceleration experienced. This would mean that frequency and waveform would have an appreciable effect, as increasing the frequency of a sine wave increases the peak acceleration. Using a square wave instead of a sine wave will cause even higher accelerations, although in this case changing the frequency would have no effect, as the peak acceleration would not change only the time under load, and this only matters with a viscous response. Perhaps Timmerman and Wu (1969) are correct when they assert that only acceleration above the region of 0.5g have an effect on the test results. Certainly when ballasts have been tested under vibration, peak acceleration has been shown to have an

effect on the state of the material. Gaskin et al. (1978) and Morgan and Markland (1981) have shown that when ballast is vibrated, frequency has no effect on the material, but the peak acceleration experienced does have consequences. Morgan and Markland tested a uniformly graded limestone of 19mm average particle size, thus the inertial properties of the particles will be different to those of ballast and the results may not be identical, and found that when loose ballast was vibrated in a box accelerations above 1g had a marked compactive effort on the material. This was the same conclusion reached by Gaskin et al. (1978). When pre-compacted material was tested, however, accelerations above 1g were found to disturb the material. From accelerometer measurements, it was found that the ballast particles lost contact with the vibrating box and each other at higher accelerations resulting in impact forces being generated when the particles came back into contact, thus explaining the compaction of the loose samples and the disturbance of the compact samples. When static beds were surcharged by vibrating loads, generated impact loads and fluidization of the ballast bed were again found to be key factors. In this case the loads and frequencies tested were out of the range of the usual cyclic loading tests, but within the range of dynamic frequencies and loads to be found in the track environment.

2.8 Triaxial Testing

The triaxial apparatus is to be used to investigate the stress-strain behaviour of the materials under test. In this section, some of the factors affecting the design of a suitable triaxial testing system are reviewed.

2.8.1 Specimen Size

The size of the specimen should be such that it is representative of the material as a whole. This section covers the factors influencing the choice of specimen size.

2.8.1(a) Specimen Diameter

The specimen diameter, D, should be sufficiently large that there are enough particles across the diameter to act as a continuum rather than a structure, thus giving repeatable and representative results. Obviously, this depends on the maximum particle size d_{max} of the soil. For this reason, the ratio D/d_{max} is often used to specify the diameter that should be used. The ideal method of determining the best D/d_{max} ratio is to carry out a series of tests with different values of D to find the smallest value of D/d_{max} at which the change in parameters obtained is negligible.

Salman (1994) carried out a review of literature on the subject, and the material available suggested that "it seems reasonable to conclude that if the material gradation is such that the proportion of particles in the maximum sieve size range is 30% or less and the ratio D/d_{max} is 6, then there is no effect of the specimen size on the test". Other researchers have used smaller values, however. Brown and O'Reilley (1991) recommended that for triaxial testing of ballast, a specimen diameter in excess of 200mm should be used, giving a D/d_{max} of 4 for the standard 50mm railway ballast, Knutson and Thompson (1978) used similar figures, Stewart (1986) used 38mm material in a 6 inch (152mm) specimen giving D/d_{max} of 4 and Alva-Hurtado and Selig (1981) used 152mm samples with 30mm material, giving a D/d_{max} of 5.

2.8.1(b) Specimen Height

In a conventional triaxial test with plain steel top and bottom platens, it can be seen that specimens 'barrel' during shearing. This is due to friction between the end of the specimen and the platen restraining the specimen from shearing outwards. This gives rise to 'dead zones' adjacent to each platen where the soil is restrained from moving freely. The sample should be sufficiently high that there is an area between these zones (called the dilating zone) that is unaffected by end restraint, and will hence be more representative of the material behaviour. For this reason, specimens have traditionally had a height to diameter ratio (H/D) of 2.

Various authors, such as Rowe and Barden (1964), Bishop and Green (1965), Duncan and Dunlop (1968), Lee (1978), Lam and Tatsuoka (1988), Goto and Tatsuoka (1988) have investigated the effect of differing H/D ratios on the strength of cohesionless materials, usually sands. Bishop and Green (1965) tested Ham River sand and concluded that reducing the H/D ratio to 1 increased the angle of friction of the material by 4-5° depending on the initial porosity of the specimen. Goto and Tatsuoka (1988) tested Toyoura sand and found that increasing the H/D ratio from 2.0 to 2.7 decreased the angle of friction by 1°.

All of the above authors have attempted to reduce the effects of end restraint by producing lubricated ends to go between the specimen and the platens. The most successful method, introduced by Rowe and Barden (1964), is to sandwich layers of silicone grease between thin rubber membranes. This can effectively eliminate end friction and thus the dead zones in the specimen, theoretically allowing the use of shorter specimens. This finding generally

appears true, but the exact effectiveness appears to vary between experiment and experiment. Bishop and Green (1965) deduced that well lubricated ends reduce the angle of friction (ϕ') of a sample where H/D=1 to that of a sample with H/D=2 and regular ends, although the peak strength occurred at a higher strain. Lee (1978) and Goto and Tatsuoka (1988), whilst agreeing that peak strength occurred at a higher strain, concluded that with lubricated ends, for dense samples ϕ' was lower and for loose samples ϕ' was higher than a conventional specimen with unlubricated ends. Lam and Tatsuoka (1988) tested specimens with lubricated ends with a wider range of H/D ratios down to 0.25. They observed that even with well lubricated ends, reducing the H/D ratio from 2 to 1 increased the value of ϕ' by 1° for dense samples and 2° for loose samples. Decreasing the value of H/D from 1 to 0.25 caused another similar increase in ϕ'.

In addition to the changes in stress/strain behaviour, Rowe and Barden, Bishop and Green, Duncan and Dunlop, Lee, and Lam and Tatsuoka all confirmed that lubricated ends give higher and more uniform volumetric strains, as the dead zones are removed and thus shearing is no longer concentrated in the 'dilation zone'. The result of this is that barrelling no longer occurs, or is much less pronounced, and there will be lower internal pore pressure gradients in the finer grained soils due to the more uniform dilation or densification as the material shears.

End lubrication is not without its problems though. Lee (1978) listed some possible drawbacks;

1. Coarse particles of material could penetrate through the cushion and bear directly on the platen.
2. With time under loading, the viscous grease can squeeze out from the ends, which could limit the time available for a test.
3. Because of the viscous nature of grease, the lubrication effectiveness may reduce with increased rates of loading.

In addition, Goto and Tatsuoka (1988) pointed out that multiple layers of grease and rubber membranes could introduce bedding errors, with the squeezing out of grease, the spreading of membranes and the penetration of particles into the lubrication layer.

Drescher and Vardoulakis (1982) carried out a theoretical investigation into the specimen height to diameter ratio and its implications for testing granular material. They presented

corrections to the observed angle of internal friction for both non lubricated and lubricated ends (as lubricated ends still have a frictional component) dependant on the height to diameter ratio of the specimen, concluding that conventional triaxial testing gives values of internal friction that are unsafe and overstate the effect of strain softening of the material. However, to apply these corrections requires accurate knowledge of the size of the dead zones within the material, information which is not normally available.

2.8.2 Specimen Monitoring

To cut down on possible errors, it is better to monitor the load and deformations inside the triaxial cell. For example, measuring the piston load with a load cell placed inside the triaxial cell will avoid errors due to friction between the piston and the triaxial cell piston bushing. Techniques are also available for internal measurement of strain, for example those of Boyce and Brown (1976) and Burland and Symes (1982). Measuring the axial strain over the middle part of the specimen in this way gives a more accurate result as it avoids possible bedding errors at the ends of the specimen and eliminates distortion of the results that would occur due to the dead zones being included in the strain measurement.

However, for situations where internal axial strain measurement is not possible, Bressani (1995) has argued that external strain measurement can be nearly as accurate. Bressani found that many measurement errors came from non-alignment of the top cap and inadequate calibration of the equipment being used. By careful calibration of the equipment and all ancillaries, careful alignment of the top surface of the specimen to ensure it is perfectly level, and use of a rotating top cap with point loading, many of the errors associated with external measurement could be eliminated. This conclusion contradicts that of Goto and Tatsuoka (1988) who found that the presence of a rotating top cap resulted in less uniform deformation. However the effect was only really apparent in loose samples where peak stresses occurred at larger strains, and hence where there was more time for cap rotation. In these cases ϕ' was reduced by about 1°.

2.8.3 Membrane correction

Salman (1994) carried out a review on the subject of correcting stresses for the effect of the specimen membrane. His conclusions were that for cases where the cell pressure is sufficient to hold the membrane firmly against the specimen i.e. no buckling of the membrane occurs, then the compression shell method proposed by Henkel and Gilbert

(1952) should be used. This theory assumes that the membrane is acting against the deviator stress rather than confining the specimen, although radial confinement may have occurred if the specimen has been consolidated, in which case this should be calculated for the post consolidation state and included in the minor principal stress. In this case, the following correction should be used;

$$\sigma_{1m} = \frac{\pi d_0 M \varepsilon}{a_c} \qquad 2.8.1$$

Where σ_{1m} is the correction to the measured compressive stress (in kPa), d_0 is the initial specimen diameter (in m), M is the membrane elastic modulus at 10% extension (in kPa), ε is the axial strain and a_c is the corrected area of the specimen at strain ε (in m^2).

Where the rubber membrane buckles during shearing, the membrane is incapable of resisting the major principal stress, but will then be adding to the confinement. In this case, the minor principal stress σ_{3m} should be corrected by the equation proposed by LaRochelle et al. (1988);

$$\sigma_{3m} = \sigma_{om} + 0.75\frac{M\sqrt{\varepsilon}}{d_0} \qquad 2.8.2$$

Where σ_{om} is the original confining stress (in kPa)

More recently Kuebris and Vaid (1990) have proposed a single system to supersede both of the above equations. These new equations take into account the change in thickness with extension of the membrane. They propose that the modulus of the rubber membrane should be measured in a similar way to that proposed by Henkel and Gilbert (1952), but the calculations should take account of the change in cross sectional area of the rubber. This change results in a constant value for the modulus rather than the decreasing value given by the old method, obliviating the need to measure the modulus at a particular strain. Once this is established, the equations for membrane restraint can be constructed to account for variations in membrane thickness during the test. In addition, these equations acknowledge the fact that axial and radial strain are interdependent, as a change in one will induce a change in the other due to the Poisson's ratio of the material. The previous equations do not acknowledge this. Thus, the corrections are;

$$\sigma'_{rm} = \sigma'_r - \frac{4E_m t_0(2+\varepsilon_v+\varepsilon_{Ma})\varepsilon_v}{3D_0(2-\varepsilon_v+\varepsilon_{Ma})} \qquad 2.8.3$$

Where σ_{rm} is the corrected radial stress (in kPa), σ_r is the uncorrected radial stress (in kPa), E_m is the Young's modulus of the rubber membrane (in kPa), ε_{Ma} / ε_v are the axial and volumetric strains in the specimen respectively, t_0 is the original thickness of the membrane and D_0 is the original diameter of the membrane (the units of the last two variables are not given, but provided they are both the same, it is immaterial).

$$\sigma'_{am} = \sigma'_a - \frac{4E_M t_0(2+\varepsilon_v+\varepsilon_{Ma})(3\varepsilon_{Ma}+\varepsilon_v)}{3D_0(2-\varepsilon_v+\varepsilon_{Ma})} \qquad 2.8.4$$

Where σ'_{am} is corrected axial stress and σ'_a is uncorrected axial stress (both in kPa)

2.9 Summary

In the past, railway maintenance was a fairly empirical process. If a length of track was particularly uneven, a gang of men was sent out to cure the problem. Over the years, increasing demands on the track, in terms of frequency and magnitude of loads and the requirement to reduce costs, forced an examination into exactly what was happening to the track, and how it behaved in order to predict and minimise the maintenance requirement. From this need sprung a desire to understand the behaviour of the materials underlying the track, especially under the repeated loading conditions to which they were subject, both in the field and in the laboratory. With this knowledge, a new generation of techniques for maintaining the railway are being developed.

However, as can be seen from this survey of the available literature there are several areas in the field of ballast mechanics where there is still a lack of knowledge concerning the behaviour of the material and how its performance may be improved. It is felt that the following points are the most important of those covered.

1. There is still a lack of detailed knowledge about the loads liable to be encountered by a particular section of ballast in the ballast bed. General vertical loads due to passing vehicles are known, although little work appears to have been carried out on the exact magnitude and frequency of abnormal dynamic loads. There is some, but far from

extensive, knowledge about lateral loads, especially in the light of possible principal stress rotation in the ballast bed.

2. Knowledge of the rate at which plastic strain accumulates in granular materials under repeated loading is confused. There are many different proposals by different authors all attempting to explain the same behaviour, and most of it explains the pattern of observed behaviour, rather than predicting the magnitude.
3. There is a considerable body of work concerning the elastic behaviour of granular materials. Much of it, however, concerns smaller, well graded material of the type generally used in highway bases, and this has not been extrapolated to railway ballast.
4. Little knowledge exists on the effects of principal stress rotation on the behaviour of ballast.
5. Virtually no work has been done on the behaviour of systems consisting of two layers of non cohesive material, such as will be found in stoneblown track.
6. There are several methods available to strengthen, and give apparent cohesion to granular materials. Not all of them have been tried on railway ballast.

Given the potential impact that the new stoneblowing machinery being brought into service could have on the process of track maintenance, and given the lack of knowledge of the effect it is liable to have on the track it is treating, it was decided that the aim of the project would be to use triaxial and model tests to investigate the behaviour of a two layer system of the type liable to be found in the track bed after stoneblowing. As an area of interest, it was also decided to do a small investigation of the possibility of reinforcing railway ballast with polymer mesh elements. From these aims, a set of objectives were drawn up.

1. To investigate the behaviour of a two layer system of large, uniformly graded granular materials with reference to the behaviour of its component materials, especially under cyclic loading.
2. To investigate the use of different sizes and types of material in the two layer system, with a view to optimising the material used by the Stoneblower.
3. To investigate the effect of differing layer geometry on the behaviour of a two layer system.
4. To investigate the effect of the addition of polymer mesh elements to railway ballast.

To meet the objectives, a series of monotonic and cyclic load triaxial tests were carried out on single and two layer specimens, with some of the two layer specimens having the layer interface oriented at different angles to the direction of the major principal stress. These tests were complemented by a limited program of model tests using the 'Half Sleeper Rig' made available by Scientifics Ltd.

The following chapters detail how the objectives were achieved, in terms of equipment design, test procedures and test results.

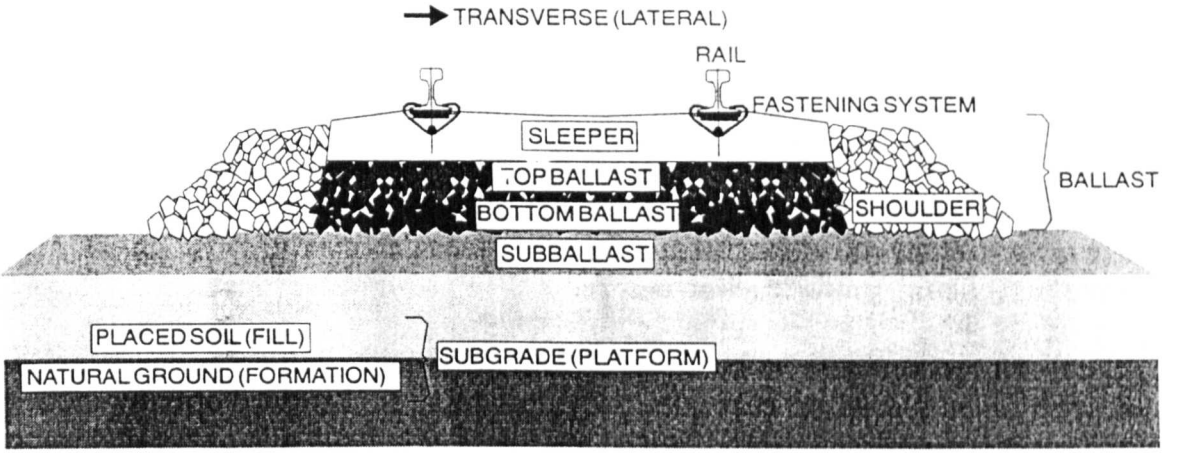

Fig. 2.1 - Track Structure Components (from Selig and Waters 1994)

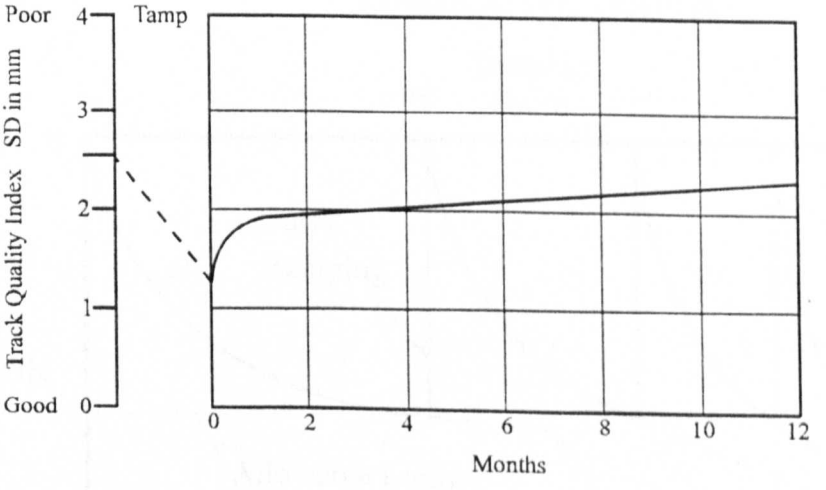

Figure 2.2 - Track Quality Index with time (from Waters, 1989)

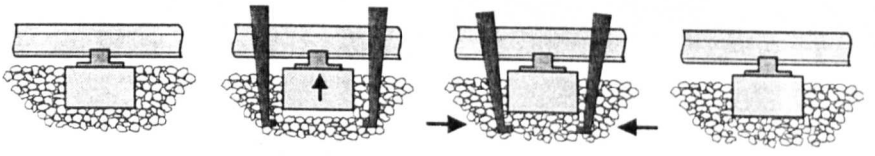

Fig. 2.3 - Schematic Diagram of the Tamping Operation

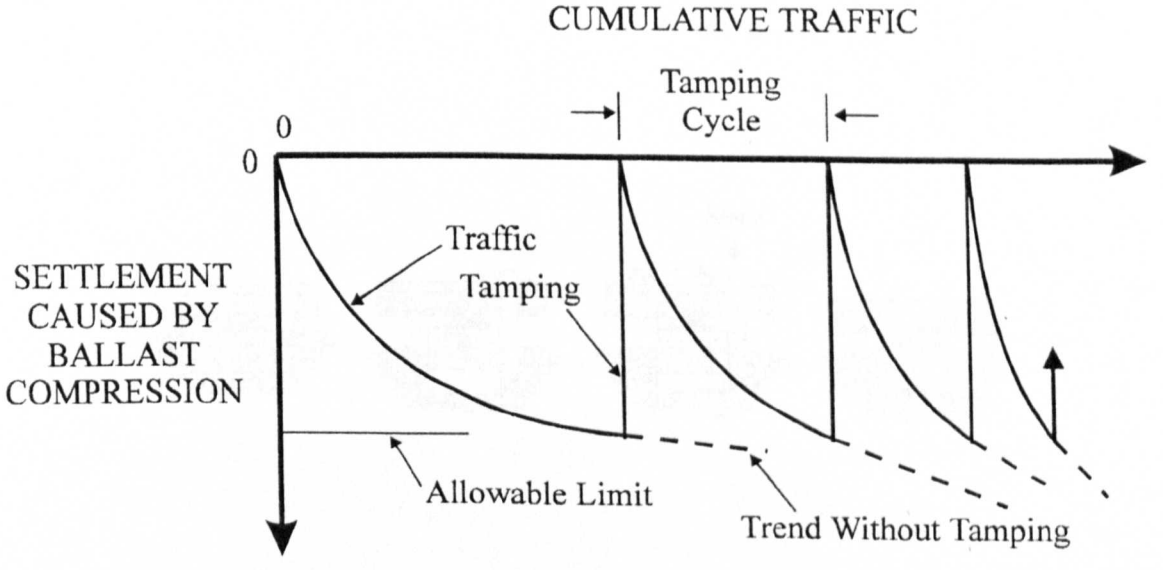

Fig. 2.4 - Ballast Settlement Over the Maintenance Cycle

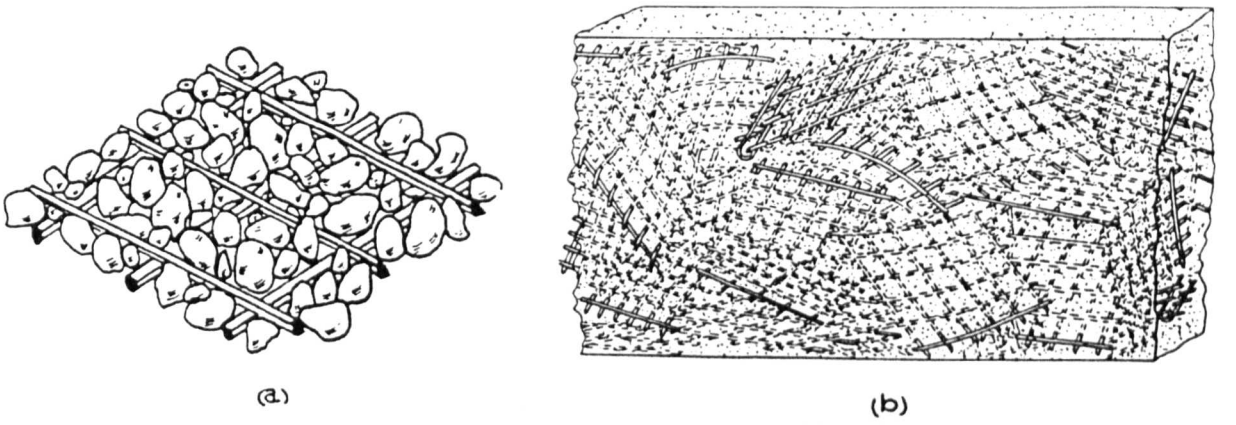

(a) Interlock with groups of particles
(b) Interlock of adjacent aggregations

Fig. 2.5 - Method of Reinforcement by Polymer Mesh Elements (from Mercer et al. 1984)

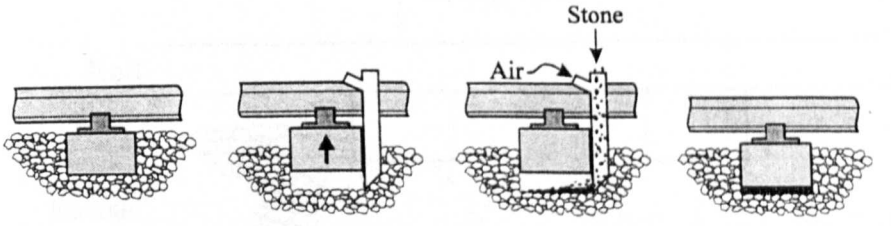

Fig. 2.6 - Schematic of the Stoneblowing Operation

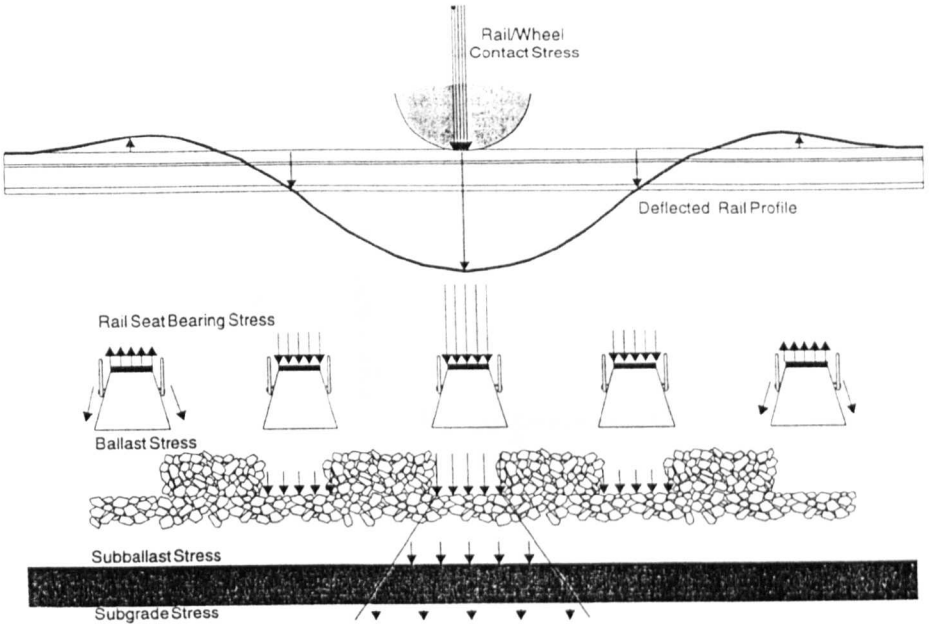

Fig. 2.7 - Typical Wheel Load Distribution Over Adjacent Sleepers (from Selig and Waters 1994)

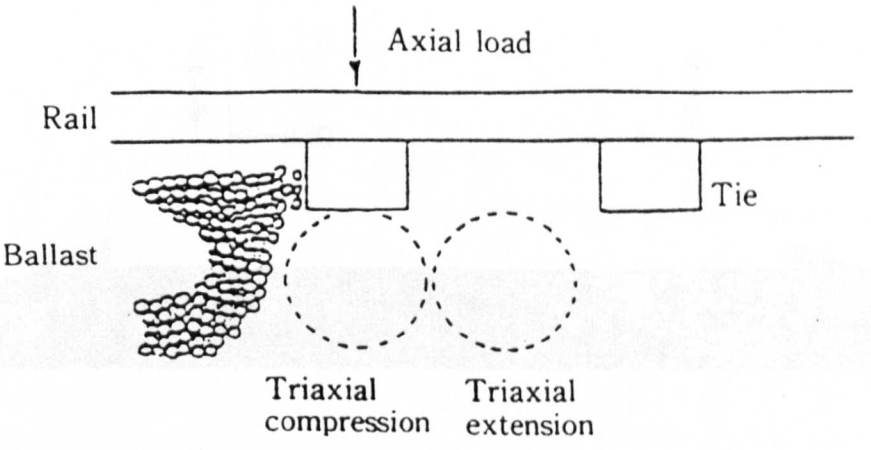

Fig. 2.8 - Load System Within the Ballast

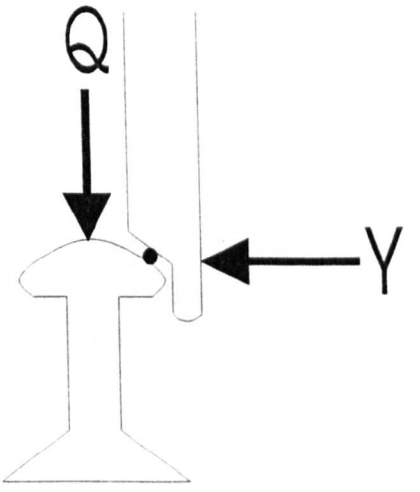

Fig. 2.9 - Force Expression at Wheel Rail Contact Point

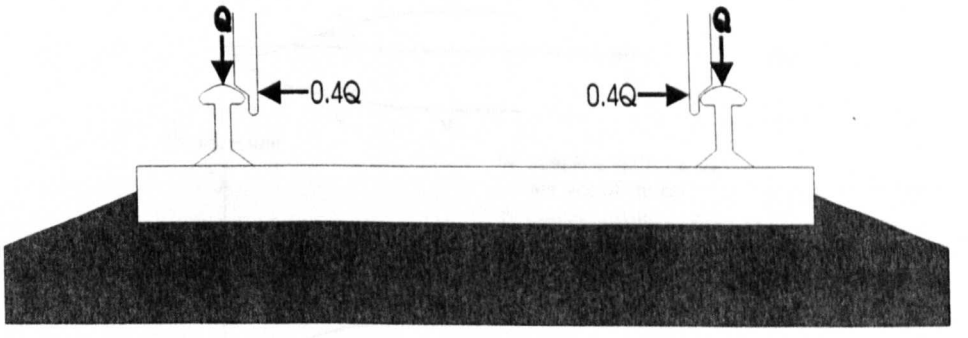

Fig. 2.10 - Gauge Spreading Forces on Straight Track

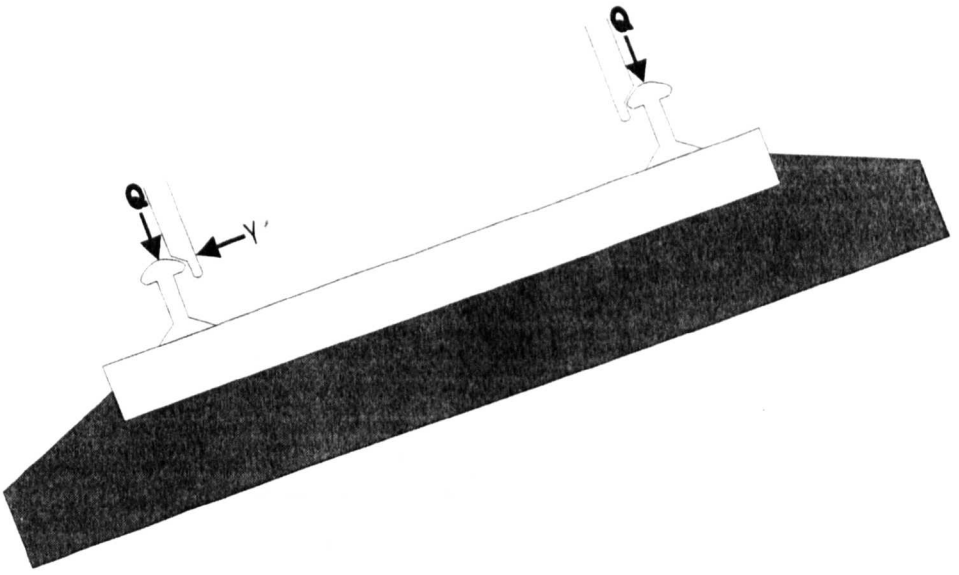

Fig. 2.11 - Low Rail Forces on High Cant Track Traversed at Low Speed

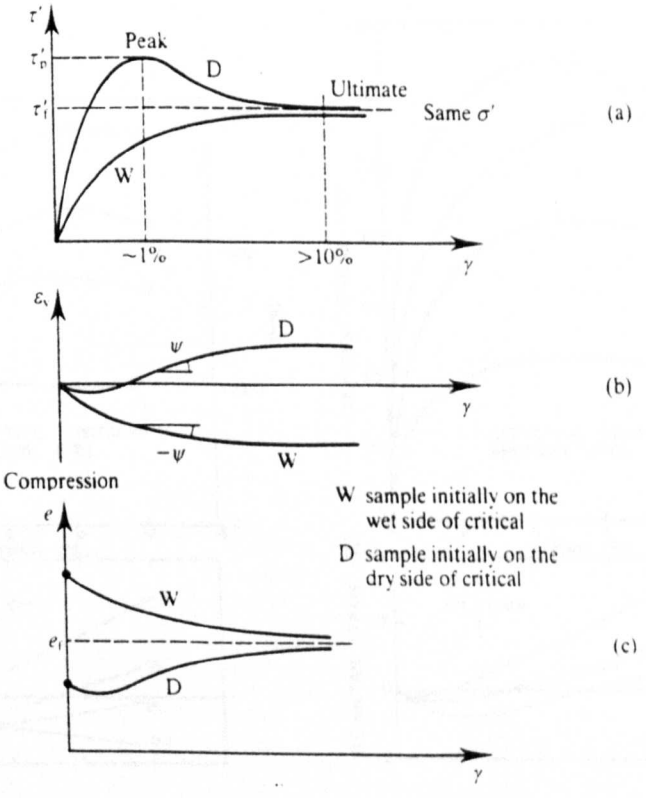

Fig. 2.12 - Typical Critical State Behaviour of a Material During Drained Shearing

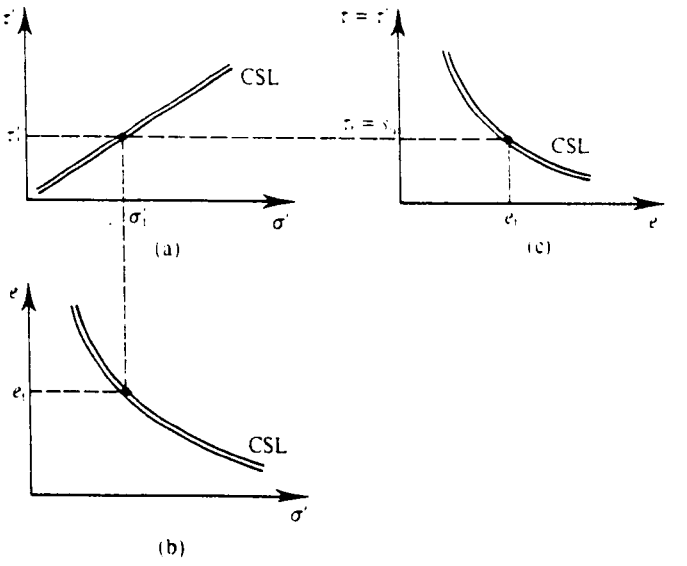

Fig. 2.13 - Relationship Between Void Ratio, Shear Stress and Confining Stress for Materials Shearing at the Critical State

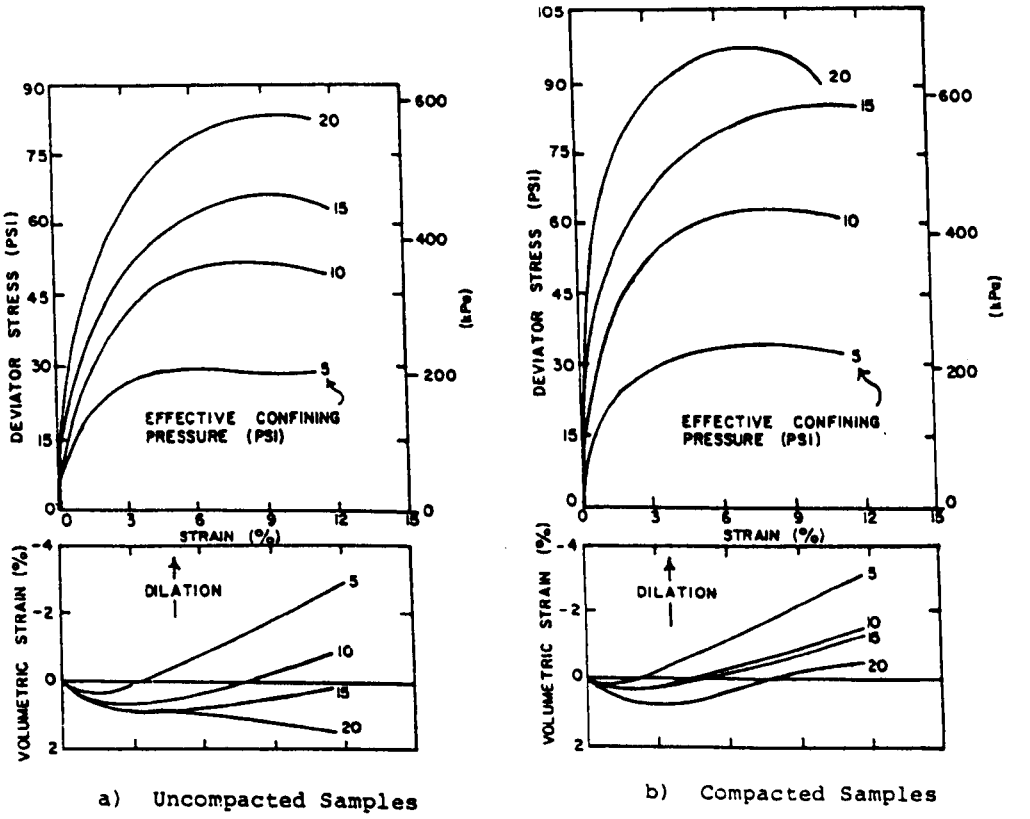

Fig. 2.14 - Typical Results For Triaxial Tests on Railway Ballast (from Alva-Hurtado and Selig 1981)

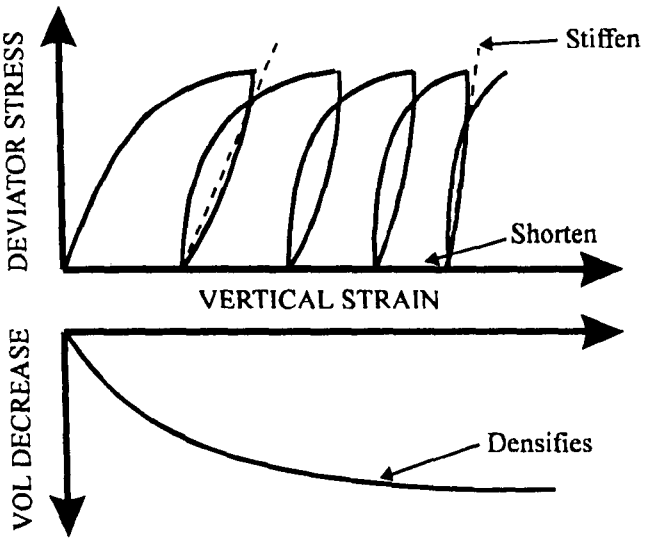

Fig. 2.15 - Idealised Behaviour of a Cohesionless Material Under Cyclic Loading

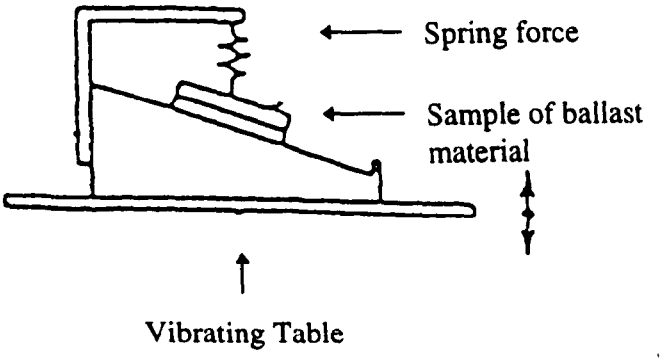

Fig. 2.16 - Apparatus for Measuring Acceleration Required to Induce Slip Between Ballast Particles (from Tarumi 1994)

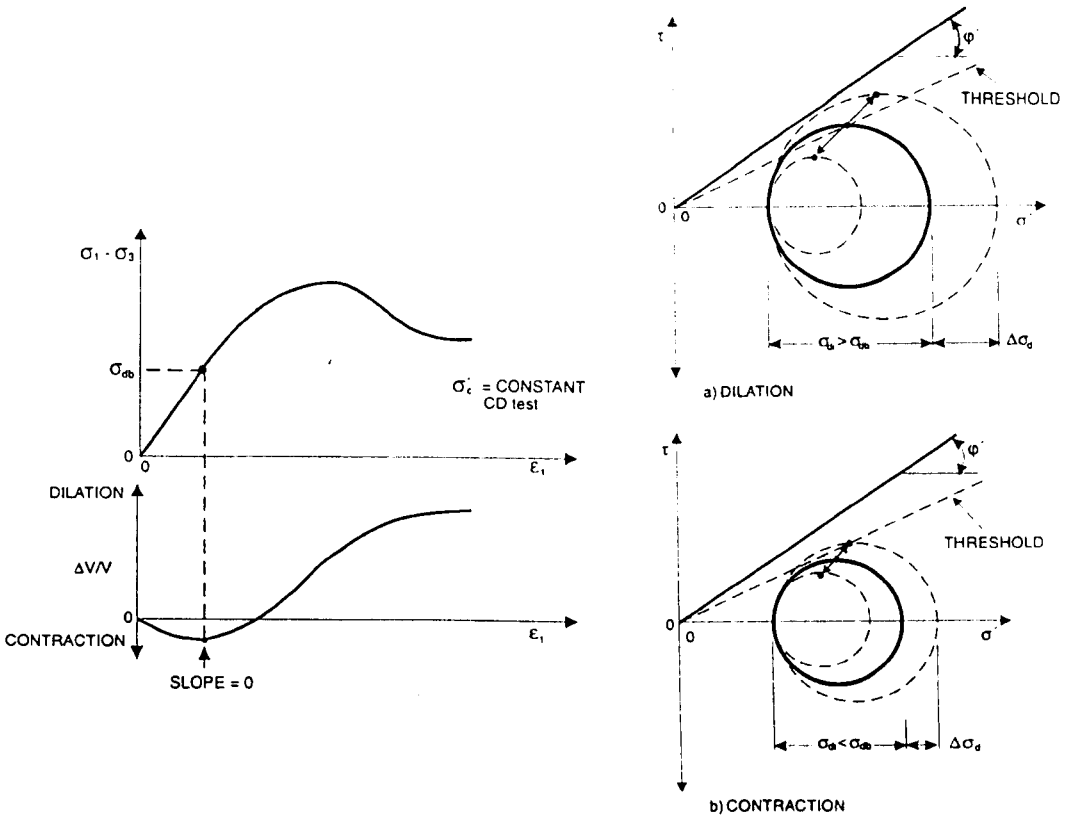

Fig. 2.17 - Method of Determining Threshold for Dilation Under cyclic Loading (from Tam 1986)

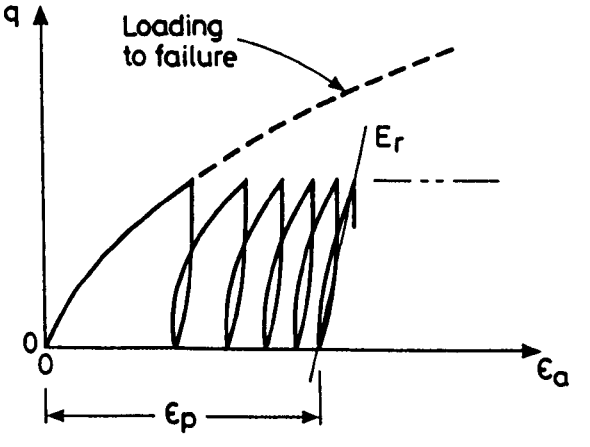

Fig. 2.18 - Definition of Resilient Modulus

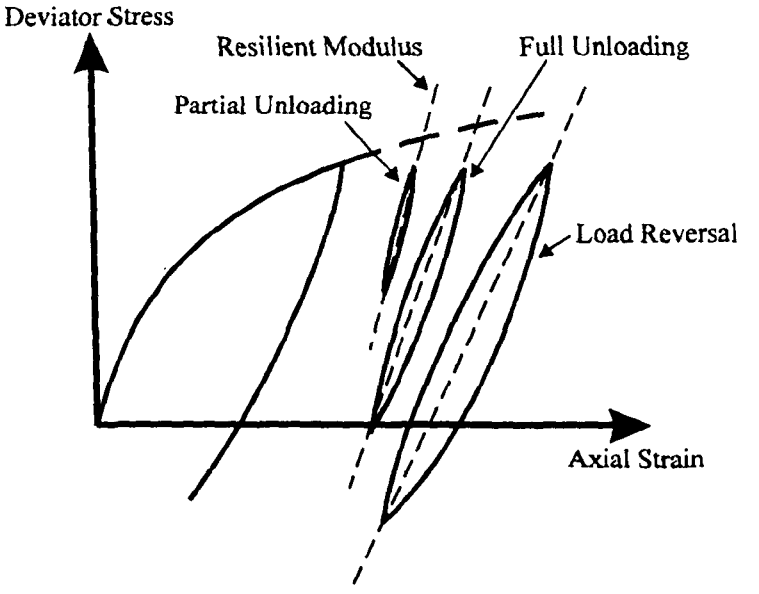

Fig. 2.19 - Effect of Degree of Unloading on Resilient Modulus (from Selig and Waters 1994)

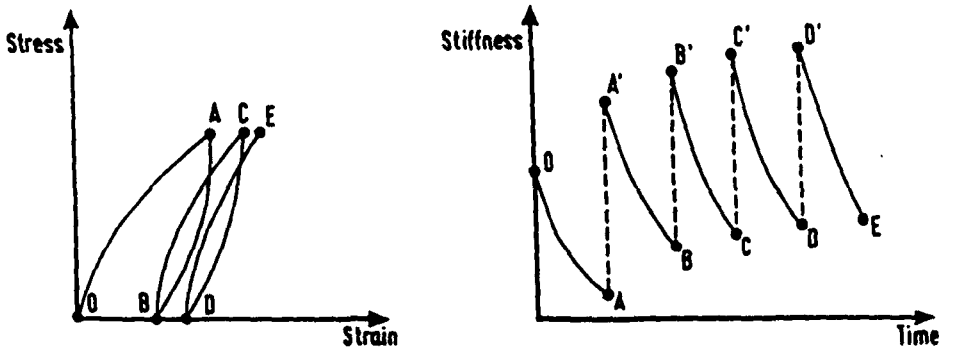

Fig. 2.20 - Change of Stiffness of Material With Reversal of Direction of Stress Increase (from Brown and O'Reilly 1991)

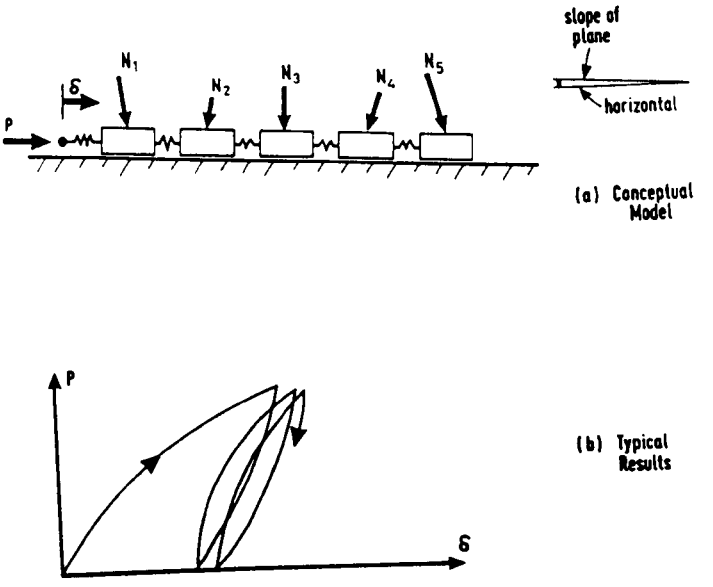

Fig. 2.21 - Simple Block and Spring Model of Cohesionless Material Under Cyclic Loading (from Brown and O'Reilly 1991)

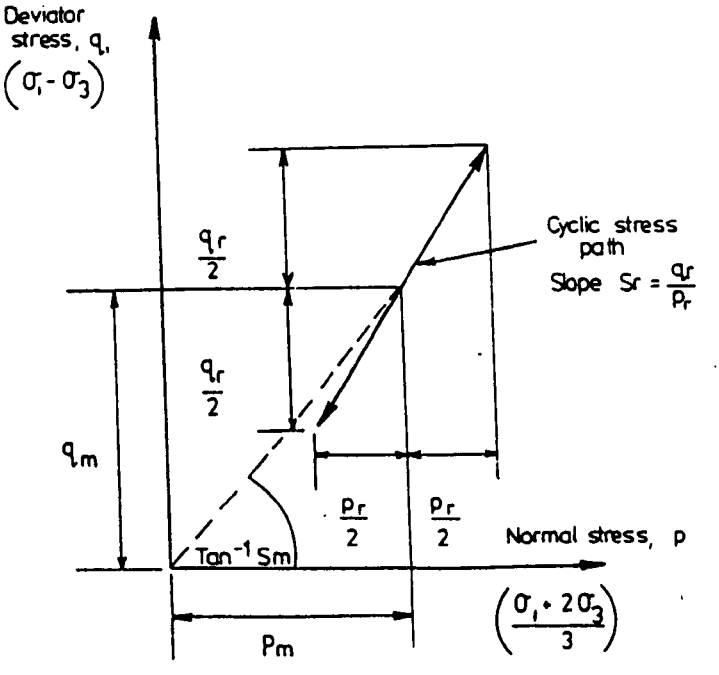

Fig. 2.22 - Definition of Terms Used by Boyce et al. (1976)

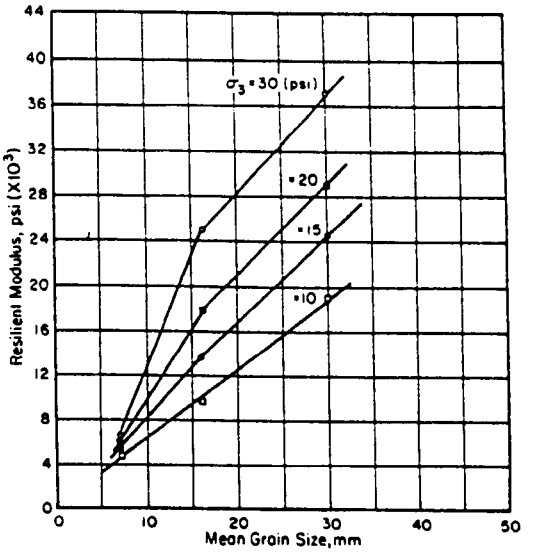

Fig. 2.23 - Relationship Between Particle Size and Resilient Modulus (from Janardanham and Desai 1983)

Chapter 3 - Development of Triaxial Apparatus

3.1 Introduction

The type of testing proposed for this project had not been carried out before at the University of Sheffield, therefore before the test programme could commence suitable equipment needed to be designed and built. The design process and its results are documented in the following sections.

3.2 The Cell

On the basis of the findings of Section 2.7 (see also Brown and O'Reilly, 1991), the testing undertaken at the University of Sheffield was carried out in a triaxial cell, shown diagramatically in Fig. 3.1 and pictured in Plate 3.1. From the literature survey (see Section 2.8.1(a) and Salman, 1994), it was established that for a conventional triaxial test to give representative results the specimen height should ideally be at least six times the maximum particle size, although a number of authors have reported work with a ratio as low as 4, and the H/D ratio should be two. Therefore, using 50mm ballast, the specimen diameter should be 300mm and the specimen height 600mm. However, the largest triaxial cell to which this project had access had an internal diameter of 296mm and height of 605mm, necessitating reduction in the size of the test specimens from the ideal. A specimen diameter of 236mm and height of 455mm was chosen, as this would give sufficient radial and vertical clearance to permit the assembly of the cell and instrumentation. The literature review gives precedents for using ballast specimens of similar size, e.g. Knutson and Thompson (1978) and Brown and O'Reilly (1991). A consequence of this reduction from the ideal size is that the results may not give absolute values for specimen parameters, but as the project is essentially a comparative one, the relative values should still be valid.

In addition to the basic cell, the end platens, cell pressure system and loading system all had to be considered, and are covered in detail in the following sub-sections, along with the vacuum system used to aid in specimen preparation.

3.2.1 Platens

Given the nature of the material under test, i.e. large uniform particle size resulting in low numbers of high stress contact points within the specimen, it was decided that lubricated ends were not appropriate for triaxial testing of this material. For the majority of the specimens, the use of a H/D ratio of two should eliminate the effects of end restraint from conventional platens. The only exceptions to this were those two layer specimens where the material interface extended into the dead zone and in these cases corrections were introduced to compensate for this.

The bottom platen was machined from mild steel with two 'O' ring grooves around the edge to facilitate the sealing of the specimen membranes by 'O' rings. This platen was then bolted to the base of the cell. In addition, the platen was drilled to allow a vacuum line to be routed into the specimen to facilitate specimen preparation. The top of this hole was covered with porous plastic sealed down with silicon sealant to prevent any fines present on the test materials from being sucked into the vacuum system.

The top platen was manufactured with identical dimensions to the bottom platen, but machined from aluminium to reduce the dead weight resting on the specimen. A 1mm thick sheet steel disc was also machined to the same diameter as the platen and placed between the specimen and the platen to stop the ballast damaging the relatively soft aluminium.

3.2.2 Vacuum system

The vacuum system was required to enable the specimen to have sufficient strength to be self supporting during assembly of the equipment. The vacuum system is shown diagramatically in Fig. 3.2 along with the plumbing system. The system consisted of a vacuum pump connected to the cell base via a vacuum gauge and a valve venting to air. The valve allowed some control over the degree of vacuum by permitting a quantity of air to enter the system.

3.2.3 Plumbing

Ideally the cell pressure should be cycled with the axial load to most accurately represent the stress regime experienced by the materials in a track bed. On the basis of previous work which showed that cyclic cell pressure could be approximated by a constant cell pressure at what would be the average pressure of the cyclic system (Brown and Hyde, 1975), a constant cell pressure system was chosen in order to simplify the equipment.

The plumbing is shown schematically in Fig. 3.2. The air pressure supply passed via an adjustable regulator, which controlled the cell pressure, and Bourdon gauge into the top of twin reservoir tanks. A cell water feed came from the bottom of the tanks and passed via a 'T' block on which the cell pressure transducer was mounted into the cell, through a control valve. There was also a vent valve on top of the cell to allow air to escape as the cell was filled from the reservoir tanks, and to allow air back in as the cell water drained back into the tanks after testing was completed. There was no pore/back pressure system as the material was tested dry.

3.3 Loading System

3.3.1 Static Loading.

The cell was mounted in a 100kN loading frame, and this was used as the loading system for the monotonic triaxial tests. The base pedestal of the frame was driven upwards via a screw thread and a set of adjustable gears. By trying various gear combinations, it was found that the highest rate of compression available was 0.96mm/min (equating to 0.22%/min with a 455mm high specimen) and so this was used.

3.3.2 Cyclic Loading

When considering a system for cyclically loading ballast specimens it was decided that it must conform to the following specification:

- It must be able to cyclically load the ballast for a pre-determined number of cycles and then shut down without intervention.
- It must be able to load the specimen to a stress of 300 kPa, as determined from Section 2.5.1 (Shenton, 1974, Esveld, 1989)
- It must be able to cycle at a speed of 1Hz in order to complete the tests in a reasonable amount of time.

A study was undertaken of the possible design methods for a cyclic load system, and it was found that the following methods were possible:

- Mechanical
- Electro - Mechanical
- Pneumatic
- Hydraulic

Of these, calculations showed pneumatics to be ruled out on the grounds of speed, mechanical was ruled out on the grounds of speed and the possible effects of fatigue, and electro-mechanical was ruled out because of an inability to achieve the required loads. This left a hydraulic system as the only possible option.

3.3.2(a) Hydraulic System

The majority of the previous cyclic loading work carried out on granular materials has been done using sophisticated commercial servo-hydraulic systems. However, such a complex commercial unit was beyond the budget of this project. It was therefore decided to design and build a suitable loading system. For simplicity, the loading system was built around a solenoid valve. The significance of this for the test programme was that the valve was only able to switch between two oil pressures, rather than having the infinitely variable output of the servo valve system, hence the equipment gave a square wave load rather than the sine wave loading used in most previous work. Sine wave loading is more representative of the loadings experienced in the field, but there is considerable work suggesting that loading waveform has no effect on the results (for example Lee and Vernese, 1978). In order to check this hypothesis, comparative tests were carried out at Scientifics Ltd. on their half sleeper rig (loaded via a servo-hydraulic system), the results of which are reported in Chapter 7.

The design of the hydraulic loading system is shown in Fig. 3.3 and the constructed system shown in Plate 3.2. It consisted of a pump to supply the oil, which was fed to the inlet of the solenoid valve via a pressure relief valve. This controlled the maximum pressure of the oil at the inlet, and hence the maximum load exerted on the specimen. There was a filter between the pressure relief valve and the return line to filter the oil that was by-passed, thus removing any potentially harmful particles present. A hydraulic ram is connected to one of the ports of the solenoid valve, and this was switched alternately between the inlet, where pressurised oil was fed into the ram thus loading the specimen, and tank return, where the

high pressure oil escaped to the reservoir and the specimen became unloaded. There was another pressure relief valve in the connection between solenoid valve and tank to ensure only oil above a pre-set pressure returned to the tank, effectively keeping a minimum pressure in the ram at all times. By this method, the ram was prevented from losing contact with the specimen, which would have resulted in impact loading when the pressure was re-applied. A bypass valve was provided around this return line pressure relief valve to allow this low pressure to be dissipated when dismantling a specimen.

The size of the ram was carefully chosen to keep the required oil pressure range of the system within manageable limits. If the ram were of too small a piston area, the maximum pressure to achieve the required load on the specimen would have been very high, and high pressure rated components would have been needed. If the ram area was too large, the maximum pressure required would have been much lower, as would have the minimum pressure to keep the ram against the specimen. If the minimum pressure were too low, it would have become difficult to adjust the minimum pressure relief valve to give the required value. By using a ram of 14.5cm^2 effective area, the maximum pressure did not have to exceed 200 bar, the recommended maximum for the solenoid when only using one of its two channels, whilst the minimum pressure needed to keep the ram against the specimen was not so low that it became difficult to adjust the minimum pressure valve.

When the system was initially built and tested, it was found that it worked but could not satisfy the cycling speed requirement due to insufficient pump capacity. This was due to the resilient deformation of the specimen being higher than expected and half of the pump capacity going to waste. It was found that the pump could not supply enough oil in the time that the ram was connected to the high pressure supply to fill the ram up to the required pressure, and so the maximum load being achieved was not sufficiently high. However, on the other half of the cycle, the capacity of the pump was going to waste as the entire oil supply was being vented back to the tank through the pressure relief valve. To cure this capacity problem, an accumulator was fitted to the pressure side of the system. This stored the excess high pressure oil produced when the ram was not connected to the pressure supply, and released it when the ram was connected to the pressure supply, thus effectively doubling the capacity of the pump. Two accumulators were fitted to the system via control valves, one for use with low pressures (below 90 bar) and one for use with higher pressures.

With the accumulators fitted, it was found that the system would operate at 0.5 Hz, half the speed originally specified but still sufficient to allow the required tests to be completed in a reasonable time.

3.3.2(b) Control System

The hydraulics were controlled by a single chip computer, known as a 'stamp' computer, from Parallax Corporation. This single chip contained memory, basic interpreter, computer and I/O circuitry, and was in this case connected to a single line LCD display. Via relays the chip controlled the main solenoid of the hydraulics system and the power supply to the hydraulic pump. It had been programmed to control the test, operating it in two stages. When it was first triggered, it cycled the solenoid at slow (0.16Hz) speed. This allowed the hydraulics to keep up in the early part of the test where the deformations of the specimen were large and there was a consequentially large demand for oil from the pump. At a point defined by the user, when the specimen deformations reduced, the control unit could be switched to high (0.5Hz) speed cycling of the solenoid valve to complete the rest of the test in a reasonable time. Throughout, the control unit recorded the elapsed number of cycles and displayed this on the LCD display. After a number of cycles pre-set by the user, the control unit stopped cycling the solenoid and shut down the power to the hydraulic pump, thus terminating the test. Therefore, the use of the computer enabled the tests to be set up and left running unsupervised, for example over a weekend.

It was decided to run each test for 100,000 cycles. Ideally, the highest number of cycles possible should have been run to simulate the long in service life of railway ballast (up to 20 million cycles), but this had to be weighed against time considerations and wear on the equipment. The figure of 100,000 was chosen as at 0.5 Hz, this could be fitted into a weekend (taking about 56 hours) and would give a reasonably representative view of long term performance. The next significant test figure, 1,000,000 cycles when plotted on a log scale, would take some three weeks.

In addition, the control unit had a manual mode allowing the user to control the solenoid, for example to test its operation, and had outputs to the logging computer to signal the operation of the solenoid and high or low speed mode to help synchronise data collection.

The circuit diagrams for the computer and the program to run it as a test controller can be found in Appendix I.

3.4 Instrumentation

3.4.1 Load

In order to eliminate piston friction from the load readings, internal measurement of load was preferred. To do this, a fatigue rated, water resistant load cell of 22.5kN load range was obtained from RDP Instruments, allowing 500kPa axial stress on a 236mm diameter specimen. This was mounted on the internal end of the cell piston with a ball and seat connection, to avoid any potentially destructive bending forces being transmitted to the load cell, between it and the top platen. By machining the seat of the mounting directly into the top platen (see Fig 3.1), and reducing the thickness of the top and bottom platens to 40mm, it was possible to accommodate a specimen of 455mm height in the cell.

3.4.2 Axial Deformation

In order to eliminate bedding errors at the ends of the specimen and some of the equipment compliance, internal measurement of axial strain is generally preferred. However, assuming a 10% strain, sensors with sufficient travel to accommodate this were found to be a minimum of 25mm in diameter. When allowances had been made for assembly clearance and the sensors clearing the expected radial deformation of the specimen it was felt that the reduction in specimen size necessary to accommodate internal measurement would reduce the D/d_{max} ratio, and hence the repeatability and representative nature of the specimen, to an unacceptably low level (see Section 2.8.1(a) and Salman, 1994). For this reason, it was decided to use external measurement for axial strain. To accomplish this, a single LVDT of 50mm travel was mounted on the cell piston, to take readings against the cell top. As discussed in the literature review, Bressani (1995) has shown that if the correct procedures are followed, external measurement can be as accurate as internal measurement.

3.4.3 Radial Deformation

As stated in Section 3.4.2, it was felt that it was not possible to include any instrumentation that would impinge on the available radial space in the cell. Therefore, in order to measure the radial deformation, the cell was cut in half and an aluminium ring was inserted (see Fig. 3.1). Three radial LVDTs were then mounted horizontally on this with an angle of 120°

between them. This allowed the direct measurement of the radial deformation without reducing the available space in the cell. It had the disadvantage though of inflexibility, as the deformation could only be measured at one height unlike, for example, a radial collar. The ring and LVDTs were positioned such that they measured the deformation at the midpoint of a 455mm height specimen after 5% axial compression.

3.4.4 Cell Pressure

Cell pressure was measured by use of a conventional 100kPa pressure transducer mounted on a 'T' block on the inlet tap of the cell.

3.5 The Data Logging System

The monitoring system was based on a Viglen 486 DX 66 computer fitted with a Strawberry Tree ACPC16 16 bit converter card with 16 A-D converters and 16 digital I/O lines.

3.5.1 Static Tests

To record the data from the monotonic loading tests, the Strawberry Tree 'Workbench' program was used. This was programmed to read from each of the sensors at 15 second intervals and record the raw data directly to disk as a text file. The layout for this can be found in Appendix II. This data was then processed at a later date using the FORTRAN program detailed in Appendix II.

3.5.2 Cyclic Tests

Due to a fault in the user logging routines supplied with the logging card, it was necessary to use the Workbench program to log data from the cyclic load tests. This program was unsuited to the task as there was no provision for recording data on a logarithmic basis as is usual when carrying out cyclic load tests on granular material. Therefore, a system was created whereby at the start of the test when the controller was in slow mode, 10 readings were taken per loading cycle. When the controller switched to high speed operation, the logging program switched to taking a pair of readings every 10 load cycles. These readings were triggered by the inputs from the control unit to ensure that they remained synchronised throughout the test. The data was saved in the form of a text file to the RAM of the computer, as the time that would have been taken to save it to disk could possibly have disrupted the timing of the readings. The data then had to be copied to the hard disk at the end of the test. The workbench layout used for this can be found in Appendix II.

This system resulted in the recording of far more data than was needed for each test. To extract the required data, a Fortran 77 program was written (see Appendix II for program listing) to read the text files into the computer, extract the required data, convert this to engineering units using calibration data supplied in separate files, and write the files back to disk. This calibrated data was then imported into Microsoft Excel where it was converted, using Visual Basic macros, into more appropriate geotechnical parameters, and basic plots of axial strain, volumetric strain, resilient modulus, plastic strain and radial strain against number of cycles were produced for each test. The main data analysis program also calibrated the data produced by the static triaxial tests, and this data was similarly converted to basic geotechnical parameters and plotted using Visual Basic macros in Microsoft Excel.

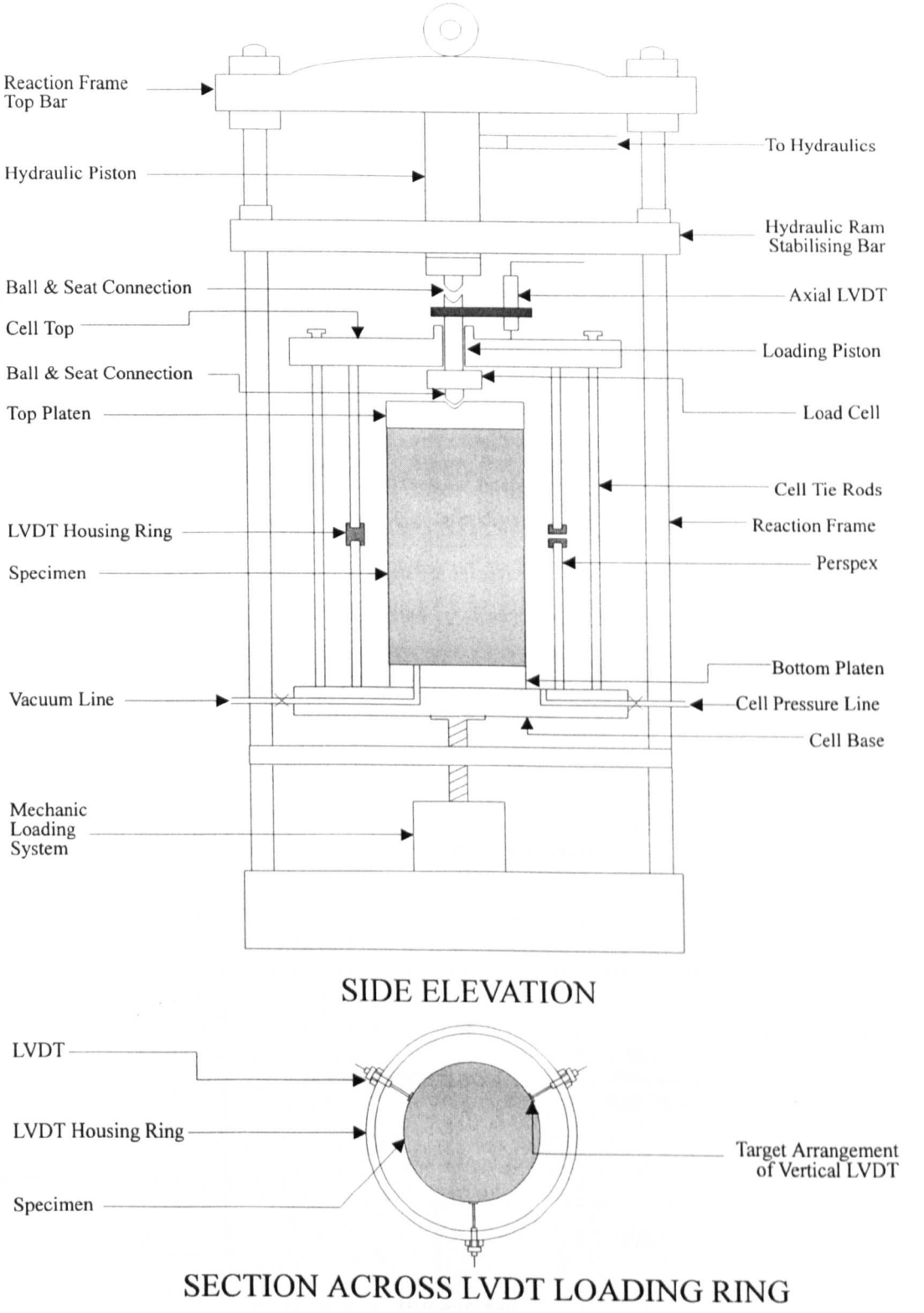

Fig. 3.1 - Diagram of the triaxial cell

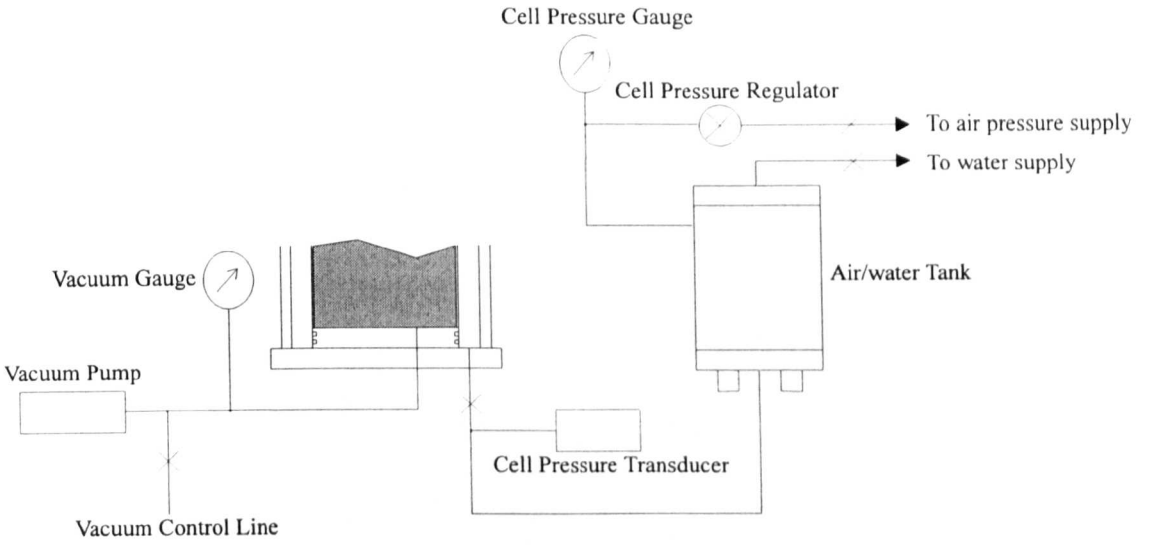

Fig. 3.2 - Diagram of the vacuum and plumbing systems

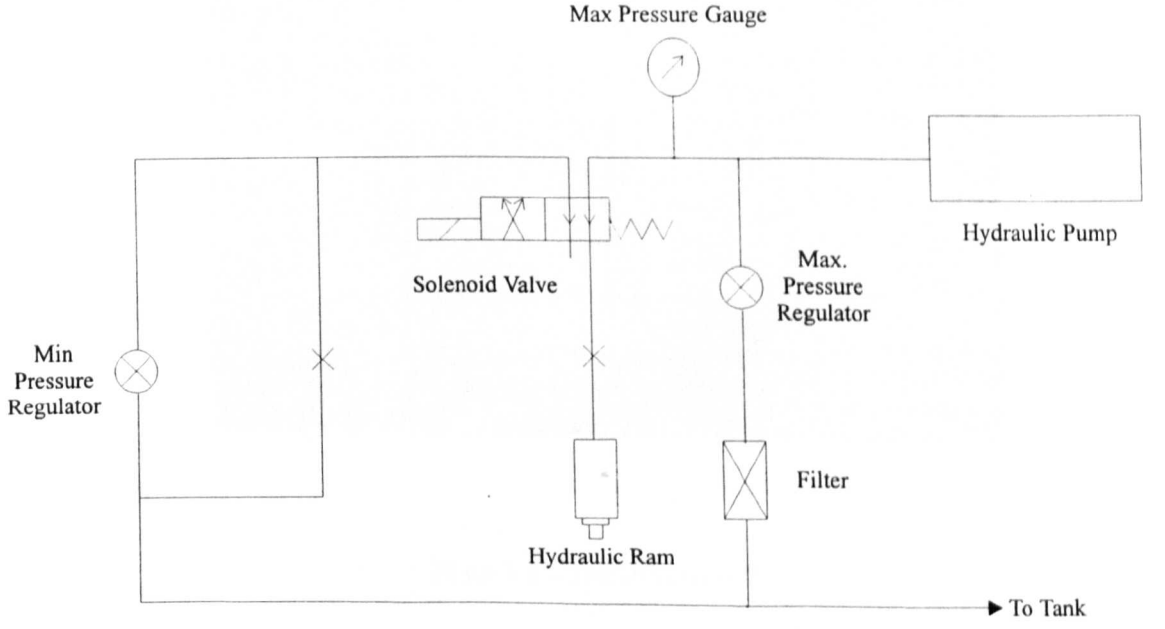

Fig. 3.3 - Diagram of the hydraulic loading system

Plate 3.1 - The triaxial cell

Plate 3.2 - The hydraulic loading system

Chapter 4 - Transducer Calibration and Data Corrections

4.1 Introduction

Good quality measurements are vital for high quality results. Instruments must have the required accuracy and range, should ideally have little drift and should be calibrated periodically to produce an accurate calibration factor. Also, good test results depend on a number of corrections being made to the data to improve its accuracy, such as correcting the axial deformation for equipment compliance.

This chapter covers the methods used to calibrate all the measuring devices, and the types and methods of corrections made to the data.

4.2 Calibrations

Table 4.1 lists the transducers used in the testing, their type, range and manufacturer's claimed accuracy. Table 4.2 lists their initial calibration factors, actual accuracy and drift with time.

The calibration data was recorded directly from the logging computer during calibration, and the data files were subsequently loaded into a spreadsheet. A linear regression was performed on the data to obtain the calibration factors for the transducers. The accuracy of each transducer was found by taking the maximum deviation from the best fit line, due to scatter in the results or hysteresis, and dividing this by the full range of the transducer. The calibration factor for the transducers was initially checked every six weeks or thereabouts, and it was found that variation in the calibration factors with time (drift) was generally negligible or very small. For this reason, a full re-calibration was only done approximately every six months. In the context of the testing programme, this meant that calibrations were done at the beginning, middle and end of testing. In the analysis, drift was corrected for by

linearly interpolating between the calibration factors with test number i.e. by equipment usage, which was in most cases uniform over time.

The exception to this was the load cell. It was found that doing a linear regression on the calibration data resulted in the greatest inaccuracies in readings being at the ends of the scale. During analysis of the data, it was necessary to accurately note the minimum load placed upon the sample and so the regression was skewed by fixing the intercept value to be that obtained during calibration. This resulted in a more accurate reading of minimum load at the expense of slightly reduced overall accuracy (R^2 was reduced from 0.999972 to 0.999956 for the final calibration)

A description of the methods used to calibrate each of the types of transducer can be found in the following sub-sections.

4.2.1 Linearly Variable Displacement Transformers (LVDT)

Two different types of LVDT were used in the research, the immersible free armature types with 25mm range used for direct measurement of the radial strains (three LVDTs), and the fixed armature type with 50mm range used for external measurement of the axial strain.

The transducers were left connected to the logging system and switched on for at least 24 hours prior to calibration. In general, the logging system was left switched on permanently. A Mitutoyo digital vernier accurate to 0.001mm was used for calibration. In the case of the free armature LVDTs, the electrical zero was found and the LVDT was then taken to each extremity of its range in steps of 2.5 mm, giving a total of ten steps over its full 25mm displacement. The calibration factor was determined from three complete cycles through the range of the transducer. The fixed armature type was taken in 0.5mm from its maximum range and calibrated from this point in steps of 5mm, again giving ten steps over its full range. Again, the calibration factor was determined from three complete cycles through the range of the transducer.

The LVDTs showed accuracies of 0.104% and 0.297% of the full scale deflection, which correspond to maximum errors of 0.012% for the axial strain and 0.063% for the radial strain respectively, both expressed as a percentage of the initial radial and axial dimensions.

The error due to drift of these transducers was found to be negligible for the axial transducer and one of the radial transducers. The drift for the other two radial transducers was noted to be significant. The three radial transducers are all from the same manufacturer and were nominally identical, and were all calibrated at the same time in the same manner, so the reason for the difference was unclear.

4.2.2 Load Cell

The Load Cell was a fatigue rated, submersible type from RDP Electronics. It was rated to 5000 lbs (22.5 kN) in both tension and compression, but was only used in compression for these experiments.

As with the other transducers, the load cell was left powered up for at least 24 hours before testing to give it sufficient time for its output to stabilise. For the purposes of calibration, the load cell was left in situ. The apparatus was assembled as for a normal test, except that the specimen was replaced by a calibrated load ring on steel blocks and no cell fluid was present. Great care was taken during assembly to ensure that the loading ring and load cell aligned vertically, thus ensuring that the loading ring was perfectly flat on its base and that no additional lateral forces would be generated during loading. The hydraulic ram control valve was then closed to lock the ram in place, and the system was loaded by manually winding the whole cell unit up and down on the loading frame. The load cell was loaded from zero load to 1000 divisions movement on the loading ring dial gauge (representing 25kN load) in steps of 100 divisions and then unloaded again in the same increments. The calibration factors were calculated from three such loading/unloading cycles. From the calibration card produced the last time the loading ring was standardised, it was found necessary to use a quadratic equation to ascertain the load on the loading ring from its dial gauge reading with the required degree of accuracy. This calculated load was then used to calibrate the load cell, which proved to have a linear response.

The accuracy of the load cell was slightly lower than the manufacturer's estimate, at 0.283% (although some of this may be contributable to the accuracy of the loading ring - 0.09%) which corresponds to an error of 1.6 kPa over the full scale. The drift of the load cell was relatively small at 76N per six months, corresponding to 1.7 kPa deviator stress at the maximum load.

4.2.3 Pressure Transducer

One pressure transducer of 100 kPa range was used in the experiments to measure the cell pressure. Again, this was left connected for at least 24 hours before calibration. A Budenberg air dead weight tester was used to calibrate the transducer in steps of 10 kPa. The load was cycled up and down in 10 kPa increments for three complete cycles, the calibration factors being calculated from this.

The accuracy of the cell pressure transducer was very good at 0.043%, corresponding to an error of 0.043 kPa. However, at 2.48 kPa per six months, the drift was significant.

4.3 Corrections

Corrections were made to several parameters to improve their accuracy. These were external axial deformation, radial stress, specimen cross sectional area, transducer output with voltage and top cap alignment.

4.3.1 External Axial Deformation

As the specimen was loaded, the loading equipment deformed slightly. Given that the axial strain was measured externally, this compliance was reflected to some degree in the total measured deformation. To increase the accuracy of the axial specimen deformation measurement, it was quantified and eliminated.

In order to do this a dummy specimen was made from high strength concrete As shown in Plate 4.1. This specimen was then coated with a thin skim of plaster of Paris at the ends and placed in a compression loading machine while the plaster set. This ensured that the ends were flat and parallel to give a true result for equipment compliance. The dummy specimen was then substituted for a real specimen in the equipment (although no cell pressure was applied) and was tested under cyclic loading and monotonic loading up to the maximum rating of the load cell. Whilst this was being done, the measured axial deformation and deviator stress were logged and used to produce a correction value.

It was found that the compliance was the same under both cyclic and monotonic loading and, within the range of the load cell, was linear. Repeating the test at every calibration also established that there was no perceptible drift in the value, with it remaining constant at

0.017 mm deformation per kN load. The dummy specimen was calculated to have a negligible deformation and no correction was made for this.

4.3.2 Radial Stress

Corrections for the radial stress due to the effect of membrane restraint were made using equation 2.8.3. This correction required a value for the elastic modulus of the rubber membrane, obtained using the method described by Keubris and Vaid (1995).

Corrections for axial and radial stress were then calculated using equations 2.8.3 and 2.8.4. These were found to be negligible as a percentage of the loads placed upon the specimens, and so the corrections were not incorporated into the final results.

4.3.3 Specimen Cross Sectional Area

As a specimen was compressed during tests, it underwent both volumetric and shear strain, with the result that it could 'barrel'. This meant that the cross sectional area, and hence axial stress on the material, could change as the test proceeded. In order to compensate for this, the most common form of correction was used. It was assumed that the barrelling was equivalent to a right cylinder of dimensions equal to the average between the ends and the midpoint of the actual sample. Knowing the original dimensions, and the deformation at the midpoint measured by the radial LVDTs, the assumed average cross section was calculated and hence the corrected stress was deduced.

4.3.4 Voltage correction

As the test proceeded, the value of the supply voltage to all the transducers may have fluctuated to a small degree. This would inevitably have altered their output, and hence the readings obtained were corrected for any deviation from the standard voltage.

In order to accomplish this, the transducers were all set to their maximum values - the axial LVDT was fixed at its fullest extent, the load cell was loaded to near its maximum limit with the concrete dummy sample in place and the pressure transducer was exposed to cell fluid at 100 kPa - and the supply voltage was varied whilst its value and the transducer outputs were monitored. It should be noted that the radial LVDTs had their own stabilised power supply and were not affected by fluctuations in the main power supply. It was not

possible to ascertain if the radial LVDTs were subject to fluctuations of this kind for any reason.

From analysis of this data, it was found that the transducer outputs varied linearly with voltage within the range of 10V ± 0.1V (see Figs. 4.1 - 4.3). The axial LVDT output was found to fluctuate at the rate of 4.593mm increase per volt increase at 49.029mm. The Load Cell output varied by 2.078kN increase per volt increase at 21.346kN and the cell pressure transducer registered 10.62 kPa increase per volt increase at 100.05 kPa

As the supply voltage was monitored at all times, these corrections could easily be calculated and fed back into the results.

However, approximately one third of the way through the testing programme, it was noted that there were very small fluctuations in the level of the supply voltage. On investigation, it was found that there was a loose connection on the power supply rail in the transducer junction box. When this was corrected, it was found that the reading of supply voltage was now steady but had increased by 0.05V. This would suggest that the previous readings had been slightly inaccurate, but the exact degree of this inaccuracy could not be quantified. For this reason it was decided not to apply the voltage correction to the data. In addition, a possible error corresponding to the change in the transducer readings with an assumed 0.05V increase in supply voltage needed to be taken into account during analysis of the data.

4.3.5 Alignment Correction

On approximately 20% of the initial, as opposed to post cyclic, monotonic triaxial tests, it was found that the deviator stress did not initially increase as expected with strain, but formed a plateau at the start of the stress / strain curve. This was always accompanied by an indication of radial expansion from one of the radial LVDTs and radial contraction from the other two. An example of this data is shown in Fig. 4.4. This was believed to be due to slight non-alignments of the top cap and piston, resulting in lateral forces being exerted by the piston on the top cap as it was forced into the ball seat. Once the lateral force reached a certain level (the plateau level), this caused the top cap to move sideways until the seat was aligned and the piston was forced fully into it. This non-alignment is shown diagramatically in Fig. 4.5. As the top cap moved, it must have moved the specimen laterally with it due to

platen / specimen friction. This would therefore explain the movement in one direction by one of the radial LVDTs and movement in the opposite direction by the others.

Given that this is a well recognised phenomenon, and that the problem never extended beyond an axial strain of 0.6%, corresponding to a movement of 2.6mm, much less than the depth of the top platen seat, it was decided to just remove the data in the affected tests up to the point where the rate of increase in deviator stress had reached a constant. In all cases, there were at least four remaining points in this zone of constant stress increase rate, and these were then used to back calculate what the values of the origin should be.

No. of Transducers	Type of Transducer	Manufacturer's Claimed Accuracy	Measuring Range	Parameter Measured
3	Free Armature Immersible LVDT	0.5% F.S. Manufacturer - RDP	± 12.5mm	Specimen Radial Strain
1	Fixed Armature DC LVDT	0.5% F.S. Manufacturer - MPE	0 - 50mm	Specimen Axial Strain
1	Immersible Fatigue Rated Load Cell	0.1% F.S.(hysteresis) 0.1% F.S.(non linearity) Manufacturer - RDP	0 - 22.5kN	Specimen Deviator Stress
1	Pressure Transducer	0.1% F.S. Manufacturer - CE	0 - 100kPa	Specimen Cell Pressure

Table 4.1 - Transducers Used in the Investigation

Transducer Type	Calibration Factor	Accuracy (% of F.S.)	R^2	Average Drift
LVDT - Radial Strain S/N 3196	12.832 mm/V	0.259	0.999991	0.212mm per six months
LVDT - Radial Strain S/N 3197	13.315 mm/V	0.297	0.999968	0.207mm per six months
LVDT - Radial Strain S/N 3195	12.798 mm/V	0.278	0.999993	0.021mm per six months
LVDT - Axial Strain S/N HS 50/7069	1484.0 mm/V	0.104	0.999997	0.067mm per six months
Load Cell S/N 491338	1135.0 kN/V +0.023	0.283	0.999943	75.6N per six months
Pressure Transducer S/N 790495	1101.1 kPa/V +0.836	0.043	0.999999	2.48kPa per six months

Table 4.2 - Calibration Factors and Accuracy of Transducers Used in the Investigation

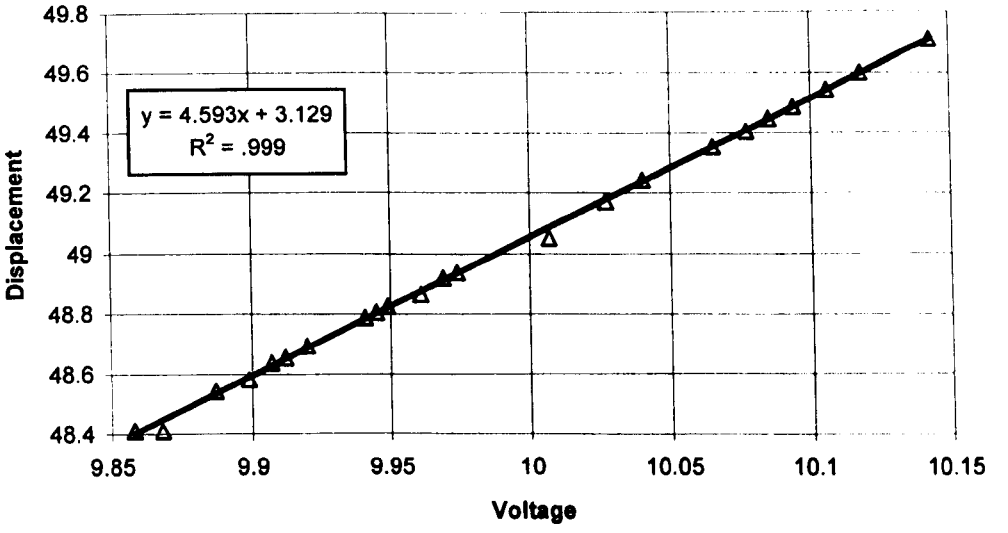

Figure 4.1 - Variation in axial displacement reading with voltage

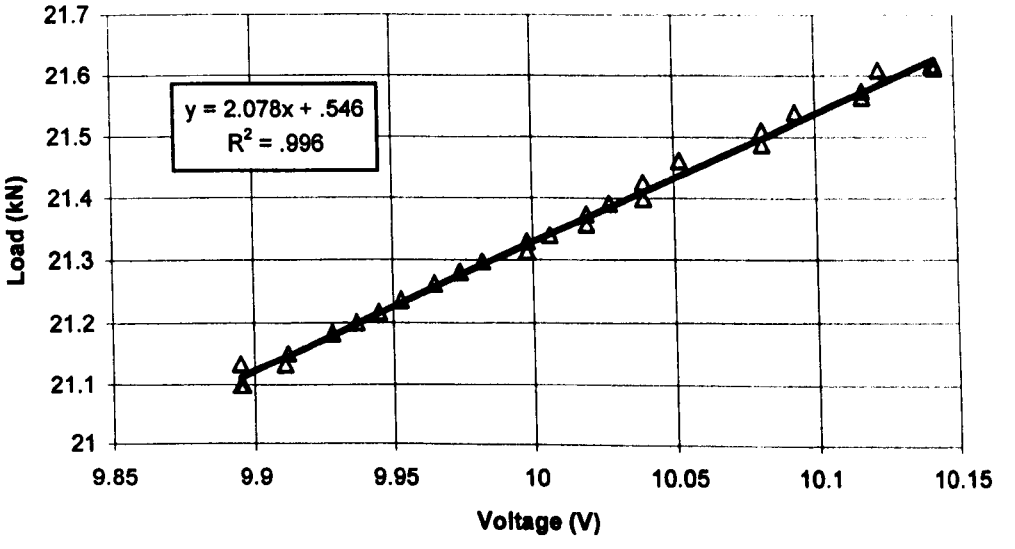

Figure 4.2 - Variation in load reading with voltage

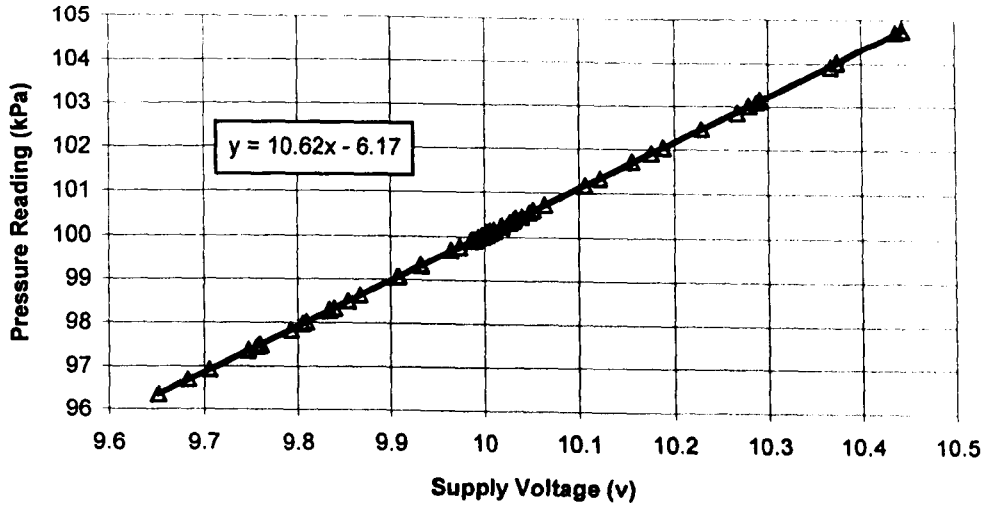

Figure 4.3 - Variation in cell pressure reading with voltage

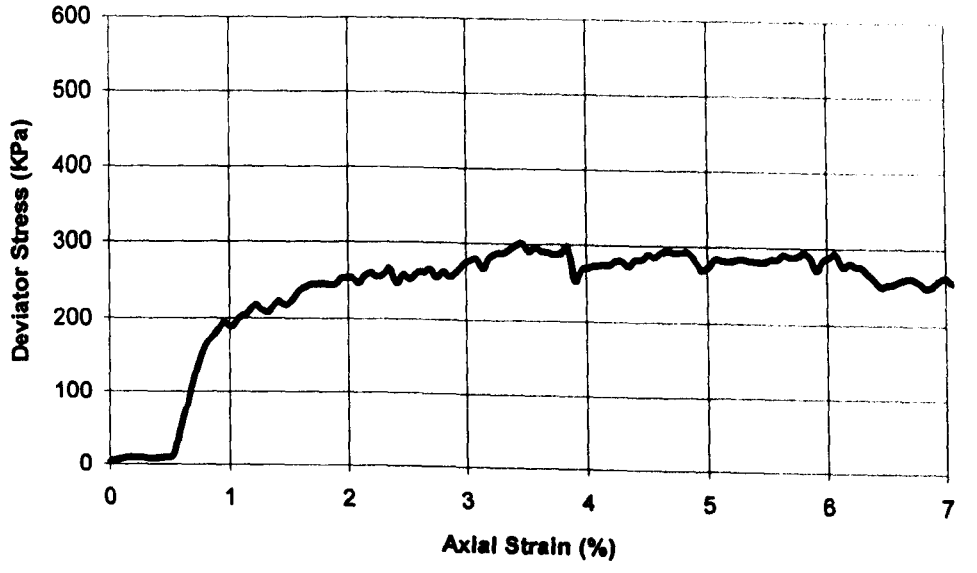

Figure 4.4 - Typical stress-strain curve resulting from non-alignment of top platen and piston

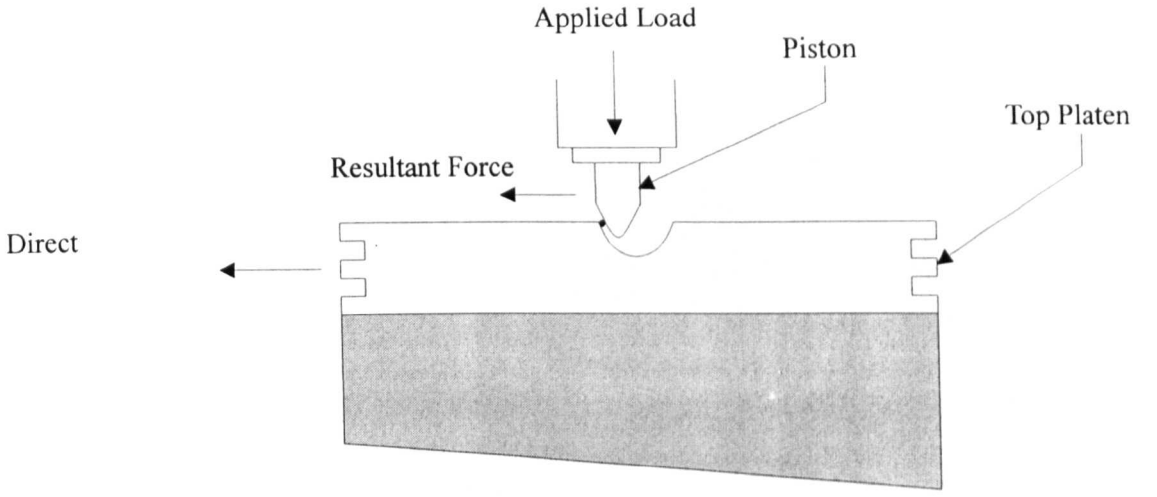

Figure 4.5 - Diagrammatic representation of top platen non-alignment

Plate 4.1 - Concrete dummy specimen

Chapter 5 - Materials and Triaxial Test Procedures

5.1 Materials

Six different materials were used in the test programme. The main one of these was the 50mm aggregate supplied by E.C.C. Aggregates. This material was a granite conforming to the British Rail specification for railway ballast (see Appendix III) except for the fact that collection from the production facility necessitated bypassing the jet washing plant. To compensate for this, the material was washed manually to remove the dust fraction. The other materials used comprised of a 20mm aggregate conforming to the Railtrack specification of Pneumatic Ballast Injector (Stoneblower) stone, which was obtained via Railtrack from an unknown source, 20mm rounded uncrushed river gravel obtained from Shardlow and 14, 10 and 6mm gradings of crushed granite aggregate obtained from A.R.C. Central Aggregates. In each case, the entirety of the material came from one batch, and the batch was thoroughly mixed before use. No material was re-used. The full specifications of each material are given below. Particle Density was measured by the gas jar method given in BS 1577:1990.

5.1.2 50mm Ballast Stone

Source: Croft Quarry, Leicestershire.

Map Reference: SP 512 965

Description: Medium Grained Granite. Mixture of grains, some comprised mainly of quartz and plagioclase feldspar giving a whiteish appearance, and others comprised of mainly quartz and orthoclase feldspar giving a pinkish appearance characteristic to material from this quarry.

Particle Density: 2.67

Grading:

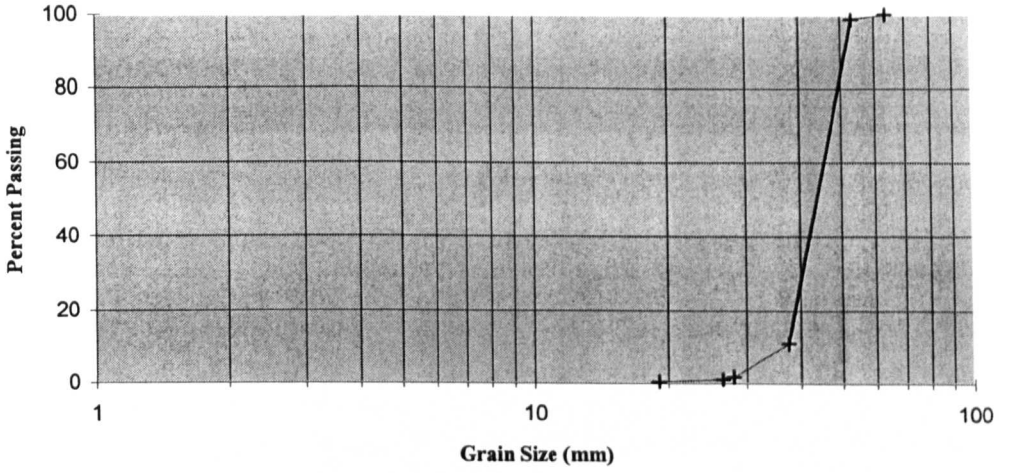

5.1.3 20mm 'PBI' Stone

Source: Railtrack

Description: Greenstone (Metamorphic) with quartzite intrusions.

Particle Density: 2.85

Grading:

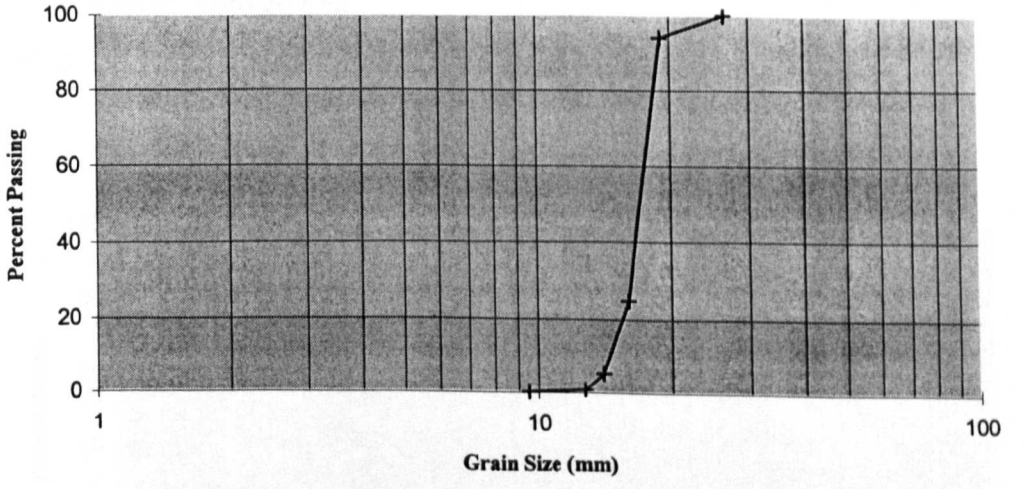

5.1.4 14/10/6 mm Stone

Source: Cliffhill Quarry, Leicestershire.

Map Reference: SK 412 110

Description: Medium Grained Granite comprised of Quartz, Plagioclase Feldspar,

Orthoclase Feldspar and accessory minerals.

Particle Density: 2.81

Grading:

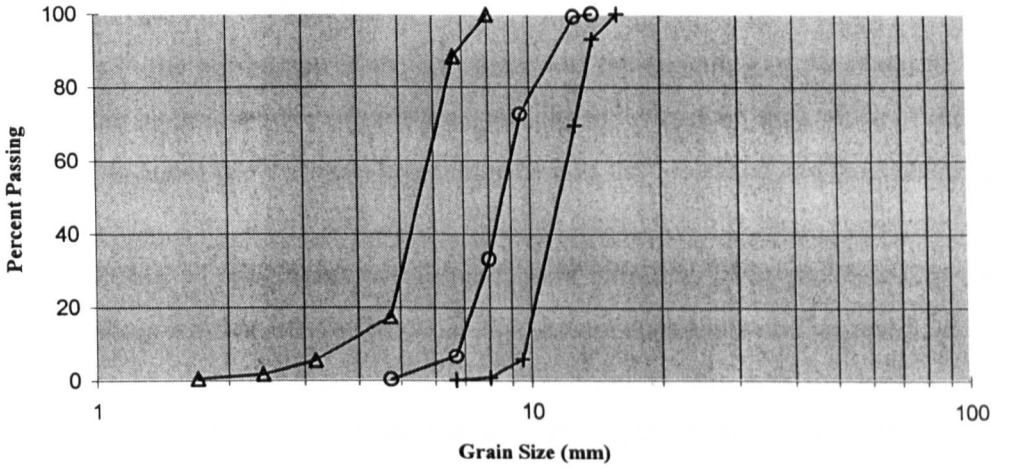

5.1.5 20mm River Gravel

Source: Shardlow

Map Reference: SK 318 305

Description: Washed, uncrushed river gravel. A mixture of quartzite and igneous rocks

Particle Density: Average 2.62

Grading:

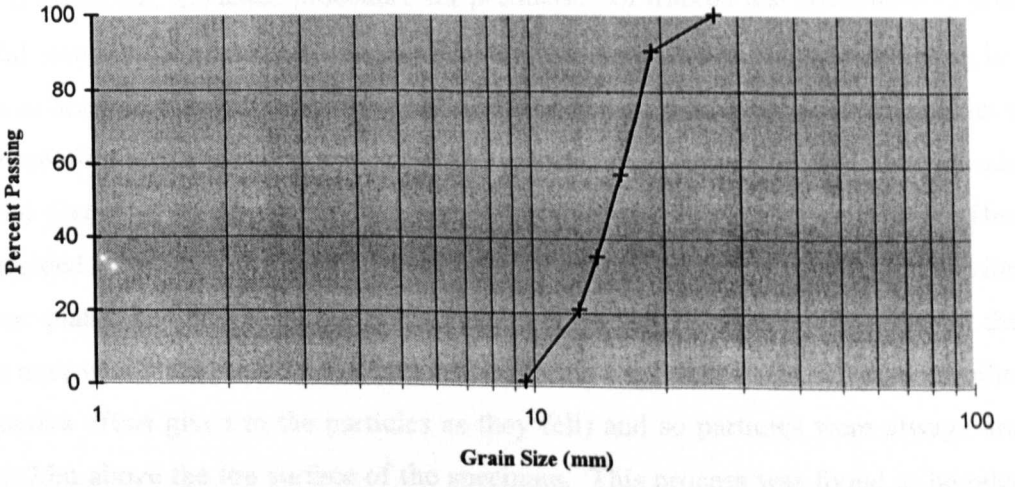

5.2 Test Procedures

This section details the procedures used for preparing the test specimens and setting up the tests. In each test series, both monotonic and cyclic load test specimens were produced in an identical manner.

5.2.1 Production of Test Specimens

The first stage in the production of the specimen was the sampling of the material. Despite the fact that the materials were of uniform grading, and therefore separation of the particle sizes was not an issue, the materials were mixed when first obtained and then placed in their storage containers. The ballast and 20mm material were stored in large aggregate bags, and the other materials, of which less was needed, were stored in 25kg plastic sacks. Material needed for testing was then shovelled out of the storage containers and air dried for 24 hours before the specimen preparation. The only exception to this was the ballast, which as mentioned in Section 5.1 needed to be washed before use. In this case, sufficient material for about eight tests was removed from the storage area at a time and washed, and was then stored next to the main supply ready for use. Stone was subsequently removed from this pile as required and air dried for 24 hours prior to the test as for the other materials.

The test specimens were constructed on the base platen of the triaxial cell to minimise disturbance during assembly of the test apparatus. To prepare the samples, a rolled aluminium mould (see Plate 5.1) was produced of 236mm internal diameter, sufficient to just sit over the base platen, inner membrane and 'O' ring seal. This mould was made in two halves, joined with eight bolts.

It was decided that the usual procedure for production of triaxial test specimens of granular material, namely compaction in measured layers, was not suitable for tests involving ballast. This was because compaction of material of this size would tend to cause unusual levelling and orientation of the particles with a flat face against the compaction tool, thus introducing artificial planes of weakness into the sample and perhaps altering its behaviour. Hence it was decided to prepare specimens by dropping the particles into a mould, whilst vibrating the base platen and mould on a vibrating table. Preliminary investigation showed that the height over which the particles fell was crucial to the final density (in effect, controlling the compactive effort given to the particles as they fell) and so particles were always dropped from 0.75m above the top surface of the specimen. This process was found to be relatively

time insensitive, as long as each particle had a couple of seconds to fall into place then time had no noticeable effect on the range of densities achieved. To compact the top of the specimen to the same degree as the rest of the material, and to produce a relatively flat contact surface at the top, it was decided to place the top platen on the top of the specimen and surcharge it. In the preliminary investigation it was found that surcharging beyond 20kg had relatively little effect, and so this weight was chosen. Specimens were surcharged for 1 minute under vibration on the vibrating table.

The specimens prepared with the smaller grained materials were produced in a similar manner, except that they proved to be more time sensitive. For this reason the materials were added steadily to the mould over a period of one minute, left for a further 15 seconds to vibrate, and were then vibrated under surcharge for 30 seconds.

To produce two layer specimens, the ballast was added up to the required level, which was marked on the inside of the membrane, whilst under vibration and surcharged. The actual height of this first layer was next measured relative to the top of the mould. The second material was then poured on top of the first under vibration, over a period of time proportional to the thickness of the top layer, and surcharged as normal.

The exception to this procedure was when producing specimens with an angled interface. In order to produce these specimens, special wooden formers were manufactured with bottom faces at the required angles (see Plate 5.2) The original idea was to place the required quantity of ballast into the mould as normal, allowing the correct volume of ballast for a 50/50 split, ballast and top layer, to be gauged accurately, and then put the angled former on top of the ballast with the usual surcharge load. Under the combination of load and vibration, they would form the ballast surface into the required angle. In practice, however, this did not work as a combination of friction against the rubber membrane, tilting of the former and resistance of the ballast to deformation prevented the former from moving downward into the ballast. The problem was overcome by placing the required quantity of ballast in the mould, stopping the vibration and then moving individual particles by hand to form roughly the correct angle for the interface and with its highest point circumferentially adjacent to one of the radial LVDT's. The surcharged former was then placed onto the ballast and vibration was restored to compact the ballast and produce exactly the required angle of surface. As with the other two layer specimens, the distance between the top of the

angled former and the top of the specimen mould was recorded to determine the position of the interface. Addition of the top layer of material was carried out by pouring sufficient stone into the mould to cover the angled ballast surface before commencing vibration, the lateral pressure of the fine grained material stopping the ballast particles from vibrating out of position and changing the angle of the interface. The rest of the material was added to the required level over a period of 30 seconds under vibration, and surcharged as normal.

The full sequence for producing a specimen was as follows. Firstly, the cell base / bottom platen was bolted to the vibrating table and the lower end of the inner sample membrane was stretched over the bottom platen. This was then secured to the bottom platen by means of an 'O' ring in the upper of the two 'O' ring grooves. The specimen mould was next placed over this, flange cutout uppermost, and an 'O' ring placed over it at the top. The membrane was then brought up the inside of the mould and stretched over the top, before being tucked under the 'O' ring to secure it in place. To manufacture a two layer specimen the required height of the first layer was marked on the inside of the membrane with chalk at this stage. The vibrating table was then switched on, and the materials were poured in so that the sample could be prepared (the exact method being dependent on the test being conducted). The buckets containing the material used for the samples were weighed both before and after pouring to determine the mass of the material used.

After specimen preparation, the vacuum pump was connected to the vacuum port on the cell base. It was necessary to start with the vacuum valve on the cell base and the vent valve in the vacuum line open. The vacuum pump was then switched on, and the vacuum line vent valve closed slowly until a vacuum of 100mm of mercury or thereabouts was shown on the gauge. Measurement of the height of the specimen was carried out by measuring the distance of the top platen below the top of the mould at the three points above the radial LVDT's. If there was more than 2mm difference between any of these values, corresponding to a tilt of 1 in 100 (i.e. 0.5°), the specimen was deemed to be unacceptable and discarded. The 'O' ring securing the inner membrane to the top of the mould was then removed, and this allowed the membrane to be lifted from around the top of the mould. The bolts holding the two halves of the mould together were then removed and the mould taken off the specimen, now supported by the vacuum. The inner membrane was then secured to the top platen by means of an 'O' ring in the lower of the two grooves.

A second, outer, membrane was put over a stretcher ring and eased over the specimen, taking care that the bottom of the membrane did not cover the cell water inlet. This membrane was secured in place with an 'O' ring in the empty grooves of the top and bottom platens.

Finally, the LVDT targets were glued to the outer membrane using silicone sealant. Their position was measured using the cell body as a circumferential guide and a tape measure to place them 240mm above the cell base. This height was chosen so that the target was at the midpoint of an average specimen after 5% axial deformation.

5.2.2 Cell Assembly

The bolts securing the cell base to the vibrating table were first removed, and the cell base/body sealing ring was smeared with grease and placed in its groove. The axial LVDT and load cell were then temporarily disconnected from their power/output sockets. After checking that the aluminium block preventing the load cell and piston from slipping out of the cell was securely in place, the cell body was lowered over the specimen using a pulley block and rotated to ensure that the body and base lined up correctly (denoted by chalk marks). The cell body was then lowered over the specimen, using a piece of plastic pipe to guide the load cell cable into the correct position and the protruding ties to locate the body precisely. The cell body was secured in place by tightening the ties, working on diametrically opposite pairs of ties at the same time.

The vacuum valve on the cell base was then closed, the vacuum pump switched off and the vacuum line disconnected from the cell base. The cell was now free to be lifted into the loading frame. When in the frame, the cell was secured in place by means of a strap around the cell and the loading frame posts. The Load Cell and axial LVDT were then reconnected to their output sockets. Having ensured that the armatures were correctly in place and the seals were greased, the radial LVDTs were bolted into their mountings, all four bolts being fully tightened. The ram stabilising bar and frame reaction bar (see Fig. 3.1) were then mounted into their correct places and screwed down.

5.2.3 Cell plumbing

The cell water line was connected to the base of the cell, and the control valve opened. Having ensured that the valves on the top of the air/water tanks were closed, and the vent

valve on the top of the cell was open, the cell pressure regulator was opened to fill the cell. As soon as water was seen to come from the vent valve on the top of the cell, the cell fluid control valve on the cell base was closed. The vent valve was then closed, and the vacuum valve opened to release the vacuum within the sample and ensure that the test was drained. Finally, the cell pressure was adjusted to the required value and the cell fluid valve was opened.

5.2.4 Commencement of Test

The procedure for starting the test depended on whether a monotonic or cyclic test was being conducted.

5.2.4(a) Monotonic test

The computer was rebooted, and the 'static' workbench setup was selected. The supply voltage was adjusted to exactly 10.000V and the filename was set on the logging icon. After ensuring that the hydraulic ram shutoff valve was closed, the compression frame platen was wound manually up to the point where the top of the piston was almost touching the hydraulic ram. The manual control wheel was locked in place, the logging was enabled and the compression frame driving motor was set to the 'cell up' position.

The test was left running until one of the LVDTs was at the point of exceeding its range, at which point the compression frame driving motor was switched off.

5.2.4(b) Cyclic Test

The computer was rebooted, to ensure the correct operation of the ramdrive, and the autoboot (cyclic load test) setup was allowed to come on. All the hydraulic valves were closed. The valve to the selection of accumulators was then opened, the appropriate accumulator being dependent on the oil pressure used. The hydraulic control unit was then switched on and the hydraulic oil pressure was allowed to stabilise. The controller was set to manual mode, and the operation of the unit checked. The supply voltage was then adjusted to 10.000 V and the logging icons set with the appropriate filenames and test descriptions. As with the static test, the cell was wound manually up to the point where the piston was almost touching the hydraulic ram. The control unit was reset, the ram control valve opened and the control unit set to automatic. The test started at low speed. After completing 50 cycles at low speed, the control unit was switched to high speed, after which the test was left to run its course for 100,000 cycles.

5.2.5 Completion of Test

After the cyclic test had been completed, the data was first moved from the ramdrive to the hard disk of the logging computer to ensure a permanent record. Provided that none of the LVDTs had reached the end of their travel, a monotonic loading test was carried out on the specimen for comparison purposes. For this, the same procedure was followed as for a normal monotonic loading test, except for the fact that the cell piston was already in contact with the hydraulic ram so that there was no need to manually adjust the elevation of the cell.

On completion of the test, dismantling of the cell was carried out in the reverse order to assembly. Attention was paid to the state of the specimen, with any unusual deformations or the presence of water being noted. Finally, the specimen was discarded along with any excessively stretched or distorted membranes, and the equipment was cleaned ready for the next test.

5.2.6 Data Processing

The data from the tests was processed using a dedicated program, covered in Section 3.4, which extracted the required data from the logging files and converted it to engineering units using data from the transducer calibrations, linearly interpolated between calibration points. This program also corrected the data for external axial strain, as detailed in Section 4.3.1. The data was then converted to standard geotechnical parameters using Microsoft Excel with corrections being made for cross sectional area (Section 4.3.3) and specimen alignment (Section 4.3.5) as necessary. Microsoft Excel was also used for any further manipulation and comparison of data.

5.3 Numbering of Test Sets

The test programme was divided into a number of different Test Series, each with a different objective. Each Series consisted of a number of weekly Test Sets. Each test set consisted of a monotonic triaxial test, a cyclic load triaxial test and a post cyclic monotonic triaxial test carried out under the same conditions and using identical starting specimens. This testing could be fitted into a week, thus facilitating easy scheduling of the programme.

The Test Sets were numbered in the chronological order in which they were carried out, with the exception of the repeatability tests of the main test series, which were designated with 'REP' instead of a number. Thus there were a total of 40 test sets and two 'REP' sets.

Test Sets 1 and 2 were trial tests, and are therefore not to be found in the analysis of results.

The test sets were then grouped into separate Test Series. Each Series considered a different set of test parameters. In order to reduce the number of tests that needed to be carried out, the test conditions were arranged so that some sets could be included in more than one Test Series. Thus, for example, Test Set 5 consists of specimens with equal layers of ballast and 20mm material, with a horizontal interface between the layers, carried out at a cell pressure of 40 kPa. This Test Set can therefore be included in Series TB, where the size of the material in the top layer is varied (in this case it is 20mm material), in Series TC where the cell pressure on two layer specimens is varied (in this case, it is tested at 40 kPa cell pressure), and in Series TD where the angle of the layer interface is varied (in this case, the angle of the interface is zero). Therefore, Set 5 appears as TB-5, TC-5, and TD-5 even though only set of experiments was carried out.

In addition, it should be noted that in Series TA, the characterisation tests for ballast and the 20mm material with a 40 kPa cell pressure were carried out at the start of the main test series, to enable analysis of the following tests to begin as early as possible, and given their importance they were then repeated at the end of the main test series. This means there are some Test Sets that are duplicated in this Test Series.

For completeness, a list of the tests carried out and test conditions in each case, listed by Set number, can be found in Appendix IV.

5.4 Test Series

The test series carried out are summarised in the following sections, with the details of the tests in each series to be found in Tables 5.1 to 5.11. In each case, the tests were carried out under standard conditions with any variation from this being listed in the tables. For two layer tests, the standard test conditions were equal layer thicknesses of each material, with the interface between the layers horizontal. The bottom layer was always ballast and the top layer was 20mm material unless stated otherwise. For all tests, the standard cell pressure was 40kPa. Under cyclic load conditions the deviator stress was cycled between 10 kPa and 250 kPa. Ideally, the consequences of different stress ranges on each of the sets of conditions would have been investigated, but this would have added an order of magnitude of complexity to an already crowded test schedule. For this reason, it was felt that a

constant load range was best for the sake of comparison, as there was also a significant amount of literature already covering the effect of varying the peak load of a cyclic load test.

5.4.1 Series TA - Characterisation of Materials Used

In order to analyse the behaviour of a two layer system, the behaviour of the individual materials was established to enable a comparison. For the 'minor' materials, this consisted of one test series, carried out with a cell pressure of 40 kPa. For the 'major' materials (i.e. ballast, 20mm stone and the rounded river gravel) a second series was also conducted at 90kPa to gain more of an insight into the behaviour envelope. Initially, the PBI stone and ballast were characterised at 40kPa cell pressure at the start of the test programme, but given the importance of these tests (forming the basis for most of the analysis) they were repeated at the end of the programme.

5.4.2 Series TB - Stone Size

For this series of tests, the 20mm stone in the two layer specimens was replaced with one of the smaller gradings of stone. The aim of these tests was to find out how the two layer system behaved when comprised of layers of differing size ratios.

5.4.3 Series TC - Effect of σ_3

This series of tests was designed to form the initial analysis of a two layer system. These specimens were tested at 30, 40, 60 and 90kPa to assess how they behaved with differing lateral stress.

5.4.4 Series TD - Effect of Angle of Interface Between Materials

Specimens were made from equal volumes of ballast and PBI stone, but with differing interface angles to test how the system behaved when the principal stress was in a direction other than perpendicular to the layers of material e.g. railway track under cornering loads - see Section 2.5.2. Specimens were produced with the interface at 11, 22, 33 and 45 degrees from perpendicular to the main axis of the specimen. Stresses were kept identical to the other tests - 40kPa cell pressure and 10kPa to 250kPa cyclic deviator stress - to facilitate comparison with the other test series. This did not directly simulate loading under cornering for a ballast bed, as that would have consisted of the same load perpendicular to the layers with an additional lateral component. However, once the behaviour under differing angles

of interface was established and given a knowledge of the behaviour of granular materials under different magnitudes of load, this could have been translated to cornering conditions.

5.4.5 Series TE - Effect of Layer Thickness

For this series of tests, specimens were made up with varying proportions of ballast and 20mm stone. These tests were designed to ilustrate the effect of varying degrees of restraint on the specimen. It was expected that each layer in the specimen would behave like a 'short' triaxial specimen, i.e. a specimen with a height to diameter ratio of less than the normal 2:1.

5.4.6 Series TF - Stone Type and Angularity

A series of tests were carried out with a different type of stone to assess whether the trends found in the other tests were peculiar to railway ballast type aggregates. In these tests, rounded river gravel was chosen as the second material for the two layer tests as it possessed particle characteristics at the opposite end of the scale to those of the granite aggregates - round, near spherical particles with relatively smooth surfaces. The material was of the same maximum particle size as the 20mm stone, and had a relatively uniform grading, although it was found to be slightly less uniform than the 20mm stone. The majority of these tests were carried out with a cell pressure of 90 kPa as it was found that the material was unable to resist the cyclic deviator stresses used with lower cell pressures.

5.4.7 Series TG - Mesh Elements

Section 2.4.1 described how randomly orientated sections of geogrid have been used in the past to reinforce granular materials such as sand. It was hypothesised that the same principle could be used to reinforce railway ballast, and so a series of tests were carried out to investigate this.

Firstly, the type of mesh to be used was chosen. The reinforcement had to work by the ballast particles penetrating the holes in the grid, and thus allowing the sections of the grid to exert a reaction force on the particle side. Unlike sand, however, this cannot occur throughout the grid, merely at a few discrete points within the system due to the large particle size and so there could not be continuous contact. If the size of the grid was too large, there would have been large amounts of deformation before the grid came into contact with the particle, which would have made the system of little use for maintaining the

geometry of a ballast bed. If the grid had been too small, the ballast particles would not have penetrated the grid sufficiently to produce a good interlock and high reaction force. Similarly, if the grid had been too flexible, there would have to been large strains in the material before the reinforcement had strained sufficiently for a reaction force to be developed. On this basis, a Tensar SS40 geogrid from Netlon was chosen as the reinforcement (see Plate 5.3). This was an orientated polypropylene geogrid with a grid spacing of 33mm and a rib thickness of 2.2/2.5 mm. This gave a high flexural stiffness and breaking strength (40kN/m), an advantage when dealing with the large stresses present in a ballast bed.

It was decided that this material should be cut into 100mm squares. This gave a 3*3 grid arrangement, as can be seen in Plate 5.3. It was felt that this was the maximum size that could be justified for a ballast bed, the bed being as little as 300mm deep in some cases. Had the grid been larger, the pieces of material could have interfered with or been damaged by maintenance procedures.

In addition to the Netlon elements, it was decided to investigate the use of another material to try and achieve the same effect. Terram 1500 by Terram Ltd. was chosen (see Plate 5.4). This was a non-woven geotextile formed from polypropylene fibres randomly orientated and heat bonded together, and had the property of being equally strain resistant in all directions, unlike woven geotextiles. It was envisaged that this material would work by becoming trapped at particle interfaces and exerting tension between these points. This material was chosen as it had the highest tensile strength of the Terram series of materials. It too was cut into 100mm square sections for use as reinforcement.

In each mesh element test, specimens were made up of ballast to which ten elements were added. These were dropped in at roughly equal spacings during specimen preparation. Unfortunately it was found during trials that this would not work, as the vibration resulted in the reinforcement 'floating' on the top of the specimen as it was prepared. The Netlon sections were a particular problem, as they were manufactured of elastic material, and any particles that landed on top of them would just bounce off. To overcome this, when each section of reinforcement had been added, two or three ballast particles were placed on top of it by hand to locate it in place, after which the ballast was added in the usual fashion. The specimens were then tested as normal, under the usual loading conditions.

5.4.8 Series TH - Repeatability of Main Test Series

Identical tests were carried out near the beginning, at the middle and at the end of the test programme to check if the results were the same in each case, and thus to show that any results and trends found from the test series were not just random. This also served as a check that the test equipment was performing consistently.

5.5 Further Tests

As explained in Section 6.3.1 it was necessary to carry out further tests to establish the behaviour of the material under differing conditions. These tests were carried out as a separate group five months after the main test programme with calibrations at the start and end of this secondary test programme. The tests carried out are listed below. All sets consisted of the cyclic load test and the post cyclic monotonic load test only.

5.5.1 Series TI - The Effect of Differing Minimum Stress During Cyclic Loading

A series of tests were carried out on two layer specimens with each test having a different minimum cycling stress. The aim of these tests was to investigate how the change in minimum stress affected the plastic and elastic strains.

5.5.2 Series TJ - The Effect of Water on the Specimen Behaviour

A test was carried out to investigate the effect of the presence of water on the deformation of the specimen. This test was carried out without any pore fluid and was drained, as for the other tests, but the materials were soaked in water for two hours before the start of the test.

5.5.3 Series TK - Repeatability

The repeatability of the secondary test programme was checked to ensure the results were consistent, and to see how they compared with the repeatability results from the main test programme.

Test Series TA - Characterisation of the materials	
Test Set	Comments
3	Characterisation of ballast
31	Repeat of Test Set 3
32	Characterisation of ballast with cell pressure of 90 kPa
4	Characterisation of 20mm stone
25	Repeat of Test Set 4 - Lost due to water leak
26	Repeat of Test Set 4 - Lost due to water leak
27	Repeat of Test Set 4
30	Characterisation of 20mm stone with cell pressure of 90 kPa
15	Characterisation of 14mm stone
17	Characterisation of 10mm stone
19	Characterisation of 6mm stone

Table 5.1 - Summary of Test series TA

Test Series TB - Variation in Stone Size With Layered Specimens	
Test Set	Comments
5	Top layer of 20mm material
16	Top layer of 14mm material
18	Top layer of 10mm material
20	Top layer of 6mm material

Table 5.2 - Summary of Test Series TB

Test Series TC - Effect of Cell Pressure on Two Layer Specimens	
Test Set	Comments
5	Cell pressure of 40 kPa
6	Cell pressure of 60 kPa
7	Cell pressure of 90 kPa
8	Cell pressure of 30 kPa for monotonic test and 35 kPa for cyclic test

Table 5.3 - Summary of Test Series TC

Test Series TD - The Effect of the Angle of Interface Between the Two Layers	
Test Set	Comments
5	Horizontal interface
9	Interface at 11° to horizontal
10	Interface at 22° to horizontal
11	Interface at 33° to horizontal
12	Interface at 45° to horizontal

Table 5.4 - Summary of Test series TD

Test Series TE - Effect of Layer Thickness	
Test Set	Comments
13	350mm Ballast, 100mm 20mm stone
5	Equal ballast and 20mm stone
14	150mm Ballast, 300mm 20mm stone

Table 5.5 - Summary of Test Series TE

Test Series TF - Use of Rounded River Gravel	
Test Set	Comments
21	Characterisation of rounded River Gravel, 90kPa cell pressure cyclic test
22	Two layer specimen, 90kPa cell pressure for cyclic load test
23	Two layer specimen with interface at 45° to horizontal, 90kPa cell pressure
24	Two layer specimen, 60 kPa cell pressure
33	Two layer specimen, 90kPa monotonic test, no cyclic test

Table 5.6 - Summary of Test Series TF

Test Series TG - Mesh Element Reinforcement	
Test Set	Comments
28	Ballast with Netlon elements
29	Ballast with Terram elements

Table 5.7 - Summary of Test Series TG

Test Series TH - Repeatability of the Main Test Series	
Test Set	Comments
5	Basic two layer test
REP2	Mid programme repeatability test. No monotonic test
REP3	End of programme repeatability test. No monotonic test
3	Ballast Characterisation
31	Repeat of Test Set 3
4	20mm material characterisation
27	Repeat of Test Set 4

Table 5.8 - Summary of Test Series TH

Test Series TI - Variation in Minimum Cycling Stress	
Test Set	Comments
37	Low minimum stress - 8kPa
35	Medium minimum stress - 17kPa
36	High minimum stress - 25kPa, lost due to water leak
38	Repeat of test set 36

Table 5.9 - Summary of Test Series TI

Test Series TJ - Effect of Water on Deformation	
Test Set	Comments
35	Materials tested dry
39	Materials soaked for 2 hours before test

Table 5.10 - Summary of Test Series TJ

Test Series TK - Repeatability of the Secondary Test Series	
Test Set	Comments
35	Standard test at start of secondary programme
40	Standard test at end of secondary programme
5	Standard test from main programme for comparison
REP2	Mid programme repeatability from main programme for comparison

Table 5.11 - Summary of Test Series TK

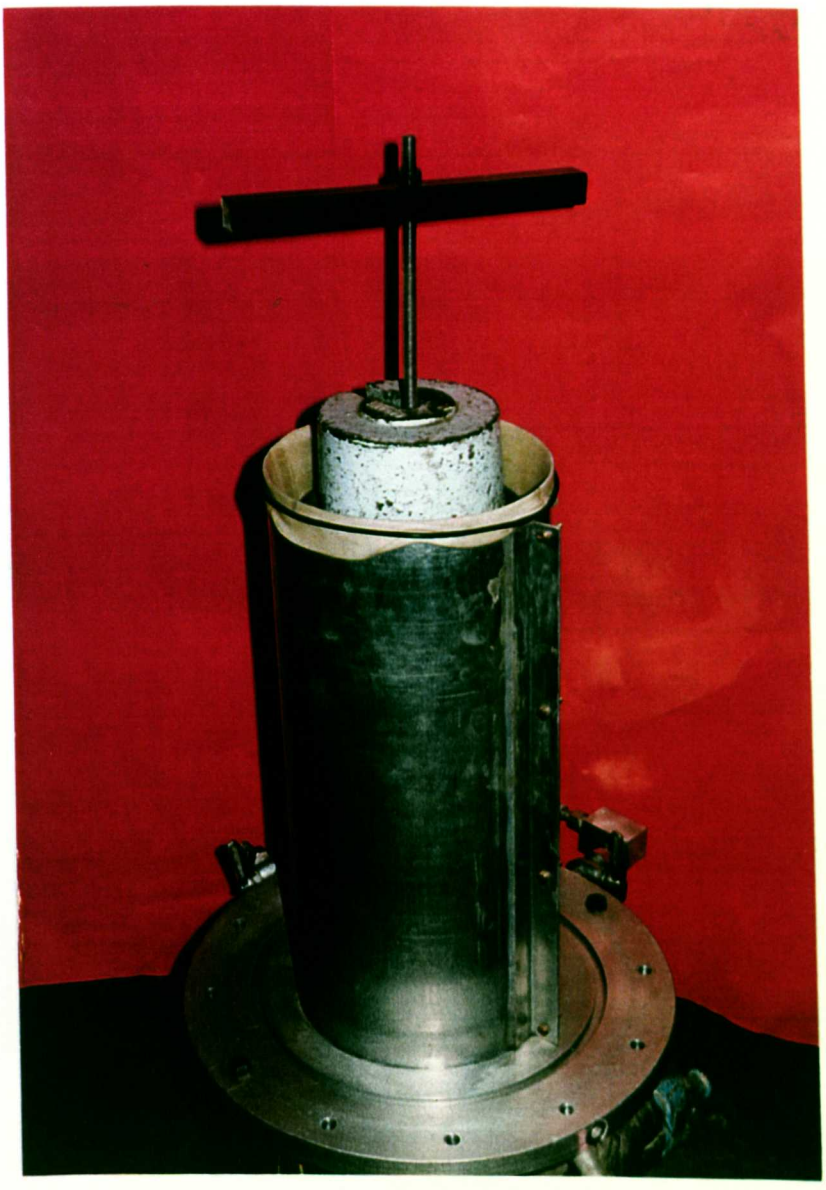

Plate 5.1 - Preparation of test specimens

Plate 5.2 - Formers for production of specimens with angled interfaces

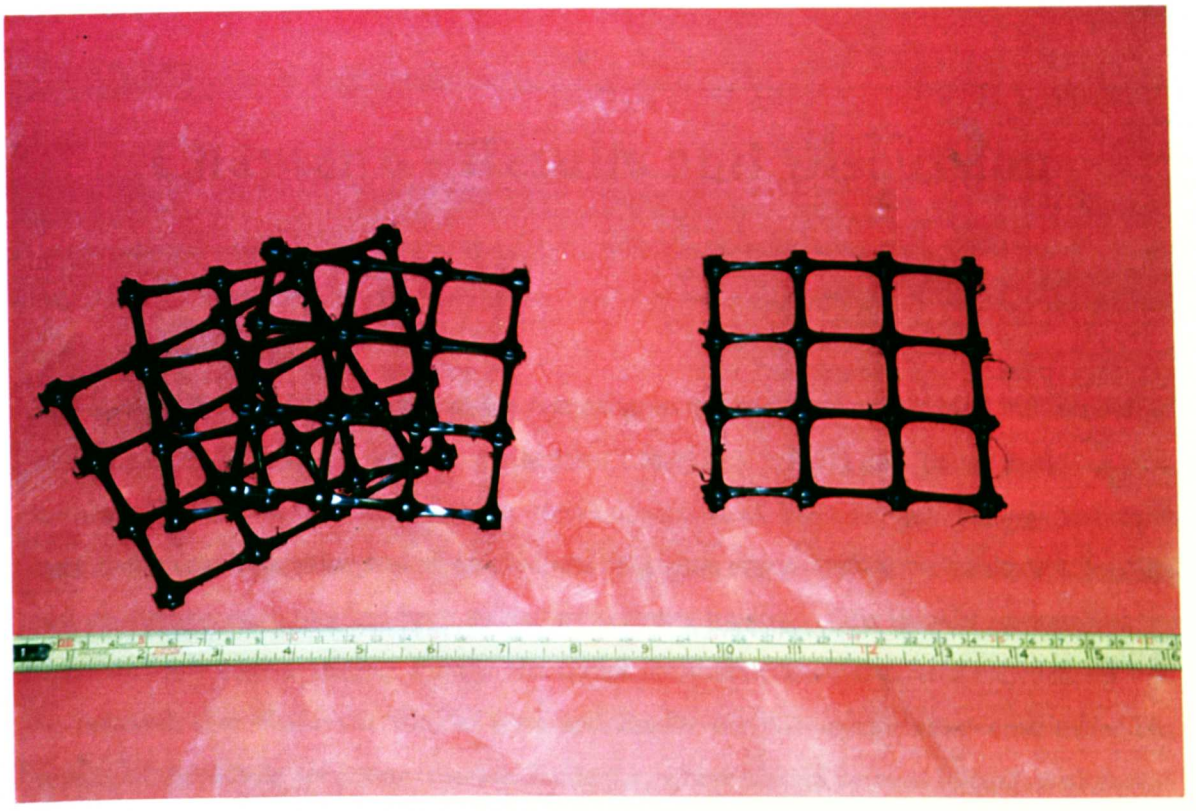

Plate 5.3 - Tensar 5540 mesh elements

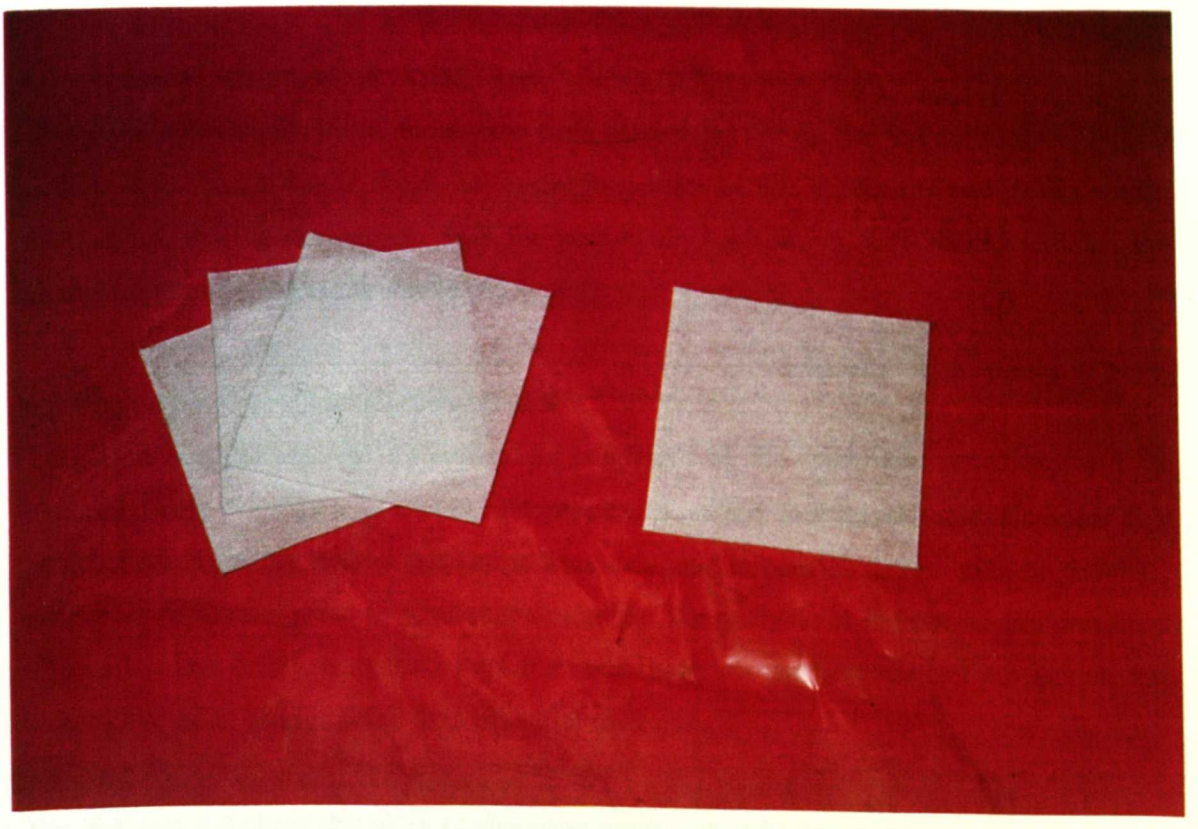

Plate 5.4 - Terram 1500 mesh elements

Chapter 6 - Results and Discussion

6.1 Introduction

In Section 5.4 it was explained that the test programme had been subdivided into a number of 'series', each having a specific objective (Tables 5.1 - 5.11) and being made up of a number of test 'sets'. Each of these 'sets' consisted of a monotonic loading test on a specimen, a cyclic loading test on an identical specimen and a post cyclic monotonic loading test on the specimen that had been subjected to cyclic loading. This chapter summarises the results of this triaxial testing. Firstly, the initial monotonic triaxial tests from each set will be covered, then the cyclic triaxial tests and finally the post cyclic monotonic tests. The results of these tests are summarised in Table 6.1, which should be read in conjunction with Tables 5.1 - 5.11 as appropriate. The implications of the results, along with those of the model tests described in Chapter 7 are discussed in Chapter 8.

6.2 Initial Monotonic Triaxial Tests

This section covers the initial monotonic tests carried out for all the test series described in Section 5.4. These results show the failure properties of the specimens and trends within each series, and by comparison with the post cyclic monotonic tests should indicate the changes caused by the cyclic loading.

6.2.1 Series TA - Characterisation of the Materials

To gain an insight into the differences in behaviour of the specimens resulting from the material being combined in layers, the properties of the individual materials were first established. Thus the tests in this series were designed to provide information on the basic properties of the materials as a reference point for the analysis of the two layer specimens. The ballast and the 20mm material are the main materials used for the test programme and so are covered in greater detail than the other materials.

Fig. 6.1 and 6.2 show the plots of deviator stress and volumetric strain respectively with axial strain for the first and second tests on ballast at 40kPa cell pressure, and the test

carried out at 90 kPa cell pressure (test sets 3, 31 and 32). The deviator stress shows trends typical of a normally consolidated granular material, with the stress increasing with strain, rapidly at first and then at a gradually lesser rate until a constant stress has been reached after about 5% axial strain. However, in this case, the deviator stress varies quite considerably around the mean value (up to ±18 kPa around an average of 240kPa for the first test carried out at 40 kPa cell pressure). This is thought to be due to slip at the interface between the large particles or breakage of particles / particle points, resulting in a slight loss of stress, which then gradually builds up with further deformation until it is of sufficient magnitude to induce further slip or breakage. This phenomenon is not seen in other results from triaxial tests on railway ballast, such as those by Raymond and Davies (1978), Alva-Hurtado and Selig (1981) and Indraratna et al. (1998). The reason for this is unknown. It is thought unlikely that it results from an increased number of particles in the sample giving a more even response, as the D/d_{max} value of the samples tested by Raymond and Davies (1978), Alva-Hurtado and Selig (1981) and Indraratna et al. (1998) are only slightly greater than those of the samples in this research (5.9, 5.0 and 5.7 respectively, as opposed to 4.7 here). It could be a function of the number of readings taken during the test, (fewer readings resulting in a smoothing out of the line), the materials used, or perhaps the presence of water in the other tests. In such tests, the water could have acted as a lubricant, resulting in a smoother and more gradual slip between particles rather than the larger jumps here.

The maximum deviator stress in this situation is hard to define due to the fluctuations in its value. For this reason, a value called the "average deviator stress" has been defined. This is calculated by averaging the results of the previous 10 readings to the point being monitored (equating to 0.55% axial strain) and effectively smoothes the fluctuations in the latter part of the test. This "average deviator stress" is the value of peak stress quoted for the initial monotonic tests in the summary of results (Table 6.1). The maximum "average deviator stress" in the first test at a cell pressure of 40 kPa of 247 kPa corresponds to a maximum principal stress ratio of 7.2. This is low compared to the results obtained by Indraratna et al. (1998), who obtained values of 12 at 30kPa cell pressure for a similarly graded material, and 18 for a slightly finer grained material.

Examination of the deviator stresses of the first and second tests on ballast at 40 kPa cell pressure, illustrated in Fig. 6.1, shows that they agree quite well. The deviator stress of the second test (set 31) does not start at zero, but this is most likely due to the sample being

fractionally too tall for the equipment and being compressed slightly as the cell was assembled. If the deviator stresses of the two tests are superimposed, they can be seen to correspond well if the repeat test is assumed to start at an axial strain of 0.25-0.33 %, which would correspond to an actual deformation of 1.25-1.5mm. If this is assumed to be the case, the "average deviator stresses" correspond almost identically until about 5% axial strain, after which they diverge slightly.

The volumetric strain, shown in Fig. 6.2, follows a similar pattern to the tests carried out on railway ballast at low confining pressures by Alva-Hurtado and Selig (1981) and Indraratna et al. (1998), with slight densification until about 1% axial strain, followed by dilation. However, the volumetric strain measured here is somewhat greater than that measured by Alva-Hurtado and Selig (1981) and Indraratna et al (1998), being 3.6% dilation at 5% axial strain as opposed to 1% dilation or less given by the other researchers at the same axial strain. Examining this behaviour in terms of CSSM (Schofield and Wroth, 1968, Atkinson and Bransby, 1978) would suggest that the material is not normally consolidated as suggested by the deviator stress, but is actually heavily overconsolidated due to its volumetric expansion. This would mean that the deviator stress had not reached a plateau, but was merely at a peak, and would start to fall again if the material were distorted further before reaching a critical state at some strain beyond the range of the equipment.

As would be expected, the increase in cell pressure of the test carried out at 90kPa results in higher deviator stresses being reached. However, the level of fluctuation of the deviator stress is also much greater, with the variations being so great that even the "average deviator stress" fluctuates significantly. It was noted that tests carried out at this higher cell pressure resulted in greater levels of particle breakage within the specimen, and so it is thought that the greater fluctuations noticed in the test at 90 kPa cell pressure were due to breakage of the particles, the smaller fluctuations noted in this test and the ones at 40 kPa cell pressure being due to breakage of the contact points and particle slippage. The maximum "average deviator stress" for the 90kPa cell pressure test equates to a maximum principal stress ratio of 5.8. This is lower than that of the 40 kPa test and equates with a value of about 8 obtained by Indraratna et al. (1998) when testing a sample at 90kPa. This would further suggest that the test specimens are actually overconsolidated, as an increase in average stress on the particles at a constant initial void ratio such as here would take an overconsolidated specimen closer to the critical state line, and so it would dilate less on

shearing and consequently the peak principal stress ratio would be lower (Atkinson and Bransby, 1978).

The volumetric strain measurements for the test at 90 kPa cell pressure follow the broadly expected path with volumetric contraction until about 1% axial strain and then volumetric expansion. The rate of volumetric expansion is less than that of the test at 40 kPa cell pressure until 2.5% axial strain, which would confirm the above observations, after which it increases sharply to a level significantly greater than the 40 kPa test. This is contrary to what would be expected from the literature, both in terms of theoretical (Atkinson and Bransby, 1978) and previously observed behaviour (Alva Hurtado and Selig, 1981, Indraratna et al., 1998). This would suggest that either the material is displaying significantly different behaviour to other soils, or that the measurements are inaccurate. Examination of the radial deformations for the individual LVDTs in the two tests (see Fig. 6.3) would suggest that the measurements are at fault, as the values from the different transducers vary considerably. It is postulated that this is due to the size of the test material. Inevitably with particles of this size, the radial LVDT targets, of 60mm by 80mm and curved with a radius of 236mm, will bridge two or three particles. Thus the measurements recorded will be severely influenced by the behaviour of individual particles rather than the material as a whole, with the consequent randomness of response. It would perhaps be more accurate to measure volumetric behaviour of large grained material by displacement of cell or pore fluid (which would entail testing with the specimen saturated). It is also thought that at large strains, there is a loss of accuracy due to the distortion of the shape of the specimen (Salman, 1994). For these reasons, the values of volumetric strain quoted in Table 6.1 for comparison are the values at 1% axial strain, as it is felt that the accuracy will be greater at low strain values.

The average density of ballast specimens prepared during the test programme was 1466 kg/m^3 with a maximum of 1476 kg/m^3 and a minimum of 1454 kg/m^3. No allowance has been made for edge voids. Assuming spherical particles of 50mm diameter, the addition or subtraction of one particle to an average sized specimen will cause a variation of 8.9 kg/m^3 in the density. Therefore, the entire difference in the density range is only caused by a variation of 2 to 3 particles.

Table 6.2 shows how these values compare with the materials used by Raymond and Davies (1978), Alva-Hurtado and Selig (1981) and Indraratna et al. (1998).

Figs. 6.4 and 6.5 show the plots of deviator stress and volumetric strain against axial strain for the first and second tests conducted on the 20mm stone at 40 kPa cell pressure, and the test carried out at 90 kPa cell pressure (test sets 4, 27 and 30 respectively). As can be seen, this material follows a similar pattern to the ballast showing behaviour expected of a normally consolidated material, with the deviator stress increasing rapidly at first, then progressively less quickly until it eventually reaches a plateau. However, it can be seen in these tests that there is a slight downward trend in the deviator stress at higher axial strains, indicative of these values actually being peak stresses. In this case, though, there is much less fluctuation of the deviator stress about the mean value than was seen with the ballast, no doubt due to the greater value of D/d_{max} in this case (11.8) resulting in the fluctuations being averaged out over the bulk of the sample.

The volumetric strains for the tests on 20mm material (see Table 6.1) show more dilation than those of the ballast tests, which is consistent with the slightly higher peak principal stress ratio seen here (Rowe, 1962). From Fig. 6.6, it can be seen that the radial deformation of the first specimen tested at 40 kPa cell pressure (test set 4) is much more uniform than in the ballast tests, as the LVDT targets will now be covering many particles and giving an average of them all. This suggests that the volumetric strain figures are more representative of their true values.

The density of the initial test specimen was 1669 kg/m^3, significantly higher than the mean of the ballast specimens due to the tighter packing that comes from smaller particle sizes, and the higher specific gravity of the material itself. The average density of the 20mm specimens was 1665 kg/m^3, with a maximum of 1683 kg/m^3 and a minimum of 1645 kg/m^3, which is almost twice the range compared with the ballast specimens. This difference corresponds to approximately 60 particles of 20mm stone.

As can be seen from Fig. 6.4, the deviator stress for the second test at 40 kPa cell pressure is significantly lower than that of first test. There was no difference in test conditions that could explain this discrepancy, although it was noted on dismantling that the specimen, whilst having failed in the usual mode of barrelling, was shifted to one side. If this were due to some eccentricity of loading, rather than damage on dismantling, it could explain the anomalous result.

The results for the 14mm, 10mm and 6mm materials can also be found in Table 6.1. They all follow a similar pattern of behaviour to the 20mm material, and have failure stresses and volumetric strains of the same magnitude.

Fig. 6.7 shows how the maximum principal stress ratio varies with particle size. A straight best fit line drawn through this data would suggest that the maximum principal stress ratio does not vary with gradation, which is contrary to the findings of Indraratna et al. (1998) who suggest that a smaller grading results in an increase in specimen strength. However, it could be imagined that a relationship such as that shown in Fig. 6.7 would be valid, where the maximum principal stress ratio increases up to a maximum level.

Some effects of the D/d_{max} ratio can be ascertained at this point. The repeatability of the results with low D/d_{max} ratios cannot safely be deduced from the few samples considered up to this point, but the results from the ballast tests are encouraging. However, the results from the 20mm stone tests, with a larger D/d_{max} (and according to Salman, 1994, sufficiently large to avoid size related effects) do not show a high degree of repeatability. The accuracy of the ballast results as absolute values is unknown, as there have been no known tests on ballast specimens large enough to give accurate values with which to compare them. The other materials have sufficiently high D/d_{max} values for them to be considered to be representative of the material.

The variability in the results arising from the D/d_{max} ratio can be considered at this point. It appears that an increase in the D/d_{max} ratio results in less fluctuation about the "average deviator stress" at a given cell pressure, and more uniform values from the radial strain transducers. These relationships are shown in Figs. 6.8 and 6.9 respectively. Fig. 6.8 shows the standard deviation of the fluctuations about the "average deviator stress" between 3.0% and 5.0% axial strain. This shows that the fluctuations appear to fit well with a negative power relationship as the D/d_{max} ratio increases. Fig. 6.9 shows that variability of the radial readings (defined as the maximum radial deformation minus the minimum radial deformation at 5.0% axial strain) follows a similar power relationship to the Standard Deviation of the fluctuation, although this will also be a function of the size of the radial targets used.

6.2.2 Series TB - Layered Specimens With Variable Stone Size

Figs. 6.10 and 6.11 show plots of deviator stress and volumetric strain against axial strain for the specimen composed of layered ballast and 20mm stone, along with the values for its component materials for comparison (test sets 5, 3 and 4 respectively). The graphs show that the two layer specimen displays the same general trends in behaviour shown by the materials in the characterisation tests. The discontinuities on the plot of volumetric strain were caused by a loose connection on LVDT 0. It can be seen from Table 6.1 that the value of peak "average deviator stress" is similar to that of the ballast, whilst the value of volumetric strain is intermediate between the materials. The standard deviation of the fluctuation about the 'average deviator stress' is 4.3 kPa, which from the previously calculated relationship corresponds to a D/d_{max} ratio of 7.05 i.e. a maximum particle size of 33.5mm, midway between the component materials.

The density of the two layer specimen, at 1570 kg/m^3, is again midway between those of the component materials. On the basis of the weight of each type of material used and the distance between the top of the specimen mould and the top of the compaction mould / top platen, the theoretical densities of the material in each layer can be calculated. These will be different to the actual densities of the materials in place, and the densities measured previously in the material characterisation tests. For example, the density of the ballast layer would be less than expected as there will have been a smaller thickness of material than previously used. This means the edge voids where the specimen meets the bottom platen / compaction mould will form a greater percentage of the specimen than they would otherwise. Similarly, the calculated density of the smaller materials will be greater than expected because some of the material will fill the edge voids of the ballast layer, and so the actual volume of material will be greater than the measured value and this will be reflected in the density. In addition, with the smaller materials some of the particles will fall through into the ballast layer during specimen production and thus be unmeasured volume. This measured density, therefore, can be used as an indication of the stability of the two layer specimen, showing how much material has migrated from the top layer of stone into the ballast. If it is compared with the average density of a whole specimen, and the particle densities are known, then an estimate of the volume of material lost into the ballast layer can be calculated. Fig. 6.12 shows the results of this process carried out on the data from the prepared specimens. As can be seen, the quantity of material 'lost' is similar for 20 and 14mm material signifying reasonable stability, as the material fills the top voids of the

ballast layer. The volume of lost 10mm material is slightly higher, suggesting that some it will be falling through deep into the ballast. The figures for the 6mm material are much higher, however, indicating that a quantity of the material is migrating downwards, and that the layers are not forming a stable interface.

Table 6.3 shows the angle of shearing resistance for the two layer specimens, along with the values for their component materials, all at 40 kPa cell pressure. As can be seen, for the specimens with 6, 10 and 14mm material the angle of shearing resistance is 1 - 3° higher than the value for the material comprising the top layer, whereas for the specimen with 20mm stone, the value is intermediate of the values for the components. It was noticed during dismantling of many of the two layer specimens that the form of failure was different to the usual barrelling failure. In these cases, the top layer of material had barrelled, but the bottom layer (ballast) was relatively undeformed. This is shown diagramatically in Fig. 6.13 and on Plate 6.1. It could be that this behaviour is due to the weaker top layer controlling the behaviour of the specimen, and being confined by the stronger ballast material underneath, thus effectively having a H/D ratio of 1. In the literature (Bishop and Green, 1965) it was reported that decreasing the H/D ratio to 1 resulted in an increase in confinement of the material, giving a rise of 4-5° in the angle of friction. This would help to account for the increase in strength noted above, but would not account for why the ballast section of the specimen could then take greater deviator stresses than ballast would if tested alone. If there were shear stresses at the interface of the two materials, as would be expected if one material were restraining another, then the effective principal stresses on the material would be increased, and it would be expected to fail at a lower deviator stress rather than a higher one. A different explanation could be that, as can be seen from Table 6.1, Test Series TA, the smaller materials all have greater dilatory tendancies than the ballast. As a result, in the two layer specimen the section comprising of smaller material will bulge more than the ballast section. This explanation would not, however, account for the strength increases seen in the two layer specimens.

6.2.3 Series TC - Effect of Cell Pressure on Two Layer Specimens

The peak "average deviator stress" and volumetric strain for tests on two layer specimens at 30, 40, 60 and 90 kPa cell pressure can be found in Table 6.1 (test sets 8, 5, 6 and 7 respectively). As the cell pressure increases the two layer specimen follows the conventional behaviour for a granular material, with a decreasing tendency towards dilation,

as the overconsolidation ratio decreases, and an increase in the level of maximum 'average deviator stress' attained. Fig. 6.14 shows the change in principal stress ratio with the change in cell pressure. As can be seen, the principal stress ratio increases with decreasing cell pressure, as would be expected with the resultant increase in overconsolidation ratio and consequent increase in dilatant tendency, causing an increased dilation component. Although there is only limited data, it appears to fit reasonably well with a relationship of the type proposed by Indraratna et al. (1998) where;

$$R_p = a(\sigma_3')^b \qquad 6.1$$

and

R_p is the maximum principal stress ratio

a is the magnitude of the principal stress ratio at $\sigma'_3 = 1$ kPa

b is an empirical index related to the degree of particle degradation.

This equation is remarkably similar to the CSSM equation describing the peak state line (Atkinson and Bransby, 1978) for a material, and should perhaps have been expressed as such given that the maximum principal stress is a function of this. The equation states that;

$$\frac{q'_p}{p'_c} = \alpha\left(\frac{p'_p}{p'_c}\right)^{\beta} \qquad 6.2$$

Where;

q'_p is the peak deviator stress

p'_p is the average stress at the peak

p'_c is the critical average stress for the starting void ratio of the material

α is the slope of the critical state line, and thus a function of the frictional properties of the soil grains

β is a function of the soil behaviour related to the dilational properties

The values of a and b given by the regression on the two layer specimen data are both lower than those obtained by Indraratna et al. (1998). This would suggest some physical difference in the stone, both in terms of surface roughness and particle shape / grading.

Fig. 6.15 shows the values for the specimens tested at 40, 60 and 90 kPa (test sets 5, 6 and 7) plotted as a Mohr-Coulomb failure envelope. This gives an angle of shearing resistance of 46° for these specimens.

6.2.4 Series TD - Effect of Interface Angle

Table 6.1 gives the analysis of the volumetric strain and peak "average deviator stress" for the specimens with differing angles of interface between the two materials (ballast and 20mm stone). This shows an essentially random pattern of maximum stress and strain reached in the test. The horizontal and 11° inclined specimens show a slightly lower deviator stress than the other specimens, but there is insufficient indication here of a trend. This would suggest that the inclination of the interface between the materials is not a factor controlling the strength of the specimen.

6.2.5 Series TE - Effect of Layer Thickness

If the values of deviator stress and volumetric strain in Table 6.1 are examined, it can be seen that the specimen with equal layers of both materials (test set 5) failed at a lower deviator stress than the specimens with unequal layers of material, and underwent less dilation. From this, it would appear that having a thin layer of material that is almost completely enclosed in the 'dead zone' gives a greater degree of confinement to the remaining layer than if the two layers are of equal thickness. If the peak deviator stresses for the specimens, and consequent values of angle of shearing resistance are compared with those of the component materials (Table 6.4), it becomes apparent that a thin layer of material in the dead zone increases the angle of shearing resistance of the material in the thick layer by 3 degrees. This increase when the thick layer 'specimen' is reduced to a H/D ratio of 1.3 - 1.5 corresponds well with the work reported by Bishop and Green (1965). However, as explained in Section 6.2.2. it is unclear how this increase comes about.

6.2.6 Series TF - The Behaviour of Rounded River Gravel

As stated in Section 5.4.6, tests were carried out on a different type of material, rounded river gravel, to see what the effect would be on a two layer system of using non-angular material. The following paragraphs detail the characterisation tests on this material, and its behaviour in the two layer system.

Figs. 6.16 and 6.17 show the deviator stress and volumetric strain for specimens produced from rounded river gravel, at 40 and 90 kPa cell pressures (test sets 21 and 33). As can be seen, they follow the same general pattern of behaviour as the angular granite materials. There is, however, a distinct downward trend for the deviator stress of the test at 90 kPa cell pressure, suggesting a peak stress and visibly less tendency to contraction of the material at the start of the test at both cell pressures than occurred with the angular materials. This is no doubt a function of the spherical particle shape, with its inherently higher initial specimen densities (an average of 1726 kg/m^3).

The maximum principal stress ratio of the specimen tested at 40 kPa was 4.1. This is significantly less than that of comparable tests using the angular materials despite the high levels of dilation, and would suggest that the frictional shear resistance of this soil is much lower than that of the granite materials. Because of this relatively low level of strength, it was deemed necessary to carry out the remainder of the testing on rounded river gravel at a cell pressure of 90 kPa in order that the specimens subject to cyclic load would not fail on the first load cycle. This value of 4.6 for the maximum principal stress ratio of the specimen tested at 90 kPa cell pressure is slightly higher than that of the specimen tested at 40 kPa. Given the increase in cell pressure, with the consequent decrease in overconsolidation ratio compared with the 40 kPa test, it would be thought that the principal stress ratio would be lower. A broadly similar value would suggest a purely frictional response, i.e. the material is not overconsolidated and dilating.

The peak "average deviator stress" for specimens of ballast and river gravel, and a two layer specimen comprised of these material, all tested at 90 kPa cell pressure, can be found in Table 6.1 (test sets 32, 33 and 22). It can be seen that in terms of maximum deviator stress and deviator stress fluctuation, the behaviour of the two layer specimen closely follows that of the ballast. This would suggest that the ballast is restraining the river gravel and indeed, the angle of shearing resistance for the two layer material is 4° higher than that of the river gravel with a H/D ratio of 2. However, it would be expected that the movement of the gravel would hide some of the fluctuation of the deviator stress of the ballast as with the other smaller material.

Fig. 6.18 shows how the deviator stress of a two layer specimen with an interface at 45° to the horizontal (test set 23) compares with a two layer specimen having a horizontal interface

(test set 22). The deviator stress builds up much more slowly with axial strain than in the conventional two layer specimen. Thus it appears that in the case of a two layer specimen using less angular material, changing the angle of the interface does have an effect on the deviator stress. Plate 6.2 shows a 45° specimen produced from ballast and river gravel. As can be seen, this has failed by barrelling, but there has been far more deformation on the side composed mainly of river gravel than on the side composed mainly of ballast. It appears that the change in geometry has reduced the restraint of the river gravel and thus it can deform and behave more as it would in a sample with a H/D ratio of 2. This could be due to the fact that on a specimen with a 45° interface angle, the section of the specimen composed of river gravel covers a large area of the shear band, rather than being confined between ballast and 'dead zone'.

Figures for the peak "average deviator stress" and volumetric strain for two layer specimens tested at 90 and 60 kPa respectively (test sets 22 and 24) can be found in Table 6.1. The volumetric strain follows conventional behaviour, with a lesser tendency towards dilation as the cell pressure increases, but the behaviour of the deviator stress is inexplicable, being significantly lower when the cell pressure is at the higher value. There is nothing in the test data or measurements from specimen production to suggest why the specimens should behave as such.

6.3 Behaviour of Material Under Cyclic Loading

As stated in Section 5.4, each of the test sets included a cyclic load test on a specimen to simulate the loading that the material would experience in the track bed. The results of these cyclic load tests are presented here, again subdivided into the test series as laid out in Section 5.4. The data from the cyclic load tests can be found in Table 6.1. For each test, this lists the permanent axial deformation after 100,000 cycles and the resilient modulus, as defined in Section 2.6.2(b) (see also Hicks and Monismith, 1971, Kalcheff and Hicks, 1973), averaged over the last 60,000 cycles of the test to smooth out random fluctuations.

6.3.1 Series TH - Repeatability of the Main Test Programme

Fig 6.19 shows a plot of deviator stress against axial strain for the first 25 cycles of the first test on ballast (test set 3). It shows the typical characteristics of granular material under cyclic loading, as would be expected from Section 2.6.2 (see also Brown and O'Reilly, 1991). However, after the first few load cycles, the stress-strain cycles on the plot start to

converge and become difficult to differentiate, hence the data is more usually plotted as axial strain against number of load cycles. Fig. 6.20 shows the plot of axial plastic deformation against the number of load cycles for the first test on a ballast specimen at 40 kPa cell pressure. As can be seen, the deformation behaves as expected from Section 2.6.2 with the majority of the deformation occurring within the first few load cycles. This response is more visible if the number of cycles is plotted on a logarithmic scale as shown in Fig. 6.21. Towards the end of the test programme, another identical test was carried out. It can be seen from Table 6.1 that there is a large discrepancy between the results with the deformation for the later test being more than twice that of the first. This was an unexpected result as a repeatability test had been carried out carried out midway through the test programme and shown results very similar to those of the test on which it was based. Fig. 6.22 shows the results of the mid programme repeatability test with its original (sets REP2 and 5 respectively), and with the values zeroed to the start of the second load cycle to eliminate any initial bedding errors. When the results of a test on the 20mm material early in the test programme were compared with a supposedly identical test later on in the programme, the same problem was apparent. The settlement in the later test (test set 27) was found to be almost three times that of the first (set 4), the details being shown in Table 6.1. This meant that it was not just a problem isolated to the ballast as a result of the lower D/d_{max} ratio. Examination of the third and last repeatability test of the original test programme (set REP3) showed that it too had deformed more than expected, but inspection of the test data revealed that the cell pressure was incorrectly set too low. This could have accounted for the discrepancy.

From the data, it appeared that something had changed in the later part of the test programme rendering supposedly identical tests incomparable. To try and identify the cause of this change, all aspects of the test were examined.

Material - Each of the materials for the tests consisted of one batch of stone that was thoroughly mixed before use. None of the material was re-used. Thus barring some unforeseen degradation of the material, it would be reasonable to assume that the stone used did not change.

Test preparation technique - The method of specimen preparation was kept constant throughout the testing period, although there was slight variation in the specimens. For

example, there was found to be variation in the finished height of the specimen, albeit on a random basis and by no more than 5%. It was also possible that the compactive effort given to the material could vary. To check this, the porosity of each finished specimen was calculated from the weight of material added, the density of the material and the final volume of the specimen. A graph of porosity with test number was then plotted (Fig. 6.23, which also shows estimated minimum and maximum porosities for the material). As can be seen, there was a slight tendency for the porosity to decrease as the test programme went on, which would suggest that if anything the deformations should have reduced slightly in the later tests. Given that the method of transporting these specimens to the test apparatus did not change, it would suggest that the test preparation technique was not the cause of the change in behaviour.

Instrumentation - The instrumentation was repeatedly calibrated, and these calibrations did not change significantly throughout the test period (see section 4.2). On the basis that it was not just one test that showed anomalous results, the possibility of the response of the instruments fluctuating between calibrations would be ruled out. As mentioned in Section 4.3.4, there was variation of the supply voltage within the test period that was not compensated for. On the basis that a voltage fluctuation of 0.05V was suspected, this would lead to load, displacement and pressure variations of 0.10 kN, 0.22mm and 0.53 kPa respectively if each transducer was at the end of its range, i.e. an error of approximately 0.5% in each case. Even cumulatively, this is not sufficient to cause the 100-200% error that is occurring, and so the instrumentation should be ruled out of the list of possibilities.

Test Conditions - There were changes in the test conditions in order to test different variables and the effect that this would have on the specimens, for example cell pressure, but in each case these were restored to their original values. A certain amount of variation is unavoidable however. For example, the cell pressure fluctuates as the load is cycled due to the finite response time of the pressure regulator, and the change in viscosity of the hydraulic oil as it heats up will cause small changes in the response of the load system. Inspection of the output data from the tests revealed, however, that there had been a change in the loading experienced by the specimens at some point in the test series. It appeared that around the point of Test 18, the minimum load experienced by the materials under cycling had reduced from 0.4 - 0.5 kN (9 - 11 kPa) to between 0.05 and 0.1 kN (1 - 2 kPa). The maximum load also fluctuated slightly, but there was no noticeable trend.

In addition to the change in load, after Test 24 there was also a problem with leaks where the membranes met the top and bottom platens. The cause of the leaks was never fully identified and the problem overcome, and several tests were lost completely due to ingress of water. It could have been possible that in other cases sufficient moisture entered the specimen to cause a change in behaviour without its presence being noticed.

Thus it could be argued that the only two possible reasons for the difference in behaviour between the earlier and later tests were the ingress of water and the change in minimum stress.

Comparison of the supposedly identical tests reveals that the change in deformation was not always a simple one. As shown in Fig. 6.24, a plot of axial strains at corresponding points in the tests for both the tests on 20mm materials at 40 kPa cell pressure reveals that the deformations in the latter test accumulated at three times the rate of those in the first test throughout the whole cycling period. Similar plots for the repeatability tests and the two ballast tests at 40 kPa cell pressure (Figs. 6.25 and 6.26 respectively) reveal that the relative rate of strain accumulation varied as the test proceeded. One feature common to all the tests with a higher deformation is the value of resilient modulus. The values of resilient modulus from Table 6.1 show that in each case the resilient modulus was significantly lower in the test where the greater deformation took place.

The presence of water is not expected to affect the behaviour of soils provided no excess pore pressures occur, although small quantities of water around the inter-particle contacts will result in soil suctions and effectively increase the confinement. However, in materials such as railway ballast fines are not present, thus little suction will be developed. Therefore, it might be thought that the presence of water would have little effect on the behaviour of ballast. However, limited previous research has found that the presence of water increases the plastic strains in the material (Eisenmann, 1984, Raymond and Bathurst, 1987, and Sato, 1995), although Pappin et al. (1992) found that in the case of a well graded, crushed limestone, the presence of water had no effect on the resilient modulus of the specimen provided drainage was allowed.

It is possible that the change in axial load could be responsible for the change in material properties, it is clear from Fig. 2.19 that the resilient modulus changes non linearly with

deviator stress. On this basis, a small change in the minimum stress during cycling could significantly affect the deformation and resilient modulus. Tests by Jeffs and Marich (1987) have shown that during box tests on ballast, reducing the minimum load experienced by material to zero results in a large increase in settlement. How much of that is due to possible impact loading from loss of contact between the material and the scale sleeper is unclear. It should be borne in mind, however, that in the case of the triaxial tests, there is always cell pressure acting on the top of the sample, thus the vertical stress never actually reaches zero as it would in a box test. Also, it should be noted that to some degree, the change in loading may be the result of the change in modulus, rather than the cause. A decrease in resilient modulus will result in an increase in elastic deformation. This means that there will be a greater travel of the loading piston in each load cycle, and thus a greater demand for oil from the pump. Because the pump is supplying oil at near its maximum capacity, this increase in demand could result in a drop in pressure and hence a slightly reduced maximum load. It was indeed noted that the maximum load in the ballast, 20mm stone and two layer tests examined were all slightly lower than average.

The resilient modulus of the specimens was felt to be the key to this problem, so to investigate the effect of the stress level on the specimen, the stresses were compared with the resilient modulus. Examination of the change in stress range (maximum stress - minimum stress) against change in resilient modulus showed only random scatter, and the change in minimum stress with the change in resilient modulus was inconclusive, which is unsurprising given the range of materials and specimen configurations tested.

6.4 Secondary Test Programme

Thus, in order to test the effects of change in minimum stress and the presence of water, an additional group of test sets were carried out (see Section 5.5 for details). In this series, two layer specimens were prepared and tested in the same manner as for the repeatability tests of the main series, except for the fact that the minimum load was varied for each test and carefully checked beforehand to ensure it was correct. In addition, one test was carried out in which the materials were soaked in water for two hours before the test, and then prepared into a specimen in an attempt to quantify the effects of wetting of the ballast.

6.4.1 Analysis in Terms of Resilient Modulus

The data was first analysed in terms of resilient modulus, as this appeared to be directly linked to the change in deformation as noted in Section 6.3.1.

6.4.1(a) Series TI - Variation in Minimum Stress

The data in Table 6.1 shows that the resilient modulus of the specimen decreases with the level of the minimum stress (test sets 35, 37 and 38). It must be remembered that the maximum stress is the same in each case, so the range of the stress (maximum stress - minimum stress) increases as the minimum stress decreases. Comparing the observed values of resilient modulus (averaged over the last 60,000 cycles of the test) with values calculated from inputting the observed values of stress experienced by the specimens into the models produced by Boyce et al. (1976), Pappin and Brown (1980) and Brown and O'Reilley (1991), as shown in Table 6.5, it can be seen that a change in modulus is predicted by all three of the models. Along with the predicted values of modulus is the factor by which it differs from the observed value, called the error factor. The values of modulus predicted by the models of Boyce et al. (1976) and Pappin and Brown (1980) are quite similar, but significantly higher than the observed values. This is surprising as the models were produced for well graded limestone, which would be expected to be significantly less stiff than railway ballast. In each case, the error factors for the middle and lower values of minimum stress were similar, but the prediction for the higher level of minimum stress was significantly different. The model postulated by Brown and O'Reilley (1991), however, has identical error factors for the middle and higher minimum stresses, but it is the lower value of minimum stress that is significantly different. It is interesting that this model, which has constants supposedly specific to granite ballast, gives predicted values that were only slightly nearer the observed values than the other two models. More data would be required to determine if this inability to predict the relative size of the modulus in each case is due to a shortcoming in the models, or just the variability of the test results. It must also be noted that these change in moduli are not the result of the slight change in stress range that accompanies the change in minimum stress. If the model proposed by Boyce et al. (1976) is used, the stress ranges for each test are entered, and the minimum stress is altered to that of the repeatability test, in each case the modulus predicted is within 4MPa of that in the case of the repeatability test.

6.4.1(b) Series TJ - Effect of Water on the Specimen Deformation

Considering the effect of the presence of water on the resilient modulus, Table 6.1 compares the resilient modulus in similar tests with and without water (sets 39 and 35 respectively). In this case, the value of resilient modulus is of a very similar value. This would suggest that the findings of Pappin et al. (1992) are correct, and that the presence of water is not responsible for the reduction in resilient modulus between supposedly identical tests in the main test series.

6.4.1(c) Series TK - Repeatability of Secondary Tests

The results of this series, analysed in terms of resilient modulus are shown Table 6.1. As can be seen, the repeatability tests follow each other closely, although they are significantly different from the repeatability tests from the main test series suggesting that the two series are not directly comparable.

6.4.2 Analysis in Terms of Plastic Deformation

If the test series is analysed in terms of plastic deformation rather than resilient modulus, a very different picture emerges.

6.4.2(a) Series TI - Variation in Minimum Stress

Comparing the tests with different minimum stress (Table 6.1) shows that a lower minimum stress does indeed cause greater settlement of the specimen than using the standard stress (approximately the same load used in the first half of the main test programme) would do. The reduction in minimum stress has in this case caused a 20% increase in plastic deformation. However, it appears that having a higher than standard minimum stress also causes greater settlement, which is unexpected given the proposed link between resilient modulus and plastic deformation (see Section 2.6.2(a) and Raymond, 1992, Raymond and Bathurst, 1994, and Sharpe, 1996). The increase in this case was 37%. If this result is not due to the presence of moisture, or a result of natural variation, then it would suggest that the link between elastic deformation, quantified as modulus, and permanent deformation is either wrong, or is only true for the modulus of the material below the ballast, where it would result in the entire ballast layer deforming upon loading rather than just the top material.

6.4.2(b) Series TJ - Effect of Water on the Specimen Deformation

Wetting of the materials results in greatly increased (68%) plastic deformation compared with the dry specimen, as illustrated by Table 6.1 (sets 35 and 39), confirming the work by Eisenmann, 1984, Raymond and Bathurst, 1987 and Sato, 1995. The test from Series TI that suffered a significant water leak (set 36) did not show a notable rate of deformation above that in the identical test later in the series (set 38). This could be due to the leak only occurring late in the test, at which point it would have little effect. Alternatively, it could be due to the water not covering enough of the specimen to result in large deformations (only the bottom third was saturated), or it could be that the very small amount of moisture noted in the specimen at the end of the second test (set 38) was sufficient to cause excessive deformation and thus in fact both specimens have deformed excessively. Assuming the scaled output of the Boyce model to be correct, the resilient modulus of the high minimum stress test would be in the region of 208 MPa, i.e. approximately the same amount greater than the medium minimum stress value as the low minimum stress value is below it. Presuming the modulus - deformation response to be linear, this would give an estimated final strain in the region of 2.15%. This would make the final strain of 3.64% an increase of 69% over the predicted value. Thus this explanation is perfectly possible.

6.4.2(c) Series TK - Repeatability

If the repeatability tests (sets 35 and 40) are compared, as shown in Fig. 6.27, it can be seen that they follow each other closely until about 30 cycles and then diverge slightly, despite being nominally identical and having very similar values of resilient modulus. If these repeatability tests are compared with the repeatability tests (also shown on Fig. 6.27) of the main series, there appears to be generally more settlement of the main series repeatability tests, although there is a significant amount of scatter. This is perhaps not coincidental with the fact that the repeatability tests from the main test series have lower resilient moduli.

6.4.3 Conclusion of Secondary Test Programme

The conclusion to be drawn from this additional test series is that the change in minimum stress that has occurred, along with the presence of water, is capable of explaining the change in behaviour observed between supposedly identical tests. For this reason, it would not be wise to compare tests carried out under the different conditions. Practically, this means that the tests carried out before Test 18 can be compared with each other, but can not be reliably compared with tests after Test 18. It may be possible to compare tests carried out

after Test 18, but care must be taken that the conditions are the same in each case.

6.5 Behaviour of Main Test Series - Plastic Deformation

The plastic, or permanent deformation of the material is perhaps the most important parameter when considering the behaviour of the material in the track bed. Ideally, there will be as little deformation as possible in the material, as deformation of the ballast bed leads to loss of geometry of the rail. Thus an understanding of how the materials deform is vital to minimising the maintenance costs of a railway.

6.5.1 Test Series TA - Characterisation of the Material

Fig. 6.28 shows the plot of the first cyclic test on a ballast specimen at 40 kPa cell pressure (test set 3). The two lines on the plot represent the deformation when loaded and unloaded. As can be seen, the majority of the deformation occurs at a constant rate for the first few hundred load cycles, and then the rate of deformation gradually reduces to a constant but low value beyond 10,000 cycles. Fig. 6.28 also shows the plot for the first specimen of 20mm stone at 40 kPa cell pressure (set 4). This follows the same basic pattern as the ballast except that the rate of settlement does not reduce until after 1000 cycles, and then it starts to increase again slightly after 60,000 cycles.

Fig. 6.29 shows a plot of the axial strain of the first ballast specimen under low load compared with the equations for axial strain given by Alva-Hurtado (1980), Shenton (1985) and Sato (1995). The formula quoted by the ORE (1970) gave deformations that were too large by a factor of ten, and thus the output from this formula has not been included. From the plot it appears that the formulae quoted by both Sato, and Shenton are of the wrong form, giving completely different patterns of deformation to the observed pattern. As no specific values were given, the Shenton and Sato formulae have had their constants estimated to fit the observed data. The formula quoted by Alva-Hurtado has been reproduced exactly, and whilst giving a more accurate form of the permanent deformation curve, the values are too small and altering the coefficients corrupts the shape. The observed data curve appears to follow a logarithmic shape on the logarithmic scale (shown in Fig. 6.30), resulting in a deformation equation of the form;

$$\varepsilon_N = \gamma LOG_{10}(\kappa LOG_{10}(\lambda N)) \qquad 6.3$$

Where ε_N is the strain after N load cycles, and γ, κ and λ are constants.

No doubt this is partly due to the fact that the deviator stress on the specimen decreases as the test proceeds. This is because the equipment does not have the ability to adjust the loading on the specimen to compensate for the increase in cross sectional area when the specimen deforms, and also that the load decreases slightly during the first couple of thousand load cycles as the equipment stabilises at an equilibrium point. Table 6.6 indicates the reduction in deviator stress for several tests in the programme. From the literature (Shenton, 1975, Klugar, 1975, Stewart, 1986, and Diyaljee, 1987), it is the largest deviator stress that controls the plastic deformation, and thus if the deviator stress decreases somewhat the rate of plastic strain will decrease significantly, possibly explaining the apparent equilibrium reached in the latter part of the test.

Examination of the ballast test data from tests at both 40 and 90 kPa cell pressure (sets 3 and 32 respectively) in terms of volumetric and shear strain gives the result shown in Fig. 6.31. As can be seen, the specimen cyclicly loaded at 40 kPa cell pressure underwent dilation whilst that tested at 90 kPa cell pressure underwent contraction, although it must be remembered that one of the tests was carried out in the early part of the test series, and one in the latter part, so some or all of the difference could be accounted for by the change in conditions. Dilation was reported by Shenton (1975) for cyclic loading on ballast under similar stress conditions to the test at 40 kPa, and the observed behaviour is consistent with the work reported by Tam (1986) and the results of the monotonic tests reported in Section 6.2.1. This behaviour could perhaps be described within the framework of CSSM (Schofield and Wroth, 1968). The specimen tested at 40 kPa would be overconsolidated, and so would tend to dilate on shearing. The increase in cell pressure would make the specimen less overconsolidated, and so it would tend more to contraction when sheared. It must be borne in mind though that the two types of test are different, and will not necessarily behave in the same way. For example, during monotonic shearing of a specimen at 90 kPa cell pressure, the specimen initially contracted, but by 2.5% axial strain the specimen had started to dilate again whereas in the cyclic test it was still contracting at this axial strain.

A similar pattern of volumetric straining was noted for the 20mm material tested under cyclic loading at 40 and 90 kPa cell pressure (test sets 4 and 30 respectively). This can be seen in Fig. 6.32.

6.5.1(a) Change in Behaviour With Particle Size

If the plastic strain against the number of cycles is compared for specimens of different particle size (Fig. 6.33), excluding that of the 6mm material where the plastic deformation exceeded the range of the equipment after 370 cycles, there is little pattern evident. However, if the materials are compared in terms of volumetric and shear strain (see Fig. 6.34) then a trend is more obvious. With the exception of the ballast, the level of shear strain appears to increase as the particle size decreases. The ballast shows the greatest level of shear strain early in the test, but reaches an equilibrium before the other materials. This could be due to the ballast having a greater reduction in deviator stress than the others, which all have similar reductions. The greater level of shear in the early part of the test contradicts the trend shown by the other particle sizes. The reason for this is not known, but would probably be a function of the low number of inter-particle contacts resulting from the large particle size, and the consequent high inter-particle forces.

Initial examination of the volumetric strains would suggest that volumetric strain is independent of particle size, and that the test on the 14mm material was anomalous. However, bearing in mind that the rate of strain of the ballast material may just be prematurely reduced, and the actual volumetric strain should perhaps be higher, then it may be the test on the 20mm material that is anomalous. This would then give a similar relationship for the volumetric strain as for the shear strain, i.e. strain increasing with a decrease in particle size, and the ballast as a material with significantly 'different' behaviour. A result such as this would concur with other results that indicate shear and volumetric strain increasing proportionally with each other. Thus it must be decided that the volumetric strain information is inconclusive.

6.5.2 Series TB - Variation in Stone Size With Two Layer Specimens

Fig. 6.35 shows a comparison between the specimen comprising of layered ballast and 20mm stone (set 5) in terms of volumetric and shear strain, along with the plots of those variables for its component materials (sets 3 and 4). This figure indicates that the shear strain of the two layer specimen is similar to that of its component materials, whilst the volumetric strain is significantly less that that of its component materials. This would perhaps indicate that the top layer of material was migrating into the lower layer and hence reducing the level of expansion of the specimen. Given the reservations about the volumetric strain expressed in the previous section, it would not be wise to rely on this.

Also, it must be noted that the radial strain measurement is taken at the midpoint of the specimen, i.e. at the interface. Given the mode of failure that was noted in Section 6.2.2, with the top layer bulging significantly more than the lower layer at large strains, the radial strain reported may not be wholly representative of the actual conditions within the specimen. For this reason, it may be more accurate to examine the behaviour at small strains only. At these strains, both volumetric and shear strain are intermediate between those of the component materials.

Fig. 6.36 plots volumetric and shear strain for the two layer specimen comprising of ballast and 14mm stone (set 16). At small strains, it can be seen that the values for the two layer specimen are similar to those of the component materials (sets 3 and 15). At higher strains the values for the two layer specimen are greater than those of the components, which corresponds with a larger value of axial strain displayed by the two layer specimen than for the components, as illustrated in Fig. 6.37. The reason for this increase in both shear and volumetric strain is unknown.

Analysis of the two layer specimen comprising of ballast and 10mm (set 18) material is displayed in Fig. 6.38. This shows that whilst the shear values for the two layer specimen and the component materials are very similar sets (3 and 17), the volumetric strain is very different, showing marked contraction of the specimen in the early stages, with some dilation later in the test. Assuming the volumetric strain measurements to be accurate, this strongly suggests loss of material from the top layer into the ballast beneath in the initial stages of the test, where a stable system of interlocking had yet to be formed, and would correspond well with the findings of Section 6.2.2.

Although it cannot strictly be compared with the earlier tests due to the change in conditions, the results for the two layer specimen comprising of ballast and 6mm material (set 20) are shown in Fig. 6.39. The plot shows that there is no volumetric contraction, as might be expected given the results of the two layer specimen using 10mm material. Whether this shows the difference in test conditions, or the potential inaccuracy of the radial strain measurement is unknown.

6.5.3 Series TC - Effect of Cell Pressure

Fig. 6.40 shows how the volumetric and shear strains of a two layer specimen comprising of

ballast and 20mm material vary with cell pressure. The specimen tested at 35 kPa (set 8) showed a large jump in both shear and volumetric strains, with both values almost doubling between 30,000 and 40,000 cycles, then returning to a rate of increase similar to that before the jump. In light of this anomaly, the values have been taken at 30,000 cycles for each specimen to facilitate comparison. In the case of the specimens tested at other cell pressures, the difference between this and the final value was minimal.

This plot shows that the two-layer specimen is very close to failure at 35kPa cell pressure, as the strains are becoming asymptotic at this point. This is confirmed by the fact that a monotonic test on a two layer specimen at 30kPa cell pressure would not resist the deviator stress used in the cyclic load experiments (see Section 6.2.3). As the cell pressure is increased, the volumetric strain tends towards contraction and the shear strain reduces, the volumetric strain converging on -0.6% and the shear strain converging on -0.9%. Due to the change in test conditions, there is insufficient data to compare this directly with the behaviour of the component materials. However, by comparison with Figs. 6.1, 6.2, 6.4 and 6.5, it can be seen that this behaviour is consistant with the behaviour described by Tam (1986), and it is also consistant with the rules of CSSM (Schofield and Wroth, 1968) as an increase in cell pressure would make the specimens less overconsolidated, and hence there would be less tendency to dilation. The increase in average effective stress on the material would also increase the frictional shear resistance of the material, and hence the shear deformation for a given deviator stress would be less.

6.5.4 Series TD - Effect of Interface Angle

Examination of axial strain, radial strain, volumetric strain and shear strain revealed no visible trends with the angle of the interface between the two materials. The only noteworthy point is that in the test with the interface at 45° to the horizontal, the radial target aligned with the highest point of the ballast layer was completely affixed to the ballast, rather than straddling the interface. With the other two targets mostly affixed to the 20mm material, the target on the ballast moved much less than the other two targets, as shown in Fig. 6.41. This confirms the observation of Section 6.2.2 that the smaller material tends to deform slightly more than the ballast.

These results would suggest that to all intents and purposes, the angle of the interface between ballast and 20mm material has no effect on the performance of the specimen.

6.5.5 Series TE - Effect of Layer Thickness

As can be seen from Table 6.1, the axial strain for both the specimens with unequal thickness of material was noticeably less than that of the specimen made up of equal thickness of material (set 5). This agrees with the findings from the monotonic loading tests (Section 6.2.5). If this is analysed in terms of volumetric and shear strain, as illustrated by Fig. 6.42, the specimens with an unequal layer thickness have lower levels of shear strain than the specimens of equal layer thickness, but volumetric strain, whilst being of similar value until 100 cycles, diverges after that point. Thus it appears that having a layer of material that lies mainly in the dead zone of the specimen acts as a restraint on the shearing ability of the specimen.

6.5.6 Series TF - Behaviour of Rounded River Gravel

As can be seen from Table 6.1, the specimen of rounded river gravel tested at a cell pressure of 90 kPa (set 21) gave a significantly greater axial deformation than either the ballast or 20mm materials when tested at 90 kPa cell pressure. This is due to its lower maximum principal stress ratio, with the consequently higher deviator stress to failure stress ratio, and thus higher deformations. The value of resilient modulus was intermediate between the values of the ballast and 20mm material.

When the river gravel was combined in a two layer specimen, however, the value of axial strain was significantly lower, and even lower than that of the two layer specimen comprising of ballast and 20mm material tested at 90 kPa cell pressure (set 7). This corresponds with the increase in strength found for such a material in Section 6.2.6, and would suggest that if the material can be sufficiently well restrained, then the tighter packing of the spherical particles results in lower levels of deformation.

6.6 Elastic Deformation Under Cyclic Loading

Even though plastic deformation is the most important parameter to consider in the context of track maintenance when analysing cyclic load tests, the elastic behaviour of the material is still important. Not only will increased elastic deformation affect the behaviour of the track superstructure, but from the findings of Section 6.3.1 it is also linked to the increased plastic deformation of the material.

Fig. 6.43 shows the graph of resilient modulus of the specimen against the number of load cycles for the first test on ballast at 40kPa (set 3). This is typical of the results from the test series, and shows a gradual increase in reslient modulus at the start of the test with the rate of increase reducing as the test proceeds. There is a certain degree of fluctuation in the value of modulus plotted over the period of the test, and for this reason the value of resilient modulus used for discussion and listed in Table 6.1 is an average of the resilient moduli taken over the last 60,000 cycles of the test. This is felt to be more representative of the material as it would behave after a period in the railway environment.

6.6.1 Series TA - Characterisation of the Material

Examination of the moduli for series A in Table 6.1 shows that all the materials fall within the band of values that would be expected from the literature, e.g. Evans (1993), Selig and Waters (1994). It appears that the particle size has little influence over the magnitude of the resilient modulus, although the values for the ballast (set 3) and the 10mm material (set 17) are a little lower than the others. As would be expected from the literature (Kalcheff and Hicks, 1973, Brown, 1974), the value of the cell pressure in the test has a much greater effect on the resilient modulus, with specimens tested at higher cell pressure having significantly greater moduli than the immediately preceding test carried out at lower cell pressure. However, equally important from examination of the data was the change in conditions that occurred midway through the test programme. As can be seen, the tests carried out at similar pressures on the ballast and 20mm materials were much lower in the latter part of the test series than in the first part. In fact, the tests carried out on these materials at 90 kPa cell pressure in the later half of the test series had only marginally greater modulus values than the tests carried out at 40 kPa cell pressure in the first half on the series. This further emphasises the findings of Section 6.4, which showed that the minimum stress in the cyclic test is highly important.

6.6.2 Series TB - Two Layer Specimens With Different Materials

It would be expected from the results of Section 6.6.1 that if the two materials in the layered specimen form a stable interface, then given that the behaviour of the materials with different particle sizes is very similar, the behaviour of the two layer specimens should be very similar. The data from the specimens with 20 and 14mm material in the top layer (sets 5 and 16) would uphold this theory. It can be seen that the value for the layered specimen of ballast and 10mm material (set 18) is significantly higher than those of the layered

specimens with the 20 and 14mm materials. However, examination of the data shows that this is the point where the minimum cyclic stress started to change. The log for the test on the layered specimen with 10mm material shows that the minimum cyclic stress increased significantly at the end of this test, which according to Section 6.4 would account for the change. The minimum stress in the cyclic test then dropped considerably, which is reflected in the value for the test with the 6mm material in the top layer of the specimen (set 20), which has a much lower value of resilient modulus. This value, however, could also be influenced by the fact that the 6mm material and the ballast do not form a very stable interface together, as highlighted by Section 6.2.2. Thus it would appear from the limited data that the size of the material in the top layer of a two layer specimen has no effect on the resilient modulus.

6.6.3 Series TC - Effect of Cell Pressure on a Two Layer Specimen

As discussed in Section 6.6.1, the cell pressure is a major influence on the value of the resilient modulus of the materials under test. Thus it would be expected that the resilient modulus of these specimens would increase with the cell pressure, and generally it can be seen from Table 6.1 that it does. However, the moduli for the tests carried out at 60 and 90 kPa cell pressure (sets 6 and 7) are very similar, which would not be expected. Examination of the test data shows no major differences in loading and Table 6.1 shows that there is less plastic deformation of the specimen tested at 90 kPa cell pressure, as would be expected, so the reason for the anomaly is unknown.

6.6.4 Series TD - Effect of Interface Angle on the Behaviour of a Two Layer Specimen

Examination of the moduli in Table 6.1 shows that there does not appear to be a pattern to the results of this test series. This would suggest that the angle of the interface has no effect on the resilient modulus of the specimen, confirming the findings of Section 6.5.4. There is significant scatter in the results however, with the specimen having an interface at 22° to the horizontal having a noticeably higher modulus. This could be due to the fact that these specimens were partially prepared by hand, thus introducing variability into the preparation procedure.

6.6.5 Series TE - The Effect of Layer Thickness

There is no obvious pattern to the results of this test series, as shown in Table 6.1. The

modulus of the two layer specimen is slightly lower when the majority of the specimen is composed of ballast, but at all times the specimens fall within the values of the two materials, as found in Series TA - Section 6.6.1.

6.6.6 Series TF - Behaviour of Rounded River Gravel

Given that the Series TF experiments were carried out in the second half of the test programme, it is perhaps wise to compare them only with the other tests carried out in the latter half of the programme. In this respect, the resilient modulus of the rounded river characterisation test (set 21) is higher than that of ballast tested at 90 kPa cell pressure (set 32), but lower than that of the 20mm granite material tested at 90 kPa cell pressure (set 30). The two-layer specimen tested at the same cell pressure had a slightly higher modulus, which is suprising as it would be expected to have a value intermediate to those of its components. The modulus of the two-layer specimen with an interface at 45° to the horizontal (set 23) however, was similar to that of the specimen of river gravel alone.

6.7 Post Cyclic Monotonic Tests

As stated in Section 5.4, monotonic loading tests were carried out on the specimens subjected to cyclic loading to compare with the initial monotonic tests and ascertain what changes the cycling had caused in their behaviour. The results of these tests, again organised by series, are summarised here.

6.7.1 Series TA - Characterisation of the Material

As before, a pre-requisite to the analysis of the two layer specimens is a knowledge of the behaviour of the component materials. The behaviour of the component materials post cycling is briefly analysed here.

Fig. 6.44 illustrates the deviator stress for a post cyclic monotonic test on the first ballast specimen tested at 40 kPa cell pressure (set 3), along with the data from the corresponding initial monotonic test as a comparison. This specimen displays characteristics of a densely packed, highly overconsolidated cohesionless material. The specimen is much stiffer and stronger than the specimen that had not been cyclically loaded, with the deviator stress quickly rising to a peak value and then tailing off gradually to an assumed eventual critical state (constant volume shearing) value beyond the range of the transducers. Such behaviour would suggest that the specimen has been further overconsolidated during the cycling phase

of the test, and is hence dilating more and so giving the peak stress. This is contrary to what has been observed in the tests though, in Section 6.5.1 it was seen that the specimen dilated during cycling, as was expected. Thus it would appear that the behaviour of these specimens is anomolous in terms of conventional soil mechanics, where it would be expected that a specimen would become weaker as it became less dense, not stronger.

As can be seen from Table 6.1, for the tests on ballast (set 3) the rate of volumetric dilation is significantly greater for the post cyclic specimen than for the initial specimen, which would reinforce the idea given by the deviator stress that the overconsolidation ratio has increased during cycling. There is always the possibility that the volumetric strain measurements could be at fault. As the specimen deforms and loses its barrel shape, the accuracy could be reduced, as previously noted. Given that the specimen is already highly deformed at the start of the post cyclic test, it would be expected that the post cyclic figure is less likely to be accurate. There is the possibility that this could explain the anomoly mentioned above, with the specimen starting to contract again after many cycles, but with the highly deformed specimen giving false volumetric strain measurements.

Table 6.1 shows how the first test carried out on ballast at a cell pressure of 40 kPa compares with the second test (set 31), supposedly carried out under similar conditions but which deformed to a much greater extent during the cyclic phase of the test. The deviator stress of the latter test can be seen to be very similar, at a peak of 384 kPa. Examination of the radial strain data for two tests (Fig. 6.45), reveals that after the initial 'elastic' phase, the radial deformation in the second test is much more smooth and uniform than that of the first test. This suggests that once the inter-particle friction has been overcome, there is some form of lubrication between the particles. This could perhaps be linked to the presence of water in the specimen or a change in surface abrasion and particle packing due to the decrease in resilient modulus under the changed conditions.

Fig. 6.46 compares the first ballast test carried out at a cell pressure of 40 kPa (set 3) with the test carried out later in the test programme at a cell pressure of 90 kPa (set 32). As would be expected, the peak deviator stress of the test at 90kPa cell pressure is higher than that of the 40 kPa cell pressure test, although not as high as might be expected. It can be seen from Table 6.1 that the specimen tested at 90 kPa cell pressure, which contracted during cycling, has shown a maximum principal stress ratio of 6.2, which is only slightly

higher than the maximum principal stress ratio of the uncycled specimen (5.9). The specimen tested at 40 kPa cell pressure, which underwent dilation during cycling, gave a maximum principal stress ratio of 11.0 after cycling, a significant increase on the figure for the uncycled specimen (7.1). Table 6.1 shows that these changes are not just due to the change in test conditions between the first and second halves of the test series, as the test set carried out on ballast at 40 kPa cell pressure in the first half of the series (set 3) shows similar trends to the test set carried out on ballast at 40 kPa cell pressure in the second half of the test series (set 31).

It can be seen from Table 6.1 that the 20mm material showed similar trends to the ballast between pre and post cycling specimens, with an increase in stiffness and strength after cycling which was most pronounced in the case of the specimen tested at 40 kPa cell pressure despite this specimen undergoing dilation during cycling.

6.7.2 Series TB - Behaviour of Two Layer Specimens

From Table 6.1, it can be seen that in terms of peak deviator stress, the behaviour of all the two layer specimens with layers of different particle sizes are very similar. There is significantly less variation in the specimens than displayed by the corresponding initial monotonic tests. Similarly, with the exception of the specimen comprising of ballast and 20mm material (set 5), the volumetric behaviour of all the specimens is much more uniform than in the initial monotonic tests. It would appear that the process of cyclic loading has perhaps re-arranged the specimens into some more uniform state. It must also be noted that all specimens have increased in strength despite undergoing dilation during cycling.

6.7.3 Series TC - Two Layer Specimens Under Differing Cell Pressures

As in Section 6.7.2, the information in Table 6.1 would suggest much more uniformity from the specimens that have undergone cyclic loading than those corresponding specimens that have not. In this case, the effect of the cell pressure appears to have been reduced with only a 20% increase in strength with an increase in cell pressure from 40 to 90kPa in the post cyclic specimens, as opposed to an increase of 100% for the initial monotonic specimens. The principal stress ratio, however, has undergone the opposite effect with the values for the initial monotonic tests being very uniform, and those of the post cyclic monotonic tests decreasing considerably with the increase in cell pressure.

If these results are plotted in the form of a Mohr-Coulomb failure envelope (see Fig. 6.47), it can be seen that cyclic loading appears to have given an apparent cohesion to the specimens, with a correspondingly lower value for the angle of shearing resistance.

If the post cyclic result for the two layer specimen tested at 90 kPa cell pressure (set 7) is plotted with the pre cycling result for that set (see Fig. 6.48), it can be seen that the deviator stress for the post cyclic stress quickly rises at the beginning of the test, peaks and then starts to reduce as would be expected from previous results. However, the deviator stress then reaches a value similar to that of the pre-cycling specimen at a similar axial strain and rises again, shadowing the deviator stress of the pre-cycling specimen. For this to occur in conventional soil mechanics, the volumetric strain rate would have to increase, decrease, and then increase again, which is not seen in any of the literature. As can be seen from Fig. 6.49 there are changes in the rate of volumetric strain during the test, but they do not correspond particularly well with the deviator stress, and may be inaccuracies in the measurement. This behaviour would suggest that the two peak strengths could be occurring by different mechanisms, the latter peak by conventional dilation as with the pre cycling specimen, and the first peak by some unknown method. Data for other tests (e.g. Fig. 6.46) shows that whilst not exhibiting two peaks, the material behaves in a similar manner. The deviator stress shows an initial peak value, and then tends to move toward the value exhibited by the corresponding specimen under initial monotonic loading. This value exhibited by the specimens in the initial monotonic test is itself a peak value, as the specimens are overconsolidated and dilating, so in a form the specimen is still showing two values for peak stress.

6.7.4 Series TD - The Effect of Variation in the Angle of Interface

As can be seen from Table 6.1, there is no particular trend evident in the value of deviator stress with interface angle in the specimen. As with the initial monotonic and cyclic tests, this would indicate that when the two layer specimen is comprised of ballast and 20mm material, the angle of the interface does not have an effect on the post cyclic monotonic stress.

6.7.5 Series TE - Effect of Layer Thickness

Table 6.1 shows that unlike the corresponding initial tests, the deviator stress behaviour of all these specimens is virtually identical. The rate of volumetric strain, however, increases

with the proportion of 20mm stone. This behaviour is unexpected given that the values for the components individually fall somewhere in the middle of this range, giving similar results to the specimen with equal layer thickness.

6.7.6 Series TF - Behaviour of Rounded River Gravel

When tested on its own, rounded river gravel gives a lower peak deviator stress than other materials tested at 90kPa cell pressure, as can be seen from Table 6.1. However, when it is tested in the form of a two layer specimen and thus more restrained, as in the initial monotonic test and the cyclic test it shows a higher degree of strength and lower volumetric deformation.

As in the initial monotonic test however, when a specimen with the material interface at 45° to the horizontal is tested, the behaviour of the specimen is more similar to that of the rounded material alone. This is thought to be due to the majority of the shear band comprising of rounded material.

6.8 Addition of Polymer Mesh Elements

Section 5.4.7 describes tests that were undertaken to investigate the use of polymer mesh elements as reinforcement in ballast. These tests involved two types of element, Netlon geogrid and Terram geotextile, cut into small pieces and added to the ballast specimens, which were then tested as normal.

The results of these tests are shown in Fig. 6.50 and in Table 6.1. It can be seen that the deviator stresses reached by the specimens with added polymer reinforcement were much lower than that of the ballast specimen alone. In the case of the Netlon elements, it is thought that the drop in strength was due to the high porosity of the specimen - 0.506 - compared with that of a typical ballast specimen - 0.450. This drop in porosity was a result of the method of preparation, involving hand placement of material, and bridging of inter-particle gaps in the material by the rigid reinforcement. The bridging of the gaps would result in fewer and weaker inter-particle contacts, and mean that considerable strain of the specimen would be required in order to deform the Netlon elements sufficiently to densify the material.

The Terram reinforcement elements were not sufficiently rigid to result in the bridging of inter-particle spaces, and so the resultant porosity of the specimen was very similar to that of ballast without reinforcement, at 0.45. In the case of this reinforcement method though, it is thought that the material, in separating the contact points of the granite particles, reduced the inter-particle friction. This friction would only be restored by the puncturing and tearing of the material as the specimen is strained, as can be seen in Plate 6.3. Having punctured the specimen, the inter-particle movement would then cause tensile forces to build up in the material. However, it is believed that the material was not sufficiently strong for these to compensate for the loss of inter-particle friction at other points not yet punctured, with the net reduction in specimen strength.

Test Series & Test Set	Description	Initial Monotonic Test				Cyclic Test		Post Cyclic Monotonic Test			
		Peak Ave. Deviator Stress (kPa)	Strain at Peak Stress (%)	Peak Principal Stress Ratio	Volumetric Strain at 1% Axial Strain (%)	Axial Strain at 100,000 Cycles (%)	Resilient Modulus (MPa)	Peak Ave. Deviator Stress (kPa)	Strain at Peak Stress (%)	Peak Principal Stress Ratio	Volumetric Strain at 1% Axial Strain (%)
TA - 3	Ballast Only	247	6.69	7.1	-0.51	3.22	144	400	0.33	11.0	1.87
TA - 31	Ballast Only	223	5.20	6.4	0.20	7.22	117	384	0.35	10.1	2.62
TA - 32	Ballast Only, 90 kPa CP	439	6.50	5.9	-0.45	2.36	149	477	4.61	6.24	0.49
TA - 4	20 mm Stone Only	265	3.22	7.6	1.29	2.80	179	418	0.23	11.4	2.73
TA - 25	20 mm Stone Only - Lost	222	2.99	6.3	1.45	9.55	139	-	-	-	-
TA - 27	20 mm stone Only	206	3.39	5.9	1.27	8.17	144	372	0.29	9.9	2.74
TA - 30	20 mm Stone, 90 kPa CP	494	3.73	6.4	0.37	1.47	191	516	0.23	6.6	1.78
TA - 15	14mm Stone Only	244	3.06	6.8	0.70	3.37	173	449	0.26	11.7	2.64
TA - 17	10mm Stone Only	259	4.00	7.2	0.86	3.46	151	443	0.28	11.5	2.64
TA - 19	6mm Stone Only	190	4.26	5.5	0.59	Failed	Failed	-	-	-	-
TB - 5	2 Layer, Ballast & 20mm	238	3.21	6.9	0.49	3.30	160	409	0.25	11.2	2.58
TB - 16	2 Layer, Ballast & 14mm	304	2.81	8.3	0.82	4.72	162	384	0.26	10.2	2.11
TB - 18	2 Layer, Ballast & 10mm	272	3.96	7.5	0.30	4.00	178	410	0.25	10.8	2.17
TB - 20	2 Layer, Ballast & 6mm	230	3.90	6.5	0.48	6.88	135	414	0.32	10.8	2.04
TC - 5	2 Layer, 40 kPa CP	238	3.21	6.9	0.49	3.30	160	409	0.25	11.2	2.58
TC - 6	2 Layer, 60 kPa CP	339	3.59	6.7	0.25	1.52	184	447	0.28	8.4	1.84
TC - 7	2 Layer, 90 kPa CP	497	4.97	6.5	-0.19	1.24	182	511	5.96	6.7	0.60
TC - 8	2 Layer, 30/35 kPa CP	223	3.49	8.3	1.69	10.71	109	-	-	-	-
TD - 5	2 Layer, Interface at 0°	238	3.21	6.9	0.49	3.30	160	409	0.25	11.2	2.58
TD - 9	2 Layer, Interface at 11°	249	4.69	7.2	0.96	3.14	145	393	0.27	10.8	3.35
TD - 10	2 Layer, Interface at 22°	283	3.45	8.1	0.51	3.17	179	415	0.28	11.3	2.33
TD - 11	2 Layer, Interface at 33°	260	2.86	7.5	0.49	3.53	147	459	0.32	12.2	2.59
TD - 12	2 Layer, Interface at 45°	278	5.56	7.9	0.29	3.48	159	412	0.29	11.2	3.66
TE - 13	2 Layer, Thick Ballast	293	3.34	8.3	1.80	2.08	149	398	0.25	10.8	1.45
TE - 5	2 Layer, Equal Layers	238	3.21	6.9	0.49	3.30	160	409	0.25	11.2	2.58
TE - 14	2 Layer, Thin Ballast	313	3.42	8.8	1.03	2.30	159	424	0.25	11.6	3.90
TF - 21	Gravel Only	128	3.26	4.1	1.35	3.37	161	431	0.26	5.7	2.27
TF - 22	2 Layer, Gravel & Ballast	414	2.91	5.5	0.58	1.07	166	524	0.32	6.8	0.71
TF - 23	2 Layer, G & B, 45° Int	371	4.63	5.1	0.22	1.35	159	452	0.32	5.9	1.60
TF - 24	2 Layer, G & B, 60 kPa	574	3.99	10.27	1.24	Failed	Failed	-	-	-	-
TF - 33	2 Layer, Monotonic Only	332	2.62	4.6	1.33	-	-	-	-	-	-
TG - 3	Ballast Only	247	6.69	7.1	-0.51	-	-	-	-	-	-
TG - 28	Ballast + Netlon element	183	7.92	5.5	-0.15	-	-	-	-	-	-
TG - 29	Ballast + Terram element	207	8.18	6.0	1.15	-	-	-	-	-	-
TH - 5	Basic 2 Layer Test	-	-	-	-	3.30	160	409	0.25	11.4	2.58
TH - REP2	Mid-Series Repeatability	-	-	-	-	2.88	160	428	0.28	11.2	2.47
TH - REP3	End-Series Repeatability	-	-	-	-	10.45	112	Failed	Failed	Failed	Failed
TI - 37	8kPa Min. Stress	-	-	-	-	3.15	162	448	0.28	12.3	1.89
TI - 35	17kPa Min. Stress	-	-	-	-	2.65	184	452	0.26	12.3	2.12
TI - 36	25kPa Min. Stress - Lost	-	-	-	-	3.23	194	422	0.26	11.6	2.50
TI - 38	25kPa Min. Stress	-	-	-	-	3.65	186	377	0.25	10.4	2.15
TJ - 35	Materials Dry	-	-	-	-	2.65	184	452	0.26	12.3	2.12
TJ - 39	Materials Wet	-	-	-	-	4.43	185	508	0.36	13.6	2.27
TK - 35	Secondary Series Start	-	-	-	-	2.65	184	452	0.26	12.3	2.12
TK - 40	Secondary Series End	-	-	-	-	2.42	182	462	0.26	12.5	2.12
TK - 5	Main Series Start	-	-	-	-	3.30	160	409	0.25	11.2	2.58
TK - REP2	Main Series Middle	-	-	-	-	2.88	160	428	0.28	11.2	2.47

Table 6.1 - Summary of triaxial test results

Author	Material	Grading (mm)	Density (kg/m^3)	Comments
Raymond and (1978)	Dolomite	5-38	1400-1700	
Alva-Hurtado and Selig (1981)	Granite	5-30	1530	Uncompacted
			1620	Compacted
Indraratna et al. (1998)	Laitite	10-50	1530	

Table 6.2 - Initial specimen densities obtained for monotonic triaxial tests on ballast

Test Specimen	Test Set	Angle of Shearing Resistance (in °, c′ = 0)
Ballast	3	49
20mm Stone	4	50
2 Layer - ballast and 20mm	5	48
14mm Stone	15	49
2 Layer - ballast and 14mm	16	52
10mm Stone	17	50
2 Layer - ballast and 10mm	18	51
6mm Stone	19	45
2 Layer - ballast and 6mm	20	48

Table 6.3 - Summary of the peak angle of shearing resistance at 40 kPa cell pressure for specimens in test Series TB, along with the values for the component materials

Specimen	Peak Average Deviator Stress (kPa)	Angle of Shearing Resistance (in °, c′ = 0)
Ballast	247	49
350mm Ballast, 100mm 20mm Stone	263	52
Equal Ballast and 20mm Stone	238	48
150mm Ballast, 300mm 20mm Stone	314	53
20mm Stone	265	50

Table 6.4 - Summary of deviator stress and angle of shearing resistance at 40 kPa cell pressure for specimens with different relative thicknesses of ballast and 20mm stone

	Test 37 Low Load	Test 35 Medium Load	Test 38 High Load
Observed Resilient Modulus (MPa)	162	184	186
Results of Predictive Models			
Boyce et al. (1976)	412	466	528
Error Factor	0.39	0.39	0.35
Pappin and Brown (1980)	395	443	490
Error Factor	0.41	0.42	0.38
Brown and O'Reilly (1991)	355	384	408
Error Factor	0.46	0.48	0.46

Table 6.5 - Comparison of observed resilient moduli with outputs from predictive models.

Test Specimen	Test Set Number	Reduction in Load (%)
Ballast	3	13
20mm stone	4	6
14mm stone	15	7
10mm stone	17	6

Table 6.6 - Drop in deviator stress during period of the test for selected tests.

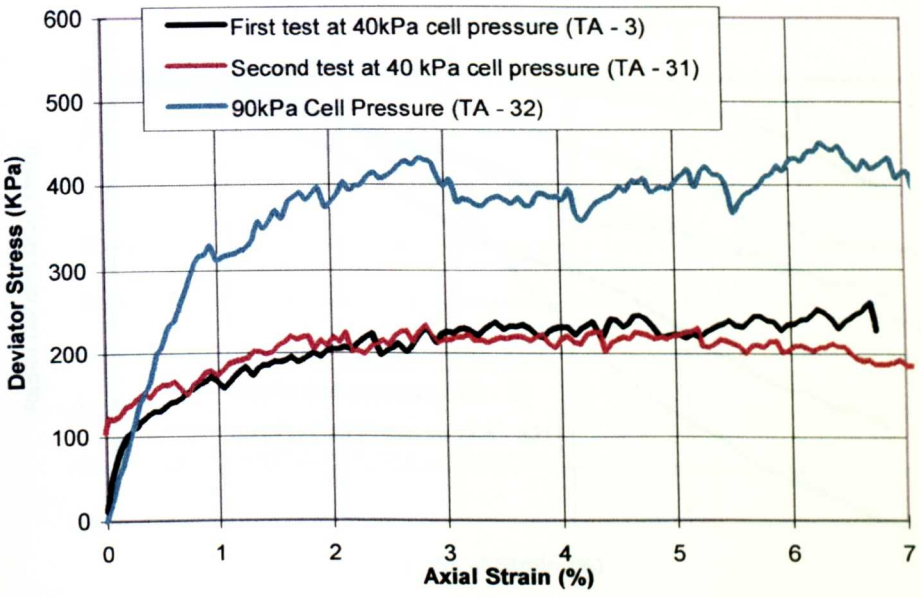

Fig. 6.1 - Deviator stress against axial strain for initial monotonic triaxial tests on ballast

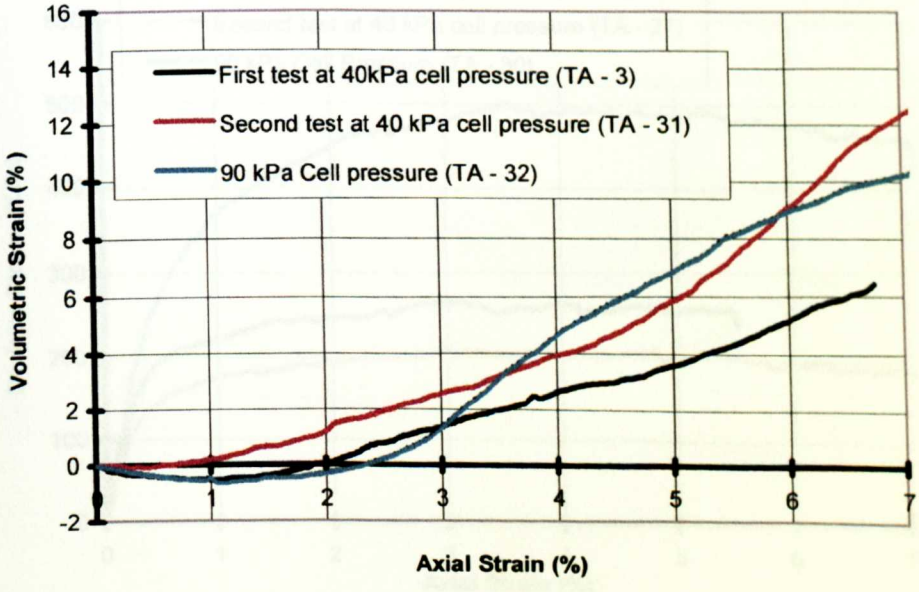

Fig. 6.2 - Volumetric strain against axial strain for initial monotonic tests on ballast

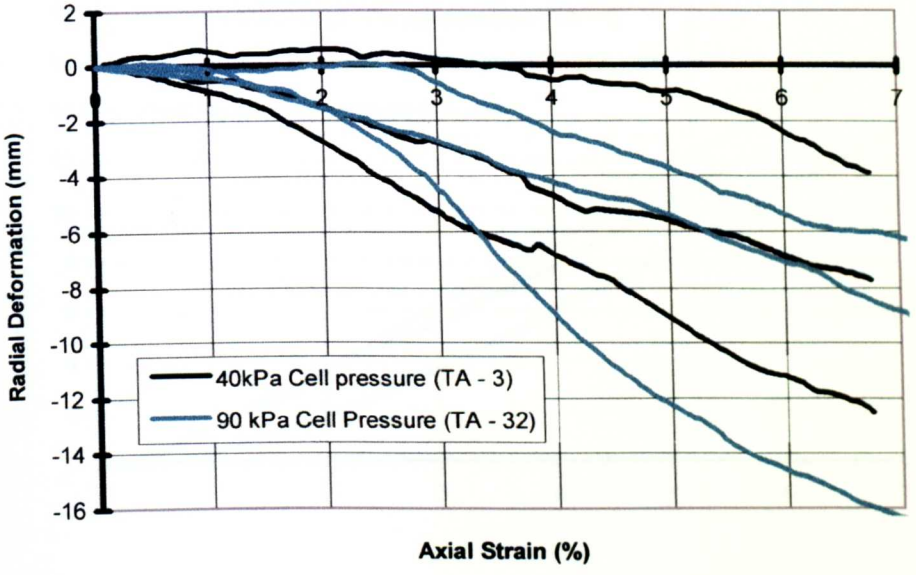

Fig. 6.3 - Radial deformation with axial strain for initial monotonic triaxial tests on ballast

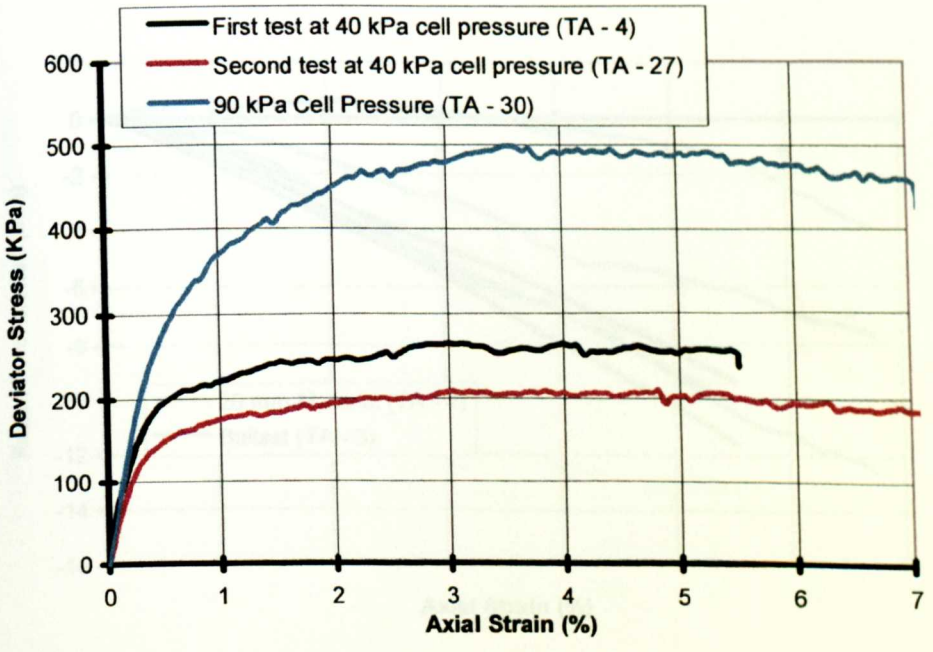

Fig. 6.4 - Deviator stress against axial strain for initial monotonic triaxial tests on 20mm material

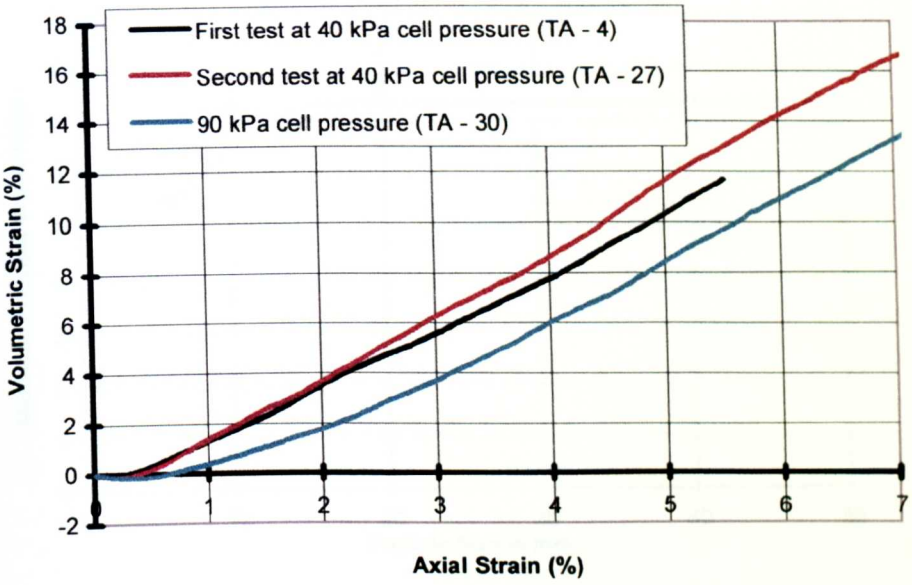

Fig. 6.5 - Volumetric strain against axial strain for initial monotonic triaxial tests on 20mm material

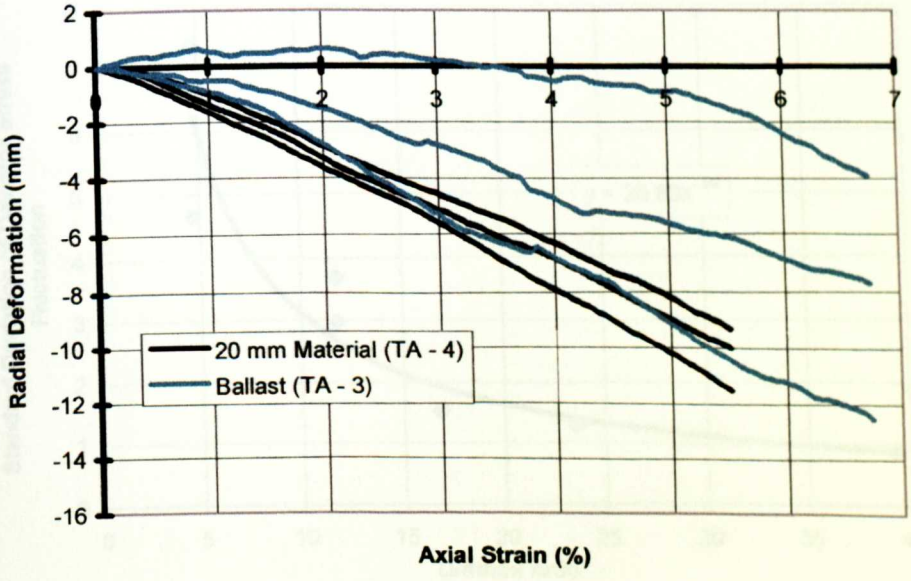

Fig. 6.6 - Comparison of radial deformation with axial strain for initial monotonic tests on ballast and 20mm material

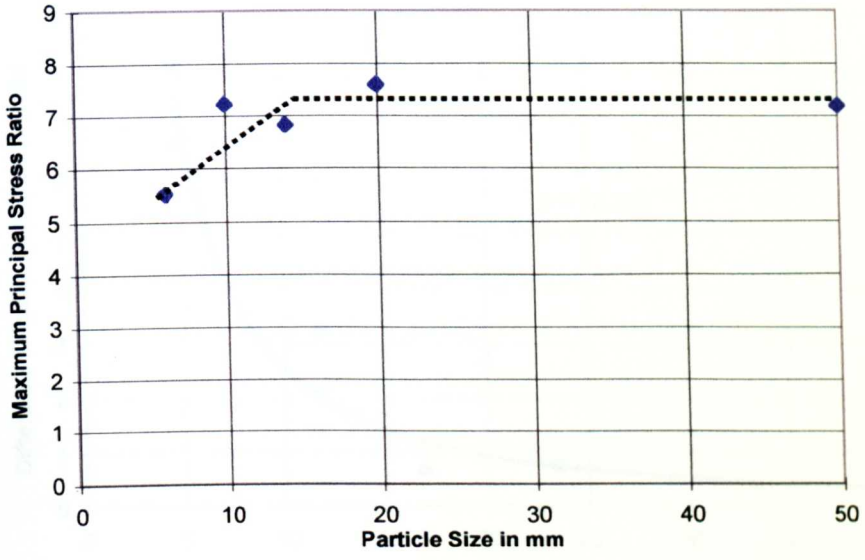

Fig. 6.7 - Variation in maximum principal stress ratio achieved with maximum particle size for tests in Series TA

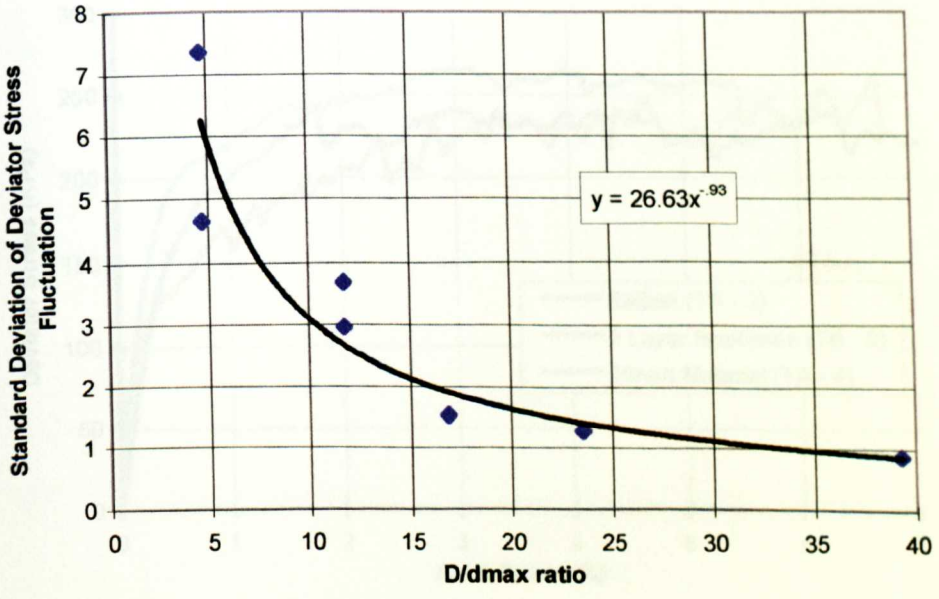

Fig. 6.8 - Variation in the fluctuation of the deviator stress during initial monotonic tests with D/d_{max} ratio for tests in Series TA

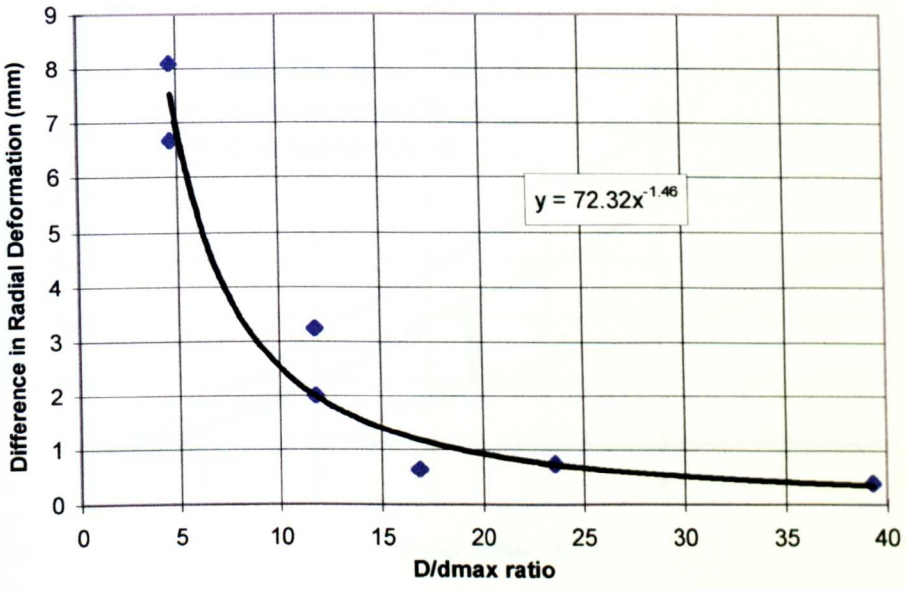

Fig. 6.9 - Variation in the difference in radial deformation with D/d_{max} ratio for tests in Series TA

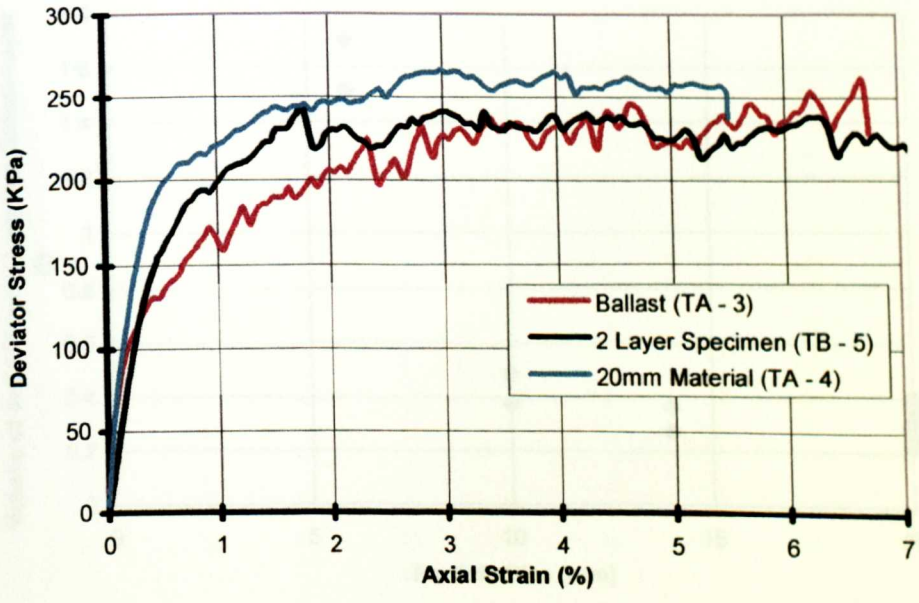

Fig. 6.10 - Deviator stress against axial strain for the initial monotonic test on a two layer specimen of ballast and 20mm material, with the values for its component materials

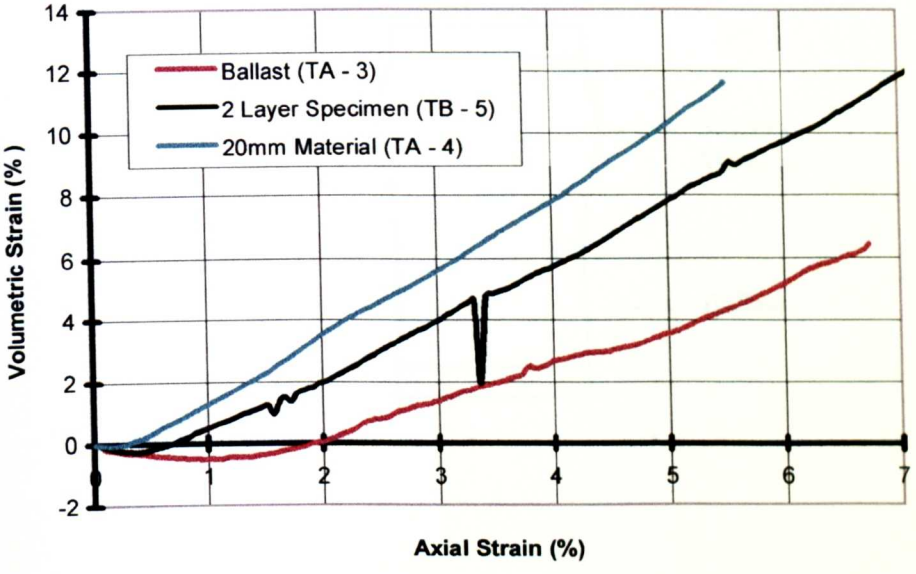

Fig. 6.11 - Volumetric strain against axial strain for the initial monotonic test on a two-layer specimen of ballast and 20mm material, with the values for its component materials

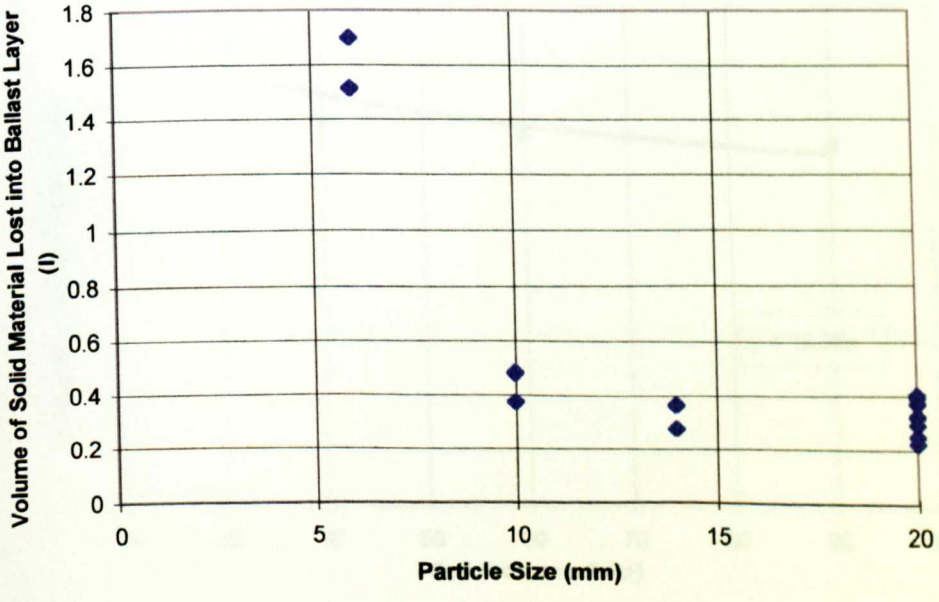

Fig. 6.12 - Volume of material lost into the ballast layer during specimen preparation against particle size for tests in Series TB

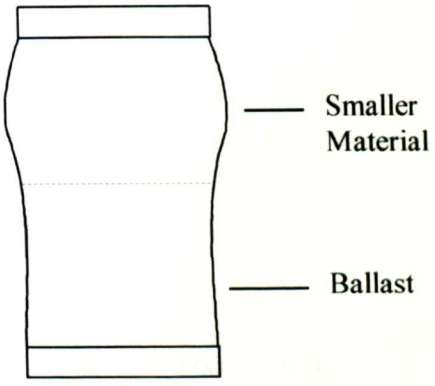

Fig. 6.13 - Mode of deformation for typical two layer specimen

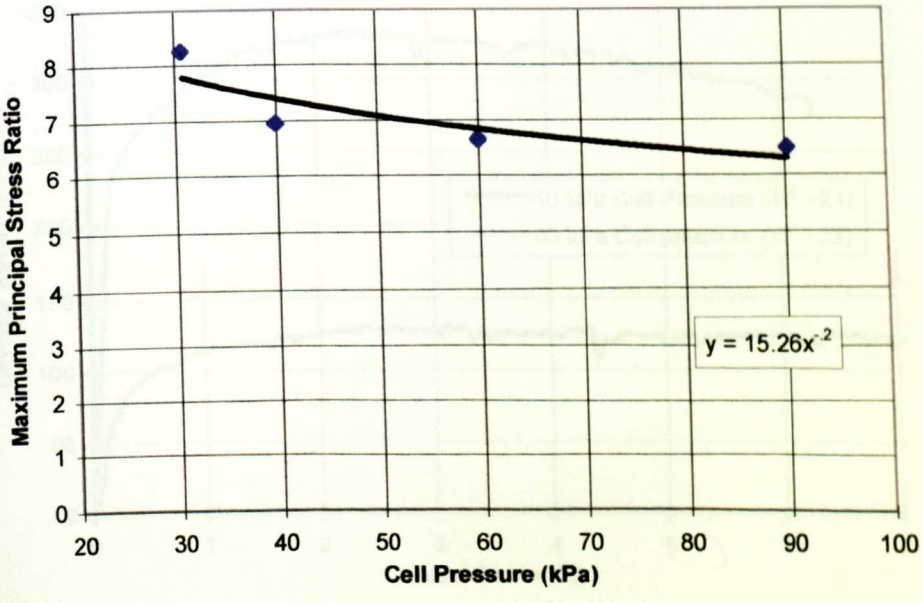

Fig. 6.14 - Change in maximum principal stress ratio with cell pressure for Tests in Series TC

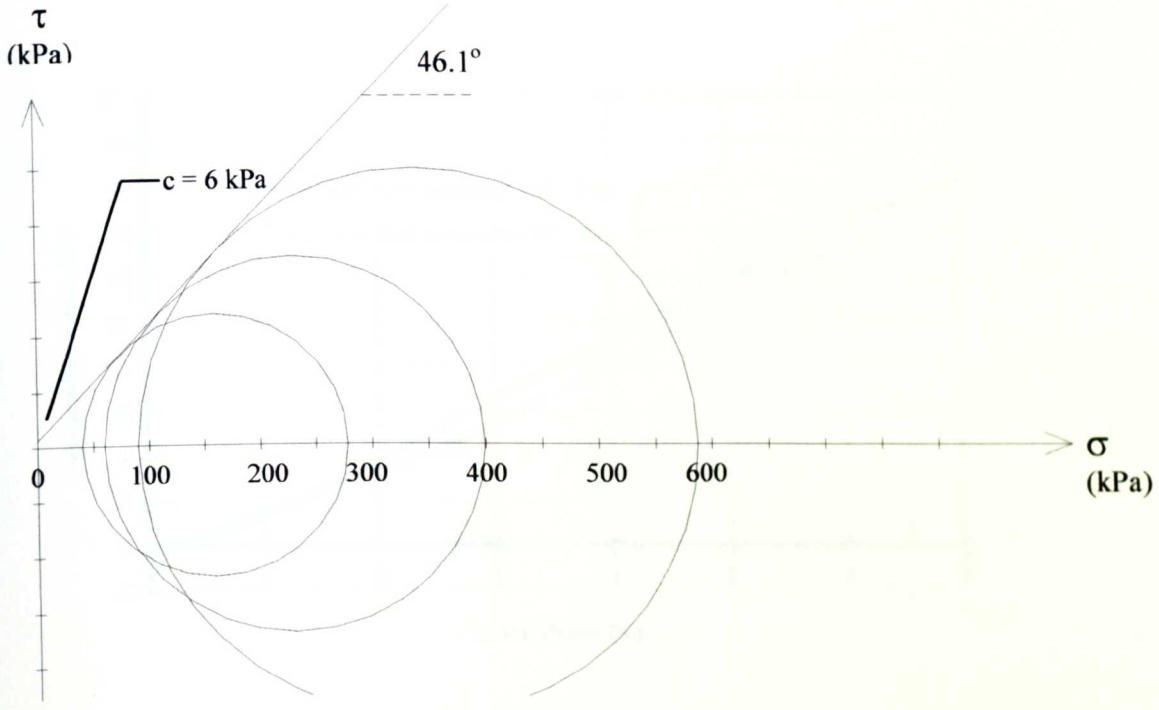

Fig. 6.15 - Failure envelope for two-layer specimens of ballast and 20mm material in initial monotonic tests from Series TC

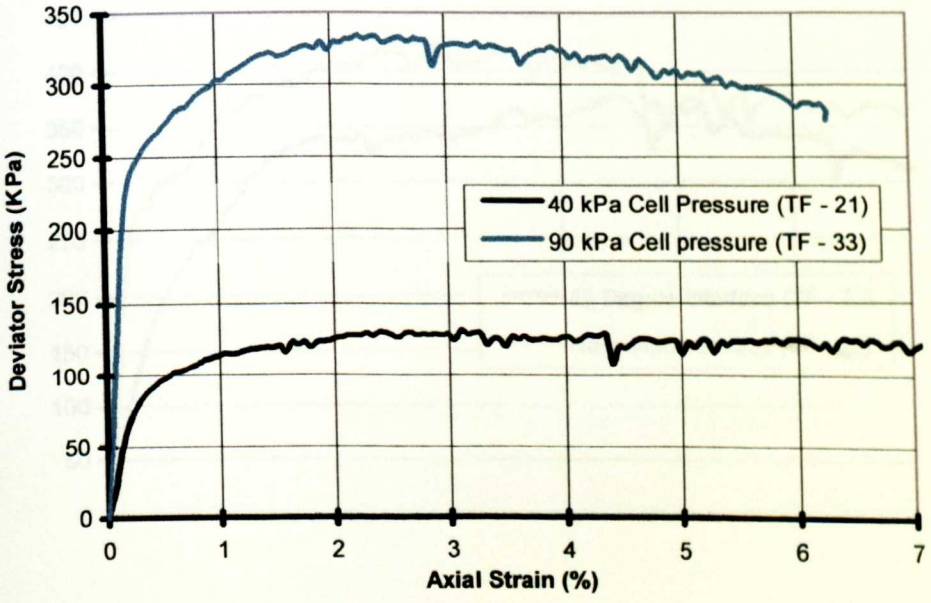

Fig. 6.16 - Deviator stress against axial strain for initial monotonic tests on rounded river gravel

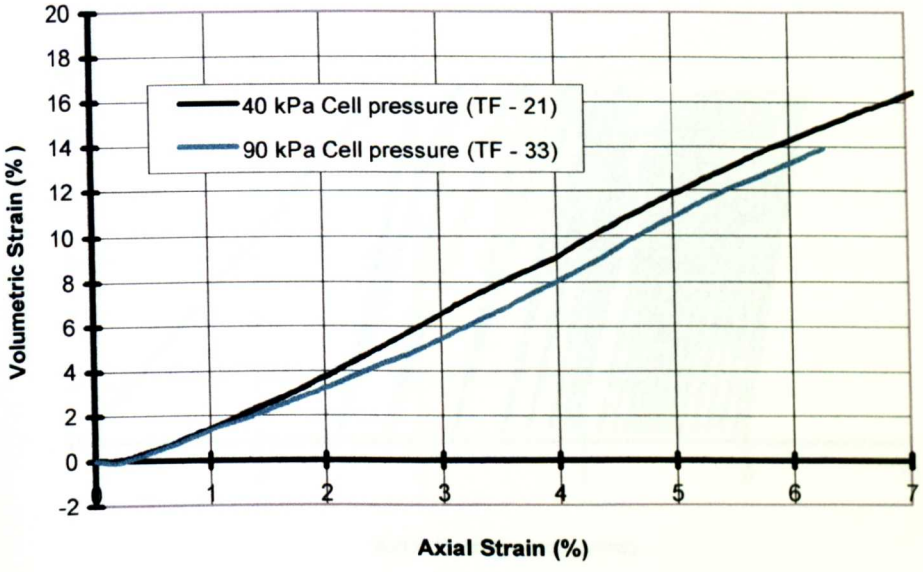

Fig. 6.17 - Volumetric strain against axial strain for initial monotonic tests on rounded river gravel

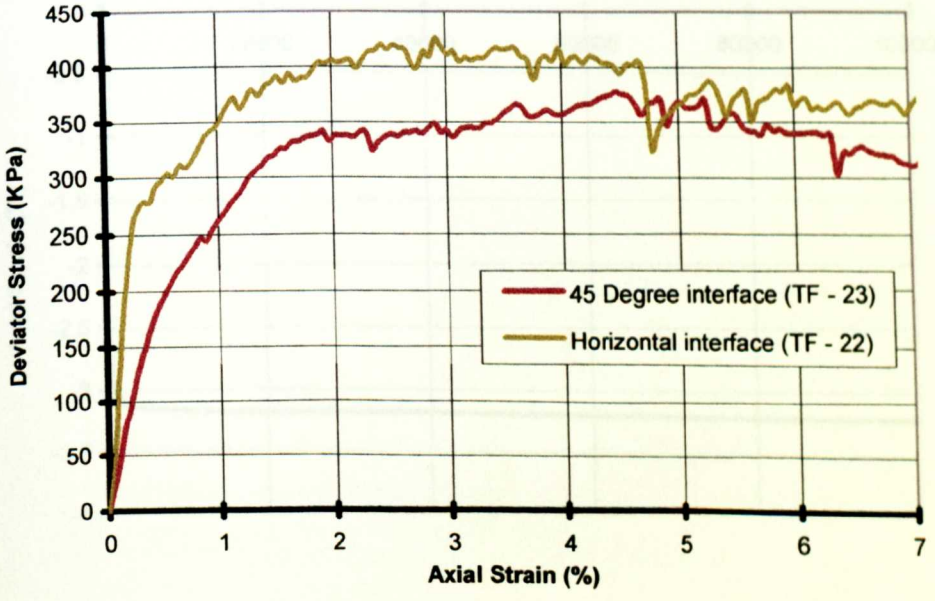

Fig. 6.18 - Deviator stress against axial strain for two-layer specimens of ballast and river gravel at different interface angles

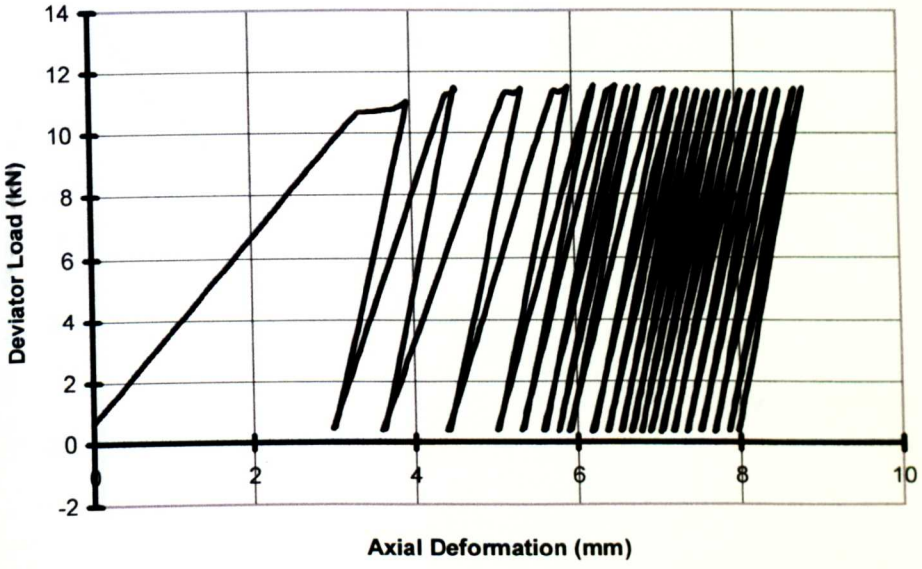

Fig. 6.19 - Deviator load against axial deformation at the start of a cyclic load triaxial test on ballast (from Test Set TA - 3)

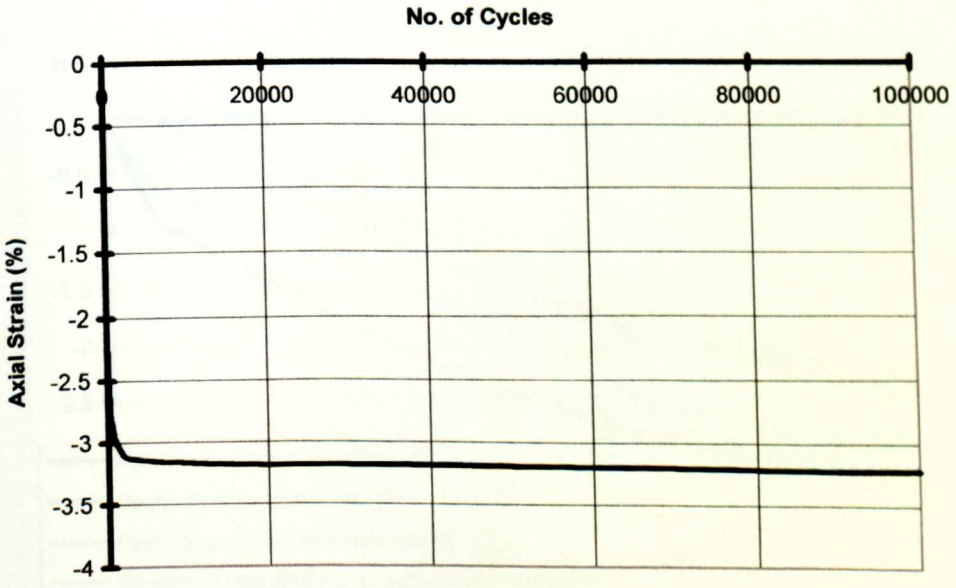

Fig. 6.20 - Axial strain against number of load cycles, for the first cyclic load test on ballast (from Test Set TA - 3)

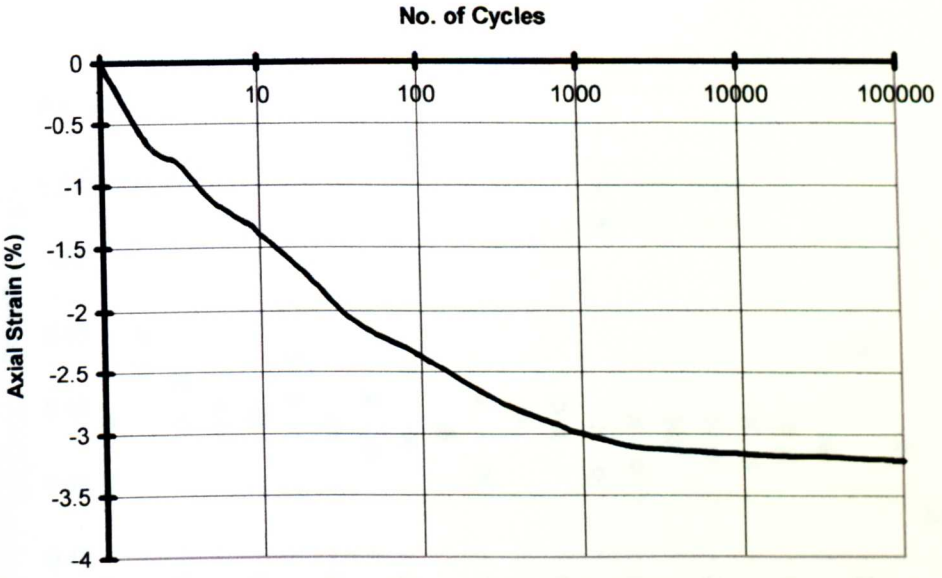

Fig. 6.21 - Axial strain against the number of load cycles on a logarithmic scale for the first cyclic load test on ballast (from Test Set TA - 3)

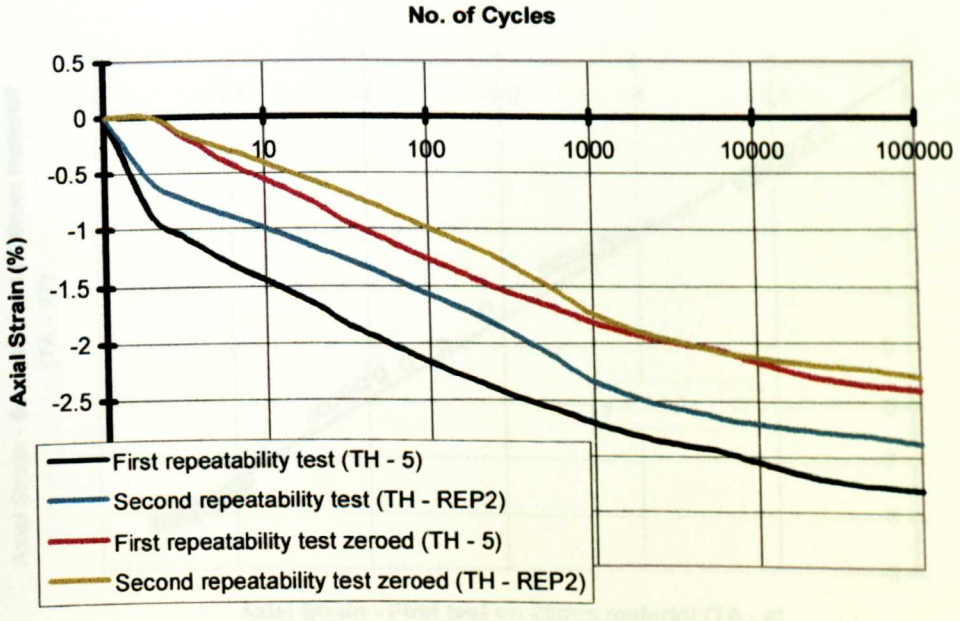

Fig. 6.22 - Axial strain against the number of load cycles for the first and second repeatability tests, along with the values zeroed to the start of the second load cycle

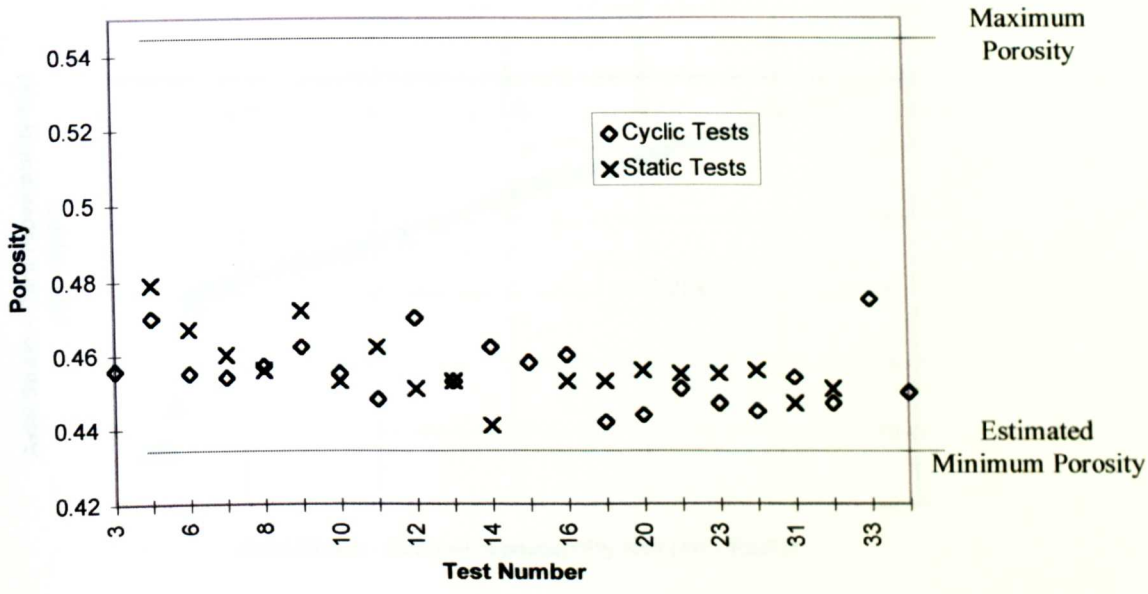

Fig. 6.23 - Porosity of the ballast specimens with progress though the test programme

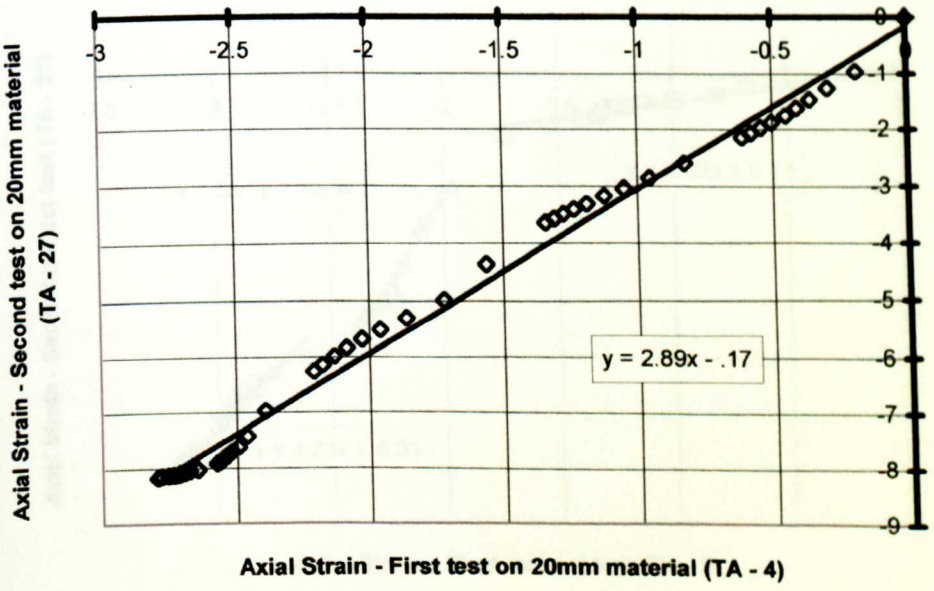

Fig. 6.24 - Comparison of axial strain at corresponding points of the first and second cyclic tests on 20mm material at 40 kPa cell pressure

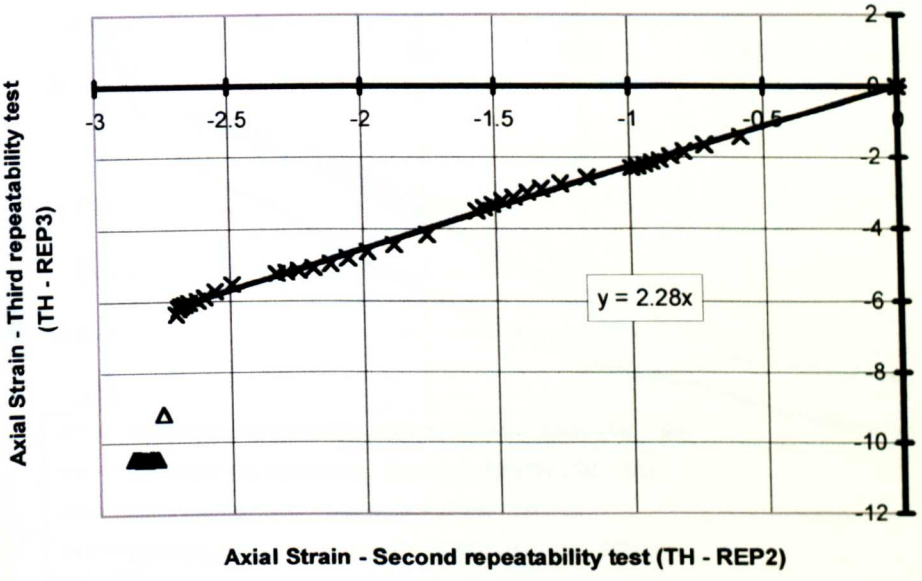

Fig. 6.25 - Comparison of axial strain at corresponding points of the second and third repeatability tests

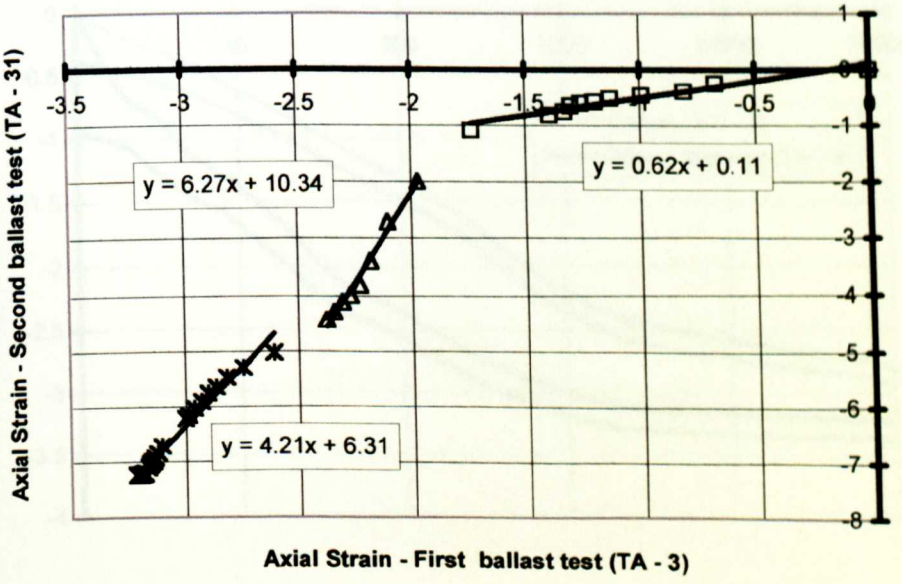

Fig. 6.26 - Comparison of axial strain at corresponding points of the first and second cyclic tests on ballast at 40 kPa cell pressure

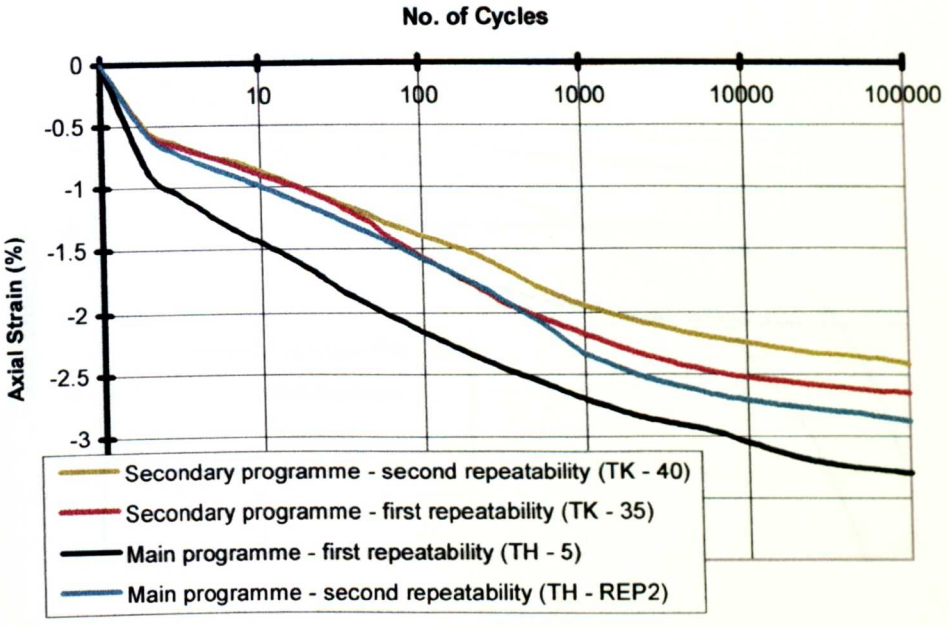

Fig. 6.27 - Axial strain against number of load cycles for main and secondary repeatability tests

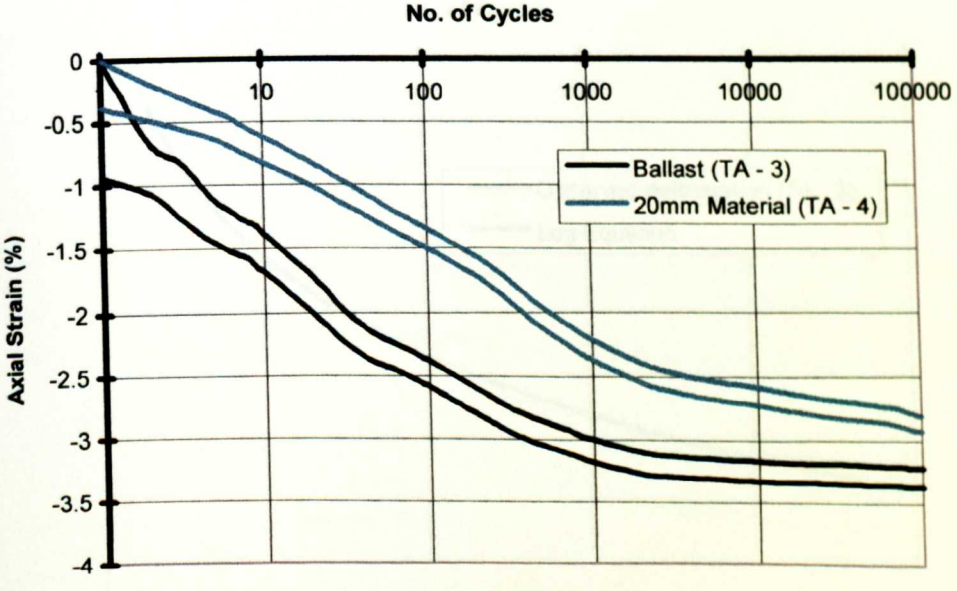

Fig. 6.28 - Axial strain against number of load cycles for cyclic tests on ballast and 20mm material

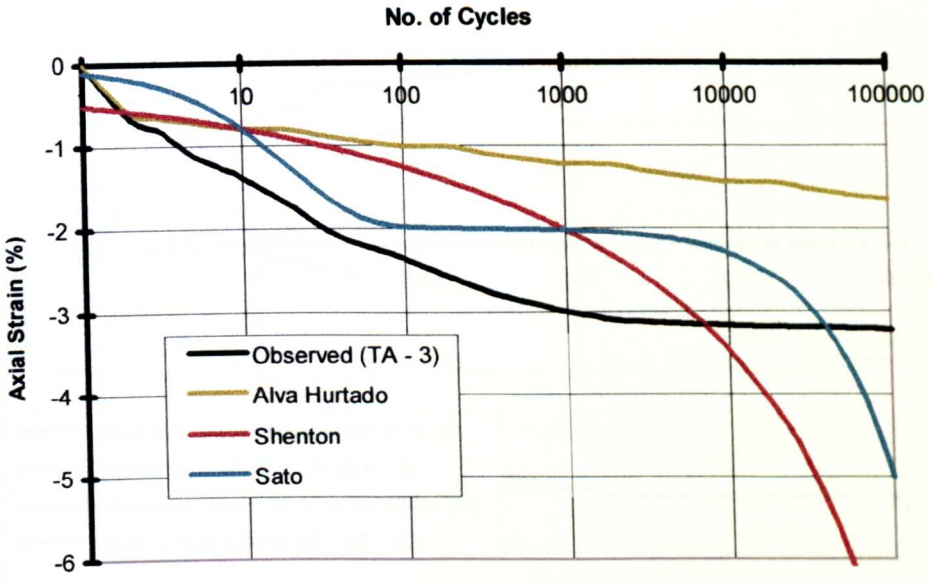

Fig. 6.29 - Observed axial strain of ballast against number of load cycles compared with predictive equations

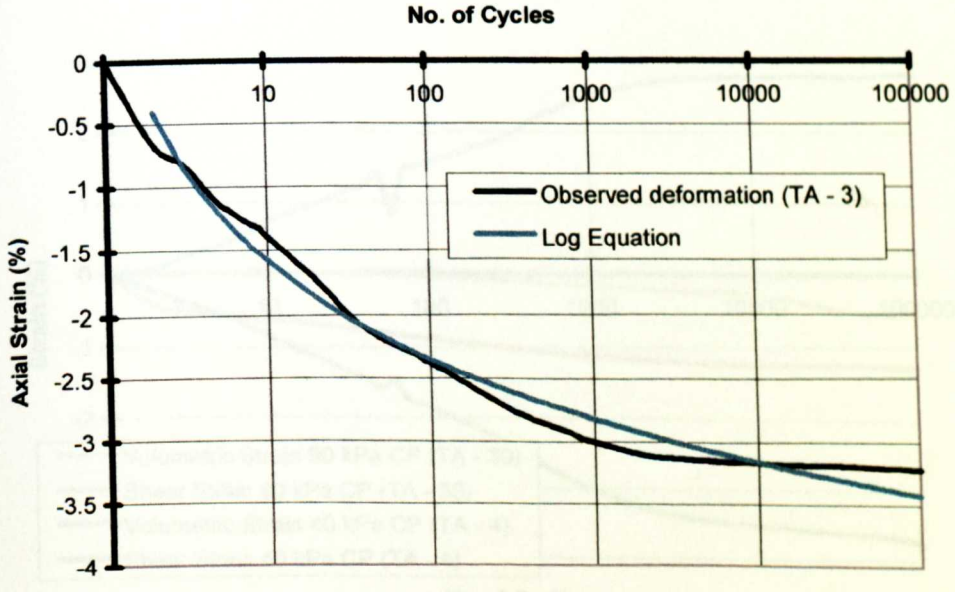

Fig. 6.30 - Observed axial strain of ballast against number of load cycles compared with log (log (N)) equation

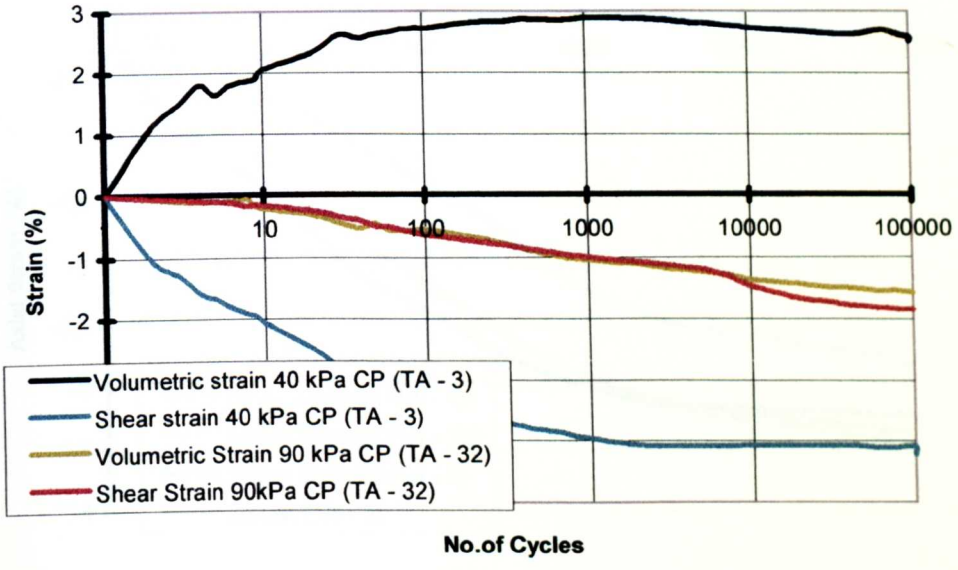

Fig. 6.31 - Volumetric and shear strain against number of load cycles for tests on ballast at 40 kPa and 90 kPa cell pressure

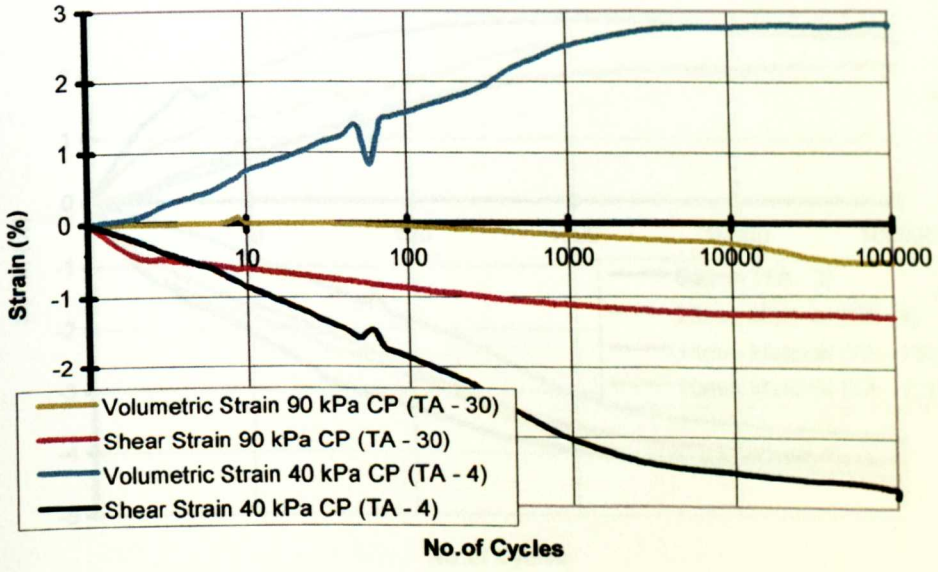

Fig. 6.32 - Volumetric and shear strain against number of load cycles for tests on 20mm material at 40 kPa and 90 kPa cell pressure

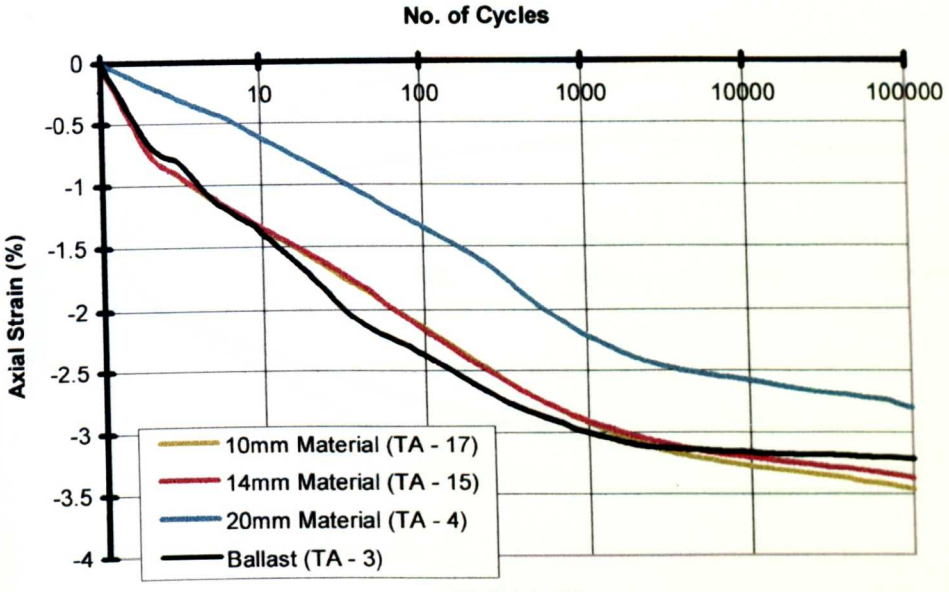

Fig. 6.33 - Axial strain against number of load cycles for different gradings of material

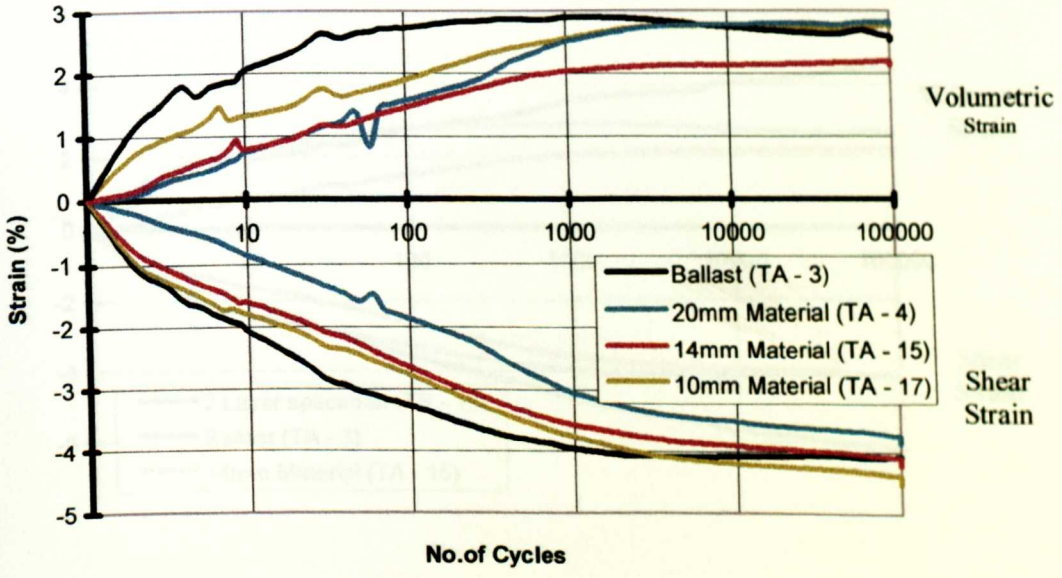

Fig. 6.34 - Volumetric and shear strain against number of load cycles for different gradings of material

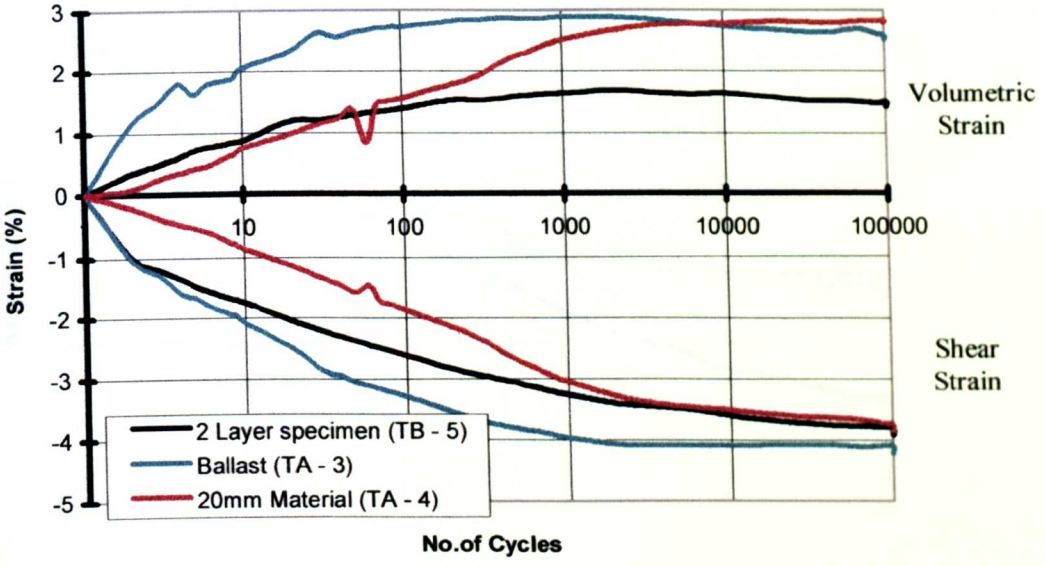

Fig. 6.35 - Volumetric and shear strain against number of load cycles for a two-layer specimen of ballast and 20mm material, with values for the component materials

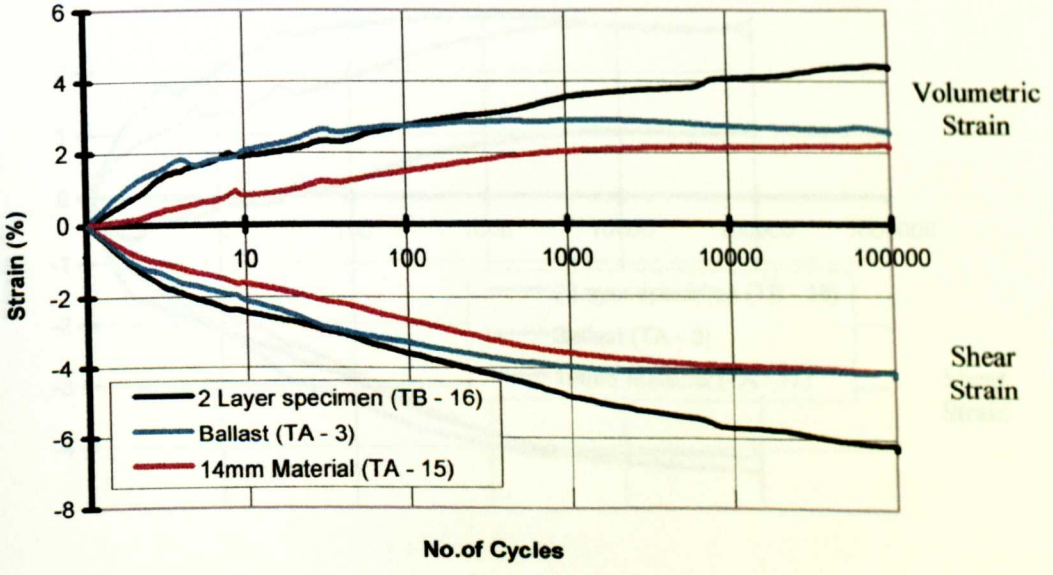

Fig. 6.36 - Volumetric and shear strain against a number of load cycles for a two-layer specimen of ballast and 14mm material, with values for its component materials

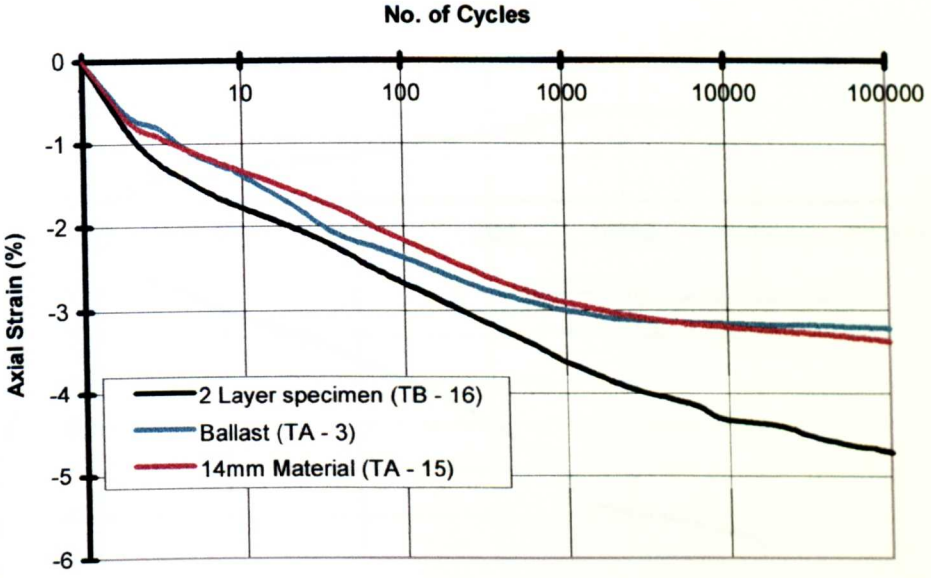

Fig. 6.37 - Axial strain against a number of load cycles for a two-layer specimen of ballast and 14mm material with values for its component materials

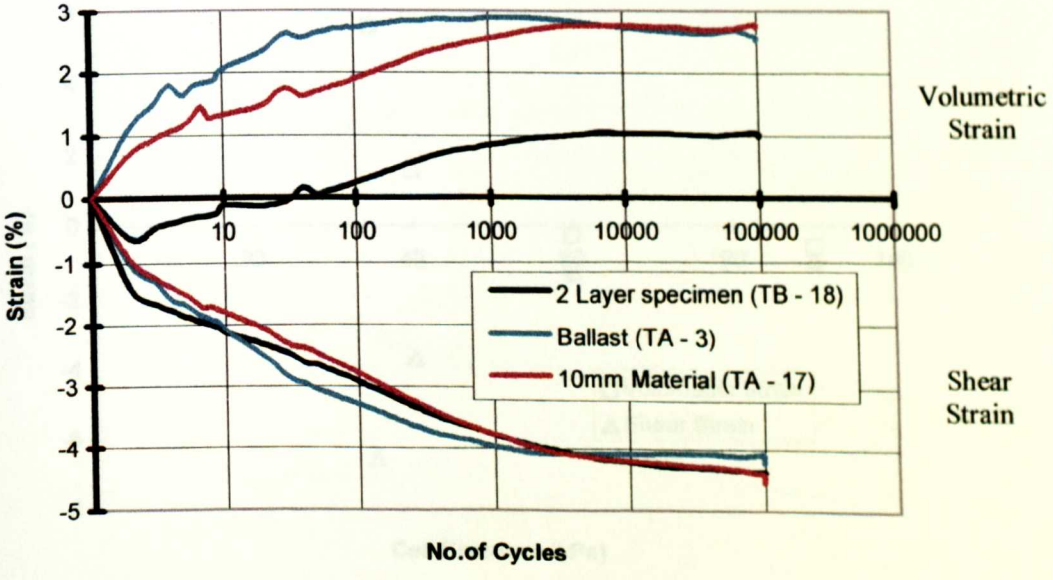

Fig. 6.38 - Volumetric and shear strain against load cycles for a two-layer specimen of ballast and 10mm material, with values for its component materials

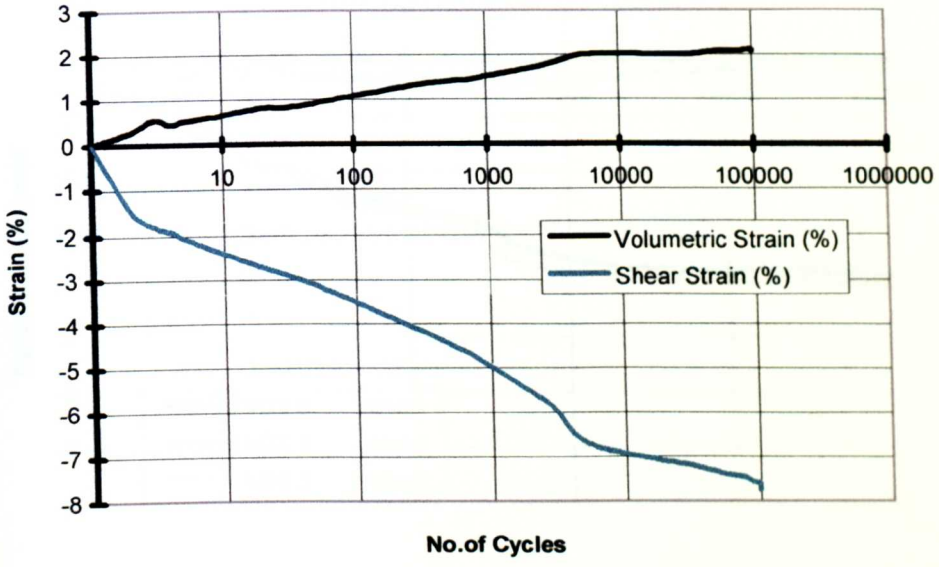

Fig. 6.39 - Volumetric and shear strain against load cycles for a two-layer specimen of ballast and 6mm material (Test Set TB - 20)

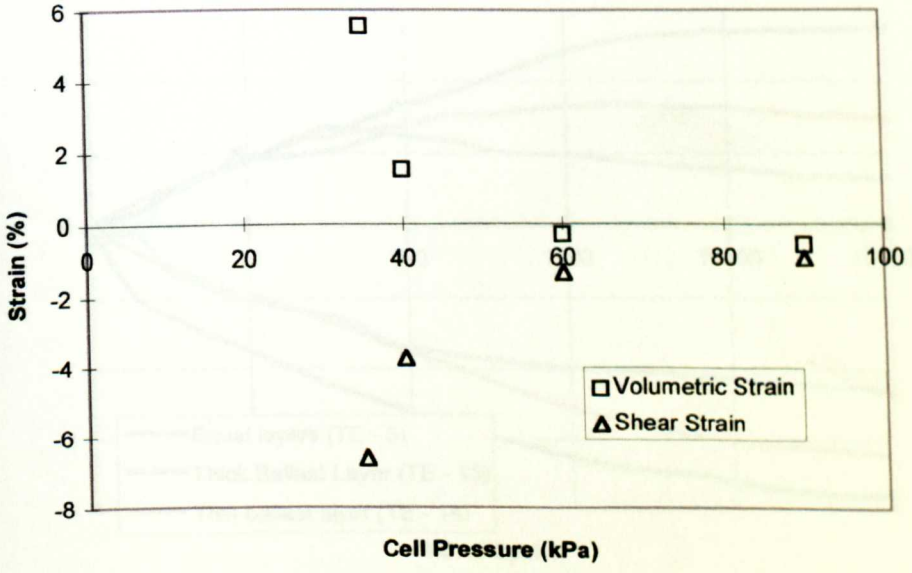

Fig. 6.40 - Variation of volumetric and shear strain with cell pressure after 30,000 load cycles for tests in Series TC

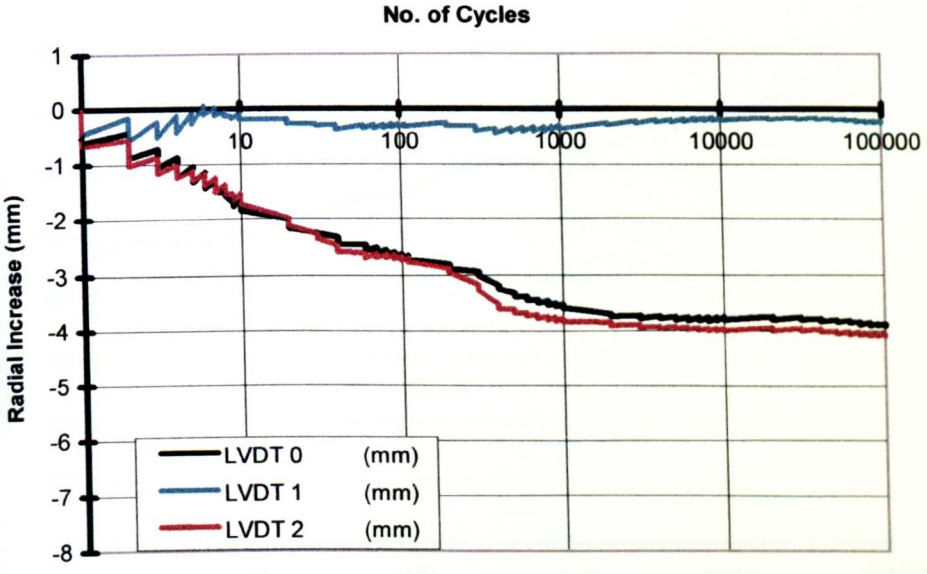

Fig. 6.41 - Radial deformation with load cycles for a two-layer specimen with the material interface at 45° to the horizontal (Test TD - 12)

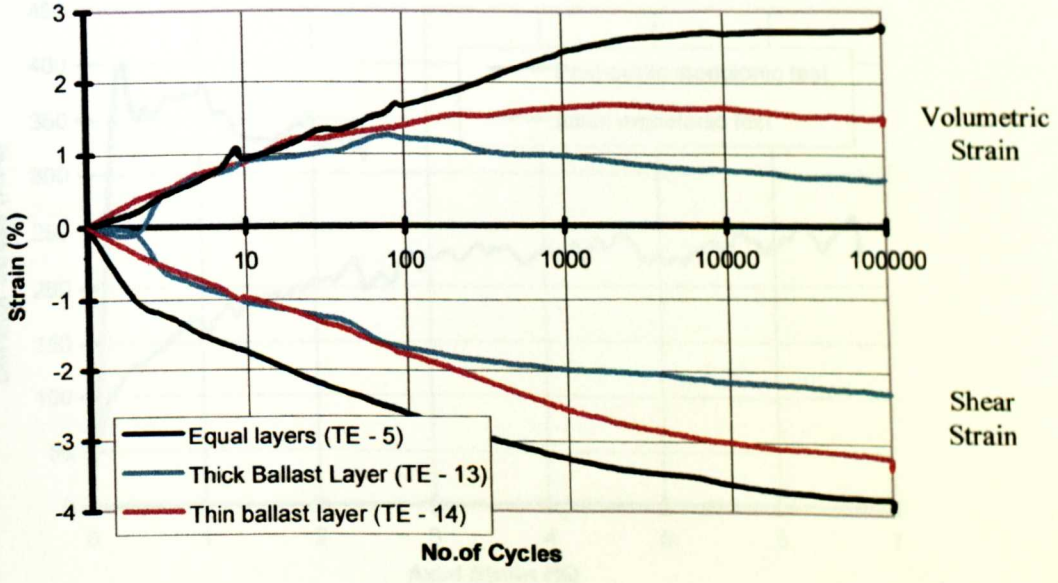

Fig. 6.42 - Volumetric and shear strain against load cycles for specimens with varying relative thicknesses of ballast and 20 mm material

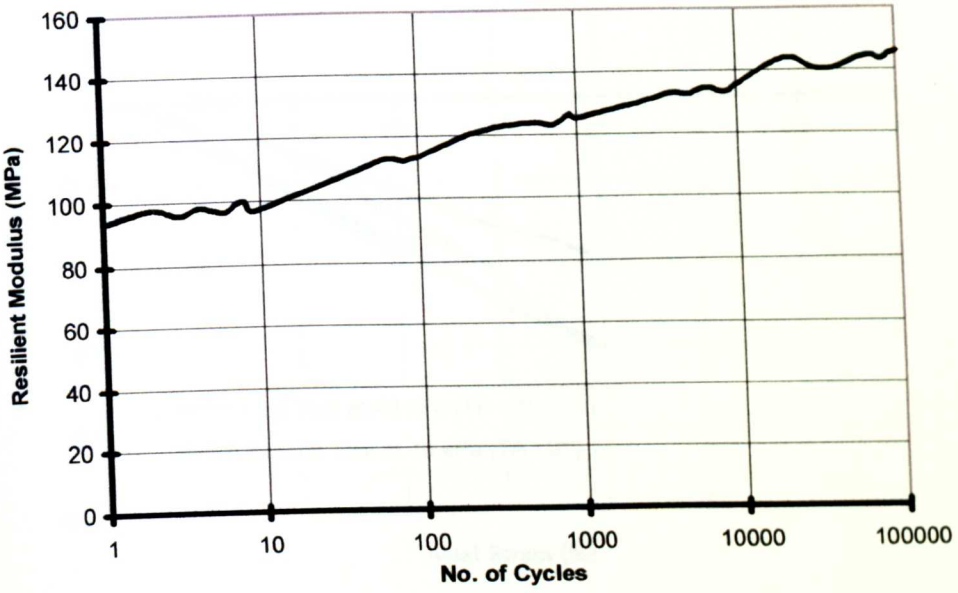

Fig. 6.43 - Resilient modulus against load cycles for the first test on ballast at 40 kPa cell pressure (Test TA - 3)

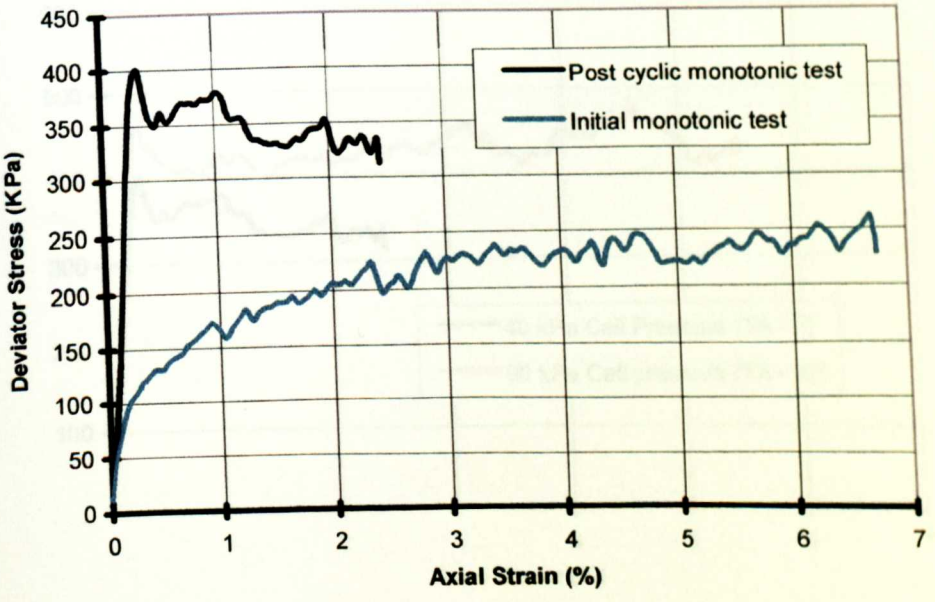

Fig. 6.44 - Deviator stress against axial strain for first initial and post-cyclic monotonic tests on ballast at 40 kPa cell pressure (Test TA - 3)

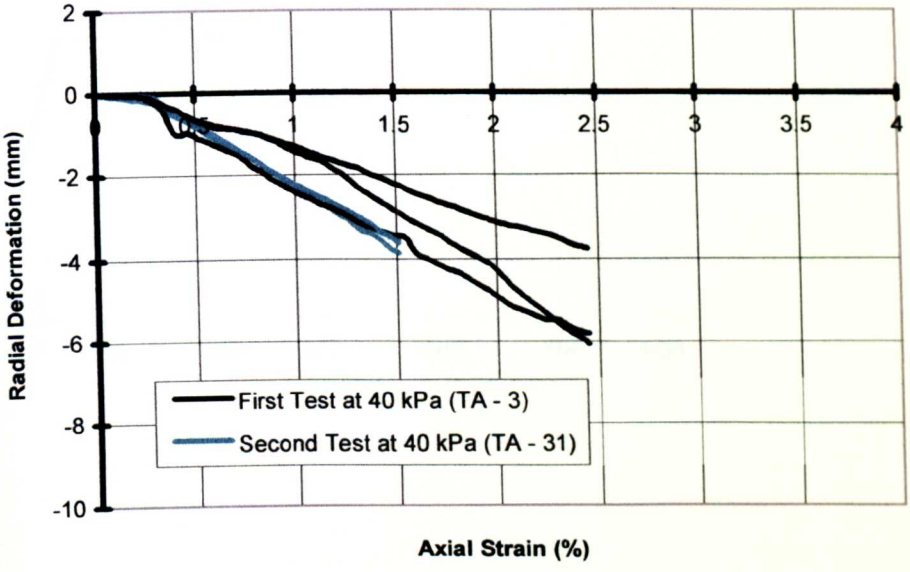

Fig. 6.45 - Radial deformation with axial strain for first and second post-cyclic monotonic tests on ballast at 40 kPa cell pressure

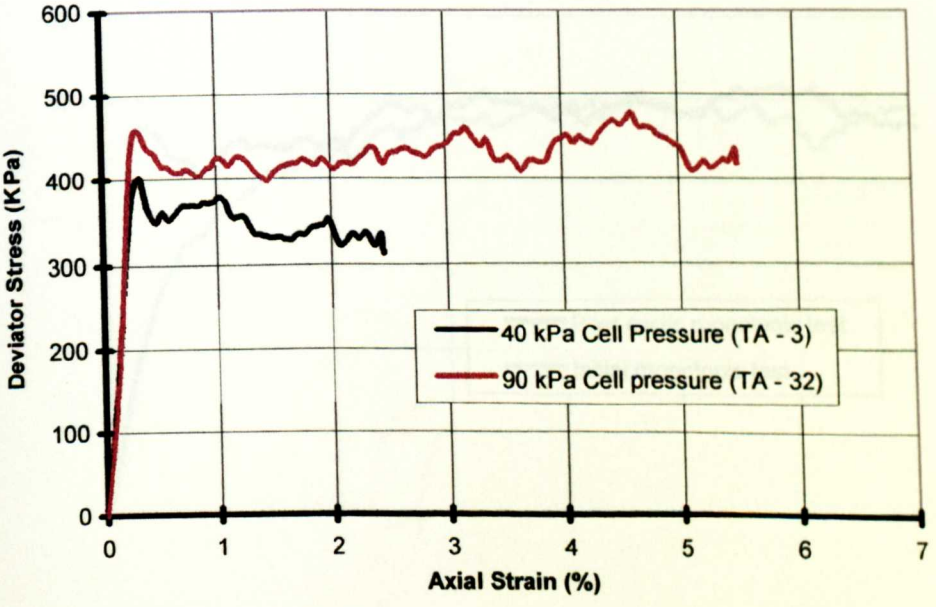

Fig. 6.46 - Deviator stress against axial strain for post-cyclic monotonic tests on ballast at 40 and 90 kPa cell pressure

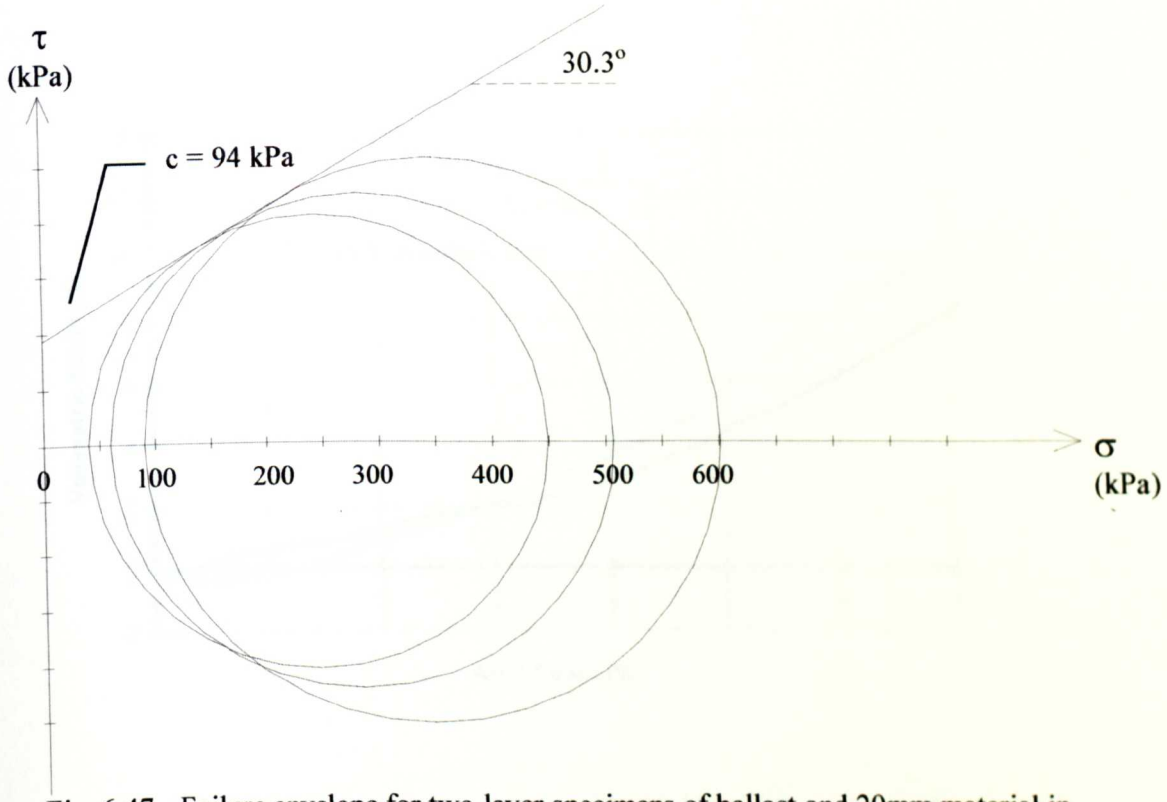

Fig. 6.47 - Failure envelope for two-layer specimens of ballast and 20mm material in post-cyclic monotonic tests

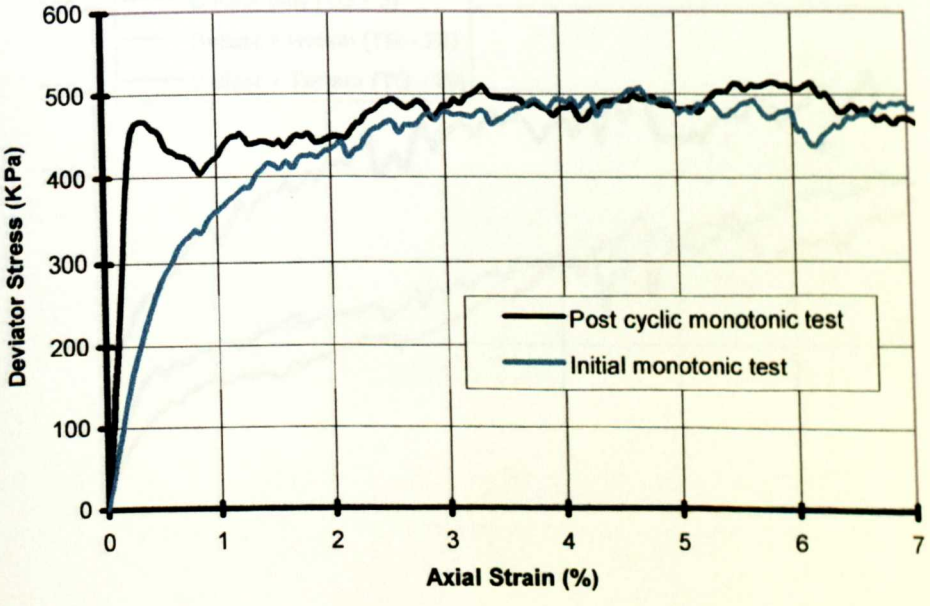

Fig. 6.48 - Comparison of deviator stress against axial strain for initial and post cyclic monotonic tests on two layer specimens of ballast and 20mm material at 90 kPa cell pressure (Test TC - 7)

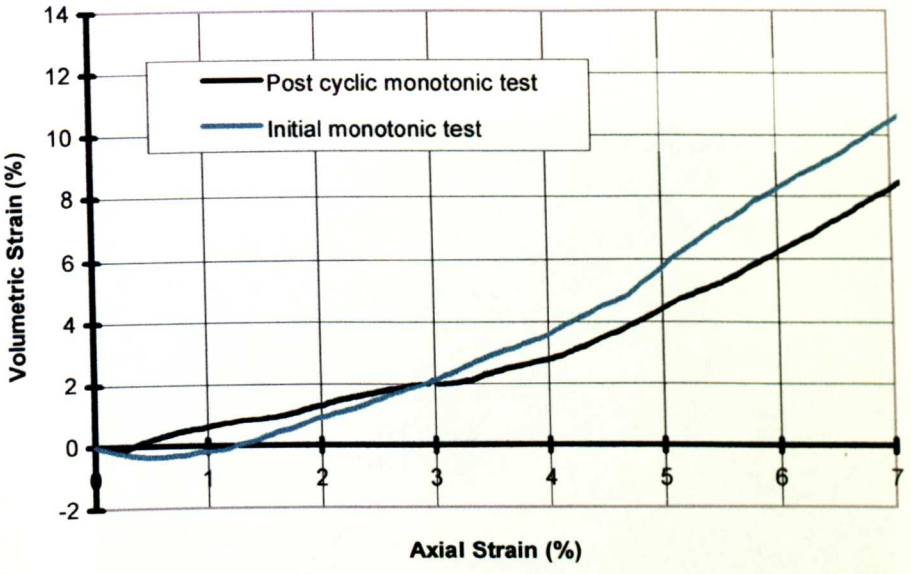

Fig. 6.49 - Comparison of volumetric strain with axial strain for initial and post cyclic monotonic tests on two layer specimens of ballast and 20mm material at 90 kPa cell pressure (Test TC - 7)

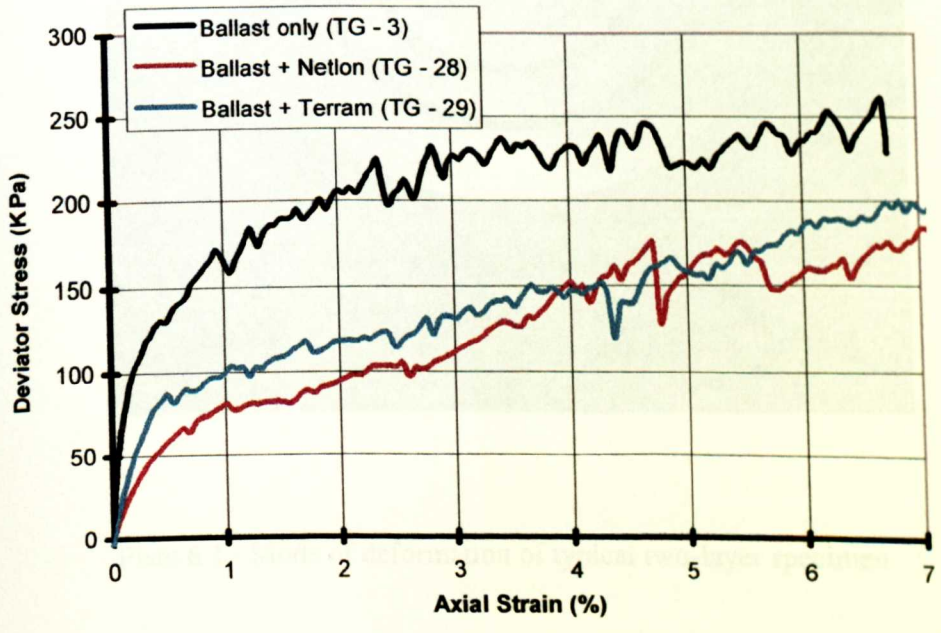

Fig. 6.50 - Comparison of deviator stress against axial strain for ballast, and ballast reinforced with polymer mesh elements

Plate 6.1 - Mode of deformation of typical two-layer specimen

Plate 6.2 - Failure mode of a two-layer specimen comprising of ballast and river gravel, with the material interface at 45° to the horizontal

Plate 6.3 - Terram reinforcement after removal from the test specimen

Chapter 7 - Model Testing

7.1 Introduction

In addition to the comprehensive triaxial testing programme, model testing was carried out at Scientifics Ltd., Derby, using their Half Sleeper Rig. This piece of equipment (Plate 7.1) was designed to model a trackbed environment. The aim of this limited study was to compare the trends noted in the triaxial tests with those in tests more closely resembling in-situ conditions.

7.2 Apparatus

The apparatus was based around a plate steel box, approximately 1000mm by 800mm by 600mm deep. A rubber mat 10mm thick with a reported modulus of 5000kN/m^2 was glued into the bottom of this to simulate the action of the track subgrade and the test material(s) placed on it.

The test bed was loaded by means of a miniature reinforced concrete 'sleeper' of dimensions 600mm by 100mm by 100mm deep (see Plate 7.2). The sleeper was restrained by two arms bolted onto it, and connected to the sides of the apparatus. These arms were articulated to prevent movement other than that in the up/down direction. In effect, they were simulating the rail in real railway track. The sleeper was loaded by a hydraulic ram via a steel ball and seat arrangement on top of the sleeper. The hydraulic ram reacted against the apex of a pair of steel girders, the connection to which permitted the ram to be angled from the vertical in any direction.

The hydraulic ram was fed via a high capacity pump and servo-hydraulic valve. This was driven from a control cabinet where the system could be set to operate in a variety of modes. Tests could be strain or stress controlled, and load waveforms, frequencies and number of cycles before shutdown could be adjusted. There was also a facility for the test to be controlled externally, for example by computer when more sophisticated test patterns were required, but this was not used for the test programme.

Integral to the hydraulic ram were transducers to measure (a) load on the sleeper and (b) how far up or down its travel the ram was (and thus how far up or down on average the sleeper had deviated from its original position). The signals from these transducers were fed back to the control cabinet, where they were decoded and could be displayed on an LED readout. There was also a facility for these to be output in the form of a voltage. Originally, the system was supplied with an Apple II computer which was connected to this output via an analogue to digital converter. This was then programmed to record loads and deformations at certain points of the test. It was felt, however, that this was not sufficiently fast for the work reported here, and there was also the question of transferring the recorded data to a PC. For this reason, a 286 PC was obtained and fitted with a logging card. This was then connected to the machine, and software was written to detect the maximum and minimum loads and deformations in each cycle, and record them on a logarithmic basis to a text file. This text file could then be loaded directly into a spreadsheet, such as Microsoft Excel, for analysis.

7.3 Calibration of Equipment

The displacement was considered to be the critical measurement for these experiments, as the load was kept identical in all cases. As the equipment had not been used or calibrated for a couple of years prior to this study, the displacement transducer was checked for accuracy. To do this, a magnetic clamp was fixed to the side of the plate steel box. Attached to this was a dial gauge which read against the flat on the end of the hydraulic ram. The ram was then cycled over the range of the dial gauge, at intervals of 2.0mm whilst readings were taken of displacement from the control cabinet and directly off the dial gauge.

From these readings, it was found that over the range of 5.30 to 7.50 cm, the displacement reading shown on the equipment was in error by a factor of 1.013, ie approximately 1.3%. This factor could then be used to correct the data obtained. Every three months or thereabouts, this reading was checked with the dial gauge. Over the period of testing, the reading was found to remain constant, no doubt due to the fact that the reading was only displayed to a relatively low accuracy of 0.1mm, which was equal to 0.1% of the range of the transducer, and hence would have had to change significantly for any difference to be noticed.

In addition to the absolute accuracy of the displacement transducer, it was felt wise to calibrate for the compliance of the equipment. To do this, the equipment was prepared as for a normal test, with the sleeper and hydraulic ram placed so as to load the plain ballast bed. Two dial gauges were then placed on magnetic clamps attached to the side of the plate steel box, measuring the deflections of the midpoints of each end of the sleeper (see Fig. 7.1). The sleeper was then loaded from zero to 20kN in steps of 2kN. At each step, the readings from the dial gauges were noted, along with the displacement reading on the equipment. From comparisons of the average of the readings from the two dial gauges with the reading off the equipment, it was found that there was a compliance which averaged out to 0.059mm per kN of load. Again, this factor could be incorporated into the results obtained to increase the accuracy.

7.4 Materials and Procedures

7.4.1 Materials

For the original investigations into the behaviour of ballast materials using this equipment by British Rail Research, a half scale representation of ballast was used (Sharpe, 1996) in order to minimise edge effects and give a more realistic number of particle contacts with the scale sleeper. The ramifications of this for particle inertia forces are unknown. A point to note is that the sleeper average contact pressure would have had to be doubled to give similar forces at the particle contacts, and it is thought that the machine would have been incapable of this at the frequencies used for this (and previous) testing. This brings into question the validity of some of previous work carried out on this equipment. Lower than required forces must have been used and it is unknown how the behaviour of the particle contacts changes with changes in force, particularly in light of the extremely high particle contact forces encountered in railway ballast which lead to breakage and high levels of abrasion.

For the reasons outlined, and the practicability of obtaining scale representations of all the different materials used in the small quantities required, it was decided to use full size materials for this study. The materials were from the same batches used in the main triaxial testing, and the descriptions of these can be found in Section 5.1. This meant that there were fewer particle contacts on the sleeper than there would be in the field, but given the alternative of obtaining another sleeper section and running the test at half the speed,

therefore significantly reducing the number of experiments that could be performed, it appeared to be the best option.

7.4.2 Test Procedures

At the start of the test programme, the ballast box was filled with new ballast and several initial tests of 1 million cycles were run to compact the bed to a point at which very little further deformation would take place. From this point, the majority of the bed remained undisturbed, with only the top section being rearranged for each new test. Any particles broken during subsequent tests were then removed on dismantling of the tests and discarded, to be replaced by new material for the next test.

The following procedure was used for running a test with this equipment:

Firstly, an approximate mass of new ballast was added to the box to replace any particles broken and to compensate for the densification of the ballast already present due to abrasion.

The bed was then agitated with a 'calibrated rake'. This piece of equipment (Plate 7.3) sat on the edges of the ballast box and was dragged along, disturbing the ballast to a set and constant depth, thereby ensuring repeatable starting conditions. The rake was dragged along, from the left side of the box to the right side five times at roughly even spacings along the length of the box. The same was done from the right to the left. The procedure was then repeated for a second time to ensure the ballast at the top of the box was fully agitated.

Next, the bed was approximately levelled with a spade. It was then precisely levelled by running a wooden gauge across it, which rested on the box sides and dropped to 75mm below the level of the sides inside the box. Any particles impeding the progress of this gauge were removed. Plate 7.4 shows this procedure.

A compressed air powered vibrating plate of similar area to the ballast box was then lifted onto the surface of the ballast bed, and run for one minute to slightly densify the upper layer of ballast and produce a flat surface for the scale sleeper to sit on.

Having prepared the ballast bed, the sleeper was then placed on its centre, allowing the hydraulic ram to be swung into an approximately correct position from its storage area at the side. The main pump was then powered up at low pressure (setup mode) and the ram lowered until the ball on the end of the ram rested just above the seat on the sleeper. The position of the sleeper was then adjusted so that when the ball was held above the seat, the ram was perfectly vertical in two orthogonal directions as measured with a spirit level (to ensure no stray lateral forces).

Having adjusted the position of the sleeper, the restraining arms were lowered and bolted into place on each end of the sleeper, and the ram lowered into the seat on the sleeper. At this point, the displacement of the ram was noted.

The pump unit was then switched to high pressure, and the load on the sleeper gradually increased to 10kN, at which point the displacement was again noted. The computer was next reset (being switched on permanently it did not need a warm up period) and the logging program run. The trip meter on the equipment was also set with the required number of loads for the test, the settings of load amplitude and waveform checked to ensure they had not changed, and the loading frequency set to 0.5Hz (to allow the hydraulics to keep up in the early part of the test). For the majority of the tests, the system was programmed to cycle the load between 2.1kN and 18.2kN, resulting in stresses of 35kPa to 303kPa below the sleeper.

The logging program and the rig were then simultaneously started. After 50 load cycles (noted on the computer display) the load frequency was increased to 6Hz and the equipment left to run for 50,000 cycles to compact the ballast bed - approximating pre-maintenance conditions.

On completion of the initial phase of the test, the data from the logging program was saved under the appropriate file name. The position of the sleeper was then marked, the restraining arms unbolted and removed and the ram withdrawn and swung to the side to provide clearance. The sleeper was then removed, taking care not to disturb the compacted ballast in the process.

Extra material was then added, as the test dictated, to simulate the maintenance procedure. To do this, a specially constructed tool was used, as shown in Fig. 7.2. The tool was placed on the box and the top nuts undone until the lower section rested on the ballast bed. The distance from top to bottom sections was measured with a ruler, and the two top nuts were wound in until the distance was reduced by an amount equal to the thickness of material to be added. The two bottom nuts were then tightened against the top bar to hold this position. This allowed the tool to be used as a gauge to control the height of material added. If there was any significant tilt on the sleeper, the length of the sleeper had to be covered in stages, with the tool being reset at every stage.

Having set the gauge tool to the correct height, material was added over the area covered by the sleeper and the tool moved across the surface of the added material. Any particles protruding into the path of the tool were removed, thus leaving a carefully controlled thickness of added material. The sleeper was then replaced in exactly the position from which it had been removed, and the same procedure followed to set the equipment running as for the start of the test, except that the position of the sleeper was already set, and that the number of cycles run for the test was generally programmed as 1,000,000. Some tests were run for longer, to test the long term behaviour of the ballast. One million cycles had been calculated to be equivalent to just over one year of traffic on an average main line.

On completion of the test, the data was again saved, and the equipment dismantled. The sleeper was removed, and notes were made regarding the distribution and condition of the added material as it was removed. Damaged ballast particles were also removed and discarded to avoid fouling of the bed.

7.5 Results and Discussion

The test series carried out and the tests within them are summarised in Tables 7.1 to 7.6. All tests were carried out with an initial 50,000 cycles of compaction to the ballast bed before the main section of the test unless stated otherwise. Similarly, all tests were carried out to 1 million cycles unless stated otherwise and all material added to the ballast bed was 20mm particle size unless stated otherwise.

7.5.1 Series MA and MB

The test programme was started with series MA and MB, which took the programme up to Test 13. At this point it was noted that the preparation technique was causing segregation of the ballast particles. Under repeated disturbance, the smaller particles were falling to the bottom of the agitated layer, with the largest particles migrating to the surface. It was felt that this was making the testing unrepresentative, with an abnormal grading resulting in fewer particle contact points on the sleeper (and thus higher contact forces) and larger voids which could result in higher levels of particle migration of the 20mm stone than would otherwise be the case. To counteract this, the preparation technique was altered. Prior to using the calibrated rake, the top layer (to a depth less than that disturbed by the calibrated rake) was scraped and mixed with a spade, thus bringing smaller particles up from below and giving the surface layer a more representative grading. Test preparation was then carried out as before.

Given that the validity of the first two test series was now in doubt, series MC and MD were carried out to replace them.

7.5.2 Series MC - Bed Characterisation

Fig.7.3 shows a plot of ballast settlement on the minimum load section of the cycle up to a million cycles. It shows the characteristic rapid build up of settlement in the early part of the test with the rate of deformation decreasing towards the end. This is more conventionally shown with the number of cycles plotted on a logarithmic scale, as in Fig. 7.4. This indicates that the settlement did not quite follow a logarithmic pattern, the rate of settlement increasing from its logarithmic value slightly towards the latter part of the test. Fig.7.4 also shows how this compares with the commonly used formulae for predicting track settlement (by ORE (1970), Shenton (1985) and Sato (1995), equations 2.6.1, 2.6.2 and 2.6.3 respectively, with unknown constants back calculated to give a best fit with the observed settlement).

As can be seen, none of the formula accurately predict the actual settlement, although for a first approximation the logarithmic settlement prediction (ORE (1970)) is a useful description. The equation by Sato (1995), however, whilst not being particularly accurate, is the only one that approaches the shape of the observed settlement, displaying a 'Double S' characteristic as the rate of settlement increases, then tails off and finally increases again

when plotted on a logarithmic scale. This would perhaps suggest that Sato's assessment of the settlement of a ballast bed comprising of two distinct processes, a rapid initial consolidation followed by a constant linear particle movement, has some credence. However, given that the experimental curves are 'flatter' than the result predicted by Sato, there could be a third process going on simultaneously that works on a logarithmic scale. This may represent densification due to abrasion at the particle contact points. Presuming contact occurs at particle corners, the more abrasion occurs the larger the particle contact will become, and thus the rate of reduction of the particle diameter will decrease as the test progresses. If this occurred logarithmically, it would then flatten the overall settlement rate.

Fig.7.5 shows how this plot (in red) compares with the settlement during the initial bed compaction from the experiments carried out in Test Series MD. The characterisation falls within the middle of the range of curves, with the majority of the plots then converging at about the 30,000 cycles mark. This suggests that the magnitude of the ballast consolidation is approximately the same in all cases, but the rate of compaction varies in each case. Perhaps this is dependent on the particular particle arrangement present in each test. This would also give confidence in the repeatability of the tests.

Fig. 7.6 shows the characterisation test compared to the settlements from the initial bed compaction of the tests from Series MB. There is a much lower degree of uniformity in these results, confirming the suspicions about the preparation technique used. Having an effectively larger grading of material on the top of the bed results in fewer inter-particle contacts and fewer support points on the sleeper, hence the outcome of the experiment is influenced to a greater degree by the arrangement of the particles present - the system is behaving increasingly as a structure rather than a continuum and giving a more random outcome.

Fig. 7.7 shows how the characterisation test compares with the 1 million cycle ballast tests from Series MA. Again the uniformity is very low. It is believed that the high settlement from the first test in Series MA was due to the incomplete compaction of the ballast bed. Only preliminary tests having been carried out before this, one of the repeat tests accidentally had a large impulsive load exerted on it at the start of the test, causing a 5.4mm drop before the cycling began with the result that settlement during the test was very low.

The other test results, however, are thought to be a product of the high degree of scatter evident with this form of bed preparation.

When assessing the behaviour of the ballast in these tests, the edge effects and the boundary conditions must be taken into account. Considering direct effects on the behaviour of the material, even if the ballast is presumed to have a 1:1 load spreading ratio with depth, (this will depend on the compaction level of the ballast in the bed) the sides of the ballast box will not contribute to the load bearing until a depth of some 350mm, equal to the depth of the main ballast layer in many track beds. The depth reached before the influence is felt from the ends of the sleeper will be less (200mm), but the influence of this will be proportionally much smaller, as shown by Stewart et al, (1984). The secondary effects, confinement from heave and horizontal confinement for the generation of lateral and longitudinal stresses, differ little from those that would be present in actual tracks, with the exception of the ends of the sleeper. Here, there would be a free boundary (the shoulder), rather than a fixed one, although it would be at a greater distance than that between the sleeper and the edge of the ballast box. Given that the average sleeper spacing is in the region of 700mm, it could be said that the arrangement accurately represents one segment of the track, with the boundaries representing the lines of symmetry between the areas of influence of each sleeper. This provides an argument for not having as large a box as possible to 'eliminate' edge effects, as has been done in the past (Sharpe, 1996). To produce significant improvement in the realism of the model, it would be necessary to model a section of the track and have a rolling load. Thus, as the load approached the sleeper under test, the lateral loads would force the material on the segment boundary towards and then away from the test sleeper as the load impinged directly on the test sleeper, then finally to its rest position as the load moved away again. Given that horizontal stresses have been shown to approach a constant with time (Stewart et al., 1984) even this would have only a limited effect on the outcome of the tests.

7.5.3 Series MD - Effect of addition of different quantities of stone

The effect of sleeper removal without the addition of stone on the ballast bed behaviour is illustrated by Fig. 7.8, showing settlements occurring after 50,000 cycles. In the characterisation test the sleeper was left in place. Having already experienced 50,000 cycles, the bed had become largely stable and little deformation was seen over the short term (1000 cycles). Not until the log scale encompassed large numbers of cycles did the rate of

deformation become evident. In the other two tests, however, at the 50,000 cycle point the sleeper was removed and replaced in ostensibly the same place. However, significant deformations occurred within a few load cycles, and in a similar pattern to the deformation at the start of a normal test. This behaviour suggests that even the act of removing and replacing the sleeper disturbs the load path within the system. Hence particle re-arrangement, and thus settlement, needs to take place in order to resist this slightly different load regime. Given that only minor disturbance would be expected to have taken place, then the amount of extra settlement that should have occurred is minimal. This is indeed borne out by the results, with the overall settlement for the disturbed case being slightly less that that for the undisturbed case. Both the tests where the sleeper was removed and replaced showed a lower rate of settlement than the characterisation test towards the end of the cycling period, by which time the effect of the disturbance should be minimal.

Longer term, i.e. post 1 million cycles, the graph starts to turn upwards, and it would be interesting to investigate how the material behaves longer term given that its life in the track on average extends to 20 times the loading experienced in one of these 1 million cycle tests. However, the testing equipment was unable to test beyond 3 million cycles.

Fig. 7.9 shows a plot of the settlement of the ballast bed with the addition of a 5mm layer of 20mm stone along with a plot of the characterisation test. This shows that a bed with added material settled less than one that had been disturbed (as it would be after tamping), confirming the theory behind stoneblowing as a method of track maintenance. It can also be seen that the load settlement relationship tends towards the same basic 's' shape as the characterisation test curve. Presumably in this case though, the settlement will be made up of two separate contributions (forming the two sections of the 's') - initially the settlement will be from the added material as it consolidates, and then as this tails off and the contribution from the added material becomes very small, the long term settlement of the ballast bed will become significant.

Fig. 7.10 shows how the settlement of the bed with 5mm of added material compared with that of a plain ballast bed after the sleeper was removed and replaced at 50,000 cycles. This is shown in terms of levels relative to the position of the ballast bed after 50,000 cycles. As can be seen, the addition of 5mm of stone gave a lift to the level of the sleeper, but on initial loading there was a significant drop as the newly placed stone compacted, resulting in an

initial lift of only 2.5mm. The level then continued to drop under repeated loading as the material compacted. The rate of settlement however was much greater than without the additional material, the net result after 1 million cycles being that sleeper level was lower than it would have been without the addition of the extra material. Given that very few 20mm particles were found to have migrated by the end of the test, the addition of extra material must have caused significant change in the load path through the material, with the result that considerable particle re-orientation, and thus settlement, must have occurred before equilibrium was restored. A phenomenon such as this illustrates that care must be taken with the design of maintenance procedures to minimise bed disturbance, otherwise the effectiveness of the maintenance procedure may be significantly reduced.

Fig. 7.11 shows the effect of adding thicker layers of stone to the ballast bed, again relative to the level of the ballast bed after 50,000 cycles. Up to a point adding further material to the bed gave a constant lift settlement relationship. In each case there was a drop of approximately 2.5mm when the material was first loaded and then the bed settled at a rate which was virtually the same in each case. The fact that these settlement curves are all virtually parallel, despite the variable thickness of the added material, would suggest that the settlement was mainly due to the ballast bed rather that the 20mm stone that has been placed on the bed.

Increasing the thickness of the layer of 20mm stone beyond 20mm, however, gave no additional benefit, and indeed increasing it much beyond 20mm appeared to be detrimental, with the sleeper level ending up lower than it if no material had been added. On dismantling of these tests, several observations were noted. Firstly, the 20mm stone appeared to have 'carved' a hole into the ballast bed, i.e. the settlement was occurring in the ballast layer directly below the sleeper, but not around it. This can be confirmed from Fig. 7.11, where it can be seen that the test where a 35mm layer of material was added settled much more than 35mm, meaning the ballast had to be contributing to the settlement. Secondly, the ballast bed upon which the 20mm stone had been placed was no longer level and the particles were no longer oriented to give a flat top surface - the particles gave the impression of having been moved. In tests with smaller layer thicknesses, the ballast bed had retained the imprint of the sleeper, i.e. a flat layer with oriented particles, even after the addition of stone. Finally, a proportion of the added stone was found to have migrated into the ballast bed, which did not occur with the smaller layer thicknesses.

To investigate this phenomenon further, on completion of the 30mm test a further 20mm thick layer of stone was added beneath the sleeper, the sleeper replaced in the same position again and an additional 1 million load cycles were exerted on the system. The results of this can be seen in Fig. 7.12. The settlement of this 20mm layer was slightly greater than that found from the addition of a normal 20mm layer to a compacted ballast bed, but nowhere near as much as would be predicted given the remaining layer thickness of approximately 35-40mm and that a total of 50mm of stone has been added. This would tend to suggest that the system has stabilised since the initial addition of stone.

Given that the behaviour of the layered system changes when the thickness of the 20mm stone layer exceeds 20mm, it was postulated that the behaviour was due to having more than one particle thickness of material in the top layer.

The reasoning behind this is that an unconfined layer of 20mm stone resulted in a lack of lateral pressure on the particles at the edge of the layer. When there is only one particle thickness of stone this has few consequences as the particles are confined by the sleeper above and the ballast below. However, when the layer is deeper than one particle there is nothing to stop the particles at the edge moving laterally when they are under load. The net result of this is that the particles around the edge of the sleeper are unable to take any load, and all the load must be carried by the material in the middle of the sleeper. This results in the axial loads from the sleeper being taken at a higher stress, which is therefore transmitted to the ballast. Having never been exposed to stress of this magnitude, the ballast directly below the sleeper will then settle significantly. The deeper the layer thickness under the sleeper, the more the load is concentrated in the middle of the bearing area and the more the ballast settles.

To check this explanation, another test was performed with a 30mm layer of 20mm stone under the sleeper. However, once the stone had been added and the sleeper replaced in position, the sides of the sleeper were packed with ballast to midway up the sleeper and 200mm away from it, effectively confining the 20mm stone layer as it should be in good quality track.

Fig. 7.13 shows the results of this test. The rate of settlement can be seen to be greater than in the case of the 20mm layer, perhaps due to less than perfect confinement, or higher rates

of settlement in the increased thickness of 20mm stone, but nowhere near that of the previous 30mm test. Obviously the application of restraint to the layer had a large bearing on its behaviour. On dismantling the 'confined' test it was also noted that there was little migration of stone and that the ballast bed appeared largely undisturbed.

To investigate this further, a test at higher load (see Test Series MF, Test 32) was undertaken to establish whether the increased stresses on the ballast would cause the observed settlements. Assuming that there is a band of one particle width (20mm) of material around the edge of the sleeper that is unconfined and thus unable to carry any load, the effective area of the sleeper would be reduced from $0.06m^2$ to $0.0336m^2$, and thus under a peak load of 18.2kN, the peak stress would become 540kPa. To simulate this with the standard experimental setup therefore requires a peak load of 32.5kN. Consequently, the ballast bed was prepared as normal and compacted for 50,000 cycles before the sleeper was removed and replaced in the same position, the peak load increased to 32.5kN, with the minimum load increased proportionally, and a further 1 million load cycles run at a reduced speed of 3Hz to allow the hydraulics to keep up. The output from this test can be found in Fig. 7.14, along with the output from the Series MD test where 30mm of stone was added for comparison. The correlation between the two tests is not perfect as can be seen, but they give a similar magnitude of settlement. This suggests that the explanation for the phenomenon is plausible but needs refinement, and investigation using more tests. The effect will of course be exaggerated by the small size of the sleeper. The loss of a 20mm band around a small sleeper will result in a proportionally greater effect than would be the case under a foundation of larger dimensions. However it should be borne in mind that technically it is the dimensions of the stone layer that are the determining factor, not the foundation.

For comparison with the results of Test Series MD, Fig. 7.15 shows the effect of different layer thicknesses of 20mm stone using the data from Test Series MB. The same basic pattern is evident, but there is less uniformity in the settlement data. It can be seen that the settlements were prone to sudden drops of 2-3mm. It is speculated that this was due to the larger grading and consequently larger forces exerted on each particle resulting in breakage of particular ballast particles crucial to the structure. Given that fewer ballast particles would be present with this grading, the loss of one particle would have a greater bearing on the settlement. As a purely subjective observation, there appeared to be less damage to the

ballast particles in Test Series MD than in Test Series MB. In addition, there was less settlement of the 30mm layer tests (both are included here) in Test Series MB.

7.5.4 Series ME - Addition of Different Materials

As with the main triaxial test series, a decision was taken to add different materials to the ballast bed in order to investigate their behaviour. This was with a view to perhaps optimising the type of material recommended for maintenance. To this end, the 14mm grading of crushed granite and rounded river gravel were tested as addition materials. The 14mm stone was in the belief that use of a smaller grading of material could achieve finer control over the lift given to the sleepers, and hence a greater standard of track geometry would result. The rounded river gravel was chosen as the round particles allow for a higher degree of compaction to be achieved than with angular particles, requiring less energy for the compaction, and resulting in less settlement of the added material. Also, this material is less likely to jam in the blowing tubes of the machine.

Fig. 7.16 shows the results of tests using 14mm stone as an addition material, in layers of 15 and 20mm thick. Also shown is the test with a 20mm thick layer of 20mm stone for comparison. The results indicate that in each case where the 14mm stone was used there was a significant drop in the sleeper level, with the sleeper in all cases ending up lower than it would have been if the system had remained undisturbed. On the basis of the particle restraint theory suggested earlier, the 15mm layer should have been more stable than the 20mm layer, but in this case they appeared to exhibit very similar levels of settlement. It may be that the layer thicknesses tested were too great for the effect to be apparent with a smaller grading, or it may be that in this extreme case, with perfectly clean ballast of virtually the largest grading permissible, the two particle sizes were too disparate for a stable system to form. It was noted on dismantling of the tests that there was significant migration of the 15mm stone into the ballast bed, and some settlement of the bed, but no great disturbance of the ballast particles. This would suggest the migration theory to be more likely.

The tests using the rounded river gravel were stopped prematurely (at 10,000 and 43,000 cycle) due to excessive settlement of the ballast bed. In the first case, there was a 30mm layer of gravel confined by ballast around the sides of the sleeper. During the test, the rounded gravel was forced outwards from the sides of the sleeper and in between the

confining ballast particles, presumably as a result of the higher lateral pressures encountered with rounded material compared to angular stone such as ballast as a result of the smaller angle of shearing resistance (37° for the gravel, as opposed to 49° for the ballast). The ballast bed under the sleeper was also noted to have settled considerably, by approximately 25mm, no doubt due to the concentration of load caused by inadequate confinement of the rounded material. In the second test, it was decided to increase the level of confinement, and to this end, a steel plate 500mm by 800 mm by 25mm thick, with a 640mm by 140mm cutout in the centre for the sleeper, was lifted over the sleeper and 30mm layer of river gravel following system preparation. The gap between the sleeper and steel plate was then packed with extra gravel, with the intention of fully confining the gravel under the sleeper. However, the test still had to be stopped after 43,000 cycles, as the gravel was being forced between the ballast bed and the steel plate. This would suggest that rounded river gravel is generally unsuitable for use as a stoneblowing material.

7.5.5 Series MF - Different Test Conditions

7.5.5(a) Stone Distribution

As already shown, the degree of bed disturbance is crucial in determining the amount of settlement that will take place when the system undergoes repeated loading. The more the load path through the system is altered, the more settlement will take place before equilibrium is restored.

In the tests that have been reported so far, any extra material was added as even layers under the sleeper. The Stoneblower, however, works in a slightly different manner. The stone is blown under the sleeper in a heap, which is subsequently loaded by passing trains thus forcing it into the bed due to the greatly increased stress caused by the small patch of stone taking the majority of the load from the sleeper. The material around this patch will heave as material underneath is displaced and this process will continue until equilibrium is reached, the heaving material meeting the same level as the blown stone being forced into the bed. Plate 7.5 shows the pattern of stoneblown material under a typical sleeper. For small lifts, this just results in a small inclusion of stone in the ballast bed, but for larger lifts up to 40mm, the quantity of stone blown in would result in a system very similar to the ones tested so far.

This method of introducing the stone has the potential to cause significantly greater disturbance of the ballast bed than by introducing the stone as an even layer, so it was decided to conduct a test that was slightly more representative of this situation in order to quantify its behaviour. In this test, two patches of stone 20mm deep, 100mm by 150mm in size and 50mm from the ends of the sleeper, were placed on a ballast bed previously compacted in the standard manner. The sleeper was then replaced in its original position and loaded 1 million times. The output from this test is presented in Fig. 7.17 along with the output from the Series MD test with a 20mm layer of stone for comparison.

As can be seen, there was significantly more settlement with the patch layer test than with a normal layer test. The initial loading of the patch layer test caused three times the settlement that occurred with the layer test, and the rate of settlement was higher at all points from there on. The total settlement in the test was over 30mm, meaning that any technique based on this pattern of stone addition would not be viable, as it would leave the track in a worse state than it was pre-maintenance. Given that the Stoneblower has been shown to improve the track over a loading period similar to that of this test (McMichael, 1997), it shows that the test does not accurately replicate the field situation.

During dismantling of the test, it was noted that there had been migration of the 20mm stone from the patches down into the ballast bed and that the material under the patches was disturbed and no longer forming a flat surface, showing that it had been subjected to high stresses. By comparison with the levelling gauge used to prepare the bed at the start of the test, it could be seen that heaving had taken place to either side of the sleeper, mostly around the area at the ends where the 20mm stone had been added. The level of heave could not be gauged accurately, but it appeared to be between 5 and 10mm. The material under the centre of the sleeper remained in a flat layer and undisturbed, although settled as the sleeper had settled to the point of contact with this material.

This behaviour would suggest that the area of the sleeper was too small to take advantage of the heave that had been caused around the patch of added material, and that to more accurately represent test conditions would require a larger model sleeper. A sleeper of greater width would be partially supported by the material that had heaved to either side, thus reducing the pressure on the added material and giving less settlement as is thought to be the case in the field. Further tests with this sleeper may or may not have given more

accurate results as it is not known whether the sudden drop in level between 70 and 80 thousand cycles was just a freak occurrence due to the increased stress and some resulting particle damage, or was a replicable effect (as it coincidentally occurs around the point where the sleeper reaches its 'pre maintenance' level and is probably re-establishing contact with the middle section of ballast, which could perhaps change the loading pattern). Without the sudden drop, the result would appear to be more realistic. This should be investigated in future studies.

7.5.5(b) Change in Loading Waveform

Given the lack of definitive information in the literature as to the effects of loading waveform on the behaviour of granular materials under cyclic loading, it was decided to carry out some comparative tests. It was hoped that this would indicate if the essentially square wave loading used in the tests carried out at the University of Sheffield would give similar results to the sine wave loading used by many researchers, used in the majority of these model tests and thought to occur in the field.

For these tests, everything was prepared in the same way as for a normal test, except the machine was switched to square wave instead of sine. The greater demands this placed on the equipment, in terms of oil demand and sudden loading, dictated that the tests must be run more slowly that the sine wave tests, and so the load was cycled at 0.5Hz.

Fig. 7.18 shows the results of these tests. Both square wave tests were conducted on plain ballast beds, and are therefore compared with the bed characterisation test from Test Series MC. As can be seen, the settlements under square wave loading were significantly greater than those under sine wave loading, with the sleeper in the square wave tests settling at 3 to 5 times the rate of the sine wave tests. Given the shape of the square wave settlement plots, that of an upward curve for the first few thousand cycles, it would suggest that the settlement was a magnified version of the settlement observed in the sine wave tests rather than an acceleration through the same process. From this, it could be speculated that the increased accelerations that the square wave loading exerts on the ballast bed cause magnified interparticle movements and abrasion, and so square wave loading exerts a more onerous set of loads on the test specimens.

7.5.6 Elastic Deformation

The accuracy of the vertical displacement measuring system (0.1mm) is insufficient to gain any meaningful information on the change in elastic deflections of the ballast bed. The recorded elastic deflections obtained for the bed characterisation test only varied from 0.4mm to 0.2mm between the start and end of the test, with the other tests giving similar values. The square wave tests gave values from 0.5mm to 0mm with significant scatter. This indicates certain limitations in the equipment.

Series MA - Characterisation of the ballast bed	
Test Number	Comments
1	Initial test to characterise the bed, no 50,000 cycles compaction
2	Repeat of Test 1
9	Repeat of Test 1 to assess if the variability of the deformation was just due to the new and uncompacted state of the bed
10	Repeat of Test 9
13	5 Million cycle test to assess longer term behaviour of the bed, no 50,000 cycles initial compaction

Table 7.1 - Summary of Test Series MA

Series MB - Effect of adding different quantities of stone	
Test Number	Comments
3	5mm layer of stone added
4	10mm layer of stone added
5	15mm layer of stone added
6	20mm layer of stone added
7	30mm layer of stone added
8	Repeat of Test 3 as data on initial compaction lost
12	Repeat of Test 7 to check result

Table 7.2 - Summary of Test Series MB

Series MC - Characterisation of ballast bed with revised test procedure	
Test Number	Comments
21	Characterisation of ballast bed, no 50,000 cycles initial compaction
14 to 20	50,000 cycles of initial bed compaction in each test prior to the addition of layers of material used to check repeatability

Table 7.3 - Summary of Test Series MC

Series MD - Effect of adding different quantities of stone with revised test procedure	
Test Number	Comments
14	25mm layer of stone added
15	35mm layer of stone added
16	30mm layer of stone added
16B	A further 20mm layer of stone added on top of that remaining at the end of Test 16. No initial 50,000 cycles bed compaction carried out
17	20mm layer of stone added
18	15mm layer of stone added
19	10mm layer of stone added
20	5mm layer of stone added
22	No stone added, test carried out to assess effect of sleeper disturbance on the bed. Test ended prematurely at 300,000 cycles
23	Repeat of Test 22, to 3 million cycles
24	30mm layer of stone added and confined

Table 7.4 - Summary of Test series MD

Series ME - Addition of different types of material	
Test Number	Comments
25	20mm layer of 14mm stone added
26	15mm layer of 14mm stone added
30	Repeat of Test 26
27	30mm layer of rounded river gravel added, with stone confinement
28	30mm layer of rounded river gravel added, with steel confinement

Table 7.5 - Summary of Test Series ME

Series MF - Effect of change in test conditions	
Test Number	Comments
31	20 mm layer of stone added under ends of sleeper only to investigate effects of stone distribution
32	Repeat of Test 22, except after the initial 50,000 cycles bed compaction, the load was increased to investigate load concentration
33	Characterisation of the ballast bed under square wave loading, no 50,000 cycles bed compaction. 1000 cycles only
34	Repeat of Test 33 taken to 5000 cycles

Table 7.6 - Summary of Test Series MF

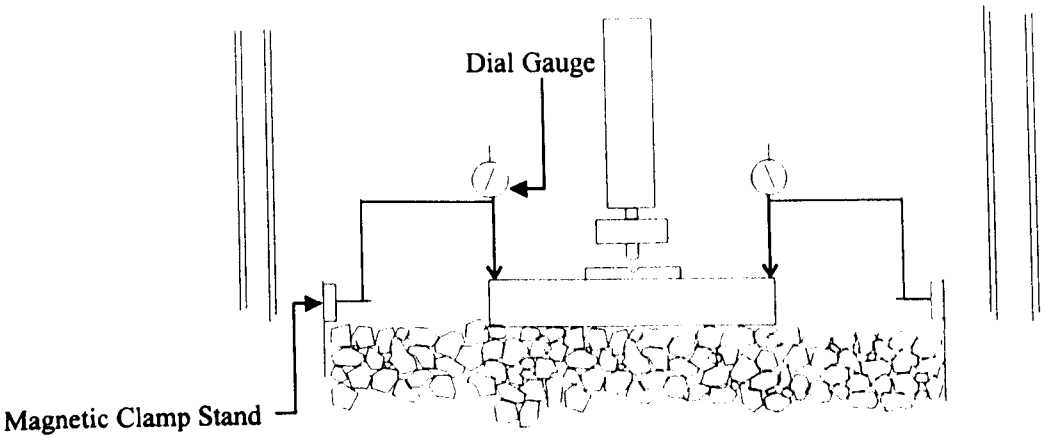

Fig. 7.1 - System for calibration of equipment compliance

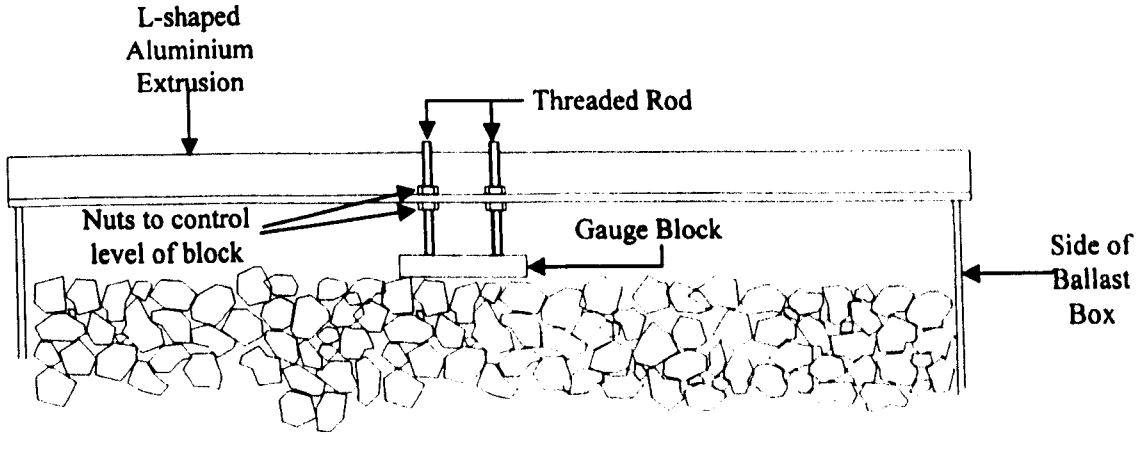

Fig. 7.2 - Tool for controlling layer thickness of added material

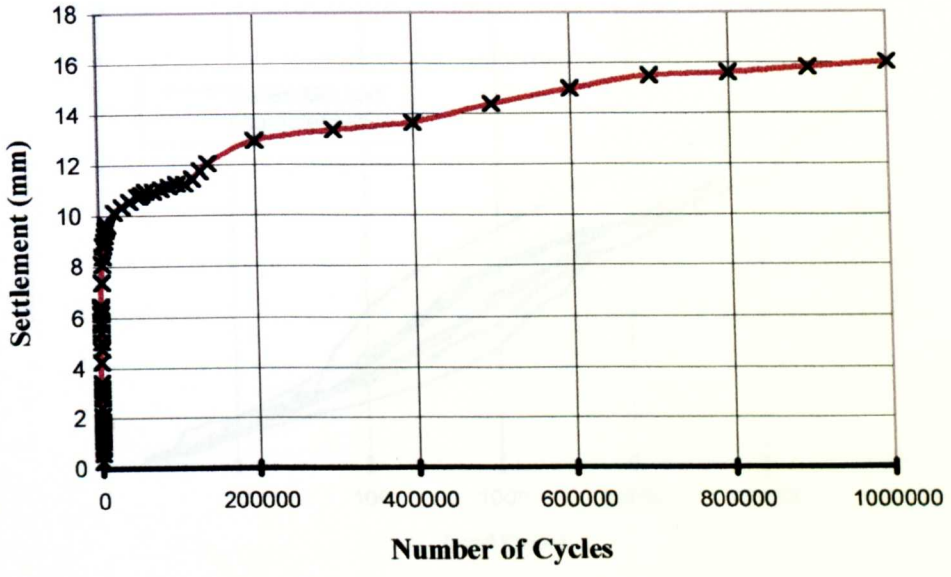

Fig. 7.3 - Settlement of the ballast bed with number of load cycles for Series MC Bed characterisation test

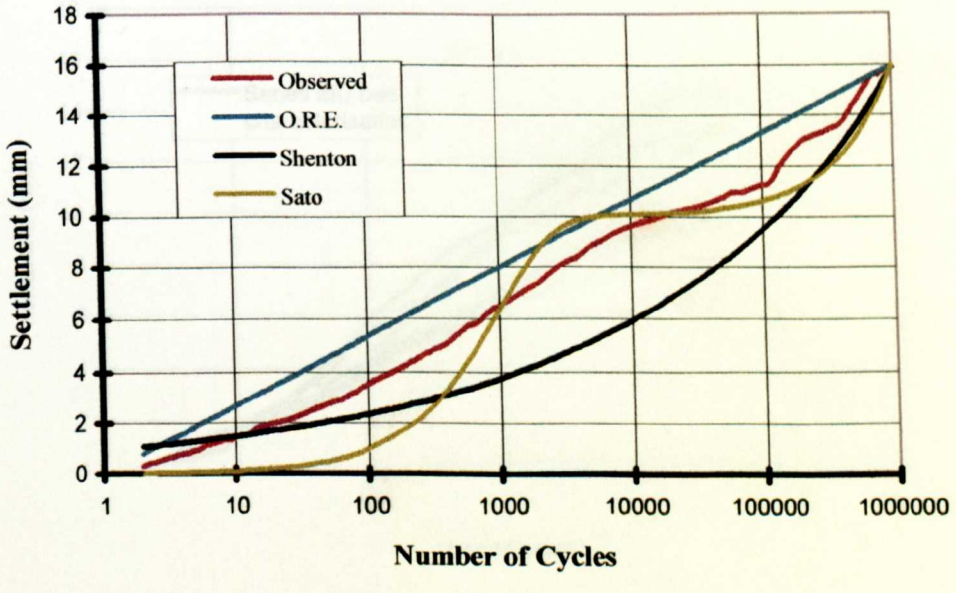

Fig. 7.4 - Observed settlement of the Series MC bed characterisation test with load cycles, compared with outputs from predictive formulae

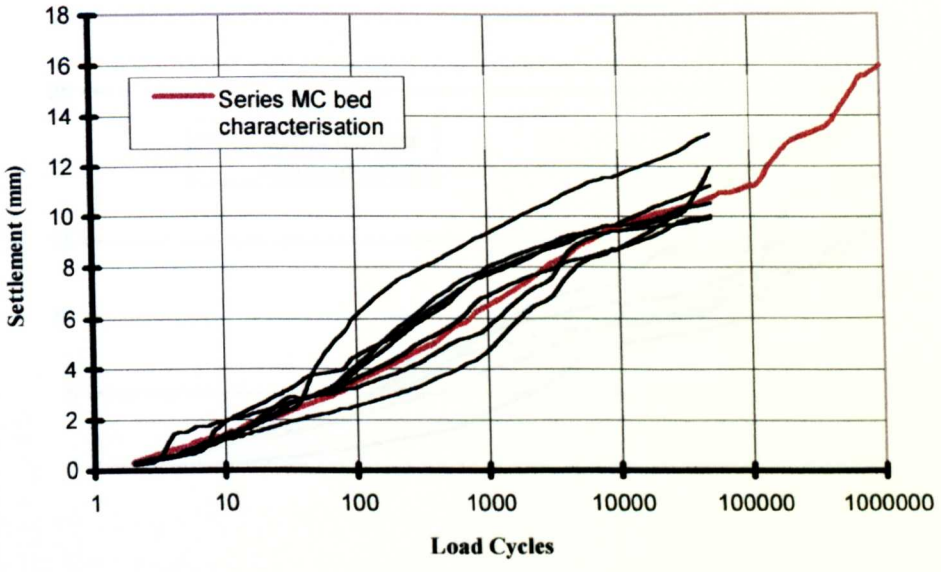

Fig. 7.5 - Comparison of settlement with load cycles for Series MC bed characterisation test and 50,000 cycle initial bed compactions from tests in Series MD

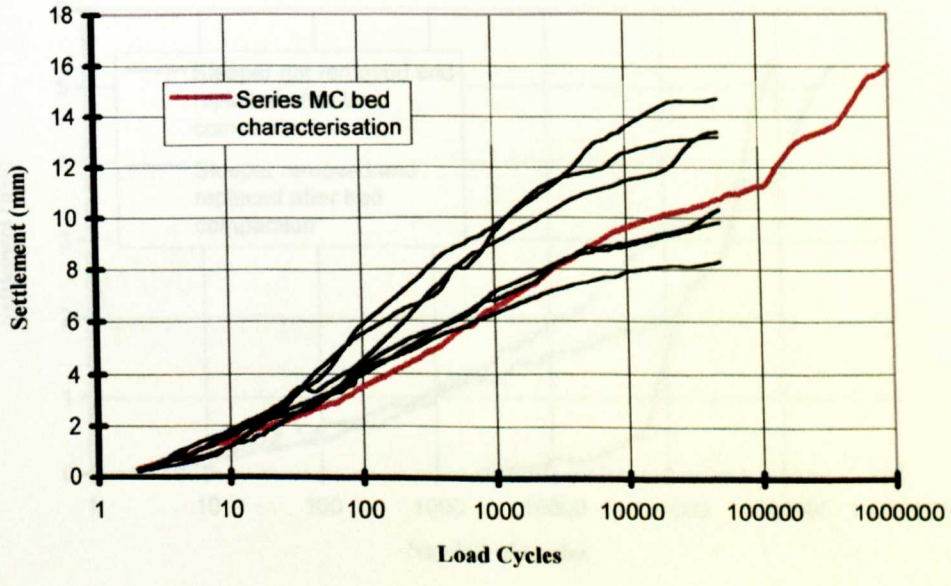

Fig. 7.6 - Comparison of settlement with load cycles for Series MC bed characterisation test and 50,000 cycle initial bed compactions from tests in Series MB

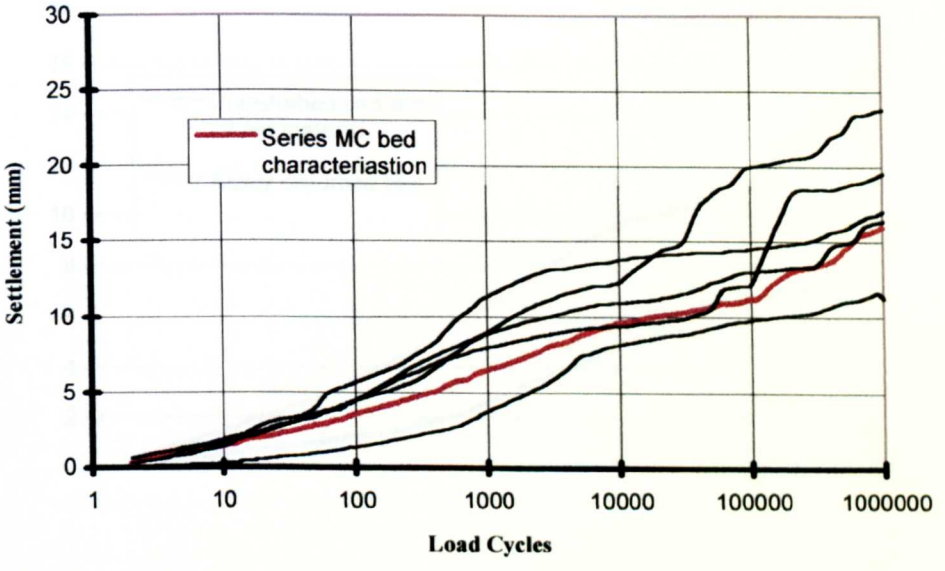

Fig. 7.7 - Comparison of bed settlement with load cycles for Series MC bed characterisation test and tests from Series MA

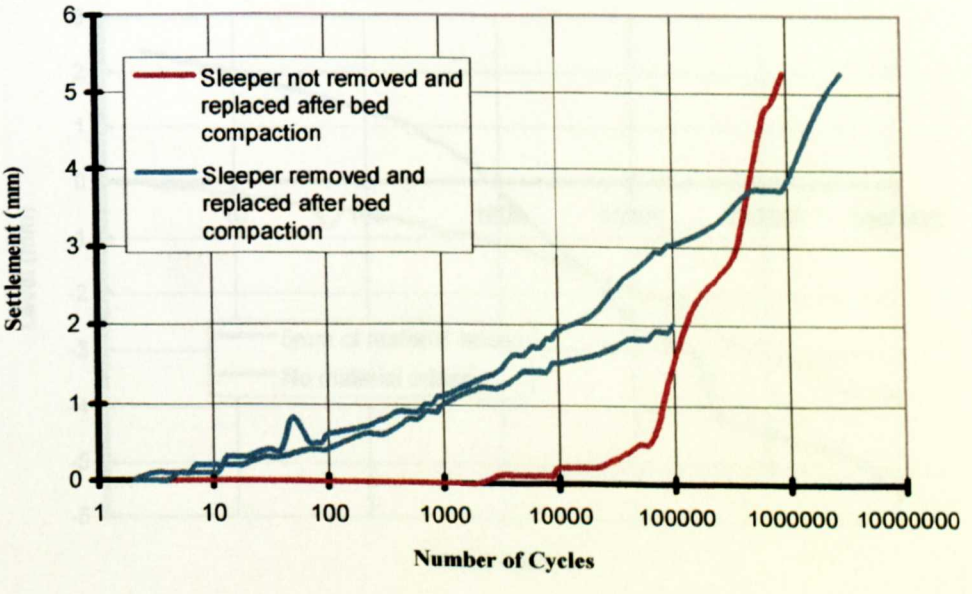

Fig. 7.8 - Settlement with load cycles after 50,000 cycles bed compaction, with and without sleeper removal

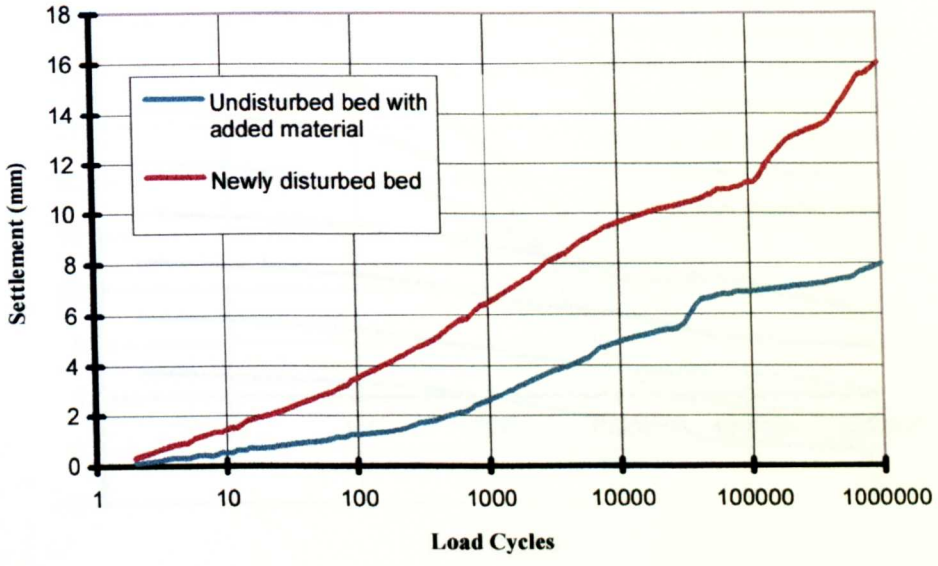

Fig. 7.9 - Comparison of settlement with load cycles when the sleeper is raised by loosening the ballast bed and raised by adding extra material

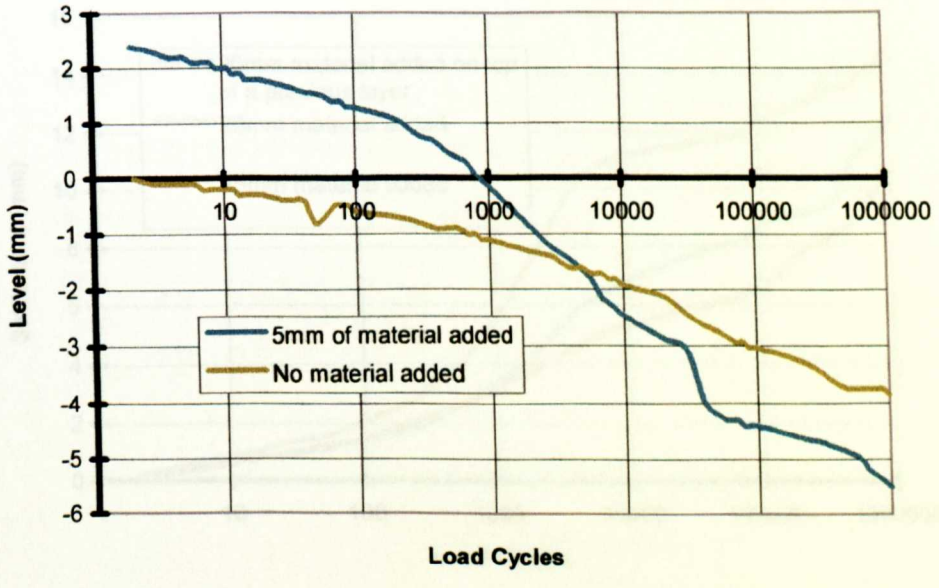

Fig. 7.10 - Comparison of overall sleeper level with load cycles for a ballast bed where no material was added and one where the sleeper level was raised with 5mm of added material

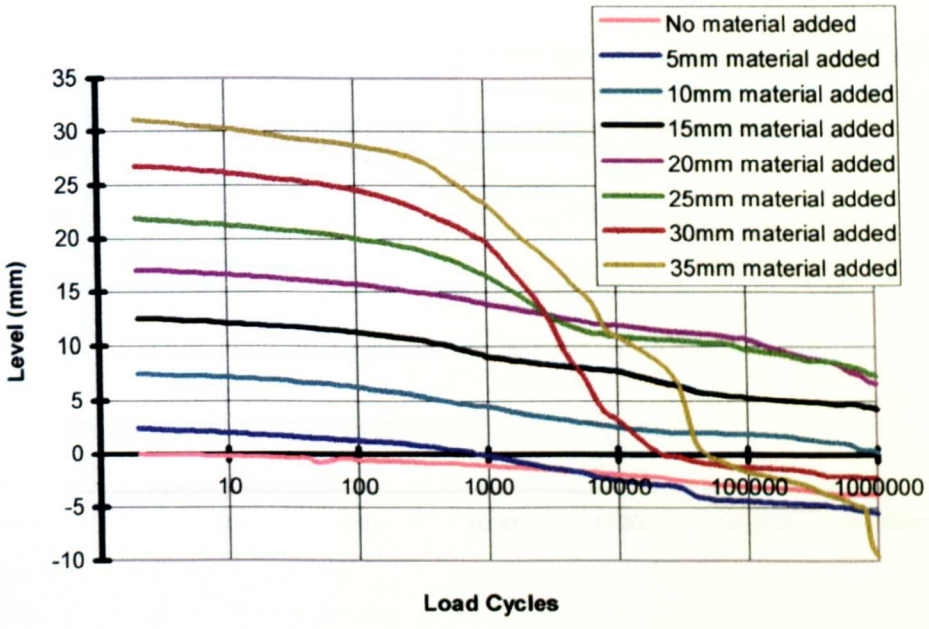

Fig. 7.11 - Comparison of overall sleeper level with load cycles for beds with the sleeper raised by various thicknesses of added material (Test Series MD)

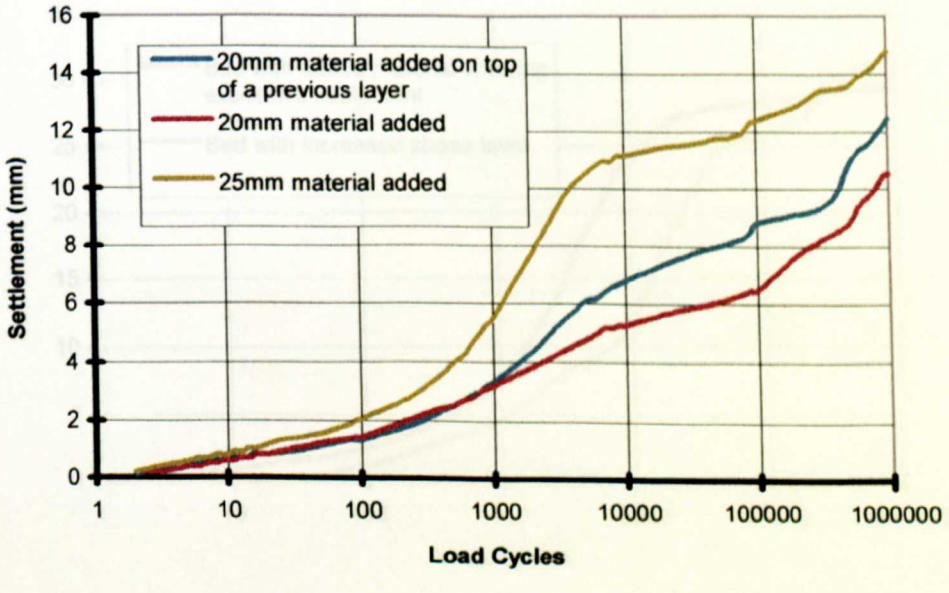

Fig. 7.12 - Comparison of settlement with load cycles of beds with 20 and 25mm of added material, and a bed with 20mm of material added on top of a previous 30mm layer

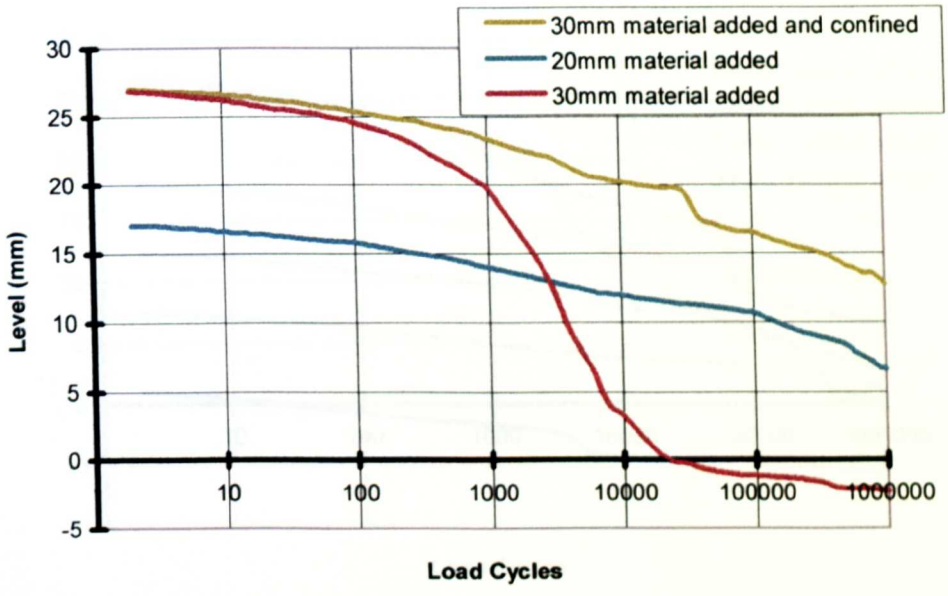

Fig. 7.13 - Comparison of overall sleeper level with load cycles for a layer of confined material and layers of unconfined material

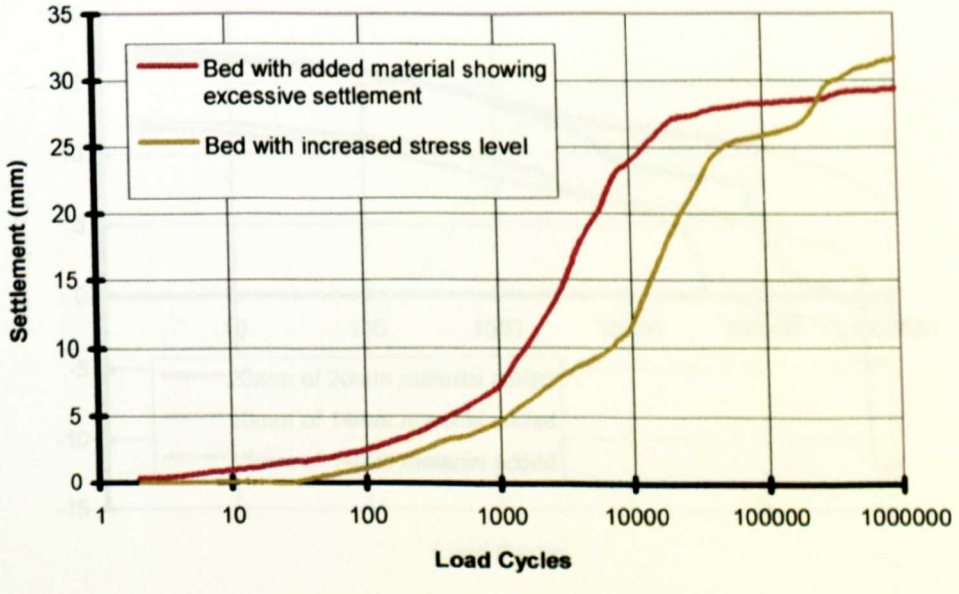

Fig. 7.14 - Comparison of settlement with load cycles for layers of added material showing excessive settlement and for a ballast bed under 540 kPa stress

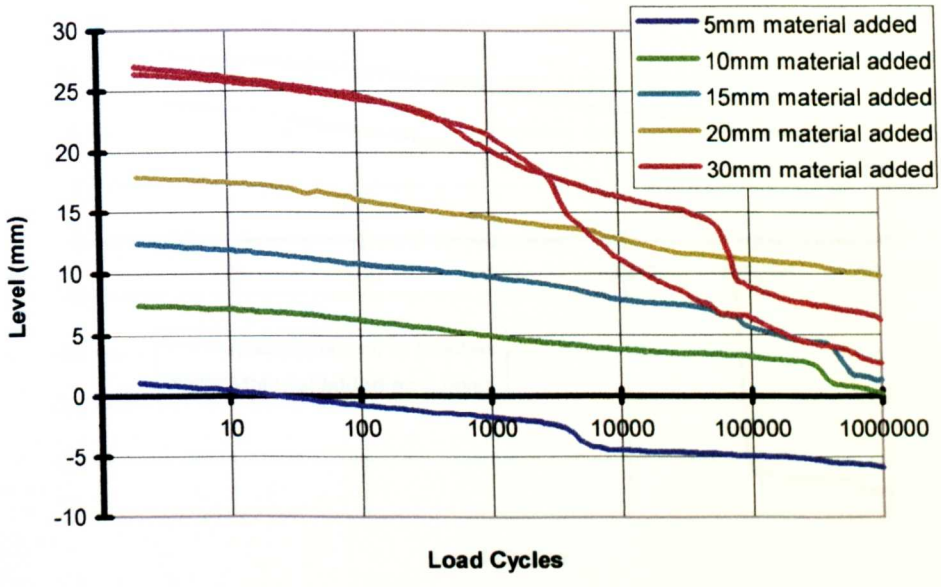

Fig. 7.15 - Comparison of overall sleeper level with load cycles for beds with the sleeper raised by various thicknesses of added material (Test Series MB)

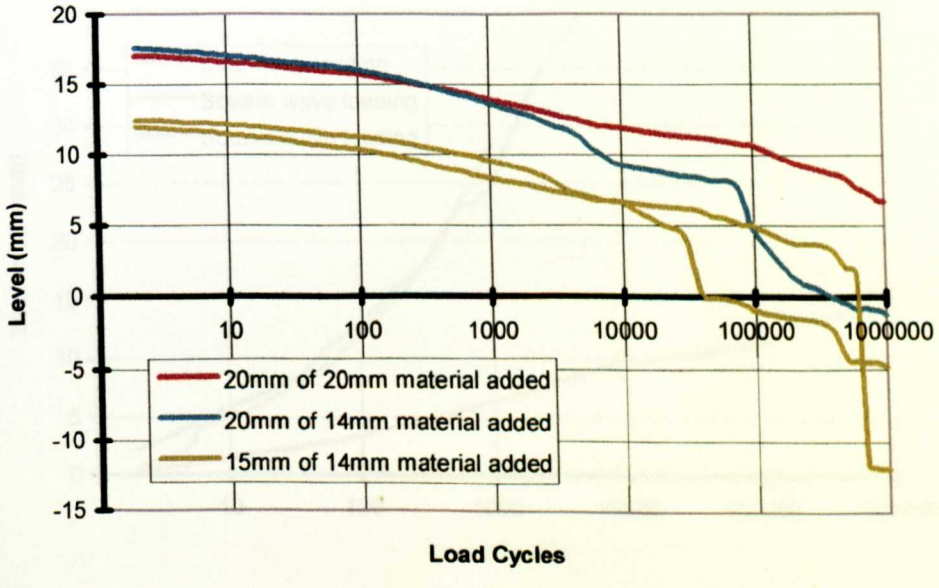

Fig. 7.16 - Comparisons of overall sleeper level with load cycles for beds with the sleeper raised by different thicknesses of 14mm material (Test Series ME) and with the sleeper raised by 20mm material

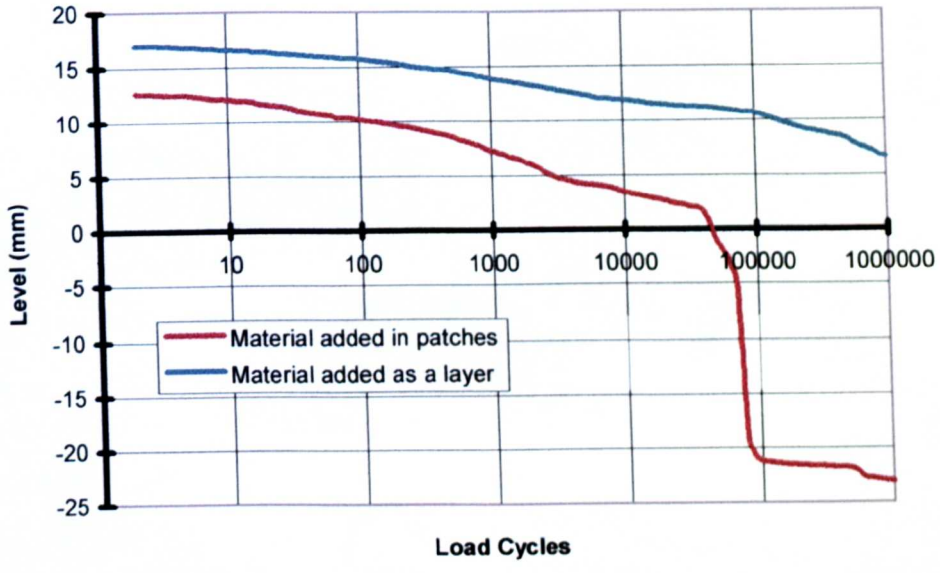

Fig. 7.17 - Comparison of overall sleeper level with load cycles for a sleeper raised 20mm by material added as a layer and material added in patches

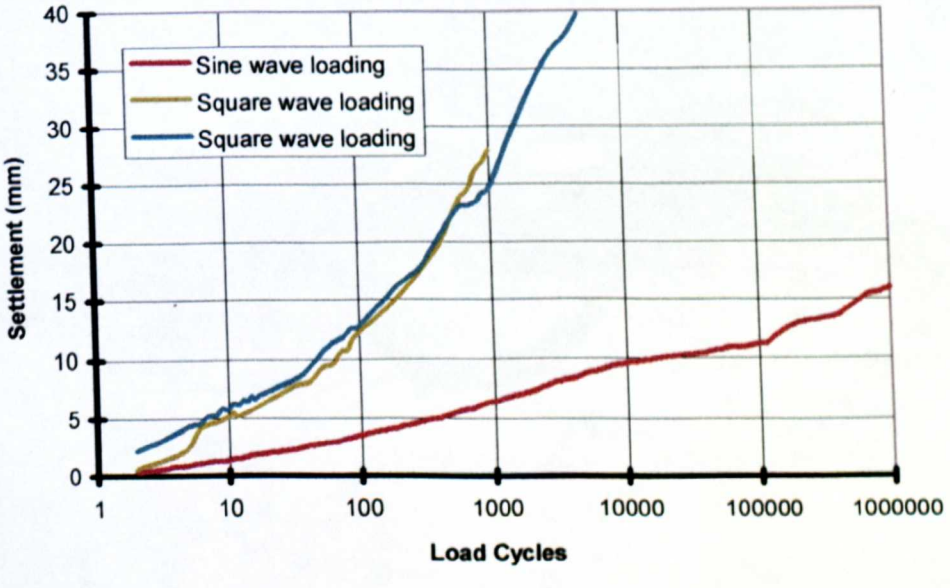

Fig. 7.18 - Comparison of settlement with load cycles for ballast beds under sine and square wave loading

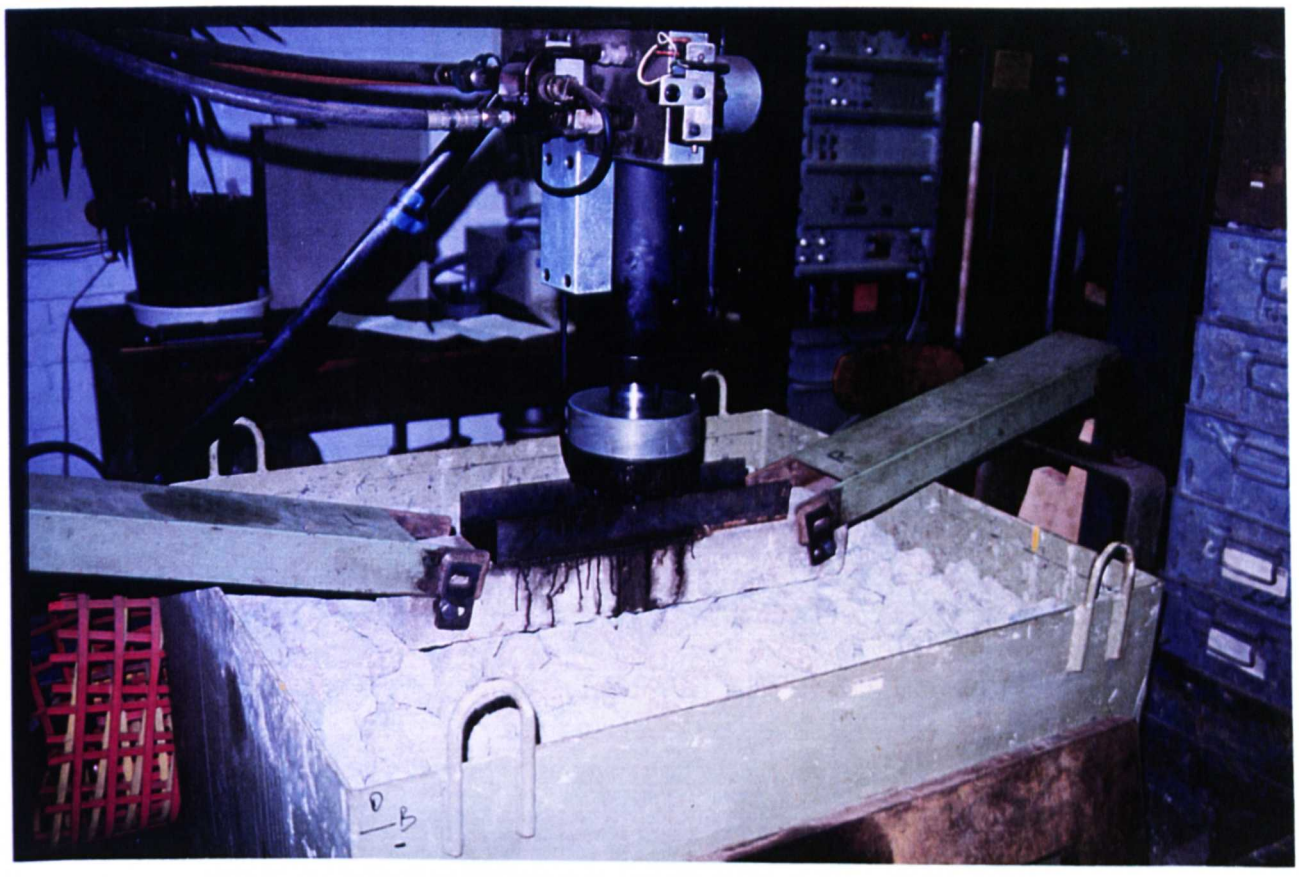

Plate 7.1 - The half sleeper rig at Scientifics Ltd

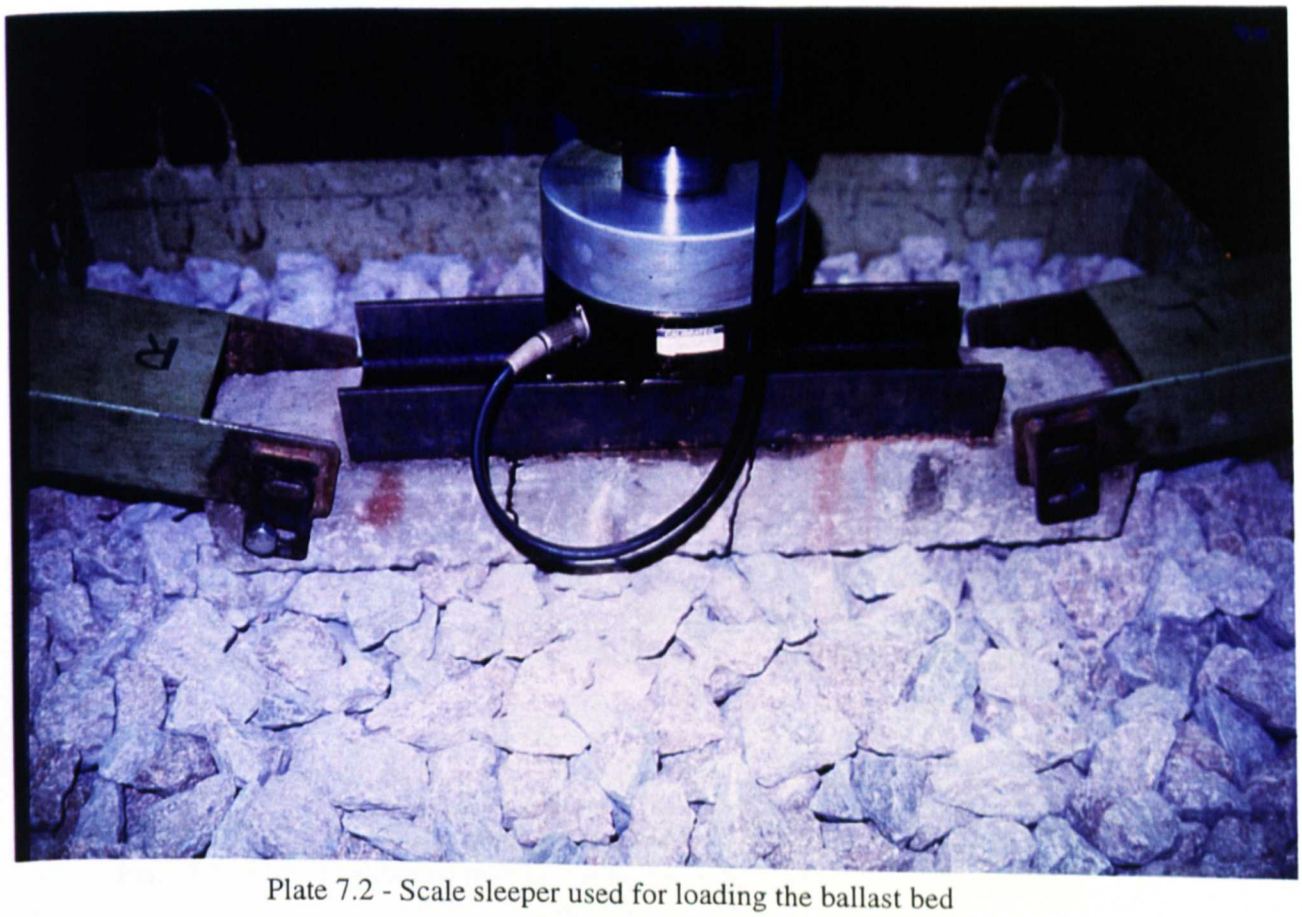

Plate 7.2 - Scale sleeper used for loading the ballast bed

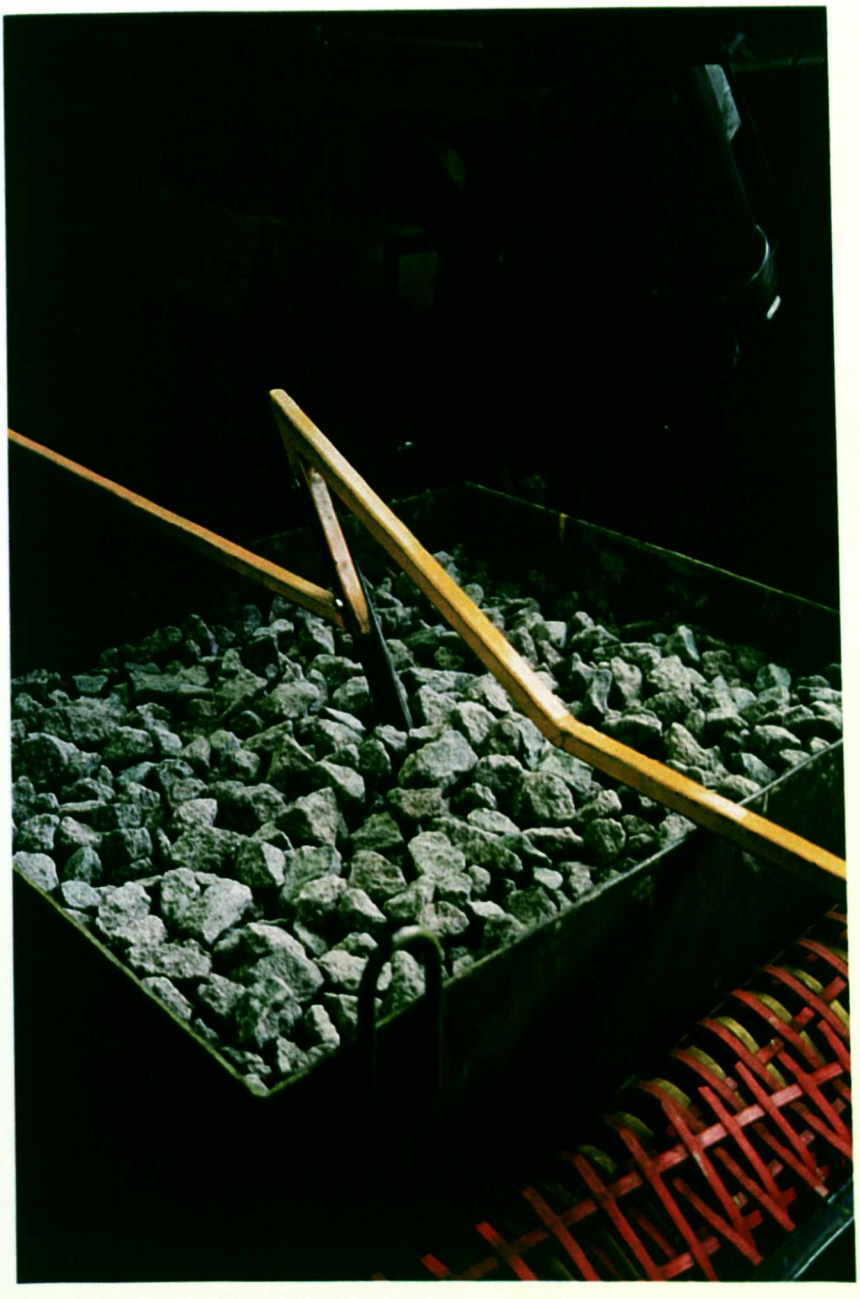

Plate 7.3 - Use of calibrated rake on the ballast load to ensure uniform starting conditions

Plate 7.4 - Use of the wooden levelling gauge to control the starting level of the ballast bed

Plate 7.5 - Pattern of stoneblown stone under a sleeper

Chapter 8 - Closing Discussion, Conclusions and Recommendations

8.1 Introduction

In Section 2.9, the aim of the research project was stated, along with a number of specific objectives. This chapter summarises how the results of the triaxial and model testing have addressed the objectives, and discusses the implications of the work with respect to the behaviour of the track bed and how it would affect track maintenance by the process of stoneblowing.

To this end, the objectives listed in Section 2.9 will be considered one at a time.

8.2 Objective 1

To investigate the behaviour of a two layer system of large, uniformly graded granular materials with reference to the behaviour of its component materials, especially under cyclic loading.

The two layer systems in both the triaxial testing and the model testing exhibit essentially the same behaviour. Both exhibit the characteristic behaviour of granular materials under cyclic loading, with the majority of the deformation occurring in the first few load cycles and the amount of permanent deformation per cycle diminishing as the test goes on. Both types of testing are also controlled by the properties of the materials - if the particle sizes are two disparate then the materials will intermix and the specimen will fail, or if one of the materials is too weak, then the system will fail. However, in the detail, the two types of testing differ considerably in the way they behave.

In the triaxial testing, it can be seen from Section 6.2.2 that it is the weaker layer of material that controls the properties of the two layer triaxial specimen. However, the behaviour of this material in turn is controlled by the degree of confinement to which it is subject. The

restraints placed upon it by the platen and the ballast in the triaxial tests effectively change its H/D ratio, and hence its strength.

In the case of the model testing, as can be seen from Section 7.5.3, the ballast rather than the smaller material controls the amount of deformation. The only control the smaller material exhibits over the settlement is in the degree to which it alters the load path of the ballast, and hence induces new settlement to take place in the ballast.

Thus it must be concluded from this that the behaviour of a two layer system is equally dependent on the testing method to which it is subject as it is the materials used.

8.3 Objective 2

To investigate the use of different sizes and types of material in the two layer system, with a view to optimising the material used by the Stoneblower.

The type of stone used in the two layer system has the ability to greatly influence the behaviour of it. A smaller stone used for the top layer may allow better control over the lift given during stoneblowing, but may not behave suitably. Similarly, a rounded material rather than an angular one may form a better packing arrangement and is less likely to block the blowing tubes of the Stoneblower, but might not reach the required strength.

8.3.1 Particle Size

The results from the triaxial testing described in Section 6.2.2 would suggest that 20mm and 14mm materials form a stable structure on a layer of ballast and 10mm material forming a reasonably stable structure, while the 6mm material tends to migrate into the ballast layer. A similar result is suggested by the cyclic test results described in Section 6.5.2. However, the results of the model testing reported in Section 7.5.4 would indicate that 14mm material is unsuitable, and is lost into the ballast bed. This must indicate some difference between the triaxial and model tests, either in terms of the grading of the ballast in the model testing still being influenced by the preparation technique or the loading conditions being different due to load concentration.

These interface stability results can be checked with the criteria for the erodibility of granular media detailed by Cedergren (1989). These criteria were originally developed to

ensure stability at the interface of different materials in granular filters and are based around the premise that if three perfect spheres have a diameter greater than 6.5 times the diameter of a smaller sphere, then the smaller sphere can pass through them (shown diagramatically in Fig. 8.1). These criteria are based around spheres and may not seem applicable to angular materials, but they are expressed in terms of material passing through a sieve aperture, and any angular material that will pass through a given sieve aperture will pass thorough the same gaps as a spherical particle which passes the sieve. In fact, angular materials will often pass through smaller gaps due to their often smaller cross sectional area compared to rounded particles of the same 'grading', thus the criteria may not be sufficiently conservative. The criteria are;

D_{15} (filter) $\leq 5\ D_{85}$ (protected soil) 8.1.1

D_{50} (filter) $\leq 25\ D_{50}$ (protected soil) 8.1.2

Equation 8.1.1 is set to ensure that the coarsest particles of the protected soil are caught in the voids between the finest particles of the filter media, thus forming a block that will trap all the material from the protected soil. The second equation (8.2.2) is present to ensure that the grading of the filter is roughly parallel to that of the protected soil, avoiding gap gradings that would allow material from the protected soil through. Given that the D_{15} value of the ballast is in the region of 37mm, this would mean the D_{85} of the finer material would have to be greater than 7.4mm to ensure stability. As can be seen from section 5.1, the 20, 14, and 10mm materials all fit this criterion, which agrees well with the results shown in Fig. 6.12 (Section 6.2.2)

Whilst the formulae quoted by Cedergren agree with the results of the triaxial testing, given the results of the model testing it would be unwise to recommend the use of material of 14mm particle size or less with this grading of ballast. It must be borne in mind though, that this is brand new ballast with the largest grading of material permitted by the ballast specification. Ballast with a grading tending slightly less towards particles of 50mm, or fouled ballast, would allow the use of smaller stone in the top layer of material. Indeed, there have been reports of hand-held stone injectors being used with 6mm material on greatly fouled ballast.

8.3.2 Use of Rounded Material

The results of Test Series TF in the triaxial testing programme showed that when adequately confined, the use of rounded river gravel with ballast in a two layer material resulted in specimens with very low levels of deformation. Because of their spherical nature, the particles of river gravel can generally reach a higher density than an angular material for a given compactive force. Also, the lack of sharp edges and points means that there is less particle breakage from the points, and the contact points are not abraded so easily, giving less opportunity for volumetric strain. However, due to the low shear resistance compared with ballast, greater confining forces are needed to mobilise the necessary interparticle friction to resist the applied loads. From the results of the model testing, Section 7.5.4, it would appear that the crib ballast is unable to provide the required lateral force, and so the material is not suitable for use within the trackbed.

8.4 Objective 3

To investigate the effect of differing layer geometry on the behaviour of a two layer system.

The geometry of a system is important as it controls the amount of load taken by a material, and where / how it will deform. Both of these factors are crucial in maintaining the geometry of a section of railway track. At a first glance, it may be thought that the two methods of investigating this, the layered triaxial test and the model test, are very different and largely incomparable. However, the common theme in both tests is the degree of particle restraint, and what effect this has on the behaviour of the material.

8.4.1 Angle of Layer Interface

The results from Section 6.5.4 and Section 6.2.4 suggest that the angle of the interface between layered specimens of ballast and 20mm material has no quantifiable effect on the behaviour of the specimen. From this, it follows that shear stresses at the interface of the material do not have any effect on the behaviour of the materials, and it is only the principal stress that controls the deformation. The practical implication of this finding is that stoneblowing curved track, where much of the radial force is taken by the sleeper ballast interface due to friction, should not have any major implications. In these situations, the frictional shear force should have no effect, and it will be the net stress on the material that should be considered. Although it is not mentioned in the literature, presumably this means that the net stress on the materials will be slightly higher than it would otherwise be in

straight track due to the combination of lateral and vertical forces, and that it will act at an angle to the vertical. This would presumably result in the material deforming in a direction other than the vertical (see Fig. 8.2). Assuming from the Prud'homme formula (see Section 2.5.2) that the lateral force would be up to one third of the vertical force, and that the sleeper pressure in straight track is 300 kPa, then the net resultant stress would be 316kPa at an angle of 18.4° to the vertical.

When two layer triaxial test specimens using river gravel were tested with the material interface at 45° to the horizontal, they were found to be significantly weaker than specimens with the horizontal interface (see Section 6.2.6). This was thought to be caused by the lower level of confinement from having the whole of the shear band comprised of gravel. This signifies that for the interface angle to have no bearing on the specimen behaviour, the material in the top layer must have very similar behaviour to that of the bottom layer.

8.4.2 Layer Thickness

In the triaxial test, when using 20mm material with ballast, having a thin layer of material (20 - 25% of the specimen height) appears to confine the rest of the specimen, thus giving it an effective H/D ratio of 1.5 - 1.6 and increasing its angle of shear resistance by approximately 3° (see Table 6.4). However, increasing the depth of the 'thin' layer to 50% of the specimen height appears to destroy this effect, due to the confinement being lost, and the specimen strength reduces to a value midway between those of its component materials. Given that the materials are so similar in behaviour (e.g. see Section 8.4.1) it is perhaps surprising that this effect occurs at all. Why should one similar material confine another similar material? When the materials are of equal thickness, they act more as one specimen and little 'confinement' takes place. Perhaps the effect is due to the method of specimen construction, with the act of orientating and surcharging the materials at the top of one layer, and then doing the same with another thin layer of material above it, causing local strengthening of the material.

In contrast, when equal thicknesses of ballast and a weaker, or more deformable, material are used to make a specimen, the ballast does act as a confinement to the weaker material and the strength of the specimen is 1-3° greater than that of the weaker material alone. This is not the 4-5° increase that would be expected from the literature (see Section 2.8.1(b) and Bishop and Green, 1965) when the H/D ratio is reduced to 1, and so the confinement is not

perfect and the stronger material (ballast) must still be deforming. Nevertheless, the stronger material is still acting as a restraint on the weaker one.

In the model testing, the confinement appears to be an issue when the thickness of the added material is greater than one particle. Without extra confinement, the lift settlement from Series MD of tests can be seen in Fig. 8.3. Fig. 8.4 shows the very different lift settlement relationship obtained from tamping as a comparison. These relationships are vital if predictive maintenance is to be carried out. If the material is blown or the track is tamped back to its correct geometry, a few months later it will have settled somewhat, and the geometry will have degraded to a certain extent. If the degree of settlement that will occur is known, extra material can be blown in or the track can be overtamped by the required amount. This will mean that initially the geometry is not perfect, but after a few months the track geometry will improve as it settles by the predicted amounts, thus moving to the desired geometry. Given the behaviour of the track described in Section 2.3 (Waters, 1989), the track should then hold its correct shape for longer.

If the added material is confined properly, as it should be in good track with crib ballast, then the lift - settlement relationship described in Fig. 8.3 should carry on in a straight line for lifts of 25 - 40mm, as the ballast bed will not be exposed to any concentrated loads, as described in Section 7.5.3. This constant lift settlement relationship would be ideal for maintenance, as it would mean that the corrected shape immediately after maintenance would stay the same as the sleepers all settled at the same rate. However, care must still be taken in the design of the maintenance level, as sleepers in other sections that have not been disturbed will not settle as much, and sleepers that have been lifted by the machine but have had no material added will settle slightly due to the small disturbances to the bed. This means there could still be differential settlement between sections of the track.

Another point to be considered is that, as described in Section 7.5.5(a) and shown in Plate 7.4, in the field the stone is blown in patches rather than in the neat layers used in this series of model tests. This would mean that with small lifts, as more stone is pneumatically injected the stone inclusion will increase in size, and thus the degree of disturbance to the ballast bed will increase. This would result in an increase in settlement on the ballast bed as the quantity of blown stone increased, until the point where the quantity of stone added was so great that it was acting as a layered system similar to the one used in the model tests, at

which point the lift settlement relationship would flatten out. Consequently, it could be imagined that the in field lift settlement relationship might actually look something like Fig. 8.5.

8.5 Objective 4

To investigate the effect of the addition of polymer mesh elements to railway ballast.

From the results of Section 6.8, it is concluded that the use of Netlon mesh elements as described in Section 5.4.7 in the ballast is not viable. The use of mesh elements with a high level of rigidity, to avoid the need for high strains in the material in order to get a reaction force from the elements, results in bridging of the particles by the elements. This reduces the density of the specimens, and the strength of the specimens is therefore affected. The use of Terram elements did not produce such a reduction in the density of the material, but then did not increase the strength of the specimen. It is thought that the tensile strength of the material was inadequate for it to develop significant confining force within the specimen.

8.6 Further Discussion

Section 6.4 showed the importance of the minimum stress in controlling the behaviour of a material under cyclic loading. From the results in this section, it can be seen that the minimum stress has a significant effect on the resilient modulus of the specimen. This behaviour has been predicted by past work in the field of highway engineering, such as Boyce et al. (1976), and Brown and O'Reilly (1991), but not generally recognised in the field of railway engineering. It also appears from Section 6.4 that the change in minimum stress also affects the plastic deformation of the specimens, although there does not appear to be a direct link between the values of modulus for a specimen and the level of plastic deformation that it undergoes.

It has been noted by several studies (Raymond, 1992, Raymond and Bathurst, 1994 and Sharpe, 1996) that the deformation of ballast in box tests is linked to the modulus of the subgrade material below the ballast, which would suggest that the plastic deformation is linked to the degree of particle movement under cyclic loading. Boyce (1980) proposes that the resilient deformation is entirely caused by deformation of the material at particle contacts and does not involve slip between particles, but this is not supported by the

evidence above. It could be that in tests with ballast overlying a compressible subgrade, the layer of ballast above has to 'flex' under loading in the same way that a beam on an elastic foundation would do. This bending behaviour would cause interparticle slip, and hence the amount of deformation in the modulus would control the degree of slip occurring, and ultimately the settlement of the ballast in the layer above. In the case of a triaxial test, the ballast at the bottom of the specimen would undergo very little interparticle slip. However, due to the low number of particles and the consequent randomness of the structure, further up the specimen the material deformation at interparticle contacts would build up to cause differential movements, and hence interparticle slip. The degree of slip would therefore be governed by the structure of the specimen, which in these specimen with a low D/d_{max} ratio is highly random.

It was also noted that the post cyclic tests carried out after the change in conditions midway through the testing programme showed smoother and more uniform deformation. This could be due to a change in material behaviour from the increased interparticle slippage.

The practical implications of this for the maintenance of railway track geometry are that not only will the rate of decay of geometry be linked to the resilient modulus of the subgrade, but also to the dead load imposed by the track. Assuming a dead load of 410kg per sleeper, and that a 100kN sleeper load gives a ballast load of 250 - 300kPa, then the minimum load experienced will be 10 - 12 kPa, i.e. similar to the nominal minimum load used in the first section of the triaxial test programme. This is of course reduced even further by the momentary uplift force from passing wheels (see Fig. 2.7). Even neglecting the uplift force, using the method proposed by Boyce et al. (1976) with estimated values of σ_3 to give the initial value of ballast modulus to be 150 MPa, calculations suggest that a doubling of the sleeper weight, which contributes most of the ballast minimum load, would in theory increase the resilient modulus of the ballast by approximately 25%. Given that the uplift load may reduce the force from the present sleeper weight to almost zero, then the effects may be more pronounced than that. As the subgrade modulus would also be expected to increase slightly, on the basis that surcharging from the weight of the ballast already contributes to the minimum stress and the dead weight of the sleeper would make a small difference, then it is possible that the settlement of the ballast could be cut noticeably.

Another effect of cyclic loading on the material is the change in failure envelope that it causes. Fig 8.6 shows both Fig. 6.15 and Fig. 6.47 combined. It can be seen that whilst the overall failure envelope has changed, giving apparent cohesion to the material, the different specimens have been affected in different ways. The tests carried out at a cell pressure of 40kPa indicate that the specimens have greatly increased in strength and stiffness despite undergoing dilation, which is contrary to the commonly accepted rules of soil mechanics (Schofield and Wroth, 1968). The specimens undergoing cyclic loading at a cell pressure of 90 kPa, however, have displayed only a small increase in the strength despite undergoing contraction. It is thought that this is due to some form of particle re-arrangement within the specimen. Because the specimen at 40kPa cell pressure is cycled close to its static failure stress, it undergoes considerable deformation and particle re-arrangement before it is able to resist the deviator stress to which it is being exposed. The specimen at 90 kPa, however, is able to resist the cyclic deviator stress relatively easily as it is a much smaller percentage (approximately 50%) of the failure stress, and so it undergoes little deformation, with the consequence that its strength is increased by a much smaller amount. It could be said that the cyclic load is 'conditioning' the specimen to be able to take a certain deviator stress, and it is this that results in the skew in the failure envelope.

One final point to consider is that according to work done by Stewart et al. (1984), the cell pressures used for these experiments are greater than the horizontal stresses to be found in ballast cycled under a load of 270kPa in a box test (see Section 2.7.1), which would be presumed to be similar to those found in a track bed. However, according to the results of this experimental programme (as discussed in Section 6.5.1) the use of a cell pressure of 40 kPa with deviator stresses of 270kPa in the triaxial test will cause dilation of the specimen. In this case then, it would be logical to conclude that the materials in the box tests would dilate on loading, which is contrary to the mechanisms that are presumed to be going on in the box tests and the ballast beds. This must again signify differences in the test conditions which must be carefully noted and accounted for when interpreting the results. It also signifies a lack of knowledge about the exact conditions within the track bed and box tests.

8.7 Conclusions

Listed below are the major conclusions that can be drawn from this work. Conclusions from both model and triaxial testing are listed separately, although it must be remembered that there is a certain amount of overlap between the two.

8.7.1 Triaxial Testing

- Providing that the materials form a stable interface, the strength of a two layer specimen is controlled by the weaker of the two layers (in these tests, the smaller grading of material). However, the behaviour of the smaller material is in turn controled by the degree to which it is confined by the other material.
- The stability of the interface between two layers of uniformly graded angular material in the triaxial test appears to agree well with the criteria for prevention of erosion in granular filters. In this case, it signifies that material of 10mm or greater will form a stable layer with the ballast used.
- The testing has highlighted the fact that the work carried out linking maximum and minimum levels of cyclic stress to resilient modulus of the material for smaller, well graded materials is also applicable to railway ballast.
- There appears to be a subjective link between the resilient modulus of a ballast specimen in the cyclic load test, and the plastic deformation that the specimen undergoes in the test.
- The degree to which the strength of a specimen is increased by the cyclic loading process depends on the ratio of cyclic deviator stress to static deviator stress at failure.
- Polymer mesh elements do not form a practical method of increasing the strength of railway ballast.

8.7.2 Model Testing

- The grading of the ballast material (in this case resulting from the preparation technique) has a significant effect on the behaviour of the material, measured here by the repeatability after 50,000 load cycles.
- Disturbance of the ballast bed will result in increased settlement. The greater the disturbance, the greater the increase in settlement. Therefore, minimisation of disturbance should be a priority.
- Thicker layers of additional material on the ballast bed, when inadequately confined, will result in large settlements. It is thought that this is due to load concentration with layers of above one particle thickness in depth.
- Of the materials tested for addition to the ballast bed, the 20mm angular material appeared to be the only one that performed to a satisfactory level.

8.8 Further Work

The work carried out has highlighted several gaps in the knowledge of the behaviour of ballast style media, which could be usefully investigated. Of these gaps, it is felt that the following three are the most important.

- An investigation needs to be carried out into the link between the resilient modulus of ballast under cyclic loading and the plastic deformation undergone by the material. This would allow the prediction of the likely future maintenance requirement of a piece of railway track to be assessed from a simple load-deflection test on it in the field.
- The value of the resilient modulus of ballast under different cyclic load paths needs to be investigated, to assess if the present formulae applicable to well graded cohesionless materials could be simply modified, or whether a new equation needs to be derived. Along with the work suggested in the previous paragraph, this would allow and assessment of the behaviour of railway track under different loading conditions, with a view to optimising the revenue - maintenance cost.
- The effect of water on the plastic deformation of granular materials needs to be quantified. This could have wide ranging applications other than railways pavements, for example on the foundations of buildings subject to cyclic load when they are built on granular soils.

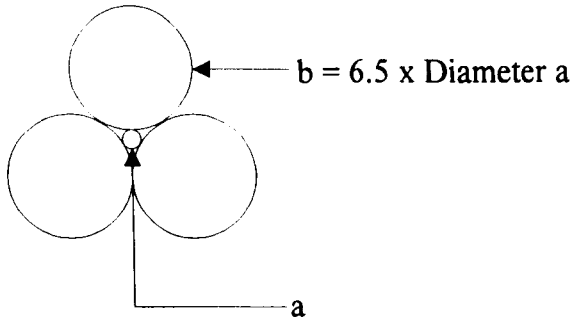

Fig. 8.1 - Theoretical basis of rules for filter media (from Cedergren, 1989)

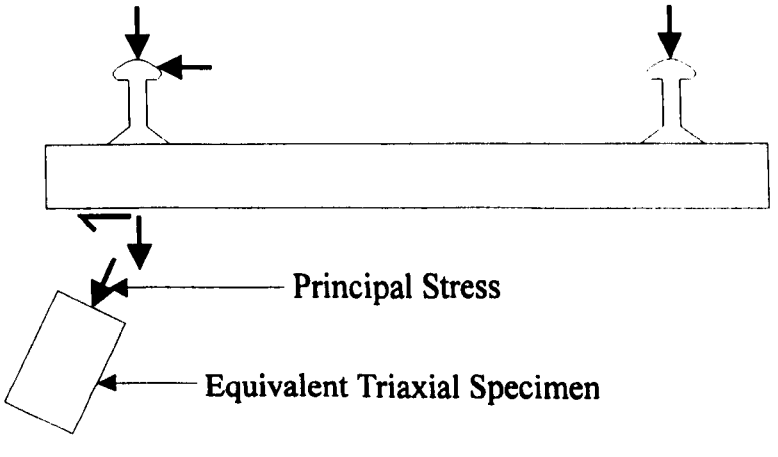

Fig. 8.2 - Resultant forces for sleeper on curved track

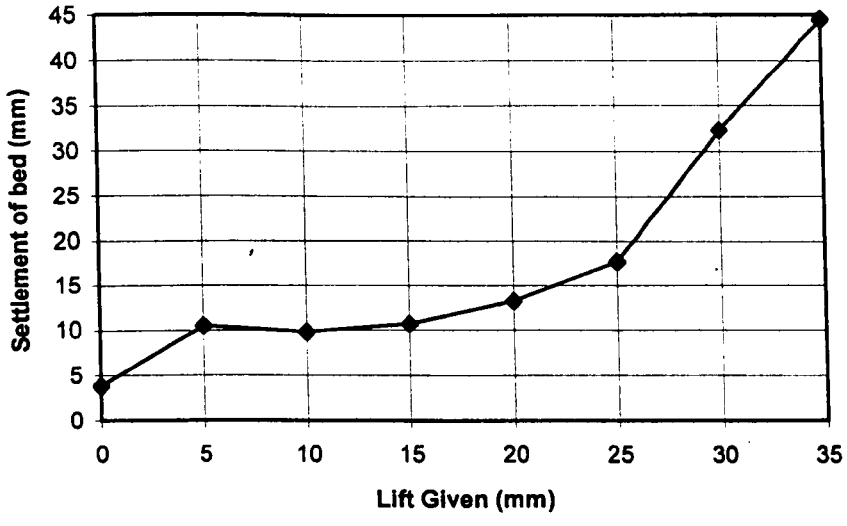

Fig. 8.3 - Sleeper lift settlement relationship from model test Series MD

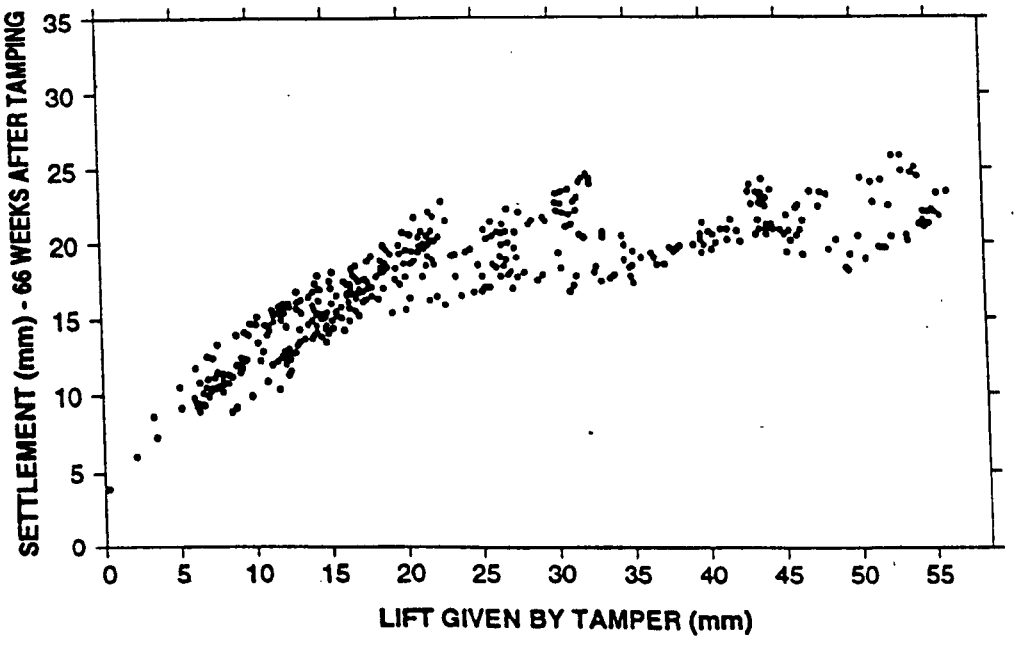

Fig. 8.4 - Sleeper lift settlement relationship from tamping (Selig and Waters, 1994)

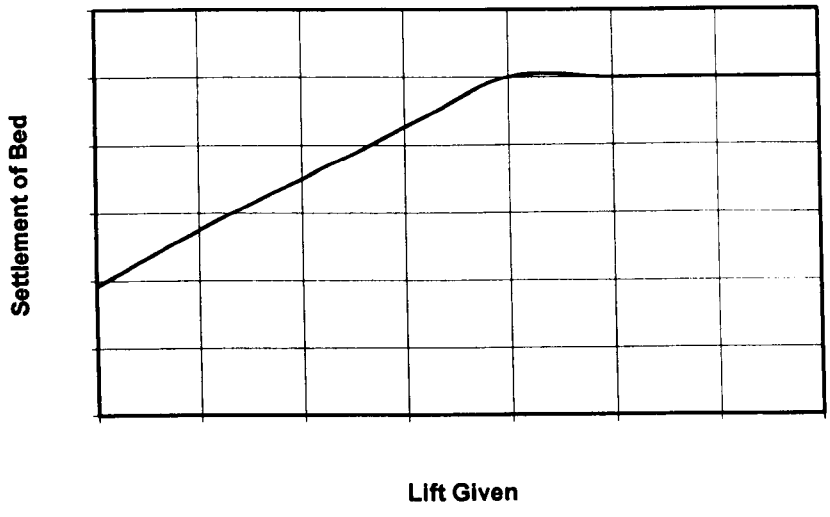

Fig. 8.5 - Proposed lift settlement relationship for stoneblowing

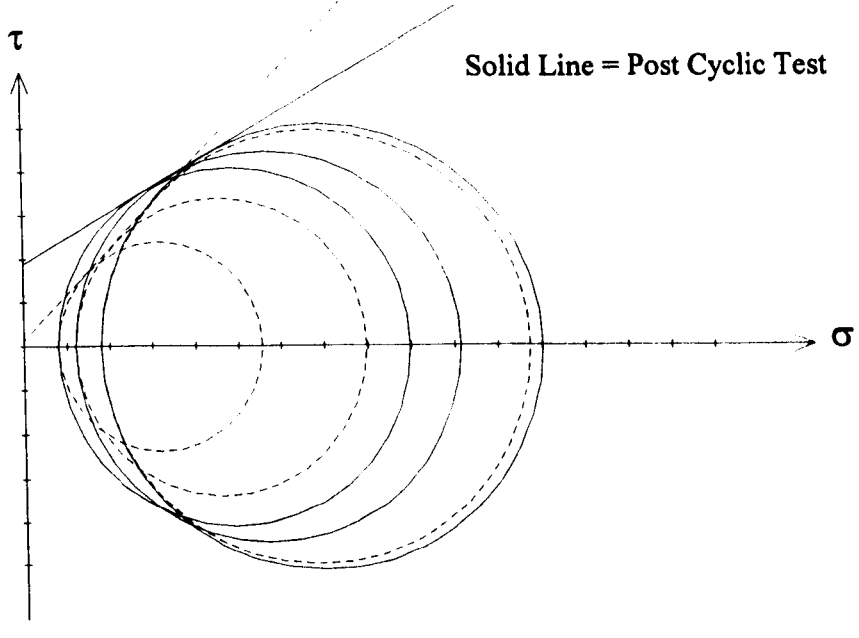

Fig. 8.6 - Comparison of failure envelopes from initial and post cyclic monotonic test on two layer specimens

References

Alva-Hurtado, J.E.D. (1980), "A methodology to predict the elastic and inelastic behaviour of railway ballast", PhD Dissertation, Department of Civil Engineering, University of Massachusetts, Amherst, Massachusetts.

Alva-Hurtado, J.E.D. and Selig, E.T. (1981), "Permanent Strain Behaviour of Railway Ballast", Proceedings of the 10th International Conference of Soil Mechanics and Foundation Engineering, Stockholm, Sweden, Vol. 1, PP 543-546.

Andrawes, K.Z., McGowan, A., Hytiris, N., Mercer, F.B. and Sweetland, D.B. (1986), "The use of mesh elements to alter the stress-strain behaviour of granular soils", Proceedings of the Third International Conference on Geotextiles, Vienna, Austria, pp 839-844.

Atkinson, J.H. and Bransby, P.L. (1978), "The Mechanics of Soils", McGraw-Hill, London

Bathurst, R.J. and Raymond, G.P. (1987), "Geogrid reinforcement of ballasted track", Transportation Research Record, No.1153, pp 8-14.

Bishop, A.W and Green, G.E. (1965), "The influence of end restraint on the compression strength of a cohesionless soil", Geotechnique, Vol. 15, No.3, pp 243-266.

Boyce, J.R. and Brown, S.F. (1976), "Measurement of elastic strain in granular materials", Geotechnique, Vol. 26, No.4, pp 637-640.

Boyce, J.R., Brown, S.F. and Pell, P.S. (1976), "The resilient behaviour of a granular material under repeated loading", Proceedings of the 8th Australian Road Research Conference, University of Western Australia, Perth, Vol. 8, pp 1-12

Boyce, J.R. (1980), "A non-linear model for the elastic behaviour of granular materials under repeated loading", International Symposium on Soils under Cyclic and Transient Loading, Swansea, UK, January 1980, Vol. 1, pp 285-294.

Bressani, L.A. (1995), "External measurement of strain in the triaxial test", Geotechnical Testing Journal, Vol. 18, No.2, pp 226-240

Brown, S.F. (1974), "Repeated load testing of a granular material", ASCE Journal of the Geotechnical Engineering Division, Vol. 100, No.GT7, July 1974, pp 825-841.

Brown, S.F. and Hyde, A.F.L. (1975), "Significance of cyclic confining stress in repeated-load triaxial testing of granular material", Transportation Research Record, No.537, pp 49-57.

Brown, S.F and O'Reilly, M.P. (1991), "Cyclic loading of soils: from theory to design", Blackie

Bryer, T. (1989), "Selection and manufacture of ballast", Third RIA Track Sector Course, Railway Industry Association, Vol. 1, Section 4, Paper 4.2.

Burland, J.B. and Symes, M. (1982), "A simple axial displacement gauge for use in the triaxial apparatus", Geotechnique, Vol. 32, No.1, pp 62-65.

Cedergren, H.R.(1989), "Seepage, drainage and flow nets", Third Edition, John Wiley & Sons.

Chiang, C.C. (1989), "Effects of water and fines on ballast performance in box tests", MS Degree project report No.AAR89-366P, Department of Civil Engineering, University of Massachusetts, Amherst, August 1989.

CIRIA (1991), "Manual on the use of rock in coastal and marine engineering", CIRIA Special Publication 83.

Di Pilato, M.A. Levergood, A.V. Steinberg, E.I. and Simon, R.M. (1983), "Railroad track substructure design and performance evaluation practices", Goldberg-Zoino and Associates Inc., Newton Upper Falls, Massachusetts, Final Report for U.S. DOT Transportation Systems Centre, Cambridge, Massachusetts, Report No.FRA/ORD-83/04.2, June 1983.

Diyaljee, V.A. (1987), "Effects of stress history on ballast deformation", ASCE Journal of Geotechnical Engineering, Vol. 113, No.8, August 1987, pp 909-914.

Drescher, A. and Vardoulakis, I. (1982), "Geometric softening in triaxial tests on granular material", Geotechnique, Vol. 32, No.4, pp 291-303.

Drnovsek, J. (1970), "Rupture line in a two layer non-cohesive medium", Soils and Foundations, Vol. 10, Part 1, pp 37-42.

Duncan, J.M. and Dunlop, P. (1968), "The significance of cap and base restraint", ASCE Journal of the Soil Mechanics and Foundations Division, Vol. 94, No.SM1, January 1968, pp 271-290.

Eisenmann, J. (1985), Discussion on papers 17-21, Track Technology for the Next Decade, Thomas Telford, London, p 274.

Esveld, C. (1989), "Modern railway track", MRT productions, Germany.

Evans, E.S.R (1993), "Track substructure guide", Report LR-CES-069, British Railways Engineering Research and Development, Civil Engineering Structures Unit, Brunel House, Derby, UK.

Ford, R. (1995), "Differential Ballast Settlement, and consequent undulations in track caused by vehicle-track interaction", Vehicle System Dynamics Special Supplement 24, pp 222-233.

Frederick, C.O. and Round, D.J. (1985), "Vertical Track Loading", Track Technology for the Next Decade, Thomas Telford, London, 1985, pp 135-149.

Gaskin, P.N., Raymond, G.P. and Powell, A.G. (1978), "Response of railroad ballast to vertical vibration", ASCE Transportation Engineering Journal, Vol. 104, No.TE1, January 1978, pp 75-87.

Goto, S. and Tatsuoka, F. (1988), "Effect of end conditions on triaxial compressive strength for cohesionless soil", Advanced Triaxial Testing of Soil and Rock, ASTM, Philadelphia, STP 977, pp 692-705.

Hamed, A.H. (1987), "Geogrid Reinforcement of ballasted track", MSc Thesis, Department of Civil Engineering, University of Birmingham, UK.

Harrison, H.D. Selig, E.T. Dean, F.E. and Stewart, H.E. (1986), "Correlation of concrete tie track performance in revenue service and at the facility for accelerated service testing-Vol. 1, a detailed summary", Battelle Columbus Laboratories and University of Massachusetts, Final Report, Report No.DOT/FRA/ORD-84/02.1, August 1984.

Hay, W.W. (1981), "Railroad engineering", second edition, John Wiley & Sons.

Henkel, D.J. and Gilbert, G.D. (1952), "The effect of the rubber membrane on the measured triaxial compression strength of clay samples", Geotechnique, Vol. 3, pp 20-29.

Hicks, R.G. and Monismith, C.L. (1971), "Factors influencing the resilient response of granular materials", Highway Research Record, No.345, pp 15-31.

Hunt, G. (1996) Personal Communication, British Rail Research, Derby, UK.

Indraratna, B. Ionescu, D. Christie, H.D. (1998), "Shear behaviour of railway ballast based on large scale triaxial tests", ASCE Journal of Geotechnical and Geoenvironmental Engineering, Vol. 124, No.5, May 1998, pp 439-449.

Janardhanam, R. and Desai, C.S. (1983), "Three dimensional testing and modelling of ballast", ASCE Journal of Geotechnical Engineering, Vol. 109, No.6, June 1983, pp 783-796.

Jeffs, T. and Marich, S. (1987), "Ballast Characteristics in the Laboratory", Conference on Railway Engineering, Perth, Australia, September 1987.

Kalcheff, I.V. and Hicks, R.G. (1973), "A test procedure for determining the resilient properties of granular materials", Journal of Testing and Evaluation, JTEVA, Vol. 1, No.6, November 1973, pp 472-479.

Keubris, R.H. and Vaid, Y. P. (1990), "Corrections for membrane strength in the triaxial test", Geotechnical Testing Journal, Vol. 13, No.4, December 1990, pp 361-369.

Klugar, K. (1975), "A contribution to ballast mechanics", Proceedings of the Symposium on Railroad Track Mechanics, Pergamon Press, pp 387-403.

Kolisoja, P. (1997), "Factors affecting deformation properties of coarse grained granular materials", Proceedings of the 14th International Conference on Soil Mechanics and Foundation Engineering, Hamburg, Germany, Vol. 1, pp 337-342.

Knutson, R.M. and Thompson, M.R. (1978), "Permanent deformation behaviour of railway ballast", Transportation Research Record, No.694, pp 47-53.

Lam, W. and Tatsuoka, F. (1988), "Triaxial compressive and extension strength of sand affected by strength anisotropy and sample slenderness", Advanced Triaxial Testing of Soil and Rock, ASTM, Philadelphia, STP 977, pp 655-666.

La Rochelle, P., Leroueil, S., Trak, B., Blais-Leroux, L. and Tavenas, F. (1988), "Area corrections in triaxial tests", Advanced Triaxial Testing of Soil and Rock, ASTM, Philadelphia, STP 977, pp 715-731.

Lee, K.L. (1978), "End restraint effects on undrained static triaxial strength of sand", ASCE Journal of the Geotechnical Engineering Division, Vol. 104, No.GT6, June 1978, pp 687-704.

Lee, K.L. and Vernese, F.J. (1978), "End restraint effects on cyclic triaxial strength of sand", ASCE Journal of the Geotechnical Engineering Division, Vol. 104, No.GT6, June 1978, pp 705-719.

Lentz, R.W. and Baladi, G.Y. (1980), "Simplified procedure to characterise permanent strain in sand subjected to cyclic loading", International Symposium on Soils under Cyclic and Transient Loading, Swansea, UK, January 1980, Vol. 1, pp 89-95.

Li, D. and Selig, E.T (1998), "Method for railroad track foundation design-II: applications", ASCE Journal of Geotechnical and Geoenvironmental Engineering, Vol. 124, No.4, April 1998, pp 323-329.

McDonald, L.M. and Raymond, G.P. (1984), "Repetitive load testing: reversal or rotation", Canadian Geotechnical Journal, Vol. 24, pp 456-474.

McMichael, P.M. (1995), Personal communication, Stoneblower Team Headquarters, Sheaf House, Sheffield, UK

Mercer, F.B., Andrawes, K.Z., McGowan, A. and Hytiris, N. (1984), "A new method of soil stabilisation", Proceedings of the Symposium on Polymer Grid Reinforcement in Civil Engineering, London, UK, Paper 8.1.

ORE (1970), "Stresses in the rails, the ballast and the formation resulting from traffic loads", Question D71, Report No.10, Utrecht, Holland.

Morgan, J.G.D. and Markland, E. (1981), "The effect of vibration on ballast beds", Geotechnique, Vol. 31, No.3, pp 367-386.

Pappin, J.W. and Brown, S.F. (1980), "Resilient stress-strain behaviour of a crushed rock", International Symposium on Soils under Cyclic and Transient Loading, Swansea, UK, January 1980, Vol. 1, pp 169-177.

Pappin, J.W., Brown, S.F. and O'Reilly, M.P. (1992), "Effective stress behaviour of saturated and partially saturated granular material subjected to repeated loading", Geotechnique, Vol. 42, No.3, pp 485-497.

Raymond, G.P. and Davies, J.R. (1978), "Triaxial tests on dolomite railroad ballast", ASCE Journal of the Geotechnical Engineering Division, Vol. 104, No.GT6, June 1978, pp.737-751.

Raymond, G.P. and Bathurst, R.J. (1987), "Performance of large scale model single tie ballast systems", Transportation Research Record, No.1131, pp 7-13.

Raymond, G.P. (1992), "Reinforced sand behaviour overlying compressible subgrades", ASCE Journal of Geotechnical Engineering, Vol. 118, No.11, November 1992, pp 1663-1680.

Raymond, G.P. and Bathurst, R.J. (1994), "Repeat load response of aggregates in relation to track quality index", Canadian Geotechnical Journal, Vol. 31, pp 547-554.

Rowe, P.W. (1962), "The stress-dilatancy relation for static equilibrium of an assembly of particles in contact", Proceedings of the Royal Society 269, pp 500-527.

Rowe, P.W. and Barden, L. (1964), "Importance of free ends in triaxial testing", ASCE Journal of the Soil Mechanics and Foundations Division, Vol. 90 No.SM1, January 1964, pp 1-27.

Salman, T.H. (1994), "Triaxial behaviour of partially saturated granular soils at low stress levels", PhD. Thesis, Department of Civil and Structural Engineering, University of Sheffield, UK.

Sato, Y. (1995), "Japanese studies on deterioration of ballasted track", Vehicle System Dynamics Special Supplement 24, pp 197-208.

Schofield, A.N. and Wroth, C.P. (1968), "Critical State Soil Mechanics", McGraw-Hill, London.

Selig, E.T. (1987), "Tensile zone effects on performance of layered systems", Geotechnique, Vol. 37, No.3, pp 247-254.

Selig, E.T. and Waters, J.M. (1994), "Track geotechnology and substructure management", Thomas Telford.

Sharpe, P. (1996), Personal Communication, Scientifics Ltd., Derby, UK.

Shenton, M.J. (1975), "Deformation of railway ballast under repeated loading conditions", Proceedings of the Symposium on Railroad Track Mechanics, Pergamon Press, pp 405-425.

Shenton, M.J. (1985), "Ballast deformation and track deterioration", Track Technology for the Next Decade, Thomas Telford, London, pp 253-265.

Stewart, H.E., Selig, E.T. and Norman-Gregory, G.M. (1984), "Failure criteria and lateral stresses in track foundations", Transportation Research Record, No.1022, pp 59-64.

Stewart, H.E. (1986), "Permanent strains from cyclic variable amplitude loadings", ASCE Journal of Geotechnical Engineering, Vol. 112, No.6, June 1986, pp 646-660.

Tam, K.H. (1986), "Volume change characteristics of dry sand under cyclic loading", MS Degree project report No.AAR85-331D, Department of Civil Engineering, University of Massachusetts, Amherst, Massachusetts, January 1986.

Tarumi, H. (1994), "Review of research on ballast and roadbed", Quarterly Report of Railway Technical Research Institute, Tokyo, Japan, Vol. 35, No.1, February 1994, pp 15-18.

Timmerman, D.H. and Wu, T.H. (1969), "Behaviour of dry sands under cyclic loading", ASCE Journal of the Soil Mechanics and Foundation Division, Vol. 95, No.SM4, July 1969, pp 1097-1112.

Timoshenko, S.P. and Goodier, J.N. (1970), "Theory of Elasticity", McGraw-Hill, 3rd Ed., London.

Waters, J.M. (1989), "Track renewals using the dynamic track stabiliser", Third RIA Track Sector Course, Railway Industry Association, Vol. 1, Section 5, Paper 5.13.

Wright, S.E. (1983), "Damage caused to ballast by mechanical maintenance techniques", British Rail Research technical memorandum TMTD15, May 1983.

Appendix I

Details of the hydraulic control unit

Control unit program

Written in 'Stamp Basic'

```
'
' Hydraulic Control Unit
' Version 9
'
' Manual / Auto
'
'
symbol clear=1      '
symbol DD_RAM=128   ' LCD Codes
symbol i_toggle=254 '

Pause 1000          ' LCD Reset at Power up

Start:
high 5              ' Solenoid off
low 4               ' Pump on

'
' Ask for and get input
'

gosub ClearLCD
serout 6,N2400,("Mode")

GetInput:
gosub KeyRead
branch b2,(GetInput,GetInput,Auto,Manual,GetInput)

'
' Manual Operation
'

Manual:
gosub clearLCD
serout 6,N2400,("Man")
ManLoop:
gosub KeyRead
branch b2,(ManLoop,Start,Switch,ManLoop,ManLoop)

Switch:
toggle 5
pause 250
goto ManLoop

'
' Automatic Operation
'

Auto:
Gosub ClearLCD
low 3               ' Indicate Low Rate
symbol Thous=1000   ' No. Cycles in Thousands
w2=200              ' High Rate Pause
w3=1000             ' Low Rate Pause


Cycle:
for w4 = 1 to Thous
    for w5 = 0 to 999
        gosub Show_w5
        gosub KeyRead
        Branch b2,(Halt,Start,Continue,Swap,Continue)
Swap:
        w1=w2
```

```
        w2=w3
        w3=w1
        toggle 3
        pause 250
Continue:
        pause w3
        toggle 5
        pause w3
        toggle 5
    next w5
gosub Show_w4
next w4

high 5          ' Ensure Solenoid
high 4          '  and Valve switched off

serout 6,N2400,("Done")
end

'
' Temporarily Halt Program
'

Halt:
gosub KeyRead
branch b2, (Halt,Start,Continue,Halt,Halt)

'
' Display Count
'

Show_w4:
b2=0
if w4 < 10 then Write_w4
b2=1
if w4 < 100 then Write_w4
b2=2
Write_w4:
b3=140 - b2
serout 6,N2400,(i_toggle,b3,i_toggle,#w4,"000")
return

Show_w5:
b2=0
if w5 < 10 then Write_w5
b2=1
if w5 < 100 then Write_w5
b2=2
Write_w5:
b3=143 - b2
serout 6,n2400,(i_toggle,b3,i_toggle,#w5)
return

'
' Clear LCD Screen
'

ClearLCD:
serout 6,N2400,(i_toggle,DD_RAM,clear,i_toggle)
return

'
' Read Keys on Pin 7
'

KeyRead:
pot 7,255,b1
for b2= 0 to 3
    lookup b2,(10,73,137,200),b3
    if b1 <= b3 then FoundKey
```

```
next
FoundKey:
return
```

Circuit Diagram of Control Unit

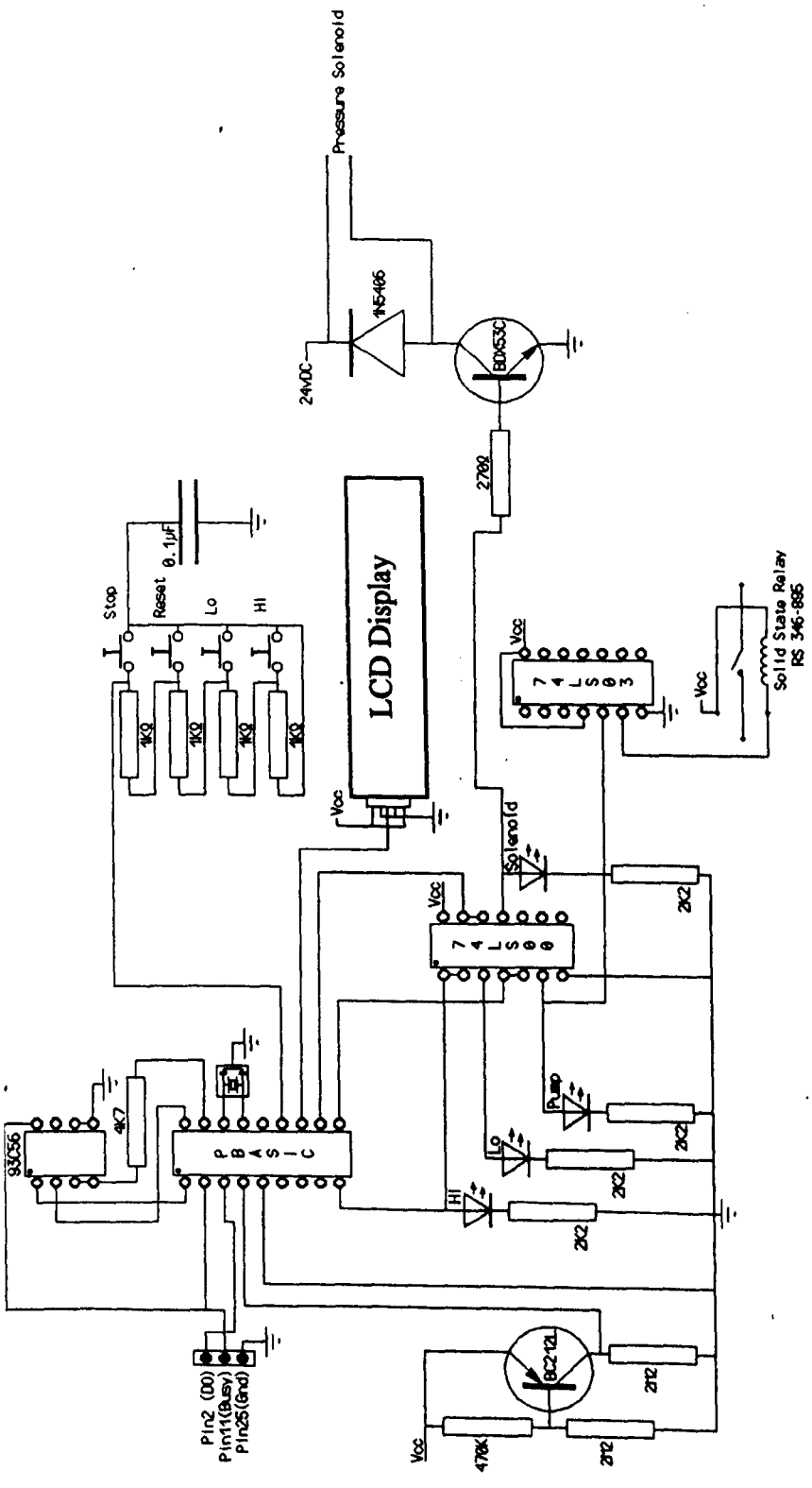

Appendix II

Details of data collection and analysis

Workbench monotonic triaxial test data recording layout

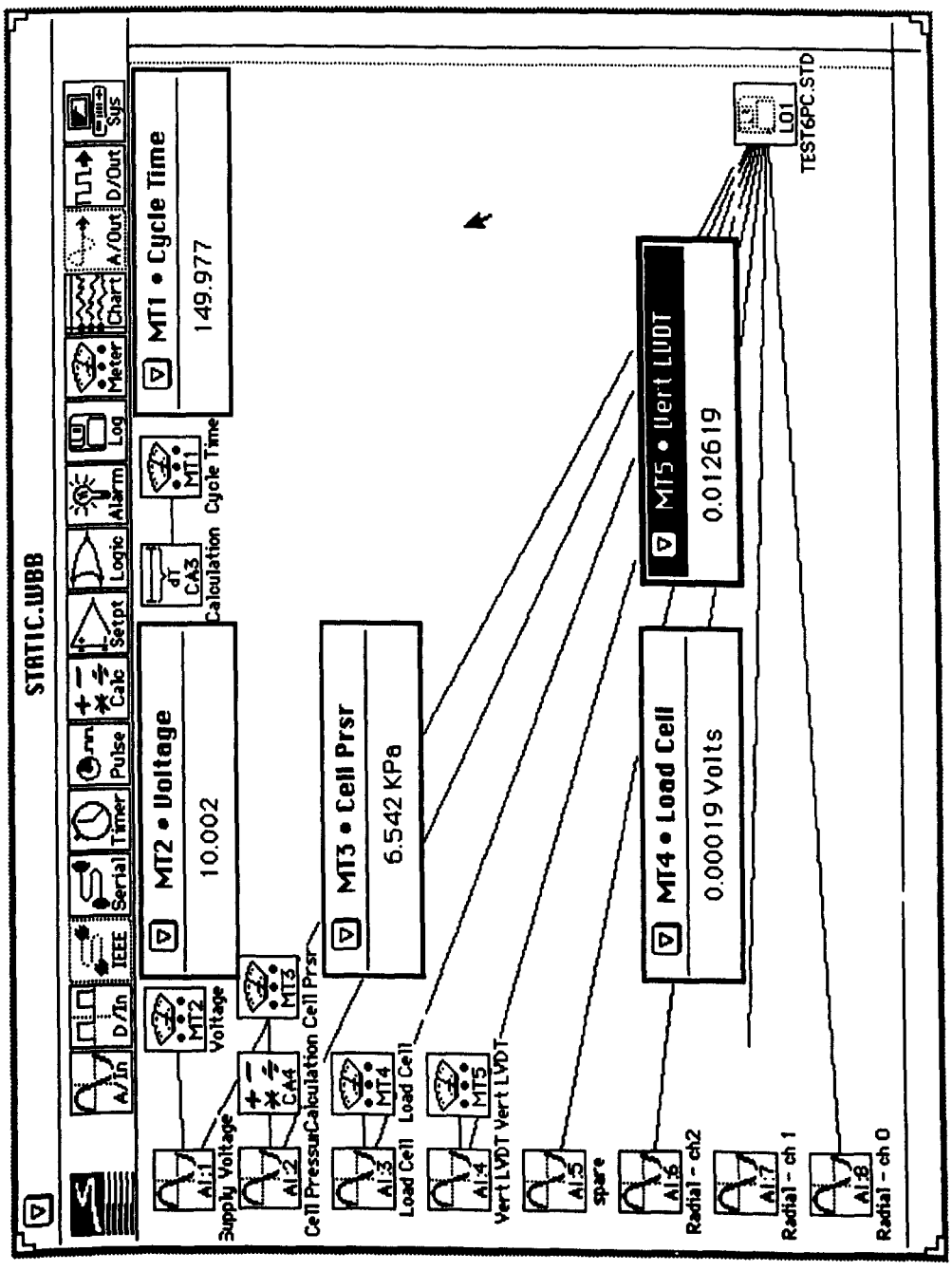

Workbench cyclic triaxial test data recording layout

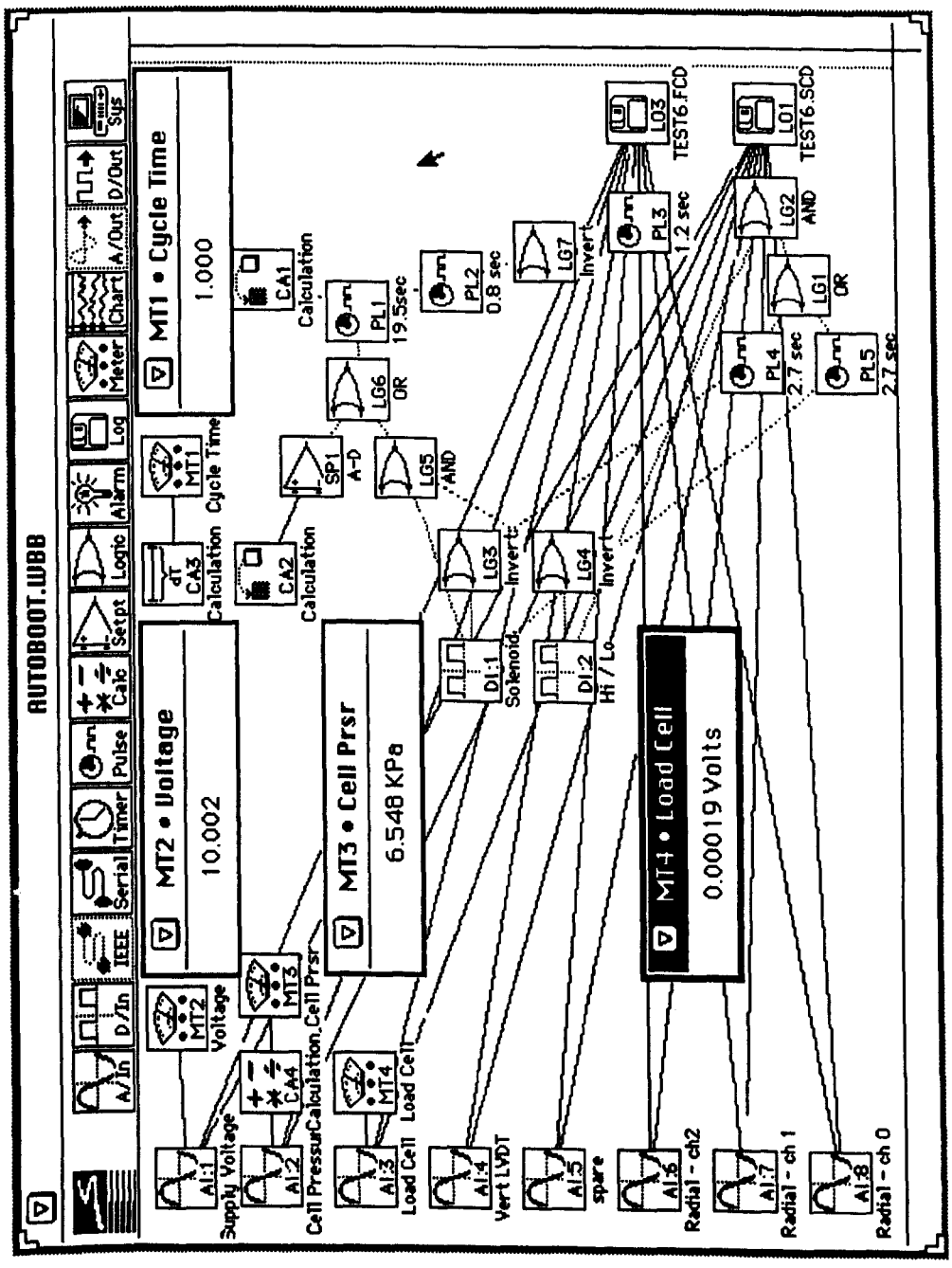

Listing of data processing program

Written for Salford FORTRAN 77 running under DBOS DOS Extender on an IBM PC compatable

```
*
* Ballast Rig Data Analysis Program V1.21
* ANDY KEY - 27 MAY 1997
*
      PROGRAM PROCESS

      CALL CLEAR_SCREEN@
      CALL HIDE_CURSOR@
      CALL WCREATE@(1,1,78,23,95,50)
      CALL POPW@(50)

      CALL WCOUP@('BALLAST RIG DATA ANALYSIS PROGRAM',95,23,1,50)
      CALL WCOUP@('ANDY KEY 1996',95,33,2,50)

      CALL MENU

      CALL KILLW@(50)

      END
*
*-----------------------------------------------------------------------
*
      SUBROUTINE MENU
*
* Subroutine to present menu and branch accordingly
*
      INTEGER ICUR,ILAST,IKEY
*
* IKEY item from keyboard
* ICUR/ILAST Item pointers
*   ICUR - current menu item
*   ILAST - menu item on last run through program
*
      CALL WCREATE@(25,10,30,4,15,40)
      CALL WCREATE@(26,11,30,4,0,41)
      CALL POPW@(41)
      CALL POPW@(40)

      CALL WCOUP@('MENU',15,13,0,40)
      CALL WCOUP@('Process Single Test',112,1,1,40)
      CALL WCOUP@('Process Multiple Tests',15,1,2,40)
      CALL WCOUP@('Exit Program',15,1,3,40)
*
* Set up windows (window 40, shadow 41) and print options
*
      ICUR=1
      ILAST=0
*
* Set up item pointers
*
 10   ILAST=ICUR
*
* Start Main Loop
*
      CALL GET_KEY1@(IKEY)
      IF (IKEY.EQ.13) THEN
            IF (ICUR.EQ.1) CALL SINGLE
            IF (ICUR.EQ.2) CALL DOUBLE
            IF (ICUR.EQ.3) GOTO20
      ELSEIF (IKEY.EQ.328) THEN
            ICUR=ICUR-1
      ELSEIF (IKEY.EQ.336) THEN
```

```
                ICUR=ICUR+1
        ENDIF
*
* Read Keyboard. If enter pressed, goto whatever section indicated
* If arrow keys pressed, change indicator
*
        IF (ICUR.EQ.0) ICUR=3
        IF (ICUR.EQ.4) ICUR=1
*
* If indicator goes out of bounds then put back in at opposite end
*
        IF (ICUR.EQ.ILAST) GOTO 10
*
* If nothing has changed since the last time, no updating to be done
* so just go and read keyboard again
*
        IF (ILAST.EQ.1) CALL WCOUP@('Process Single Test',15,1,1,40)
        IF (ILAST.EQ.2) CALL WCOUP@('Process Multiple Tests',15,1,2,40)
        IF (ILAST.EQ.3) CALL WCOUP@('Exit Program',15,1,3,40)

        IF (ICUR.EQ.1) CALL WCOUP@('Process Single Test',112,1,1,40)
        IF (ICUR.EQ.2) CALL WCOUP@('Process Multiple Tests',112,1,2,40)
        IF (ICUR.EQ.3) CALL WCOUP@('Exit Program',112,1,3,40)

        GOTO 10
*
* Something has changed, so unhighlight previously selected option
* and highlight newly selected option
* Then loop back to beginning
*
 20   CALL KILLW@(40)
        CALL KILLW@(41)
        RETURN
*
* exit option chosen, so kill windows and return
*
        END
*
*-----------------------------------------------------------------------
*
        SUBROUTINE SINGLE
*
* Subroutine to process data from single test - static or dynamic
* Allows choice of test data (STD or SCD/FCD) and calibration file (CAL)
*
        CHARACTER FILENAME*12,CALIBRATION_FILE*12,TEST*1,HEADER*255
        DOUBLE PRECISION CALIB
        DIMENSION CALIB(18)
*
* Set up variables
*  TEST used for analysing chosen filename
*  HEADER used to read in headers from calibration file
*  IA/IB general variables
*  CALIB double precision array for storing calibration values
*   - passed to analysis routine
*
        CALL WCREATE@(1,1,78,23,95,31)
        CALL POPW@(31)
        CALL WCREATE@(1,1,38,23,59,30)
        CALL POPW@(30)

 5    CALL WCOUP@('Select Test Data to be Processed:',63,1,2,30)
        CALL SELECT_FILE@('*.S?D',FILENAME,*10)

        CALL TRIMR@(FILENAME)
        TEST=FILENAME(11:11)
        CALL TRIM@(FILENAME)
        IF (TEST.NE.'T'.AND.TEST.NE.'C') GOTO 5

        CALL WCOUP@(FILENAME,63,1,3,30)
```

```
*
* Set up window and select data file to be processed (anything with S*D suffix)
*  if * not = T or C ie .STD or .SCD (will pick up associated FCD file later)
*  then choose again
* Print name of selected file in window as a reminder
*  if ESC key pressed during selection goto 10 - ie quit routine and return to
*  main menu
*
        CALL WCOUP@('Select Calibration File to be Used:',63,1,5,30)
        CALL SELECT_FILE@('*.CAL',CALIBRATION_FILE,*10)

        CALL WCOUP@(CALIBRATION_FILE,63,1,6,30)
*
* Select Calibration file to be used (.CAL files)
*  if ESC pressed during routine goto 10 - quit and return to menu
*
        OPEN (UNIT=30,FILE=CALIBRATION_FILE,STATUS='OLD')
        READ (30,900) HEADER
        READ (30,900) HEADER
*
* Open calibration file and read in first header
*
        READ (30,*) CALIB(1),CALIB(2),CALIB(3),CALIB(4),CALIB(5),CALIB(
  C6),CALIB(7),CALIB(8)
*
* Read in first line of data
*
        READ (30,900) HEADER
        READ (30,900) HEADER
*
* Read in second header
*
        READ (30,*) CALIB(9),CALIB(10),CALIB(11),CALIB(12),CALIB(13),CA
  CLIB(14),CALIB(15),CALIB(16)
*
* Read in second line of data
*
        READ (30,900) HEADER
        READ (30,900) HEADER
*
* Read in last header
*
        READ (30,*) CALIB(17),CALIB(18)
        CLOSE (30)
*
* Read in last of the data and close file
*
        IF (TEST.EQ.'T') THEN
                CALL STATIC(CALIB,FILENAME)
        ELSE
                CALL CYCLIC(CALIB,FILENAME)
        ENDIF
*
* If test character (from filename) is T, ie .sTd file, then goto static
*  analysis subroutine
* if not, then test character must be C, ie .sCd file, hence goto cyclic
*  analysis subroutine
*
 10  CALL KILLW@(30)
        CALL KILLW@(31)
        RETURN
*
* Job done - close window and return to menu
*
 900  FORMAT(A)

        END
*
*-----------------------------------------------------------------
*
```

```
      SUBROUTINE DOUBLE
*
* Subroutine to process data from multiple tests - static or dynamic -
* with incremental calibrations between two points
* Allows choice of test data (STD or SCD/FCD) and calibration files (CAL)
*
      CHARACTER FILENAME*12,CALFILE1*12,CALFILE2*12,HEADER*255
      CHARACTER TEST*1
      INTEGER IA,IB,IC
      DOUBLE PRECISION CALIB,CAL1,CAL2
      DIMENSION CALIB(18),CAL1(18),CAL2(18),FILENAME(50),TEST(50)
*
* Set up variables
*  FILENAME storage, in order, of files to be processed
*  HEADER used to read in headers from calibration file
*  TEST flag to test filetype
*  IA/IB/IC general variables
*  CAL1/2 start/finish calibration values
*  CALIB double precision array for storing calibration values
*    - passed to analysis routine
*
      CALL WCREATE@(1,1,78,23,95,31)
      CALL POPW@(31)
      CALL WCREATE@(1,1,38,23,59,30)
      CALL POPW@(30)
*
* Set up window
*
      CALL WCOUP@('Select Start Calibration:',63,1,2,30)
      CALL SELECT_FILE@('*.CAL',CALFILE1,*20)

      CALL WCOUP@(CALFILE1,63,1,3,30)
*
* Select First Calibration file to be used (.CAL files)
*  if ESC pressed during routine goto 10 - quit and return to menu
*
      CALL WCOUP@('Select End Calibration:',63,1,5,30)
      CALL SELECT_FILE@('*.CAL',CALFILE2,*20)

      CALL WCOUP@(CALFILE2,63,1,6,30)
*
* Select Second Calibration file to be used (.CAL files)
*  if ESC pressed during routine goto 10 - quit and return to menu
*
      OPEN (UNIT=30,FILE=CALFILE1,STATUS='OLD')
      READ (30,900) HEADER
      READ (30,900) HEADER
*
* Open FIRST calibration file and read in first header
*
      READ (30,*) CAL1(1),CAL1(2),CAL1(3),CAL1(4),CAL1(5),CAL1(6),CAL
     C1(7),CAL1(8)
*
* Read in first line of data
*
      READ (30,900) HEADER
      READ (30,900) HEADER
*
* Read in second header
*
      READ (30,*) CAL1(9),CAL1(10),CAL1(11),CAL1(12),CAL1(13),CAL1(14
     C),CAL1(15),CAL1(16)
*
* Read in second line of data
*
      READ (30,900) HEADER
      READ (30,900) HEADER
*
* Read in last header
*
```

```
        READ (30,*) CAL1(17),CAL1(18)

        CLOSE (30)
*
* Read in last of the data and close file
*
        OPEN (UNIT=30,FILE=CALFILE2,STATUS='OLD')
        READ (30,900) HEADER
        READ (30,900) HEADER
*
* Open SECOND calibration file and read in first header
*
        READ (30,*) CAL2(1),CAL2(2),CAL2(3),CAL2(4),CAL2(5),CAL2(6),CAL
  C2(7),CAL2(8)
*
* Read in first line of data
*
        READ (30,900) HEADER
        READ (30,900) HEADER
*
* Read in second header
*
        READ (30,*) CAL2(9),CAL2(10),CAL2(11),CAL2(12),CAL2(13),CAL2(14
  C),CAL2(15),CAL2(16)
*
* Read in second line of data
*
        READ (30,900) HEADER
        READ (30,900) HEADER
*
* Read in last header
*
        READ (30,*) CAL2(17),CAL2(18)

        CLOSE (30)
*
* Read in last of the data and close file
*
        CALL WCOUP@('Select files to be processed:',63,1,8,30)
        CALL WCOUP@('Press ESC to finish',63,1,9,30)
        IA=1
        IB=10
*
* Display 'enter files' prompt and set up file counter/print offset
*
 5  CALL SELECT_FILE@('*.S?D',FILENAME(IA),*7)

        CALL TRIMR@(FILENAME(IA))
        TEST(IA)=FILENAME(IA)(11:11)
        CALL TRIM@(FILENAME(IA))
        IF (TEST(IA).NE.'T'.AND.TEST(IA).NE.'C') GOTO 5
*
* Choose file, and check it is a legal file type
*
        CALL WCOUP@(FILENAME(IA),63,6,IA+IB,30)
        IA=IA+1
        IF (IA.GT.12) THEN
                CALL SCROLL_UP@(30)
                IB=IB-1
        ENDIF
        GOTO 5
*
* If file OK, print it up for reference, increment file counter and do again
*  if have chosen more than 12 files, will be at bottom of screen, so scroll up
*   one line and reduce offset (or would try printing below bottow of window)
*  pressing ESC key causes jump out of routine
*
 7  IA=IA-1
*
* When finished choosing (ESC key) reduce IA by 1 as incremented then exit
```

```
*
      DO 10 IB=1,IA

            DO 15 IC=1,18
            CALIB(IC)=(((IB-1)/(IA-1))*(CAL2(IC)-CAL1(IC)))+CAL1(IC)
15    CONTINUE

            IF (TEST(IB).EQ.'T') THEN
                  CALL STATIC(CALIB,FILENAME(IB))
            ELSE
                  CALL CYCLIC(CALIB,FILENAME(IB))
            ENDIF

10  CONTINUE
*
* Loop through each file in turn (total of IA files)
* Set the calibration array to its correct proportion through the distance
*   between start and end calibrations (IA-1/IB-1 of the way through)
*
* If test character (from filename) is T, ie .sTd file, then goto static
*   analysis subroutine
* if not, then test character must be C, ie .sCd file, hence goto cyclic
*   analysis subroutine
*
20  CALL KILLW@(30)
      CALL KILLW@(31)
      RETURN
*
* Job done - close window and return to menu
*
900  FORMAT(A)

      END
*
*-----------------------------------------------------------------------
*
      SUBROUTINE CYCLIC(CALIBRATION,FILENAME)

* NOT PROGRAMMED FOR ADDITIONAL PARAMETERS
*
* Subroutine to process cyclic test data IN DOUBLE PRECISION
* CALIBRATION - Array containing calibration data
* FILENAME - File to be processed
*
      CHARACTER HEADER1*128,HEADER2*128,FILENAME*12,TEMP*12
      INTEGER*4 ISEC,IMIN,IHRS,ILINE,IPROCESS,ILOG,IUD,IOUT
      INTEGER*4 IA,IB,ITIME
      DOUBLE PRECISION CALIBRATION,LINE,OUTPUT,MAX,MIN,LMAX,LMIN
      DIMENSION CALIBRATION(18),LINE(8,3),OUTPUT(9,120)
*
* HEADER1/2 - For transfering headers between files
* ISEC/MIN/HRS - time data, ITIME sum of these three
* ILINE - line being processed
* IPROCESS - next line of data to be stored
* ILOG - logarithmic increment for next line of data to be stored
* IUD - indicates whether on up or down part of cycle
* IOUT - line of ouput array where next lot of data to be stored
* CALIBRATION - holds calibration data for each channel
* LINE - array for holding three consecutive lines of data for processing
* OUTPUT - array for holding processed data until dumped to file at end
*       extra element for line number
* MAX/MIN - max/min axial LVDT values from last cycle
* LMAX/LMIN - max/min load from last cycle
*
      CALL PREPROCESS(FILENAME)
*
* Invoke preprocessor to convert data into readable form and store in
*  temporary file ~SCRATCH.TMP
*
      CALL WCREATE@(26,11,30,4,0,20)
```

```
          CALL POPW@(20)
          CALL WCREATE@(25,10,30,4,76,21)
          CALL POPW@(21)
*
* Puts information window on screen
* 20 - Shadow
* 21 - Window
*
          CALL WCOUP@('Processing Cyclic Test Data',79,2,0,21)
          CALL WCOUP@(FILENAME,79,10,1,21)
          CALL WCOUP@('Cycle - ',79,9,2,21)
          CALL WCOUP@('Cycle Required - ',79,5,3,21)
*
* Set up line counter, log counter, up/down counter and open scratch file for
* reading. Read in headers and first line of data, which is then stored in
* output array as it represents initial conditions. Then read in next line
* of data - first to be processed, hence stored in LINE array. Finally set
* max/min to first LVDT value in LINE array.
*
          ILINE=1
          IPROCESS=1
          ILOG=1
          IUD=0
          IOUT=2
          OPEN (UNIT=20,FILE='C:\~SCRATCH.TMP',STATUS='OLD')
          READ (20,900) HEADER1
          READ (20,900) HEADER2
          READ (20,*) IHRS,IMIN,ISEC,OUTPUT(1,1),OUTPUT(2,1),OUTPUT(3,1),
   COUTPUT(4,1),OUTPUT(5,1),OUTPUT(6,1),OUTPUT(7,1),OUTPUT(8,1)
          OUTPUT(9,1)=1.0
          READ (20,*) IHRS,IMIN,ISEC,LINE(1,1),LINE(2,1),LINE(3,1),LINE(4
   C,1),LINE(5,1),LINE(6,1),LINE(7,1),LINE(8,1)
          MAX=LINE(5,1)
          MIN=LINE(5,1)
          LMAX=0.0
          LMIN=-0.01
*
* Main Program Loop
*
 10   DO 20 IA=1,8
                    LINE(IA,3)=LINE(IA,2)
                    LINE(IA,2)=LINE(IA,1)
 20   CONTINUE
          READ (20,*,END=40) IHRS,IMIN,ISEC,LINE(1,1),LINE(2,1),LINE(3,1),
    CLINE(4,1),LINE(5,1),LINE(6,1),LINE(7,1),LINE(8,1)
*
* Move last line data to LINE-2 and line before that to LINE-3
* Load new line of data into LINE-1
*
          IF (IUD.EQ.0) GOTO 30
*
* If on downward part of cycle, skip upcycle routine
*
          IF (LINE(6,2)-LINE(6,1).GT.0.05*(LINE(6,2)-LMIN)) THEN
                    IB=2
                    IF (LINE(5,2)-LINE(5,3).GT.(MIN-LINE(5,3))*0.05) THEN
                              IB=3
                    ENDIF
                    IUD=0
                    MAX=LINE(5,IB)
                    LMAX=LINE(6,IB)
*
* If load in last line more than 5% lower than previous line, have peaked
*  ie end of this half of the cycle, and line 2 (IB=2) is endpoint
* If then axial position of this is more than 5% lower than the line before
*  that (line 3), have caught it on the way down and line 2 is rogue data
*  hence line 3 (IB=3) is the endpoint
* Set IUD the 0, indicating now on a downward portion, and MAX to peak LVDT
*  reading
*
```

```
* Line counter NOT incremented as this is only done after a full cycle
* ie when have reached bottom peak aswell
*
                IF (ILINE.EQ.IPROCESS) THEN
                        DO 25 IA=1,8
                        OUTPUT(IA,IOUT)=LINE(IA,IB)
 25             CONTINUE
                        OUTPUT(9,IOUT)=ILINE
                        IOUT=IOUT+1
                ENDIF
*
* If this line is the next one wanted for storage (IPROCESS) then put the
* contents of the appropriate line of LINE into the current point on the
* output array, along with the line number
* Again IPROCESS NOT incremented until have done bottom half of cycle too
* but of course, IOUT MUST be incremented else data will be overwritten
* later
*
        ENDIF
        GOTO 10
*
* When have done all this, or if were still on upward curve in the first
* place, go round loop again
*

*
* Now downcycle part of routine
*
 30   IF (LINE(6,2)-LINE(6,1).LT.0.05*(LINE(6,2)-LMAX)) THEN
                IB=2
                IF (LINE(5,3)-LINE(5,2).GT.(LINE(5,3)-MAX)*0.05) THEN
                        IB=3
                ENDIF
                IUD=1
                MIN=LINE(5,IB)
                LMIN=LINE(6,IB)
*
* If load in last line more than 5% higher than previous line, have peaked
* ie end of this half of the cycle, and line 2 (IB=2) is endpoint
* If then axial position of this is more than 5% higher than the line before
* that (line 3), have caught it on the way up and line 2 is rogue data
* hence line 3 (IB=3) is the endpoint
* Set IUD the 0, indicating now on a downward portion, and MIN to peak LVDT
* reading
*
                IF (ILINE.EQ.IPROCESS) THEN
                        DO 35 IA=1,8
                        OUTPUT(IA,IOUT)=LINE(IA,IB)
 35             CONTINUE
                        OUTPUT(9,IOUT)=ILINE
                        IOUT=IOUT+1
                        IPROCESS=IPROCESS+ILOG
                        IF (IPROCESS/ILOG.EQ.10) ILOG=ILOG*10
                ENDIF
*
* If this line is the next one wanted for storage (IPROCESS) then put the
* contents of the appropriate line of LINE into the current point on the
* output array, along with the line number
* IOUT is incremented, and IPROCESS is increased by ILOG (as whole cycle now
* complete). If IPROCESS is now 10 times the size of ILOG then have got all
* the tens, or hundreds, or thousands, and ILOG must be multiplied by 10 to
* start on the next range up. This gives roughly logarithmic data extraction
* ie 1,2,3,4,5,6,7,8,9,10,20,30..80,90,100,200,300...800,900,1000,2000,etc.
*
                CALL SET_CURSOR_POSW@(21,17,2)
                CALL PRINT_I4@(ILINE)
                CALL SET_CURSOR_POSW@(21,22,3)
                CALL PRINT_I4@(IPROCESS)
                ILINE=ILINE+1
*
```

```
* Having reached end of the bottom half, cycle is complete so ILINE can be
* incremented. This and IPROCESS are then printed on-screen
*
        ENDIF
        GOTO 10
*
* When have done all this, or if were still on downward curve in the first
* place, go round loop again
*
 40  IF (ILINE.EQ.IPROCESS) THEN
                DO 45 IA=1,8
                        OUTPUT(IA,IOUT)=LINE(IA,2)
 45       CONTINUE
                OUTPUT(9,IOUT)=ILINE
                IOUT=IOUT+1
                IPROCESS=IPROCESS+ILOG
                IF (IPROCESS/ILOG.EQ.10) ILOG=ILOG*10
        ENDIF

        CALL SET_CURSOR_POSW@(21,17,2)
        CALL PRINT_I4@(ILINE)
        CALL SET_CURSOR_POSW@(21,22,3)
        CALL PRINT_I4@(IPROCESS)
        ILINE=ILINE+1
*
* When reached end of data, end of cycle too, but would not normally be
* registered. So, end of cycle routine repeated here
*
        ILINE=ILINE/10
        ILINE=ILINE*10
*
* ILINE rounded to nearest 10 as from now on (FCD file) readings only taken
* every 10 cycles.
*
*  / by 10 to remove last digit (fraction thrown away)
*  * 10 to get back to correct magnitude
*
        ITIME=ISEC+IMIN*60+IHRS*3600
*
* Calculate time at which last reading taken, so can sift through crap at
* start FCD file to find where real data starts
*
        CLOSE (20)
        CALL ERASE@('C:\~SCRATCH.TMP',IB)
*
* Have finished with that file, so close and erase it
*
        CALL TRIMR@(FILENAME)
        TEMP=FILENAME(1:9)//'FCD'
        FILENAME=TEMP
        CALL TRIM@(FILENAME)

        CALL PREPROCESS(FILENAME)
*
* Convert filename from SCD to FCD and pre-process it
*
        OPEN (UNIT=20,FILE='C:\~SCRATCH.TMP',STATUS='OLD')
        READ (20,900) HEADER1
        READ (20,900) HEADER2
*
* Open preprocessed file + read in headers
*

 50   READ (20,*,END=80) IHRS,IMIN,ISEC,LINE(1,1),LINE(2,1),LINE(3,1),
   CLINE(4,1),LINE(5,1),LINE(6,1),LINE(7,1),LINE(8,1)
        IF (ISEC+IMIN*60+IHRS*3600.LE.ITIME) GOTO 50
*
* Read through lines of data until get past time when slow data finished
* ie eliminating rubbish from start file
*
```

```
      READ (20,*,END=80) IHRS,IMIN,ISEC,LINE(1,1),LINE(2,1),LINE(3,1),
     CLINE(4,1),LINE(5,1),LINE(6,1),LINE(7,1),LINE(8,1)
*
* When have reached this point, read next line (matched pair of previous
* reading) as this too wants discarding, as cycle after last of SCD file
* hence not wanted
*
*
* MAIN LOOP
*
 60   READ (20,*,END=80) IHRS,IMIN,ISEC,LINE(1,1),LINE(2,1),LINE(3,1),
     CLINE(4,1),LINE(5,1),LINE(6,1),LINE(7,1),LINE(8,1)
      READ (20,*,END=80) IHRS,IMIN,ISEC,LINE(1,2),LINE(2,2),LINE(3,2),
     CLINE(4,2),LINE(5,2),LINE(6,2),LINE(7,2),LINE(8,2)
*
* Get pair of readings
*
      ILINE=ILINE+10
      CALL SET_CURSOR_POSW@(21,17,2)
      CALL PRINT_I4@(ILINE)
*
* Increment line counter accordingly (as only every 10th reading taken now)
*
      IF (ILINE.LT.IPROCESS) GOTO 60
*
* If this is not the next line data required, go back to start of loop
* and do again
*
      DO 65 IA=1,8
            OUTPUT(IA,IOUT)=LINE(IA,2)
            OUTPUT(IA,IOUT+1)=LINE(IA,1)
 65   CONTINUE
      OUTPUT(9,IOUT)=ILINE
      OUTPUT(9,IOUT+1)=ILINE
      IOUT=IOUT+2
      IPROCESS=IPROCESS+ILOG

      IF (IPROCESS/ILOG.EQ.10) ILOG=ILOG*10
      CALL SET_CURSOR_POSW@(21,22,3)
      CALL PRINT_I4@(IPROCESS)
*
* If these lines are the next wanted, copy them to output array, along with
* their line nos.
* Increase array pointer to next free point and IPROCESS to next line required
*
      IF (IPROCESS.EQ.100000) IPROCESS=99990
      GOTO 60
*
* Fudge counter, as switching from SCD to FCD loses cycle and prog
* is looking for last cycle after test stopped, hence must take previous
* lot of data
*
* Loop back
*

*
* Having finished going through raw data, must convert it to usable data
* First close old file and put up new dialog window
*
 80   CLOSE(20)
      CALL ERASE@('C:\~SCRATCH.TMP',IB)
      CALL KILLW@(21)
      CALL WCREATE@(25,10,30,4,76,21)
      CALL POPW@(21)
      CALL WCOUP@('Calibrating Data',79,6,1,21)

*
* Then go through each line of the output array in turn
*
      DO 85 IB=1,IOUT-1
```

```
            DO 90 IA=1,8
c             OUTPUT(IA,IB)=OUTPUT(IA,IB)*OUTPUT(8,1)/OUTPUT(8,IB)
              OUTPUT(IA,IB)=OUTPUT(IA,IB)*CALIBRATION(IA*2-1)+CALIBRATI
   CON(IA*2)
 90     CONTINUE
*
c Calibrate for computer drift by comparing start and current voltage
c - SUSPENDED DUE TO FAULTY CHANNEL 1 CONNECTION
*
* Convert each row of raw readings to engineering units using calibration
*  REAL VALUE = (RAW READING * SLOPE) + INTERCEPT
*
            OUTPUT(5,IB)=OUTPUT(5,IB)-CALIBRATION(17)*OUTPUT(6,IB)
*
* Adjust axial deformation for system deflection
*
 85   CONTINUE
*
* Go back and do next line
*

*
* When all calibration done, convert filename to PCD, delete it if it
*  already exists, and open output file
*
          CALL TRIMR@(FILENAME)
          TEMP=FILENAME(1:9)//'PCD'
          FILENAME=TEMP
          CALL TRIM@(FILENAME)
          CALL ERASE@(FILENAME,IB)
          OPEN (UNIT=21,FILE=FILENAME,STATUS='NEW')
          CALL WCOUP@('Writing output file',79,5,1,21)
          CALL WCOUP@(FILENAME,79,9,2,21)


          WRITE (21,900) HEADER1
          WRITE (21,900) HEADER2
*
* Put headers on output file
*
          DO 100 IA=1,IOUT-1
                  WRITE (21,910) OUTPUT(1,IA),OUTPUT(2,IA),OUTPUT(3,IA),OU
   CTPUT(4,IA),OUTPUT(5,IA),OUTPUT(6,IA),OUTPUT(7,IA),OUTPUT(8,IA),OUT
   CPUT(9,IA)
 100  CONTINUE
*
* Dump results from output array to file
*
          CLOSE (21)
          CALL KILLW@(21)
          CALL KILLW@(20)
*
* Having finished, close output file and kill information windows
*
          RETURN

 900  FORMAT(A)
 910  FORMAT(9F16.8)


          END
*
*-----------------------------------------------------------------------
*
          SUBROUTINE STATIC(CALIBRATION,FILENAME)

* NOT PROGRAMMED FOR ADDITIONAL PARAMETERS LIKE VOLUMETRIC STRAIN

*
* Subroutine to process static test data IN DOUBLE PRECISION
```

```
* CALIBRATION - Array containing calibration data
* FILENAME - File to be processed
*
      CHARACTER *128 HEADER1,HEADER2,FILENAME*12,TEMP*12
      INTEGER ISEC,IMIN,IHRS,ILINE,IA,IB
      DOUBLE PRECISION CALIBRATION,CHAN,OUTPUT
      DIMENSION CALIBRATION(18),CHAN(8),OUTPUT(8,250)
*
* HEADER - Misc. character variable for transfering header data between files
* ISEC/MIN/HRS - For reading time data from file, although data not needed here
* CALIBRATION - Holds calibration data. 2 numbers (M(x),C) for each channel
* CHAN - Holds each batch of 8 channel readings for processing
* OUTPUT - Holds processed data until end, when it is dumped to file
*      200 Batches of 8 channels is theoretical maximum generated by
*      static test at 4 readings per min (@1 mm/min) for 50mm travel
*
      CALL PREPROCESS(FILENAME)
*
* Call preprocessing routine to convert data into readable form and place
* it in file ~SCRATCH.TMP
*
      CALL WCREATE@(26,11,30,4,0,20)
      CALL POPW@(20)
      CALL WCREATE@(25,10,30,4,76,21)
      CALL POPW@(21)
*
* Puts information window on screen
* 20 - Shadow
* 21 - Window
*
      CALL WCOUP@('Processing Static Test Data',79,2,0,21)
      CALL WCOUP@(FILENAME,79,9,1,21)
      CALL WCOUP@('Line - ',79,10,2,21)
*
* Initialise line counter, open file for reading and load up header
*
      ILINE=1
      OPEN (UNIT=20,FILE='C:\~SCRATCH.TMP',STATUS='OLD')
      READ (20,900) HEADER1
      READ (20,900) HEADER2
*
* Start Main Loop
*
 10   READ (20,*,END=30) ISEC,IMIN,IHRS,CHAN(1),CHAN(2),CHAN(3),CHAN(4
     C),CHAN(5),CHAN(6),CHAN(7),CHAN(8)
*
* Read in a line of data
*
      DO 20 IA=1,8
            CHAN(IA)=CHAN(IA)*10/CHAN(8)
            CHAN(IA)=CHAN(IA)*CALIBRATION(IA*2-1)+CALIBRATION(IA*2)
 20   CONTINUE
*
* Adjust for voltage (assuming 10v base value)
* Convert row of raw readings to engineering units using calibration values
* REAL VALUE = (RAW READING * SLOPE) + INTERCEPT
*
      CHAN(5)=CHAN(5)-CALIBRATION(17)*CHAN(6)
*
* Adjust axial deformation for system deflection
*
      DO 25 IA=1,8
            OUTPUT(IA,ILINE)=CHAN(IA)
 25   CONTINUE
*
* Put adjusted values in output array
*
      CALL SET_CURSOR_POSW@(21,17,2)
      CALL PRINT_I2@(ILINE)
```

```
          ILINE=ILINE+1
*
* Print line counter and increment
*
          GOTO 10
*
* Loop back
*
 30   CLOSE (20)
          CALL ERASE@('C:\~SCRATCH.TMP',IB)
*
* Having read all the data, close the temporary file and delete it
*
          DO 35 IA=(ILINE-1),1,-1
                OUTPUT(5,IA)=OUTPUT(5,IA)-OUTPUT(5,1)
 35       CONTINUE
*
* Take first LVDT reading from all the other values, so static tests
*  always start from zero - for comparison
*
          CALL TRIMR@(FILENAME)
          TEMP=FILENAME(1:9)//'PSD'
          FILENAME=TEMP
          CALL TRIM@(FILENAME)
          CALL ERASE@(FILENAME,IB)
          OPEN (UNIT=21,FILE=FILENAME,STATUS='NEW')
          CALL WCOUP@('Writing output file',79,5,2,21)
          CALL WCOUP@(FILENAME,79,9,3,21)
*
* Revise filenemae to .PSD suffix and open output file in this name
* Put this information on screen
*
* Must use TEMP variable as putting FILENAME=FILENAME(1:9)//PSD causes a crash
*
          WRITE (21,900) HEADER1
          WRITE (21,900) HEADER2
*
* Put headers on output file
*
          DO 40 IA=1,ILINE-1
                WRITE (21,910) OUTPUT(1,IA),OUTPUT(2,IA),OUTPUT(3,IA),OU
   CTPUT(4,IA),OUTPUT(5,IA),OUTPUT(6,IA),OUTPUT(7,IA),OUTPUT(8,IA)
 40   CONTINUE
*
* Dump results from output array to file
*
          CLOSE (21)
          CALL KILLW@(21)
          CALL KILLW@(20)
*
* Having finished, close output file and kill information windows
*
          RETURN

 900  FORMAT(A)
 910  FORMAT(8F16.8)

          END
*
*-----------------------------------------------------------------------
*
          SUBROUTINE PREPROCESS(FILENAME)
*
* Data Pre-Processor
* Loads data in as text and converts time string to 3 numbers, hours, minutes
* and seconds, and then saves everything to a scratch file. This can
* then be read directly as numerical data by main program as non numerical
* characters are no longer present
*
```

```
      CHARACTER FILENAME*12,DATAIN*256,DATATEMP*248,DATAOUT*256
      CHARACTER TSEC*2,TMIN*2,THRS*2

      INTEGER ILINE
*
* Initialise line counter (ILINE) and put counter window on screen with shadow
* window handle - 10
* shadow handle - 11
*
      ILINE=1
      CALL WCREATE@(30,15,22,2,0,11)
      CALL POPW@(11)
      CALL WCREATE@(29,14,22,2,42,10)
      CALL POPW@(10)
      CALL WCOUP@('PRE-PROCESSING DATA',47,1,0,10)
      CALL WCOUP@('Line -',47,5,1,10)
*
* Set up files for reading / writing
* unit 10 - READ
* unit 11 - WRITE
*
      OPEN (UNIT=10,FILE=FILENAME,STATUS='OLD')
      OPEN (UNIT=11,FILE='C:\~SCRATCH.TMP',STATUS='NEW')
*
* Transfer header to scratch file
*
      READ (UNIT=10,FMT=900) DATATEMP
      WRITE (UNIT=11,FMT=900) DATATEMP
      READ (UNIT=10,FMT=900) DATATEMP
      WRITE (UNIT=11,FMT=900) DATATEMP
*
* Main program loop
*
* Read in line of data
*
 100  READ (UNIT=10,FMT=900,END=200) DATAIN
*
* Separate out hours, mintues and seconds from colons - leave rest of data
*
      THRS=DATAIN(1:2)
      TMIN=DATAIN(4:5)
      TSEC=DATAIN(7:8)
      DATATEMP=DATAIN(9:256)
*
* Form into output line
*
      DATAOUT=THRS//' '//TMIN//' '//TSEC//DATATEMP
*
* Save to output file
*
      WRITE (UNIT=11,FMT=900) DATAOUT
*
* Update line counter in window
*
      CALL SET_CURSOR_POSW@(10,12,1)
      CALL PRINT_I2@(ILINE)
      ILINE=ILINE+1
*
* Loop back
*
      GOTO 100
*
* No More Data - close down files, kill windows and end subroutine
*
 200  CALL KILLW@(11)
      CALL KILLW@(10)
      CLOSE (10)
      CLOSE (11)
      RETURN
*
```

```
* Format statements for loading data
*
 900  FORMAT (A)

          END

* ----------------------------------------------------------------------
```

Appendix III

Summary of the specification for track ballast (BR 1203) -
July 1985 (Amended May 1988)

1. The Ballast shall be hard and durable natural stone.

2. The Ballast must be angular in shape with all dimensions nearly equal and free form dust.

3. In interpreting the requirements of this specification, reference shall be made to current British standards, viz: BS 812: Methods of sampling and Testing, except for the Wet Attrition Test where the values are to be derived from a test carried out in accordance with BS 812: 1951 Clause 27.

4. The Ballast shall consist of a mixture of sizes mainly between 50mm and 28mm to conform to the limits of the following table.

Square Mesh Sieve		
63mm	-	100% to pass
50mm	-	100 - 97% to pass
28mm	-	20 - 0% to pass
14mm	-	2 - 0% to pass
1.18mm	-	0.8 - 0% to pass

In the wagon these sizes must be evenly distributed.

5. Flakiness Index - Maximum Permissible Value 50%

Elongation Index - Maximum permissible Value 50%

or

Not more than 2% by weight of particles shall have a dimension exceeding 100mm.

Not more than 25% by weight of particles shall have a dimension exceeding 75mm.

6. The Wet Attrition Value shall not exceed 4% for ballast supplied

7. A 50kg sample of Ballast shall be taken at the time of tendering and from time to time as the Engineer decides for the purposes of quality control.

Appendix IV

Summary of conditions for each test, listed by test Set number

Main Test Series

Test Set	Materials	Layer Thickness	Cell Pressure (kPa)	Orientation of Material Interface	Comments
3	Ballast Only	-	40	-	-
4	20mm Stone Only	-	40	-	-
5	Ballast & 20mm Stone	Equal Layers	40	Horizontal	-
6	Ballast & 20mm Stone	Equal Layers	60	Horizontal	-
7	Ballast & 20mm Stone	Equal Layers	90	Horizontal	-
8	Ballast & 20mm Stone	Equal Layers	30/35	Horizontal	Initial Monotonic 30 kPa, Others 35 kPa
9	Ballast & 20mm Stone	Equal Layers	40	11° to Horizontal	-
10	Ballast & 20mm Stone	Equal Layers	40	22° to Horizontal	-
11	Ballast & 20mm Stone	Equal Layers	40	33° to Horizontal	-
12	Ballast & 20mm Stone	Equal Layers	40	45° to Horizontal	-
13	Ballast & 20mm Stone	350mm Ballast, 100mm 20mm Stone	40	Horizontal	-
14	Ballast & 20mm Stone	150mm Ballast, 300mm 20mm Stone	40	Horizontal	-
REP2	Ballast & 20mm Stone	Equal Layers	40	Horizontal	-
15	14mm Stone Only	-	40	-	-
16	Ballast & 14mm Stone	Equal Layers	40	Horizontal	-
17	10mm Stone Only	-	40	-	-
18	Ballast & 10mm Stone	Equal Layers	40	Horizontal	-
19	6mm Stone Only	-	40	-	-
20	Ballast & 6mm Stone	Equal Layers	40	Horizontal	-
21	River Gravel Only	-	40/90	-	Initial Monotonic 40 kPa, Others 90 kPa
22	Ballast & River Gravel	Equal Layers	90	Horizontal	-
23	Ballast & River Gravel	Equal Layers	90	45° to Horizontal	-
24	Ballast & River Gravel	Equal Layers	60	Horizontal	-
25	20mm Stone Only	-	40	-	Lost Due To Water Leak
26	20mm Stone Only	-	40	-	Lost Due To Water Leak
27	20mm Stone Only	-	40	-	-
28	Ballast & Netlon Elements	-	40	-	Initial Monotonic Test Only
29	Ballast & Terram Elements	-	40	-	Initial Monotonic Test Only
30	20mm Stone Only	-	90	-	-
31	Ballast Only	-	40	-	-
32	Ballast Only	-	90	-	-
33	Ballast & River Gravel	Equal Layers	90	Horizontal	Initial Monotonic Test Only, to Complete Set 21
REP3	Ballast & 20mm Stone	Equal Layers	40	Horizontal	-

Secondary Test Series

Test Set	Materials	Layer Thickness	Cell Pressure (kPa)	Orientation of Material Interface	Comments
35	Ballast & 20mm Stone	Equal Layers	40	Horizontal	Minimum Cyclic Stress Set To Exactly 17 kPa
36	Ballast & 20mm Stone	Equal Layers	40	Horizontal	Lost Due To Water Leak
37	Ballast & 20mm Stone	Equal Layers	40	Horizontal	Minimum Cyclic Stress Set To Exactly 8 kPa
38	Ballast & 20mm Stone	Equal Layers	40	Horizontal	Minimum Cyclic Stress Set To Exactly 25 kPa
39	Wet Ballast & 20mm Stone	Equal Layers	40	Horizontal	Minimum Cyclic Stress Set To Exactly 17 kPa
40	Ballast & 20mm Stone	Equal Layers	40	Horizontal	Minimum Cyclic Stress Set To Exactly 17 kPa